Chapter 1

Introduction

Knowledge begets knowledge. The more I see, the more impressed I am - not with what we know - but with how tremendous the areas are as yet unexplored.

John H. Glenn (1921-)
American Astronaut, US Senator 1974

THE research presented within this thesis focuses on the development and evaluation of trajectory design and guidance tools for the terminal area flight phase of reusable launch vehicles (RLVs). The research consists of three areas of interest for the terminal area flight phase. The first area of research involves the development of a trajectory design tool based on optimisation through the parameterisation of the vehicle steering commands. The second area of research involves the extension of a guidance method to the terminal area flight phase including a simulation tool for evaluation of the guidance under off-nominal conditions. The third area of research involves the evaluation of the terminal area flight phase, utilising sensitivity studies of the trajectories to determine the influences of off-nominal conditions.

1.1 Background and Motivation

The next generation of reusable launch vehicles requires significant improvements in order to reduce launch costs, increase safety and provide for various mission scenarios. A key aspect of these improvements will be advanced guidance systems (Hanson, 2002). The re-entry of a reusable launch vehicle (RLV) through the atmosphere tra-

ditionally consists of three distinct phases; hypersonic re-entry, terminal area flight and approach and landing. Most research on advanced guidance concepts has concentrated on improvements of existing methods and advanced guidance concepts for the ascent and hypersonic re-entry flight phases. However, in order to provide substantial improvements in performance investigations into the terminal area flight phase and the approach and landing phase must also be investigated.

The research presented in this thesis focuses on the terminal area flight phase as a next step extension to the research previously conducted on the hypersonic re-entry flight phase (Telaar, 2005). Improvements in the terminal area and approach and landing flight phases can provide significant improvements in vehicle safety and mission flexibility. Improvements in the guidance systems ability to compensate for off-nominal conditions such as atmospheric disturbances could significantly reduce the number of launch delays, increase vehicle safety and the rate of mission success.

The terminal area flight phase, also know as the Terminal Area Energy Management (TAEM) phase, is the transitional phase between hypersonic re-entry and the approach and landing phases. Consequently within the terminal area flight phase several important events occur. These include: a Mach transition (transition from supersonic to subsonic speeds) and alignment of the vehicle with the runway centreline whilst reaching the appropriate final attitude, altitude and velocity to facilitate a safe landing. The flight phase is made more complicated as the re-entry vehicles used are generally un-powered (that is without thrust) and consequently must glide to the landing site. However, these vehicles predominantly have poor glide capabilities and lower lift-to-drag ratios when compared to vehicles such as planes or gliders. Consequently this flight phase requires a complicated guidance program or specialised methods in order to meet all the above requirements.

The development of terminal area guidance methods for re-entry vehicles was first investigated in the 1970's for lifting body type vehicles (Hoffman et al., 1970). The lifting body research was then incorporated and extended within the US Space Shuttle program which at the time of writing is the only operating reusable launch vehicle with a terminal area flight phase (Ehlers and Kraemer, 1977). At the commencement of this research there had been only minor interest into improvements and new methods for trajectory design and guidance methods applied to the terminal area flight phase.

In recent years, over the course of the research presented in this thesis, there has been greater interest in advanced guidance methods for the terminal area flight phase. However, these improved and new methods have yet to provide detailed results. Currently in publicly available literature there is a lack of published data for the terminal area flight phase including sensitivity studies and proven advanced guidance methodologies.

The optimisation and guidance methods utilised within this study are an evolution of the methods originally published in the 1970's and further developed at the Institute for Space Systems (Institut für Raumfahrtsysteme) Universität Stuttgart. The methods parameterise the trajectory using the vehicle steering commands utilising non-linear programming and gradient based techniques to perform trajectory design and guidance updates. It is important to note that these methods have not previously been applied to the terminal area flight phase. Consequently this study provides a different approach for trajectory design and guidance of lifting entry vehicles during the terminal area flight phase than previously investigated in literature.

1.2 Objectives and Scope

The primary objective of this research is the further development and successful application of the steering command parameterisation methodology to the terminal area flight phase. Another important addition of this thesis to scientific literature is the inclusion of detailed sensitivity studies for the terminal area flight phase.

While this thesis does not present a completely proven method of guidance, since it has not been flight tested, it has been substantially evaluated utilising computer simulations. Computer simulations were used for evaluation, since a full flight test program of the software was well outside the scope of this research due to funding limitations.

The developed trajectory design and guidance programs for the terminal area flight phase were intended to be adaptable and flexible to various vehicles and missions. Consequently the evaluation of the trajectory design and guidance programs were performed for two completely different vehicles and their associated missions. Although this method is intended to be applicable to various lifting re-entry vehicles the evaluation of more than two vehicles was considered outside the scope of this research

due to time and funding limitations. Additionally the availability of detailed vehicle aerodynamic models is limited in publicly available literature. An added benefit of the evaluation of two completely different vehicles and missions allowed for sensitivities of the proposed method and the terminal area flight phase to be investigated since vehicle specific traits could be identified.

1.3 Thesis Organisation

Chapter 2 provides an overview of previous, current and emerging trajectory design and guidance methodologies. The current gaps in literature are highlighted throughout and summarised in the conclusion. It also includes a small discussion of optimisation techniques since the trajectory design techniques are based on non-linear programming and optimisation. A specific focus on the review of guidance methodologies is given to the terminal area flight phase. However, conceptual and advanced developments for other flight phases are also briefly discussed.

Chapter 3 discusses the methodology used within this research including the trajectory design and guidance programs. Additionally there is a discussion of the various models, the off-nominal conditions (applied errors) and the assumptions and limitations of the techniques utilised.

Chapter 4 presents the two vehicles and their associated missions that were used in the development and evaluation of the programs. The sub-orbital Hopper concept vehicle and the sub-orbital X-33 Single Stage To Orbit (SSTO) vehicle are discussed in sections 4.1 and 4.2 respectively.

Chapters 5 and 6 present the investigations and evaluations of the trajectory design and guidance programs, respectively. Also included are the sensitivity studies results and a comparison to other methodologies previously published in literature. Both chapters also include a discussion and conclusion of the results and findings for the investigations and evaluations of the associated program. Chapter 5 combines the evaluation of the two vehicles in single discussion. However, Chapter 6 separates the evaluation for the two vehicles due to the amount of results and for ease in comparison to other methods in literature.

Chapter 7 provides an overall conclusion of the investigations and findings of the

research presented in this thesis. A suggestion on possible future work to extend this field of research is also included. The Appendices A, B, C and D which follow provide more detailed information on the simulation environment, numerical methods, the developed Hopper vehicle speed brake model and modification to the steering profiles for various off-nominal conditions.

Chapter 2

Literature Review

The study of an idea is, of necessity, the story of many things. Ideas, like large rivers, never have just one source. Just as the water of a river near its mouth, in its final form, is composed largely of many tributaries, so an idea, in its final form, is composed largely of later additions.

Willy Ley (1906 - 1969)
In Rockets, Missiles and Space Travel, 1951

NUMEROUS different methodologies are currently available for the trajectory design, optimisation and guidance of reusable launch vehicles. The goal of this section is not to provide an entire review of trajectory design, optimisation and guidance for launch and re-entry vehicles. This topic has consumed considerable space in academic journals, such as the Journal of Spacecraft and Rockets, Journal of Guidance, Control and Dynamics, Acta Astronautica, Advances in Space Research, Aerospace Science and Technology and Progress in Aerospace Sciences. Common methods of optimisation are discussed in section 2.1. Since trajectory design and guidance is often discussed in unison in literature these two topics have also been grouped here and are discussed in section 2.2. A primary focus of the highlighted literature of this chapter will be those methods directly related to the terminal area flight phase as discussed in section 2.3. However, a brief overview of other guidance methods is included for completeness and since some methods could also be potentially applied to the terminal area flight phase. The emphasis in this chapter is on improved trajectory design and guidance methods which take advantage of modern computer systems and also

to highlight new emerging methods.

2.1 Optimisation

Within this study trajectory design is performed using the non-linear gradient based NLPQL optimisation sub-routine contained within the International Mathematics Standards Library (IMSL). However, there are various other methods that can be utilised for optimisation. The intention of this thesis is not to provide a summary of optimisation methods. A summary of numerical optimisation methods for trajectory optimisation is presented in Betts (1998). The various types of optimisation methods have been grouped into three distinct categories gradient methods, genetic algorithms and simulated annealing. These methods are each discussed in sections 2.1.1, 2.1.2 and 2.1.3 respectively.

2.1.1 Gradient Methods

Gradient based algorithms are the traditional optimisation methods. They are based on Newtonian methods which employ a search along the gradients of the function. The algorithms utilise the derivatives of the function in order to determine the local gradients. A minimum is found when the derivatives are equal to zero (Speyer et al., 1971). Gradient methods have been widely used for optimisation on a large variety of problems due to their simple methods (Speyer et al., 1971). However, these methods have the disadvantage that they can fail at singularities where no derivative of the function exists. Another problem of gradient methods is that they are only able to find local minima and not the global minimum without restart or the introduction of randomness (Goldberg, 1989). Since only local optima are found the gradient methods are relatively computationally efficient requiring only evaluation of a single point and not a population of points like other random based methods, such as genetic algorithms discussed in section 2.1.2.

2.1.2 Genetic Algorithms

Genetic algorithms are search algorithms based on genetics and natural selection (Goldberg, 1989). The algorithms use *genes*, *chromosomes* and several other methods to produce a solution. Generally genetic algorithms are useful for binary encoding in the form of strings however, more advanced algorithms can be used with non binary numbers. Genetic algorithms work on a coding of the parameter set and search from a population (Goldberg, 1989). An advantage of genetic algorithms is that the evaluation of derivatives and auxiliary knowledge is not required. The evaluation is performed by an objective function similar to a cost function (Goldberg, 1989).

The numbers or inputs called *chromosomes* are placed into a string called a *gene*. The contents of the *gene* are randomly generated and then this is used to evaluate the problem and determine the outcome (Goldberg, 1989). The level of fitness of each *gene* determines whether it will be *reproduced* in the next stage. The fittest *genes* are determined by an objective function which is a measure that is maximised similar to the cost function of gradient based methods. The process of natural selection then takes over and the fittest *genes* are taken to the next stage of the *mating pool* (Goldberg, 1989). The next stage is mating where the fittest *genes* are combined through a process known as *crossover* thus combining the previous *genes* to produce the new offspring (Goldberg, 1989). These offspring are then evaluated against the problem and again the fittest are kept and so the process continues until an optimal solution is found (Goldberg, 1989).

There are several things that have been incorporated into genetic algorithms to cope with drawbacks of this method. *Mutation* allows for greater diversity in the gene pool. It is possible using the method of crossover that the genes will converge to a certain *genes* type that may eliminate a possible solution (Goldberg, 1989). Thus whilst the solution tends to a similar solution this may not be the optimal solution but perhaps a local optimum. *Mutation* allows a small percentage change for each of the *chromosomes* within a *gene* to mutate or change to another value. Consequently genetic algorithms can be utilised as global optimisers (Goldberg, 1989). *Elitism* allows for a certain percentage of the upper population to be kept (Goldberg, 1989).

The formulation of genetic algorithms must be carefully suited to the problem in order to get the required output. For trajectory optimisation there are generally n number of *genes* and each would have to be evaluated at each stage depending on the coding of

the parameter set. This could be computationally intensive for flight path integration resulting in n evaluations for each new gene pool. Consequently this method is computationally demanding and therefore unsuitable for on-board implementation. The method could however be usefully to find the global optimal solution off-line.

2.1.3 Simulated Annealing

Simulated annealing is an optimisation method named due to an analogy to the annealing process used when heat treating metals. Annealing is a process of heating and then slowly cooling metals to remove defects as it allows the atoms to redistribute to their lowest energy setting. An optimisation method has been designed to simulate the annealing process where an effective temperature is used as an equivalent (Kirkpatrick et al., 1983). Simulated annealing also utilises a cost function that is minimized but it can also be utilised as a global optimiser using the Metropolis algorithm (Metropolis et al., 1953). The Metropolis algorithm allows *bad* steps that increase the cost function in order to search for a better solution (Kirkpatrick et al., 1983). Using a probabilistic method given by equation 2.1 the algorithm can have more 'bad' steps at higher effective temperature T.

$$\exp\left(\frac{-\Delta F}{k_B \cdot T}\right) > R_n \tag{2.1}$$

Where ΔF is the change in the cost function, k_B is the Boltzmann factor and R is a random number on the interval $(0,1)$. The effective temperature is used as a control factor and as the system reaches steady state the temperature can be decreased. The use of the effective temperature allows for large variations to occur at high values and then as the system is cooled via an annealing schedule only small changes are allowed at lower effective temperatures.

A modification of simulated annealing to speed up the process is to accept all changes that decrease the cost function and all those changes that increase the cost function by less than a fixed threshold (Dueck and Scheuer, 1990). The threshold level is then lowered similar to the lowering of the temperature in metal annealing.

The advantage of simulated annealing is the global optimisation properties however, similar to genetic algorithms an increased computational effort is required to

perform the evaluations at every step to see if the cost function is improving before proceeding to the next step. The effective temperature or threshold introduces more computational complexity and the evaluations must also be performed at the various levels.

2.1.4 Summary of Optimisation Methods

The gradient based methods were selected for several reasons. The major reason was that this research is an extension of already existing methods discussed in section 2.4.3 and therefore the methods previously used were adopted, modified and extended to perform this study. Another major reason for the selection of gradient based methods is because of their widespread use and that previous testing has been performed to verify the algorithms suitability through the studies Schöttle (1988); Burkhardt (2001); Tetlow (2003); Gräßlin (2004); Telaar (2005). Although the random based methods of simulated annealing and genetic algorithms provide the ability to perform global optimisation this was not specifically necessary for the trajectory design. For the trajectory design of this study the determination of the optimal solutions produced from various initial guesses were evaluated by the user. This is discussed more in Chapter 5 and in detail in section 5.9. The simulated annealing and genetic algorithm can also be more computational intensive due to their global optimisation of the problem. By using a gradient method possible trajectory solutions could be generated rapidly and then verified by the user.

2.2 Trajectory Design and Guidance

There has been and continues to be, considerable interest and research into the development of new trajectory generators and guidance systems for launch vehicles. Trajectory design is generally performed by advance optimisation tools, such as the tool developed in this study for the terminal area flight phase. However, new emerging methods also include the trajectory design process within the guidance programs or utilises a similar formulation to design the trajectories and then perform guidance. Some of the new emerging methods include fuzzy logic design and neural networks. Conse-

quently the trajectory design methods for the terminal area flight phase are discussed in conjunction with guidance methods of section 2.3.

The purpose of a guidance system is to generate a set of commands in order to guide the vehicle from an initial state to a desired final state. There are several different types of guidance methods available for launch and entry vehicles and they often depend on their application. Expendable launch vehicles have a guidance system that is only required to place the payload into orbit and is often designed only for the specific mission. Reusable launch vehicles require the guidance system to accommodate more flight phases including ascent, re-entry, terminal area and approach and landing. Consequently these guidance systems need to be able to cope with a variety of flight conditions and often different mission profiles. Although there are many different types of guidance systems they can be grouped into two distinct types implicit and explicit.

2.2.1 Implicit Guidance

Implicit guidance also known as open loop guidance produce command profiles based on predetermined reference trajectories. The reference trajectories are designed prior to the launch. From these reference trajectories the required steering commands are then determined for the vehicle. Implicit guidance is predominantly used for atmospheric ascent flight. An example of this is the US Space Shuttle which utilises preselected pitch and yaw profiles based on the conditions determined prior to the launch (McHenry et al., 1979; Bordano et al., 1991). Implicit guidance is used for atmospheric ascent because with existing methods it is difficult to model all of the aerodynamic forces on a vehicle in real time during this flight phase (Hanson et al., 1995).

The advantages of implicit guidance is that it takes up minimal on-board computational effort as the profiles are calculated prior to launch. Since the profiles are not determined by an on-board guidance computer there are no issues with solution convergence or stability. An additional advantage is that provided the mission conditions are consistent with the precomputed reference trajectories then the vehicle should reach the final conditions accurately.

The disadvantages of implicit guidance is that it requires considerable pre-mission planning to account for all the expected conditions at the time of launch. This pre-

mission planning can be expensive in terms of both time and money. Leung and Calise (1994) state that implicit guidance has often caused launch delays for the US Space Shuttle due to large winds not conceived for during mission planning. The pre-computed guidance commands are only suited to the mission profiles considered and can not be adapted if the profiles differ. Consequently if the flight conditions or mission profile differs from the reference trajectory it can result in large deviations from the required final conditions or even mission failure.

2.2.2 Explicit Guidance

Explicit guidance or closed loop guidance schemes are the other type of guidance methods utilised. Explicit guidance utilises real time methods for on-board trajectory updates or generation. From the on-board trajectories the command profiles can be generated and adapted to the current flight conditions.

The advantages of explicit guidance methods are that they can adapt to current flight conditions. Consequently if unexpected flight conditions arise the trajectory can be adapted to take them into account and theoretically reduce the requirements for launch delays. The real time trajectory generation methods reduce the amount of pre-mission planning that must be performed. However, there must still be some analysis prior to launch to ensure that these methods work effectively.

The disadvantage of explicit guidance schemes are that they generally require large amounts of computational effort in comparison to implicit or open loop guidance. However, there has been considerable research into reducing the computational requirements of explicit methods. Considerable focus has been given to the exoatmospheric ascent and re-entry mission phases. Examples of such work are given in Hanson et al. (1995) and Hanson and Jones (2004). New methods of explicit guidance are also taking advantages of advances in intelligent computing including the use of fuzzy logic and neural networks as a method of reducing the computational requirements.

The current focus of research in guidance technologies for launch and entry vehicles is advanced explicit guidance methods. The several programs around the world include work on these method for the Japanese Hope-X, European Sänger, Hermes and Hopper and the US Space Shuttle, Orbital Space Plane, X-33, X-34, X-38 and DC-X vehicles.

2.3 Terminal Area Trajectory Design and Guidance Methods

There are existing methods available for terminal area guidance and with the numerous recent reusable or semi-reusable launch vehicle development programs there has been an increasing interest in the development of new and more effective methodologies. The original terminal area guidance methods were developed in the early 1970's for lifting body vehicles (Hoffman et al., 1970). This research later became part of the research and methods developed for the US Space Shuttle program (Ehlers and Kraemer, 1977). Using the final US Shuttle method called Terminal Area Energy Management (TAEM) as a basis new methods have been developed (Naftel and Powell, 1993). These methods have evolved over time and through the numerous missions flown. However, with the development of the next generation of launch vehicles namely RLVs improved guidance methods are required to have reduced cost, increased mission flexibility and in some cases operate autonomously. The following subsections provide a brief overview of the past, current and emerging methods for terminal area guidance.

2.3.1 Lifting Body Vehicle Guidance

An early terminal area guidance scheme called landing approach guidance originally developed for lifting body vehicles is discussed in Hoffman et al. (1970). The guidance scheme was designed to deliver a vehicle at an altitude of 9 km and approximately 20 to 25 km away from the runway during subsonic glide conditions. The aerodynamic and vehicle model used is representative of a NASA M2 type lifting body.

The guidance scheme utilised altitude as the independent variable (Hoffman et al., 1970). The state variables were the vehicle heading and the two position variables in the horizontal plane (Hoffman et al., 1970). Angle of attack and bank angle were used as the control variables. The equations of motion were simplified by the quasi-steady subsonic glide conditions (Hoffman et al., 1970). These conditions assume that rate of change for velocity and flight path angle are negligible and therefore can be assumed to be zero.

The guidance scheme relies upon calculated feedback gains determined from the nominal trajectory (Hoffman et al., 1970). A detailed derivation of the guidance scheme

is included in Hoffman et al. (1970). The profiles for the state variables and control histories were stored on-board as a function of altitude (Hoffman et al., 1970). During the flight the actual positions and heading were estimated from measurements and then compared to the nominal values to determine the deviation which were used to modify the nominal control histories (Hoffman et al., 1970).

The landing approach guidance scheme was tested for numerous off-nominal conditions including aerodynamic, density, mass, atmospheric winds and initial condition errors (Hoffman et al., 1970). The guidance scheme worked effectively in simulations under all the conditions tested as the final condition errors were quite small (Hoffman et al., 1970). The method for reshaping the trajectory due to the perturbations works effectively with the new trajectories representing only small deviations from the nominal. However, various combinations of the applied errors and a complete evaluation was not provided in public literature.

An advantage was that the simple methods based on feedback gains make for an easily implemented guidance program. Although this method did not deal with some of the other requirements of terminal area flight, such as a supersonic to subsonic transition or greater altitudes and distance to target, the method could possibly be extended to perform terminal area guidance.

2.3.2 US Shuttle Terminal Area Energy Management (TAEM)

Terminal Area Energy Management (TAEM) is the method utilised by the US Space Shuttle Orbiter. This method developed in the 1970's (Ehlers and Kraemer, 1977) and considered to be the benchmark as it is still in use and the only method which has received significant flight testing for verification. The US Shuttle Orbiter TAEM guidance tracks an energy versus range profile by varying the energy dissipation rate (Ehlers and Kraemer, 1977). The energy dissipation rate can be modulated by three distinct methods:

- Turning away from the runway, thus increasing the range-to-go and providing a greater period in which the energy can be dissipated;
- Varying dynamic pressure, an increase in dynamic pressure produces an increase in drag and consequently increases the rate of energy dissipation;

• Varying the speed brake, an aerodynamic decelerator, where an increase in deflection results in increased drag and consequently increased rate of energy dissipation.

The modulation of the dynamic pressure implicitly modifies the angle of attack and was used due to the greater accuracy achieved with a dynamic pressure sensor over the angle of attack sensor (Ehlers and Kraemer, 1977).
The TAEM guidance consists of three distinct sub-phases with an additional subphase to facilitate off-nominal conditions (Ehlers and Kraemer, 1977). Figure 2.1 provides a visual representation of the TAEM guidance phases.

Phase 0 Named the S-turn phase is the auxiliary phase provided to allow dissipation of excess energy by turning away from the Heading Alignment Cylinder (HAC) (Ehlers and Kraemer, 1977). The HAC was later referred to as the Heading Alignment Cone as the path followed by the US Shuttle Orbiter is that of a spiral (Moore, 1991). The utilisation of maximum dynamic pressure and maximum speed brake during this phase results in the maximum achievable energy dissipation rate (Ehlers and Kraemer, 1977).

Phase 1 The Acquisition phase controls the flight path, such that the current trajectory is tangent to the HAC. The rate of energy dissipation is controlled by modulating

Figure 2.1 – TAEM guidance phases (Ehlers and Kraemer, 1977)

dynamic pressure and in the subsonic flight range by modulating the speed brake deflection as well as dynamic pressure (Ehlers and Kraemer, 1977).

Phase 2 The Heading Alignment phase controls the US Shuttle Orbiter to track the HAC. The HAC is a virtual cone generated by the guidance system that allows the US Shuttle Orbiter to turn and align with the runway while dissipating energy (Moore, 1991). Energy dissipation while following the HAC is facilitated by dynamic pressure modulation and speed brake deflection (Ehlers and Kraemer, 1977).

Phase 3 The pre-final guidance phase operates on the displacement and displacement rate of the vehicle to achieve the final approach plane (Ehlers and Kraemer, 1977). The longitudinal axis has the speed brake deflection modulated to control dynamic pressure in order to achieve the required air speed (Ehlers and Kraemer, 1977). The US Shuttle Orbiter's elevons are then used to control altitude and glide slope (Ehlers and Kraemer, 1977).

TAEM utilises energy versus range functions where the guidance system attempts to track a nominal function based on a fixed mid-range speed brake position combined with a mid-range dynamic pressure value assuming no wind (Ehlers and Kraemer, 1977). Other energy versus range profiles are utilised to allow for implementation of the Phase 0 S-turns and repositioning of the HAC to the minimum entry point (Ehlers and Kraemer, 1977). There are four possible positions for the HAC depending on the energy state of the vehicle, the nominal value or the minimum entry point when the vehicle is at a low energy state, each with the HAC placed left or right of the runway centreline (Moore, 1991).

The US Shuttle TAEM guidance method, mentioned above and discussed in detail within Moore (1991) and Ehlers and Kraemer (1977), although well suited to the US Space Shuttle Orbiter requires extensive modification for application to other re-entry vehicles. Examples of this can be seen in the studies Naftel and Powell (1991); Powell (1993); Naftel and Powell (1993). Additionally the initial and final vehicle states are vehicle specific and required extensive analysis and study of the guidance system's performance in order to determine the appropriate state variables and their tolerances. The guidance system used was originally designed in the early 1970's. There have

however been significant advances in the modelling of vehicle dynamics and atmospheric disturbances in the past quarter of a century. These advances would allow for greater analysis of the sensitivities of TAEM guidance strategies and consequently a more robust and efficient guidance system.

Barton et al. (2002) points out that during the development of the US Space Shuttle guidance programs the engineers were limited by the memory and computational capacity of the computers at the time. Consequently modern RLVs which utilise some of the Shuttle's guidance techniques are limited by these old methods (Grubler, 2001). The US Shuttle Orbiter relies upon considerable pre-mission planning for the generation of ascent, descent, TAEM and landing guidance and control (Bordano et al., 1991). According to Bordano et al. (1991) a study conducted in 1988 for the Space Shuttle Liquid Rocket Booster (LRB) found that of the \$258.4 M cost per launch \$32.3 M is spent on Mission Operations Directorate (MOD) representing 12.5% of the overall cost. The MOD costs are directly related to staffing requirements for the development of the guidance system, including the 8 alternate guidance schemes required for varying weather conditions and several abort scenarios (Bordano et al., 1991). More specific information on the varying areas of development can be found in Bordano et al. (1991), although how much of the pre-mission cost is associated with the TAEM flight region is currently unavailable. Hanson et al. (1995) states that approximately 20% of each missions cost is due to mission design. However, Hanson et al. (1995) goes further than Bordano et al. (1991) by stating that it is not primarily due to the generation of trajectories but that most of the cost is related to the efforts required to verify the trajectories to ensure vehicle and crew safety.

If the redundant mission planning and design and the large staffing requirements could be reduced considerable, amounts of time and money could be saved. One possible method for achieving such saving would be by utilising an on-board trajectory propagation method. A reduction in the time to develop a mission profile and its implementation would significantly increase the number of achievable flights per year of a launch vehicle and consequently reduce the overall cost of each mission. The use of a robust on-board trajectory propagation method could reduce the launch and re-entry delays commonly experienced by the US Space Shuttle program (Bayle, 1984). These launch delays are traditionally attributed to poor weather conditions which could be

adapted for by on-board trajectory propagation (Bayle, 1984). In some cases the poor or changing weather conditions could be accounted for within a new trajectory propagation by taking into account the most current weather readings instead of the monthly averages used within most atmospheric models.

The US Shuttle Orbiter utilises an energy over weight profile as a function of range-to-go (Ehlers and Kraemer, 1977), due to the simplified geometric segments in the TAEM trajectory the ground track and range-to-go is easily calculable. However, this also imposes limitations on the TAEM trajectory (Grubler, 2001; Barton et al., 2002).

The Shuttle TAEM guidance always places the HAC at a fixed location downrange from the runway. Although there is currently the option to move the HAC it can only be repositioned to the minimum entry point (Grubler, 2001; Moore, 1991). Consequently there are limitations on the trajectory which do not allow for the optimal re-entry trajectory, fine tuning or adaptations to other styles of ground tracks (Barton et al., 2002). The HAC placement can also force the Shuttle to switch from low energy versus range to high energy versus range (Grubler, 2001). This can be problematic since during the HAC the Shuttle must be at subsonic speeds (low energy) in order to be able to follow the spiral. If however, the vehicle is at supersonic speeds (high energy) it will lack the manoeuvrability required to follow the spiral trajectory (Grubler, 2001; Barton et al., 2002).

During the acquisition phase (Phase 1) the constant bank acquisition to the HAC is modelled as a constant radius arc segment (Barton et al., 2002). Although this is valid for small angles of rotation it may not be valid for large gliding turns since the US Shuttle Orbiter will follow a ground track more representative of a spiral then a constant radius arc segment (Barton et al., 2002). This can be important in abort scenarios which may require large acquisition turns in order to return to launch site or in the selection and flight to an alternative landing site (Barton et al., 2002).

Perhaps the largest limitation of the Shuttle TAEM guidance is the decoupling of the longitudinal and lateral guidance. The longitudinal guidance utilises an energy profile where the wings are level in order to predict the ground track and range-to-go (Grubler, 2001; Barton et al., 2002). Consequently the range-to-go ignores the large effects that bank angle has on the vehicle's lift vector which can significantly alter the vehicle's energy and range (Grubler, 2001; Barton et al., 2002). Although the longitudi-

nal guidance does include a correction to account for the energy loss due to a non zero bank angle a better solution would be to combine the longitudinal and lateral guidance. The decoupling was most likely made to reduce computational effort and segment the problem for the multiple central digital computers on-board the US Shuttle Orbiter.

Summary of Shuttle deficiencies:

- No coupling between the longitudinal and lateral guidance;
- Use of fixed predetermined geometric shapes;
- Limited adjustability of trajectory generated prior to mission;
- Costly off-line trajectory generation;
- Limited adaptability for off-nominal conditions;
- Limited abort capability.

Despite these drawbacks the US Shuttle TAEM guidance method has performed well over all flights, consistently delivering the crew safely to the landing site. However, if the areas of deficiency could be removed or improved upon a more robust guidance method could be realised, allowing for improved reliability in the TAEM flight region. Additionally if on-board trajectory generation could be utilised there would be a significant cost saving in pre-mission planning. Another possible benefit of advanced terminal area guidance could provide for autonomous operation of unmanned re-entry vehicles.

2.3.3 Charles Stark Draper Laboratory Development

Barton et al. (2002) identified the deficiencies in the Shuttle TAEM guidance, as discussed in section 2.3.2, while a new method for generating TAEM trajectories was investigated. The new method, developed by Grubler (2001), from the Auto Landing I-load Program (ALIP) developed by Barton and Tragesser (1999) and AutoLanding I-load Program 3D (ALIP3D) developed by Girerd (2001), utilised non linear equations of motion in 3 degrees of freedom (3DOF). However, unlike previous trajectory propagators which used inertial velocity and time as the independent variables the method

of Grubler (2001) utilised altitude instead of time and dynamic pressure instead of inertial velocity. The equations of motion utilised for traditional trajectory propagation were retained but were reformulated in terms of the new independent variables. This procedure further developed by Barton (2001) known as Kernel Extraction Protocol (KEP) enabled the trajectory to be designed based on the desired characteristics, such as the dynamic pressure constraints. Subsequently the dynamics and control history required was then able to be extracted from the generated trajectory for online optimisation (Barton et al., 2002). The use of fixed altitude intervals allowed the boundary conditions to be accurately represented.

Barton et al. (2002) stated that by using the dynamic pressure as the main variable the iterations for the equations of motion were more robust since the dynamic pressure had a slower rate of variation than the variables traditionally used in trajectory propagation. Additionally it was convenient to use dynamic pressure because many of the vehicle trajectory constraints were directly related, such as the dynamic pressure limits and targeting conditions (Barton et al., 2002). Using the KEP equations of motion Grubler (2001) designed a trajectory generator that did not rely upon predetermined fixed geometric shapes a significant limitation of the US Space Shuttle Orbiter TAEM method.

The method developed called Sub-optimal Nodal Application of the Kernel Extraction (SNAKE) propagated trajectories through a three step process (Barton et al., 2002). Step 1 utilised a dynamic pressure schedule that satisfied the required range to reach the approach and landing target whilst maintaining the vehicle limitations (Barton et al., 2002). Thus for the various dynamic pressure levels below the vehicle limitations and above the maintainable flight envelope the available ground tracks ranges were produced.

Step 2 then formulated the required ground track for the vehicle, using the real time ground track solver (Grubler, 2001). The altitude steps were predetermined and as such allowed the exact number of nodes for the altitude to be known, which was implemented as the same number of nodes for the ground track. SNAKE calculated the turning capability of the vehicle for a given vehicle normal acceleration using a spiral ground track generated using a constant vehicle normal acceleration (Grubler, 2001). The spiral ground tracks allowed the generation of a look up table for heading angle

changes to be produced which allowed the maximum heading angle change between successive segments to be determined (Grubler, 2001). Additionally SNAKE was able to modify the ground track length depending on larger values of the bank angle which due to coupling required steeper flight path angles and shortened the ground track length (Barton et al., 2002).

Step 3 rapidly propagated a trajectory based on the the ground track and dynamic pressure schedules. The propagation utilised KEP and three nested loops with heuristic rules in order to achieve a balance between the equations of motion (Grubler, 2001).

Proto-SNAKE was a prototype rapid trajectory generator that used the SNAKE methods developed by Grubler (2001). The steps were performed as per the SNAKE methods, however for step 2 Proto-SNAKE used a forced steer to zero method in order to produce the ground track (Barton et al., 2002). The forcing scheme developed by Grubler (2001) utilised two phases, the first forced the trajectory to use the maximum allowable heading turn at each node until the cross range error was zero. However, this often results in overshooting the runway with regards to downrange, as shown in figure 2.2(a). Consequently the second phase forced the nodes to bend beyond the required cross range and subsequent nodes to bend back towards the zero cross range in order to reduce the downrange error to zero, as shown in figure 2.2(b) (Grubler, 2001).

The full derivations and development can be found in Grubler (2001) and Barton et al. (2002). Unfortunately because of the forcing nature, Proto-SNAKE did not recognise all possible paths and consequently the ground track produced was always of

Figure 2.2 – Steps of the Proto-SNAKE trajectory generator (Barton et al., 2002)

the same form and not necessarily the optimal solution (Grubler, 2001). Additionally there were ground track errors since any adjustment of the ground track through heading changes modified the flight path angle, but the ground track segment lengths were dependent on the flight path angle (Grubler, 2001). Grubler (2001) pointed out that the error in the ground track could be removed by the inclusion of a corrector which would remove the errors in flight path angle at each successive interval, in this case altitude steps. Unfortunately this was never implemented. Another possible problem with this method was that the maximum turning capability of the vehicle was always utilised. In case of off-nominal conditions there would be only limited ability to adjust the trajectory. It would be worthwhile to provide margins to the turning rates in order to ensure controllability as demonstrated by the sensitivity studies and results of sections 5.3, 6.1.2 and 6.2.3.

Demonstrations of Proto-SNAKE have revealed that despite the error in flight path angle and ground track the trajectory propagator was able to develop a trajectory that delivered the vehicle to the required approach and landing interface (ALI) point. Unfortunately only two thirds of the final positions in the study fell within the required tolerances for the ALI (Grubler, 2001). Grubler (2001) predicted that the use of a corrector would allow for significant improvement in the results. The fact that a majority of the trajectories were adequate solutions was proof that there is potential for further developments based on this method. Proto-SNAKE effectively removed the requirement for predetermined fixed geometric shapes as well as provided an on-board trajectory propagation scheme removing some of the significant limitations of the US Shuttle TAEM method.

There were a few other limitations to Proto-SNAKE. Grubler (2001) identified that there were discontinuities in the derivative of the density profile since it was a combination of three separate polynomials derived from the ATMOS4 density profile used by Orbital Sciences Corporation. This was a problem because the flight path angle was dependent on the density derivative with respect to altitude (Grubler, 2001). Additionally Grubler (2001) recommended that the density model should be smooth and discontinuous. However, the actual density profile flown by an atmospheric entry vehicle is rarely smooth, large density variations, such as those mentioned in section 3.2.1 could have a dramatic affect on Proto-SNAKE. The effects of density variations was

never investigated by Grubler (2001) and as such the extent of their affect on trajectory propagation can not be quantified. Consequently this suggests that a different modelling method or independent variable should be utilised to eliminate the need for a smooth density profile.

In the generation of the KEP equations of motion, Grubler (2001) identified that the guidance method could not cope with wind gusts. However, it could cope with steady head and tail winds. Grubler (2001) also stated that while variations in the size of the altitude steps were looked at no optimal altitude step size was investigated. Precision was increased by using more iterative points, decreasing the size of the altitude steps, though it was found that by having large step sizes the propagator could move past instabilities for the steepest trajectory used (Grubler, 2001). Thus a study would be required in order to quantify the requirements of the optimal altitude step before the step size could be investigated further.

Although the study undertaken by Grubler (2001) detailed the effects of some uncertainties on the entry corridor it did not include all the known common uncertainties. Grubler (2001) looked at the effect of density curve variations, continuous head and tail wind, aerodynamic coefficient errors and mass property errors. However, it did not clearly identify the influence of these on the terminal area trajectory rather than the entry corridor. Consequently studies are required to provide clear sensitivity studies on a variety of off-nominal conditions that have yet to be covered, such as constant directional winds, wind gusts, density variations and shears, varied atmospheric models, sensor errors as well as the aerodynamic coefficient errors and mass property errors covered by Grubler (2001). As with most other literature there is no definitive sensitivity study for the terminal area flight phase.

Grubler (2001) did develop a method for solving the ground track using optimisation techniques in MATLAB^{TM}however, this was time consuming due to the solver's slow convergence speed. As such this method was unsuitable for on-board trajectory propagation, one of the the key requirements of the study. Further study into a better optimisation method coupled with remodelled KEP equations of motion and an improved ground track would produce a fast efficient method for on-board trajectory generation.

2.3.4 Pre-Landing Maneuvering Stage

The Russian/Soviet Buran-Energia launch system shown to the right of the US Space Shuttle in figure 2.3 utilises a slightly different method to that of the US Space Shuttle TAEM method (Kirpischikov, 1997). There is little published data, especially in English, about the Buran guidance systems however, the paper Kirpischikov (1997) details the general concept. The flight phase was called the Pre-Landing Maneuvering Stage and similar to the US Shuttle TAEM method consisted of several sub-phases. The sub-phases used were different to that of the US Shuttle approach. The five sub-phases were:

- A spiral of turn-away;
- Spiral of corrective turn;
- Tangent to the Heading Adjustment Cylinder (HAC);
- Arc of HAC circle;
- Finishing straight line to the Key Point.

The overall Pre-Landing Maneuvering Stage is shown in figure 2.4. The Key Point was the ALI point of other terminal area guidance methods. The key difference to the Shuttle's TAEM is that the first two sub-phases form a S-turn which provides margins early within the trajectory to cope with off-nominal conditions and dispersion from the descent stage (hypersonic re-entry). Whereas the S-turn in the US Shuttle TAEM method was only invoked under high energy conditions.

The Pre-Landing Maneuvering Stage guided the Buran vehicle from an altitude of 20 km down to an altitude of 4 km. Excessive energy was dispersed by three methods:

- Change of trajectory with the help of turns;
- Change of dynamic pressure;
- Change of the lift-to-drag ratio.

The Buran method utilised the modifications to the trajectory in combination with programmed changes in the lift-to-drag ratio and dynamic pressure (Kirpischikov,

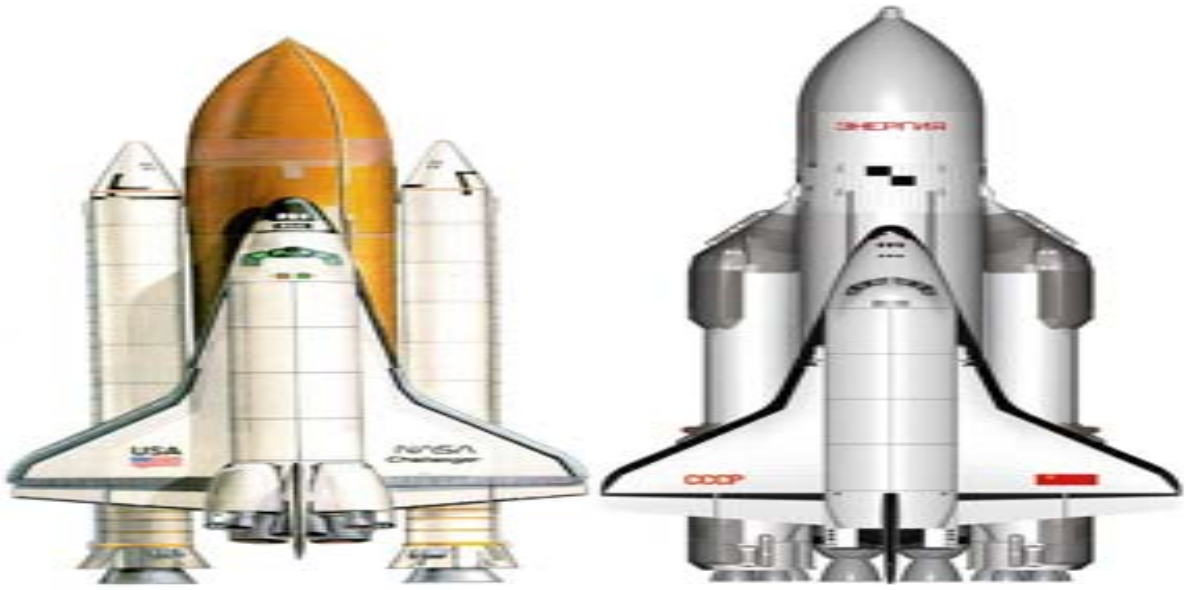

Figure 2.3 – Russian Buran-Energia launch system (right) in comparison to the US Space Shuttle system (left)

NOTE: This figure is included on page 26 of the print copy of the thesis held in the University of Adelaide Library.

Figure 2.4 – Buran Pre-Landing Maneuvering Stage (Kirpischikov, 1997)

1997). Four possible versions of reference trajectories were produced one for each of the different HAC placement points (Kirpischikov, 1997) as seen in figure 2.5. The four reference trajectories were then compared to determine the trajectory most suitable for the Buran vehicle's current energy state. If all reference trajectories had excessive energy then a turn way from the runway was performed (Kirpischikov, 1997).

Above Mach 0.8 the guidance and control algorithm stabilised the trajectory around the calculated 3D reference trajectory (Kirpischikov, 1997). Below Mach 0.8 the navigation was performed by stabilisation around the ground track for the horizontal plane nd terminal guidance in the vertical plane (Kirpischikov, 1997).

This method was very similar to the US Shuttle TAEM method and therefore had similar disadvantages, such as lack of adaptability to off-nominal conditions and no coupling between the longitudinal and lateral guidance. One advantage of this method was that the first two stages together represent an S-turn early in the trajectory which was an effective method of including margins for off-nominal conditions. The guidance ethod was also computationally efficient and could operate autonomously as observed in the successful first Buran mission on the 15th of November, 1988 (Abramov et al., 2003). Similar to the US Shuttle TAEM method significant improvement could be made to the Pre-Landing Maneuvering Stage through coupling of longitudinal and lateral dynamics and applying modern computing methods to the trajectory design and updates. Additional information on the Pre-Landing Maneuvering Stage could

NOTE: This figure is included on page 27 of the print copy of the thesis held in the University of Adelaide Library.

Figure 2.5 – Buran Pre-Landing Maneuvering Stage for different conditions (Kirpischikov, 1997)

also provide for more knowledge of the terminal area flight phase and identify areas for possible improvements.

2.3.5 EADS-ST Development

The Buran, Pre-Landing Maneuvering Stage method for terminal area guidance was further developed by the flight control team at European Aeronautic Defence and Space Company, Space Transportation (EADS-ST) (Vernis and Ferreira, 2005). The method utilised the Buran method combined with a trajectory planner that did not rely upon optimisation similar to the methods of Barton et al. (2002). The guidance scheme then tracked the reference profile with the horizontal and vertical controls decoupled (Vernis and Ferreira, 2005).

The trajectory planner utilised multiple sub-phases as given in figure 2.6. Theses sub-phases consisted of:

- Preliminary energy dissipation S-turn (only used when there is excessive energy);
- An acquisition S-turn to HAC intercept;
- HAC homing;
- HAC tracking.

The trajectory planner assumed the S-turn could be approximated by a spiral modelled by a polynomial. Four way points (P1,P2,P3 and P4) were then used to define the trajectory. P1 correspond to the TAEM entry point (TEP), P2 to the end of the S-turn, P3 to the end of the HAC homing and P4 to the end of HAC tracking (Vernis and Ferreira, 2005). The trajectory was planned by a four step process (Vernis and Ferreira, 2005):

- Placement of the S-turn at TEP according to velocity and heading conditions;
- Delta V stepping along the spiral until intercepting the HAC homing line;
- The kinematics of the waypoints P2, P3 and P4 were then calculated;
- If the conditions at P4 did not reach the required nominal entry point (NEP) a preliminary S-turn was added.

NOTE: This figure is included on page 29 of the print copy of the thesis held in the University of Adelaide Library.

Figure 2.6 – EADS-ST TAEM strategy (Vernis and Ferreira, 2005)

The guidance method utilised bank angle, angle of attack and speed brake control (Vernis and Ferreira, 2005). The method had a few assumptions including a flat earth model, equilibrium glide, no aerodynamic lateral force, isothermal atmospheric model and piecewise lift-to-drag profile (Vernis and Ferreira, 2005). The guidance method was applied to the Atmospheric Re-entry Experimental Spaceplane (ARES) vehicle (Vernis and Ferreira, 2005). The results showed that with various initial conditions the guidance was still able to achieve the required final conditions (Vernis and Ferreira, 2005). The trajectory design and guidance method were also tested in combination with a re-entry method previously tested, detailed in Vernis and Ferreira (2003) and was found to work effectively.

The advantages of this method were that it did not rely upon an optimisation method for trajectory planning which made it computationally efficient and applicable to real time operation. The trajectory planner also had been shown to be useful in backward propagation to determine suitable TEP locations, useful for pre-mission planning (Vernis and Ferreira, 2005) .

The disadvantages of this method were similar to those of the Shuttle since the method relied upon a HAC and decoupling of the horizontal and vertical control. These limitations made the guidance less adaptable than other methods that did not rely upon fixed HACs. There were also errors present in the trajectory design due to the decoupling of the horizontal and vertical controls however the guidance was

successful during simulations.

2.3.6 Previous Hopper Vehicle Developments

There has been some previous development work on trajectory design and guidance systems for the terminal area flight phase of the European sub-orbital Hopper concept vehicle. The methods were developed at Astrium a subsidiary of European Aeronautic Defence and Space Company (EADS) Space. Two different concepts were developed and preliminary testing was performed for a comparison. The first method detailed in Camara et al. (2002b) was a development of the US Shuttle TAEM guidance with notable simplifications and improvements. The second of the concepts was a development based on the work performed by Grubler (2001) and Barton et al. (2002) utilising some simplifications and improving on the trajectory planning method (Büchner, 2003).

The method detailed in Camara et al. (2002b) extended the basic method of the US Shuttle TEAM but attempted to make the method more flexible by reducing the number of phases and allowing the constrained geometric segments to become flexible. The method used three phases instead of the four utilised by the US Shuttle TAEM eliminating the auxiliary S-turn phase. The trajectory planner utilised four way points that could be repositioned for greater flexibility although in Camara et al. (2002b) only the initial way point was varied during simulations. Although there was the potential for considerable improvement and greater flexibility by varying the location of the other way points.

The method of Camara et al. (2002b) used the way points as a way to define and calculate the geometric segments of the trajectory. These geometric segments were then combined with the altitude, lateral and energy controller to generate the steering commands for angle of attack, bank angle and speed brake setting (Camara et al., 2002b). The commands were also passed through second order low pass filters to ensure that the vehicle was able to track the trajectory (Camara et al., 2002b). There were two separate altitude controllers; during supersonic flight the angle of attack command was obtained from the set of on-board profiles and during subsonic flight the angle of attack was calculated by converting the altitude, sink rate and vertical acceleration (da Costa, 2003).

The results from a 2100 simulation Monte Carlo run which involved variations of the initial vehicle states displayed impressive results (da Costa, 2003; Camara et al., 2002b). However, these results did not take into account the numerous other off-nominal conditions. Although based on the US Shuttle TAEM it remained to be seen how this improved method would cope with off-nominal conditions, such as winds and aerodynamic errors. In the review of the current status of development, da Costa (2003) identified that the modified US Shuttle TAEM did not make effective use of the complete ranging capabilities of the Hopper vehicle which was suggested to be related to the use of predefined geometric segments in this case related to the placement of the way points. However, further investigation into varying the way point locations could have improved the versatility of the method, but was not performed.

The second investigation detailed in Büchner (2003) utilised a method more closely related to that of Grubler (2001) although there were many notable differences between the two concepts the key ideas were similar. The similarities included the utilisation of maximum glide and dive boundaries and the generation of the trajectory ground track using the altitude as the independent parameter and investigating the effective turning rate limitations of the vehicles (Büchner, 2003). Unlike the method in Grubler (2001) the new method of Büchner (2003) did not translate the equations of motion in terms of dynamic pressure and solved some of the problems associated with the way that the ground track was determined.

Büchner (2003) utilised a separate method for determining the vertical profile and the ground track of the trajectory. Using a reference dynamic pressure versus altitude profile the limits of the dynamic pressure were determined by the maximum glide and dive trajectories similar to Grubler (2001). The altitude was utilised as the independent variable because it was made to be monotonically decreasing, this required the flight path angle to be within specified limits (Büchner, 2003). The trajectory was generated through a two step process involving the generation of the vertical profile first from which the required ground track profile could be generated with the necessary heading changes to reach the required target ALI point (Büchner, 2003).

To produce the vertical profile both the maximum dive and glide trajectories were determined in a similar manner to that of Grubler (2001). The maximum dive trajectory used the maximum dynamic pressure limit of the vehicle and the maximum

glide utilised the maximum lift-to-drag ratio in order to provide the greatest amount of range (Büchner, 2003). Using these two reference profiles the mean of the two was taken to provide significant trajectory margins and then a polynomial curve was fitted to provide a smooth profile (Büchner, 2003). Using the equations of motion the required angle of attack and flight path angle could be determined from the dynamic pressure profile. Although the vertical profile relating to the dynamic pressure did not consider the bank angle in the first step, the angle of attack and flight path angle were modified later to accommodate the changes in dynamic pressure caused by the changes of the bank angle (Büchner, 2003). The next stage was to design the ground track and required bank angle commands in order to align with the runway centreline. The major improvement over the method of Grubler (2001) was the development of the ground track. Several methods were investigated for the development of the ground track which included a shooting method similar to Grubler (2001), constrained optimisation of heading change with respect to altitude parameterised as a vector and optimisation using cubic polynomials (da Costa, 2003). The use of the cubic polynomials was found to be the best option as it provided the best results (da Costa, 2003).

The maximum turning rates of the vehicle were determined using constant bank angle turns in a similar method to Grubler (2001). A tabular form of maximum turning rate versus Mach number was then developed (Büchner, 2003). Cubic polynomials were generated for parameterising the turning rate with respect to altitude (Büchner, 2003). The linking of the polynomials had to be smooth enabling some simplification in the calculation of coefficients as several coefficients could be determined from others (Büchner, 2003). The problem was that due to the modelling, the constraints could not be directly applied to the polynomial coefficients as they had no direct relationship to the final position accuracy, turning rate and heading, resulting in an unconstrained optimisation of the ground track (Büchner, 2003). This was alleviated by including the constraints in the objective function (also known as a cost function) penalising the profile to ensure that the required corridor constraints were adhered too (Büchner, 2003). Monte Carlo simulations were performed including initial condition variations that showed good results.

The results for both of the developed guidance methods took into account initial condition dispersions and showed promising results (da Costa, 2005). However, both

methods required further verification and testing for the various other off-nominal conditions. Consequently neither of these two studies provided significant information for the sensitivity of trajectories in the terminal area flight phase. Further investigations into these methods could possibly provide an improved guidance scheme over the US Shuttle TAEM method. A comment provided in Büchner (2003) stated that the computational requirements for the program required significant reduction for implementation as an on-board guidance program. Therefore additional development work would be required in-order to make the on-board trajectory generation method viable for reusable launch vehicles. The simplified US Shuttle TAEM method of Camara et al. (2002b) also required additional development as the repositioning of the way points to other locations was not achieved. The repositioning of these way points would allow for an improvement over the US Shuttle TAEM as the ground track would not be constrained. However, the longitudinal and lateral coupling of the guidance would still be present in the method of Camara et al. (2002b).

2.3.7 Barron Associates Incorporated Development

An improved approach and landing guidance method previously presented in Schierman et al. (2001a,b, 2002, 2003, 2004a,c) was extended to the terminal area flight phase (Schierman et al., 2004b). The guidance method developed utilised an on-board adaptive guidance system based on trajectory command reshaping (Schierman et al., 2004b). The guidance method consisted of two main elements the guidance gain adaptation and online trajectory command reshaping. The guidance gain adaptation is an adaptive back stepping approach that delivers commands to the inner-loop which contains the reference model bandwidth utilised to schedule the outer-loop guidance gains (Schierman et al., 2004b). The guidance gain adaptation allowed the identification of anomalous events, such as a control effector failure (Schierman et al., 2004b).

The online trajectory command reshaping is known as the Optimum-Path-To-Go (OPTG) approach (Schierman et al., 2004b). The OPTG provided real time trajectory command reshaping for the vehicle with a regular interval of 1 Hz (Schierman et al., 2004b). The OPTG method consists of four steps, three of which are conducted off-line. The steps are:

1. Off-line trajectory optimisation formulation, which structures the optimisation for taking into consideration the mission segment, objective function, initial and final condition, critical parameters, constraints and the governing equations of motion (Schierman et al., 2004b). Critical parameters are those parameters that convey the vehicles performance, such as the upper and lower bounds of the lift and drag forces (Schierman et al., 2004b);

2. A database of neighbouring extremals was generated off-line via optimisation by successively varying critical parameters and initial conditions (Schierman et al., 2004b). Libraries were generated for the numerous trajectory results by repeating the optimisation for various downrange locations (Schierman et al., 2004b);

3. To enable online use a non linear function modelling tool was used off-line to generate polynomial neural networks (PNNs) that mapped the current vehicle states and critical parameters to basis coefficients describing the associated trajectory (Schierman et al., 2004b). The use of PNNs reduced the amount of data and allow efficient searching of the extremals;

4. The PNNs were then interrogated on-board with the current vehicle state and critical parameters used to compute the appropriate basis function (Schierman et al., 2004b). Disturbances and errors were taken into account by augmenting the PNNs with an on-line coefficient correction algorithm which ensured that the final conditions were met (Schierman et al., 2004b). The new trajectory commands were then calculated from the new basis function (Schierman et al., 2004b).

The extension of the OPTG method to the terminal area flight phase focused on the HAC turn of the traditional US Shuttle TAEM method (Schierman et al., 2004b). The method was evaluated for two different vehicles the X-34 and X-37. Each vehicle utilised a different method for optimisation. The X-34 vehicle utilised time as the independent variable with the cost function focused on minimising the vertical acceleration and consequently the normal acceleration of the vehicle (Schierman et al., 2004b). The cost function for the X-34 vehicle studies also included reducing the final condition errors. The optimisation formulation for the X-37 vehicle included the energy as the independent variable since it was monotonically decreasing and well defined for

the flight phase (Schierman et al., 2004b). The use of the energy as the independent variable eliminated the need for the final velocity constraint and the inclusion of the final time as a decision variable (Schierman et al., 2004b). The cost function for the X-37 vehicle trajectory similar to the X-34 vehicle also included the minimisation of the vertical acceleration (Schierman et al., 2004b). The cost function for the X-37 vehicle also minimised the dynamic pressure variations from the nominal profile as the baseline guidance tracked the desired dynamic pressure profile (Schierman et al., 2004b). The angle of attack and bank angle were utilised as the decision variables (Schierman et al., 2004b). The angle of attack and bank angle limits as well as the equations of motion were included within the constraints (Schierman et al., 2004b). A more detailed description of the two optimisation methods was provided in Schierman et al. (2004b).

The aerodynamic models of the two vehicles were incorporated into a set of PNNs with the lift and drag coefficients as a function of angle of attack and Mach number (Schierman et al., 2004b). The PNNs were utilised for trajectory base functions and aerodynamic models since they were thought to be faster than traditional table look up methods (Schierman et al., 2004b).

The results showed that the OPTG guidance method was effective for both vehicles during the HAC tracking portion of the terminal area flight phase. Although the results only covered a portion of the terminal area flight phase the methodology utilised provided promising results and could have possibly been extended to the rest of the terminal area flight phase.

Optimisation is generally too computationally intensive for on-line implementation but the PNNs provide an innovative solution. The use of the PNNs provide a fast and computationally efficient method for modifying the trajectories in real time based on optimised solutions. The PNNs used for the aerodynamic models was also inventive and could possibly provide gains in computational efficiency over tabular look up methods. The optimisation within the OPTG method combined the horizontal and vertical planes which eliminates a limitation of the US Shuttle TAEM method where decoupling of the longitudinal and lateral guidance was performed. The optimisation method for the trajectories also allows the placement and size of the HAC to be varied eliminating another limitation common to methods based on the US Shuttle TAEM methodology. Schierman et al. (2004b) states that high vehicle energy conditions re-

sulted in wider HAC turns and low vehicle energy conditions resulted in tighter HAC turns which corroborates results observed in the initial optimisation and analysis studies of this research (Chartres et al., 2005a).

There are disadvantages to utilising the OPTG method as numerous optimisations must be performed to form the basis functions for the PNNs which requires considerable pre-mission planning. The optimisation process could be implemented to operate automatically however presumably the trajectories must also be analysed for suitability and therefore would require a large amount of pre-mission effort, a disadvantage of the US Shuttle TAEM method. Solutions generated from the OPTG method under off-nominal conditions produced undesirable ground tracks, where the vehicle headed further away from the runway and then turned back. These trajectories were unsatisfactory since under the influence of off-nominal conditions, such as head or tail winds, it would be possible for the vehicle to be unable to achieve that required target conditions.

2.3.8 Rose-Hulman Institute of Technology Development

Methods for trajectory design and guidance have been developed using simplified vehicle dynamics combined with a fuzzy logic inference system (Burchett, 2004). The method was developed to allow for non discrete trajectories since fuzzy logic allows for a continuum of values for the various trajectory parameters (Burchett, 2004). Burchett (2004) utilised simplified vehicle dynamics and environmental models including an exponential density model for the atmosphere.

The fuzzy logic method allowed for the trajectory design to be performed by three distinct channels ground track, altitude and dynamic pressure. The adjustable trajectory parameters for the horizontal channel were the HAC turn radius and position from runway threshold (Burchett, 2004). The vertical channel reference trajectory used the initial and final conditions as constraints. The vertical path was defined as a polynomial intersecting at the ALI point with appropriate altitude and slope (Burchett, 2004). The polynomial was defined based on the flight path angle, distance from runway, required altitude and an adjustable parameter (Burchett, 2004). HAC position, radius and the adjustable parameter of the cubic polynomial were determined via a developed fuzzy logic inference system based on current energy state and health of control

surfaces (Burchett, 2004). According to Burchett (2004) the calculations were similar to those utilised for the US Shuttle TAEM method.

The fuzzy logic guidance system developed included three sub-phases based on the US Shuttle TAEM. The three sub-phases were acquisition, HAC turn and pre-final. For each of the sub-phases the relevant inputs were utilised to determine the bank angle commands (Burchett, 2004). During the acquisition phases the fuzzy inference system was effectively acting as a proportional controller directing the heading angle to the HAC centre (Burchett, 2004). The HAC turn sub-phase utilised the turn radius error, bearing to HAC centre and turn direction as inputs to the fuzzy inference system to determine the corresponding bank angle values to track the HAC (Burchett, 2004). For the pre-final sub-phase the relevant components for the vehicle position and velocity perpendicular to the runway centreline were used to determine the commands to align the vehicle with the centreline (Burchett, 2004). The bank angle commands were also computed with regards to the maximum available bank angle and smoothed by a first order unity gain low pass filter. The filter included a cut of frequency of 0.5 rad/s and also alleviated controller saturation (Burchett, 2004).

Another fuzzy logic system was used to determine the negative Z axis acceleration guidance commands. The fuzzy inference system for the negative Z axis acceleration commands used altitude error, vertical velocity errors, dynamic pressure and Mach number as inputs (Burchett, 2004). The fuzzy inference rules acted as a proportional-derivative controller aligning the vehicle with the correct glide path (Burchett, 2004). More details and a complete description of the fuzzy inference system is provided in Burchett (2004).

Both the trajectory design and guidance methods were developed for the X-33 vehicle and evaluated in the NASA Marshall Space Flight Centre simulation software Marshall Aerospace Vehicle Representation in C (MAVERiC). Results are presented in Burchett (2004) including cases for degraded control surfaces. Dispersions of the initial conditions were also included to determine the operating range of the fuzzy logic methods (Burchett, 2004). The results showed the effectiveness of this method but were not tested under a wider variety of off-nominal conditions, such as poor atmospheric conditions or aerodynamic coefficient errors.

The fuzzy logic method provided a continuous solution and that was not bound

by discrete parameter points that are used in other terminal area flight phase methods. Thus allowing the trajectory to be more adaptable and even to cope with control surface degradation which was simulated using reduced bank angle limits. Fuzzy logic was able to adapt the trajectory in real time utilising an operating frequency of 2 Hz (Burchett, 2004). The fuzzy logic system was developed to be adaptable to other reusable launch vehicles although it would require modifications and retuning to provide the best results.

Although the fuzzy logic terminal area flight phase methods for trajectory design and guidance were successful they still have some associated disadvantages. Fuzzy logic methods require considerable ground based analysis to train the networks and individual development for each mission which adds to mission costs. During development a large amount of trial and error was required to tune the fuzzy inference system (Burchett, 2004). The dynamics of this method were simplified assuming no induced drag which is capable of causing large errors in final conditions. The dynamics also assumed that the angle of attack was small. This was often not the case in trajectory design studies discussed in Chapter 5 as sometimes large angles of attack were required to increase vehicle drag. The guidance method decoupled the vertical and horizontal motion which could have caused errors although there was a correction factor for the bank angle it would be better to implement the two channels jointly.

2.3.9 University of Missouri-Columbia Development

Kluever and Horneman (2005) presented a guidance methodology for the terminal area flight phase based upon on-board reference trajectory generation. The method did not rely upon on-board pre-computed reference profile tracking like the US Shuttle TAEM method (Kluever and Horneman, 2005). The trajectories were however based on the US Shuttle TAEM method with similar sub-phases including acquisition, HAC and pre-final (Kluever and Horneman, 2005).

A reference trajectory was generated on-board using a trajectory planning method based on altitude profiles. The reference trajectory consisted of two altitude profiles with ground track range as the independent variable. The ground track segments were computed based on a set of parameters that defined the geometric segments. A detailed description of the ground track prediction was included in Kluever and Horne-

man (2005). Figure 2.7 displays a reference TAEM trajectory, the three sub-phases and intersection point using the on-board trajectory planner.

The two altitude profiles were quadratic polynomials, defined by a set of coefficients. The two quadratic profiles were created such that their point of intersection provides continuity in both the altitude and altitude rate with respect to range (Kluever and Horneman, 2005). The profiles also have defined points for initial and final conditions. These attributes allowed the determination of the coefficients to be simplified. The coefficients for the polynomials were found through geometric calculations and the manipulation of the equations of motion. The commands for bank angle and normal acceleration were determined from the designed reference trajectory. The full method for determining the quadratic altitude profile coefficients and command signals is provided in Kluever and Horneman (2005).

The trajectory planing method operated via a four step process: ground track prediction, propagation of the acquisition trajectory which was the first quadratic profile, propagating the second quadratic profile for the HAC turn and pre-final alignment and the final step was the selection of the most suitable reference path (Kluever and Horneman, 2005). The first quadratic was propagated using the vehicle energy divided by the weight with downrange as the independent variable, this was combined with an Euler integration scheme (Kluever and Horneman, 2005). The energy was used instead

Figure 2.7 – TAEM reference trajectory (Kluever and Horneman, 2005)

of velocity or dynamic pressure because it was monotonically decreasing and had an almost linear slope (Kluever and Horneman, 2005). The second quadratic was propagated in a similar manner except the downrange was propagated with the vehicle energy as the independent variable (Kluever and Horneman, 2005). Path constraints for final condition margins, dynamic pressure and vehicle loads were also included within the trajectory propagator.

The guidance method made use of the on-board trajectory planner by generating new reference trajectories for the current vehicle and environmental data (Kluever and Horneman, 2005). Potential ground tracks were determined by iterating a set of values for the three most influential parameters. The most influential parameters were those that determined the location and radius of the HAC. Several trajectories were propagated until a solution was provided that respected the constraints and met the final ALI requirements (Kluever and Horneman, 2005). When a flight path constraint was violated the propagation scheme was terminated and the next iteration was evaluated (Kluever and Horneman, 2005). Once the reference trajectories were obtained the optimal trajectory was determined by selecting the trajectory that maximised the dynamic pressure margins (Kluever and Horneman, 2005). The commands for bank angle and normal acceleration were then determined from the selected trajectory using both open and closed loop control (Kluever and Horneman, 2005). A more detailed explanation of scheme is provided in Kluever and Horneman (2005).

Kluever and Horneman (2005) also optimised the terminal area flight phase trajectories using inverse dynamics with the equations of motion rewritten with ground track distance as the independent variable. The flight path and azimuth were utilised as the optimisation parameters with discrete linear profiles equally spaced over ground track distance (Kluever and Horneman, 2005). The cost function attempted to minimise the difference in the flight path angle and azimuth values. A two stage approach was taken for the optimisation (Kluever and Horneman, 2005). The first stage was to perform optimisation without the final velocity or dynamic pressure constraints which satisfied the position constraints and eliminated the need for a vehicle model (Kluever and Horneman, 2005). The ground track was also attempted to be minimised by supplementing the cost function. The determined solution with the discrete linear profiles for flight path angle and azimuth were then used as an initial guess for further optimisation.

The second stage of optimisation removed the minimisation of the ground track from the cost function and included the final velocity and dynamic pressure constraints.

The results presented in Kluever and Horneman (2005) demonstrated that the trajectory planner and guidance worked effectively. The results so far have been promising with the new method successfully guiding the vehicle to the final conditions while respecting the constraints Kluever and Horneman (2005). The guidance was also evaluated under off-nominal conditions with the inclusion of initial state dispersions and drag deviations (Kluever and Horneman, 2005). However, the on-board guidance was assumed to have *perfect knowledge* of the drag variations which meant that only the ability of the trajectory planner to accommodate the drag variations was investigated. It would have been more interesting to see if the guidance could cope with the drag variations without any knowledge of the applied errors.

The trajectory design and guidance methods presented in Kluever and Horneman (2005) did not include a speed brake setting as has been utilised by almost all other terminal area flight phase methods. It would seem that the on-board trajectory design method of Kluever and Horneman (2005) provided additional margins to cope with off-nominal conditions without the need of a speed brake. Consequently additional margins could be provided by including a speed brake.

2.4 Other Guidance Methods

The next generation of launch and entry vehicles are intended to provide significant increases in mission success and safety whilst also decreasing costs. Advanced guidance and control methods have been highlighted as one possible area to investigate in order to achieve these goals (Hanson, 2002). Section 2.3 focused on the guidance methods that were directly related to the terminal area flight phase. There are however new developments in guidance methods for other flight phases that have yet to be applied to the terminal area flight phase which may provide some benefit. The most obvious methods are those new developments related to ascent and atmospheric re-entry of vehicles especially reusable launch vehicles. Possible extensions and modification of these methods might result in highly flexible and adaptable programs that are able to guide a vehicle through an entire mission including ascent, hypersonic entry, terminal

area flight and approach and landing phases.

2.4.1 Ascent Guidance

There has been continuous improvement and research into the field of guidance for launch vehicles, most has been conducted as part of the development programs for the Evolved Expendable Launch Vehicles (EELVs) and various reusable launch vehicles (RLVs). An overview and evaluation of several methods for the ascent of launch vehicles was provided in Hanson et al. (1995). The paper addressed whether advanced explicit guidance methods were better for the atmospheric portion of ascent than traditional implicit guidance methods. However, Hanson et al. (1995) also includes discussion of some of the various methods utilised for ascent guidance.

Skalecki and Martin (1993) utilised a guidance method of multiple shooting combined with non-linear programming to solve two point boundary value problems. Multiple shooting distributes the trajectory into multiple numerically integrated section (Skalecki and Martin, 1991). Each portion includes the state variables from the commencement of the next portion as the required final conditions. The states are numerically integrated to propagate them to the desired states (Skalecki and Martin, 1991). Where portions meet the actual states are compared to the expected states and then the states are reset for the next portion (Skalecki and Martin, 1991). The portioning of the trajectory allows for errors to be realised at the the intersection points instead of at the end of the trajectory where cumulative errors can result in large deviations (Skalecki and Martin, 1991). Skalecki and Martin (1991) state that multiple shooting includes more reliable convergence and reduced computational effort over singular shooting methods, such as that discussed in section 2.4.3. The reduced computational effort is achievable since each propagation of the states via integration only has to integrate over a portion of the trajectory instead of the entire trajectory as with singular shooting methods.

The multiple shooting guidance method of Skalecki and Martin (1993) was also applied to other mission phases such hypersonic entry and aerobraking (Skalecki and Martin, 1993). Therefore there is the possibility that it could be extended to the two point boundary value problem for the terminal area flight phase. The guidance was adaptive being able to cope with off-nominal conditions, such as atmospheric distur-

bance and mission profile changes including different payload masses (Skalecki and Martin, 1993).

Leung and Calise (1994) utilised a hybrid approach combining collocation with a analytical perturbation approach. The method allowed the large errors normally introduced by atmospheric effects when using the bilinear tangent law to be overcome (Leung and Calise, 1994). Consequently a single form of guidance, utilising the bilinear tangent law, is able to perform for the entire ascent flight from launch to precision orbit insertion (Leung and Calise, 1994). The analytic nature and application of the method was well suited to the ascent flight phase but would require considerable modification and reformulation to be applicable to the terminal area flight phase.

Although some methods of ascent guidance could possibly be applied to the terminal area flight phase they would require considerable reformulation or modification. Improved ascent guidance methods have been focused on overcoming launch delays traditionally caused by atmospheric disturbances. However these trajectories terminate at exoatmospheric altitudes where the influence of the atmosphere are minimal. The methods utilised for entry flight of vehicles are more likely to be modified or extended to encompass the terminal area flight phase than methods utilised for ascent.

2.4.2 Re-entry Guidance

Considerable effort and research was recently conducted in the US on improved entry guidance methods . A summary and evaluation of some of the improved entry guidance methods was conducted at NASA Marshall Space Flight Center and presented in Hanson and Jones (2004). Entry methods utilise similar vehicle dynamics and control signals as those of the terminal area flight phase. Although most of the improved methods for entry flight have been developed with only the hypersonic re-entry flight phase in mind attributes or entire methods, could possibly be extended to the terminal area flight phase.

Dukeman (2002) utilised a trajectory tracking entry guidance method with feedback gains for the linear control law generated off-line using Linear Quadratic Regulator (LQR) theory. The reference trajectory profile consisted of reference states and control as a function of energy (Dukeman, 2002). The reference states included range-to-go, altitude and flight path angle (Dukeman, 2002). The reference controls were angle of

attack and bank angle (Dukeman, 2002). The lateral guidance utilised a similar method for bank reversal as the US Shuttle method discussed in Harpold and Graves (1979). The longitudinal guidance utilised profile tracking of a pre-determined reference trajectory (Dukeman, 2002). Dukeman (2002) does state that the method was not expected to be as robust as methods which utilise on-board trajectory re-generation. However, it was stated that the reference trajectory tracking could be combined with an on-board trajectory planner which would reduce the possibility that the loaded reference profiles are unsuitable for the current conditions (Dukeman, 2002).

Another method developed at NASA Marshall Space Flight Center was presented in Zimmerman et al. (2003). The method called Eguide was a numerical predictor-corrector guidance method that used numerical integration and a Newtonian method to determine trajectories on-board (Zimmerman et al., 2003). Eguide consisted of two separate parts, the first for controlling the vehicle during the heating phase of entry and the second part when the heat rate control is no longer necessary (Zimmerman et al., 2003). The first phase manipulates the aerodynamic lift and maintains a constant heat rate governed by an analytical bank angle control law (Zimmerman et al., 2003). The second phase used trajectory control to meet the TAEM interface requirements (Zimmerman et al., 2003). The angle of attack profile was predetermined (Zimmerman et al., 2003). Reference heat rate, initial bank angle, bank-angle rate and the time to switch between the parts were all chosen as parameters to define the trajectory (Hanson and Jones, 2004). The trajectory solution was continually resolved on-board to correct for errors and dispersions (Zimmerman et al., 2003). The trajectories were then tracked using the LQR guidance methodology of Dukeman (2002). The use of predictor-corrector methodologies seems to be favoured by many of the improved guidance methods detailed in this chapter highlighting the advantages of explicit guidance over implicit methods.

An improved method of the acceleration guidance previously used for the Apollo and US Shuttle vehicles during re-entry has been under development at the Flight Dynamics and Control Laboratory of the University of California, Irvine (Mease et al., 2004). The method named Evolved Acceleration Guidance Logic for Entry (EAGLE) extends the longitudinal entry guidance of the US Shuttle to include the lateral guidance (Saraf et al., 2004). The guidance method consist of two parts the first a trajectory plan-

ner and the second a trajectory tracking law (Saraf et al., 2004). The trajectory planner generated reference profiles for drag and lateral accelerations that provided commands for angle of attack and bank angle (Mease et al., 2002). A feedback linearization based non-linear controllers tracked the reference profiles (Leavitt et al., 2002). The results presented in Saraf et al. (2004) provided a very detailed analysis of the effectiveness of the EAGLE method under a variety of off-nominal conditions.

The phenomenon known as quasi equilibrium glide combined with a predictor corrector methodology was utilised by Shen and Lu (2004) and Lu (1999) for entry guidance. Quasi equilibrium glide assumes a shallow and nearly constant flight path angle combined with bank angle modifications (Shen and Lu, 2003). The entry trajectory problem was decomposed into two sequential one-parameter search problems (Shen and Lu, 2003). The three dimensional trajectory takes into account the lateral and longitudinal motion of the vehicle (Shen and Lu, 2004). The results using the quasi equilibrium glide method proved promising and revealed the methods ability to adapt to a variety of off-nominal conditions (Shen and Lu, 2004).

The advances in the various entry guidance methods, discussed in this section, reveal that improved methods are favouring the utilisation of on-board trajectory regeneration to adapt to errors and off-nominal conditions. There are two methods to achieve this the first is to use a reference trajectory that is stored on-board and then updated and the second is to use an on-board trajectory planner. Explicit guidance is more suited to adapting the trajectory in real time to initial condition dispersions and off-nominal conditions, combined with greater computational capacity of on-board computers these methods are providing significant improvements over traditional reference profile tracking methods.

2.4.3 IRS Programs

The trajectory design, optimisation and guidance studies conducted in this research are an evolution of the methods developed at the Institut für Raumfahrtsysteme (IRS), Universität Stuttgart. The optimisation and guidance programs utilise non linear programming techniques combined with steering command parameterisation to generate and evaluate trajectories. The optimisation program makes use of the optimisation routine NLPQL from the International Mathematics Standards Library (IMSL) and the

guidance program makes use of an accelerated Gradient Projection Algorithm (GPA). A detailed description of the optimisation and guidance programs is provided in Chapter 3 including the problem formulation and methods utilised to solve the problem.

The IRS programs throughout their development have been successfully applied to a variety of ascent and re-entry missions for a variety of vehicles. The programs were originally developed for re-entry capsules including the Concept of a Lifting Body for Re-entry Investigations (COLIBRI) capsule (Schöttle et al., 1997; Burkhardt, 2001). The IRS programs have previously been used in comparison to obtained flight data for verification of models with the Micro Re-entry Capsule (MIRKA) (Tetlow et al., 1999). The optimisation and guidance programs have also been applied to re-entry vehicles, such as the recently cancelled X-38 crew return vehicle, where the programs was utilised for the hypersonic re-entry flight phase (Burkhardt et al., 1999; Gräßlin et al., 2002, 2003). There have also been studies performed for a conceptual fly back booster and ascent missions (Tetlow et al., 2001, 2005).

The most recent development has been the application to the sub-orbital Hopper concept vehicle. The guidance program was further developed to be used for both the ascent and re-entry phases of the mission (Gräßlin et al., 2003; Telaar, 2005). A recent study showed that the guidance program (with some modifications) could be successfully applied to the ascent abort flight phase (Schwientek, 2004; Schwientek and Telaar, 2004). These result showed encouragement that the guidance program could be extended to the terminal flight area phase which has similarities with the ascent abort flight phase.

The advantages of the IRS programs are that they do not rely upon predefined geometric segments and combine the longitudinal and lateral guidance for a more accurate solution. These characteristics effectively eliminated two of the most prominent disadvantages of the US Shuttle TAEM method. The IRS programs are also well suited to on-board implementation as discussed in Wallner et al. (2002). However, the IRS programs require considerable computational effort and therefore flight computers with adequate computational speeds, similar to current generation desktop computers, would be required.

Another disadvantage of the methods used in the IRS programs are that there is no guarantee that the solution will converge with the restoration steps. However, Hanson

and Jones (2004) states that the risk of convergence can be reduced by storing a nominal trajectory which is used as long as conditions do not require a new trajectory. In the case of the IRS guidance program the stored reference trajectory is always available on-board.

2.5 Discussion of Literature

A direct comparison of previous trajectory design and guidance methods for the terminal area flight phase discussed in section 2.3 is difficult. The difficulties arise from the limited amount of published data on some methods, such as the Russian/Soviet Buran-Energia launch system. Other difficulties occur because there has been no effective comparative study of the methods utilising the same simulation environment and vehicle models. Many of the methods discussed in section 2.3 include various restrictions on the trajectories related to the different vehicle types and mission profiles.

The greatest problem in a comparison of the various methods is due to their self imposed limitations, such as the inclusion of a HAC or redefinition of the flight dynamics during problem formulation, which produces a certain type of trajectory, as was seen with the Proto-SNAKE method discussed in section 2.3.3. Compounding the issue is the lack of published results and detailed studies for each of the methods, which could possibly reveal the suitability of one method over another.

A general comparison of the various methods reveal that each has its own advantages and disadvantages. The methods developed after the US Shuttle TAEM method identify the trajectory design and guidance methods as a possible way of increasing mission flexibility and safety whilst also reducing costs. A majority of the methods utilised monotonically increasing or decreasing functions in defining the steering command or trajectory profiles as they were determined to be the most suitable. Many of the methods attempted to improve the guidance results by utilising explicit guidance to either reshape the reference trajectory and/or update the steering commands.

Methods derived from the US Shuttle TAEM or Buran Pre-Landing Maneuvering Stage guidance inherited some of their limitations, although improvements were made in flexibility of the trajectories some limitations, such as the decoupling of the longitudinal and lateral guidance channels still remained. Methods such as those discussed

in sections 2.3.5 and 2.3.6 included correction factors to mitigate against introduced errors. These methods provided promising results. It is unclear whether these correction factors were entirely effective or provided a benefit due to the reduced computational time in comparison to methods, such as those in sections 2.3.3 and 2.3.7 where the longitudinal and lateral guidance channels were coupled. The in-ability to provide a comparison is again due to the lack of published results providing detailed analyse of these methods.

The fuzzy logic method, discussed in 2.3.7, was utilised for storing large amounts of data including previously optimised trajectories and vehicle aerodynamics. The fuzzy logic method provided an innovative solution to the high computational requirements normally associated with on-board table look up interrogation. However, the generation of numerous trajectories to account for all conceivable off-nominal conditions would require considerable pre-mission planning and analysis and therefore a high associated cost. Similarly the use of a fuzzy inference system for guidance, discussed in 2.3.8, required considerable off-line training and trial and error experimentation to tune the system for an accurate response to off-nominal conditions.

The way point method of Camara et al. (2002b) provided promising results. However, the ability to reposition the way points was never fully investigated or demonstrated with only the initial position being modified. More advanced methods such as those of Grubler (2001), Büchner (2003) and Kluever and Horneman (2005) provided more promising results. These methods perform on-line trajectory reshaping in order to cope with off-nominal conditions.

The methods of Grubler (2001) and Büchner (2003) are similar both rely upon trajectory reshaping utilising information provided from maximum dive and glide trajectories combined with turning rates from constant bank angle turns. The limitations and problems associated with the Proto-SNAKE trajectory planner indicated that a trajectory generation method based on SNAKE required more investigation and utilisation of a non forcing method. Büchner (2003) developed an improved method that removed some of the limitations of the Proto-SNAKE trajectory planner. However, Büchner (2003) stated that the computational requirement was still the most important issue to work on since it was too high for on-board implementation.

Kluever and Horneman (2005) presented a trajectory reshaping method that used

a select few parameters to reshape the geometric segments of the trajectories. Since the method only relied upon a few select parameters to define the trajectory profile the computational load was suitable for on-board implementation. Initial results proved promising but they did not provide a detailed analysis of the methods suitability under a wide variety of off-nominal conditions.

The majority of methods discussed in this chapter were developed for a single type of vehicle and the associated mission, such as those methods discussed in sections 2.3.2, 2.3.3 and 2.3.8. Considerable modification and development would be required to make the methods suitable to other vehicle and mission types. However, some methods, such as those discussed in section 2.4.3 and 2.3.7, were able to be adapted to other vehicles and missions with minimal modifications. These methods provide a significant advantage as they reduce development time and complexity therefore reducing overall system costs.

The use of steering commands to define trajectories has been shown to provide significant benefit as the trajectories are adaptable to off-nominal conditions and do not rely upon achieving fixed way points or trajectory shapes. Additionally the use of the steering commands removes the need to determine the steering command profiles from other types of profiles such as vehicle accelerations or dynamic pressure used in reference trajectory tracking methods.

The study of Telaar (2005) utilised the IRS programs for the ascent and re-entry phases as the use of the same guidance program for multiple phases of the mission could provide greater flexibility, reduce complexity and reduce system costs. By utilising a single on-board guidance concept different guidance programs would not be required for the different mission phases, as has traditionally been required. This would reduce the overall system complexity and cost.

Although this research focused on improving trajectory design and guidance methods and providing detailed sensitivity analysis of the terminal area flight phase these were not the initial primary aims of the research. Initially the research was focused on determining the suitability of extending the optimisation and guidance programs discussed in section 2.4.3 and Chapter 3 to the terminal area flight phase. This research revealed that the methods were well suited to the terminal area flight phase (Chartres et al., 2005b,a). Therefore the focus switched from proving the suitability to further de-

veloping the methods and performing detailed evaluations of the methods combined with investigations of the terminal area flight phase.

A clear outcome from the literature reviewed in this Chapter indicates that there have been numerous publications discussing trajectory design and guidance methods for the terminal area flight phase. However within these publication there is a lack of published data on the sensitivities of the terminal area flight phase. Additionally there is a lack of published data on detailed evaluations of improved and new methods for both trajectory design and guidance. The studies of section 2.3 rarely provided a detailed analysis of a large amount of off-nominal conditions or significant simulation verification with a variety of these off-nominal conditions. The majority of the studies include an explanation of the methodologies but present only limited results. Additionally of the results presented they generally only include a limited number of applied error which is insufficient to provide a detailed evaluation.

There are several possible reasons for the lack of published data on the terminal area flight phase sensitivities and evaluation of improved and new trajectory design and guidance methods. Most of these studies were published in conference or scientific journal papers where size restrictions limit the amount of information able to be presented. However, investigation into larger documents such as technical reports and theses revealed that in many cases larger more thorough evaluations were not performed. A possible reasons for this is that most of the studies were also conducted under funding contracts for proposed concept vehicle programs, such as the X-33 vehicle, where once the funding was exhausted or the program stopped further study was not possible. Other programs did not allow for publications due to either lack of funding or timing constraints this was the case with X-33 vehicle TAEM investigations conducted at NASA Marshall Space Flight Centre (Dukeman, 2004).

Many different models were utilised in the studies of these chapters for the vehicle and environment models. The use of higher order models was generally only used for simulation environments and the low order or simplified models and dynamics were used for on-board calculations due to the computational efficiency. Some studies of the terminal area flight phase however used low order or simplified models for the simulation environments to initially prove the concept of the methodologies. Whereas comparative studies of ascent and re-entry methodologies, such as Hanson et al. (1995) and

Hanson and Jones (2004), utilised higher order models. Therefore this study adopted high order models for the simulation environment as the results and methods could be better integrated with the results and methods of other re-entry studies.

2.6 Conclusions From Literature

The improved and emerging methods presented in section 2.3 provide numerous possibilities for further research to achieve advanced trajectory design and guidance methods. However, a primary motivation of this research, also mentioned in section 1.1, is to further develop the optimisation and guidance methods of section 2.4.3. Some previous work conducted on the optimisation and guidance programs has been applied to abort and booster fly back of reusable launch vehicles, namely the studies of Schwientek (2004), Schwientek and Telaar (2004), Tetlow et al. (2005) and Telaar (2005). However, trajectory design and guidance for the terminal area flight phase has never been performed using the steering command parameterisation method investigated within this research. Therefore the method utilised within this research would provide another innovative method different to those presented in section 2.3.

The other methods of section 2.3 provided promising results but most had inherent limitations due to either inheritance for the US Shuttle method, problem reformulation or large amount of user interaction, such as the training of fuzzy inference systems and neural networks presented in sections 2.3.8 and 2.3.7 respectively. The online trajectory reshaping methods provided the most promising results for the terminal area flight phase as they were able to adapt to a variety of off-nominal conditions by modifying the reference trajectory.

The outcome from the literature discussed throughout this chapter has revealed that:

- There is currently a lack of detailed analysis of the terminal area flight phase including the major influences and sensitivities to off-nominal conditions;
- Improved methods of trajectory planning and guidance for launch and entry vehicles could provide significant improvements in reliability, mission flexibility and safety whilst also reducing costs;

- There has been some focus on advanced methods for guidance of lifting entry vehicles for the terminal area flight phase however these methods have not been sufficiently evaluated under a large variety of off-nominal conditions;
- Methods based on US Shuttle TAEM or Russian Buran Pre-Landing Maneuvering Stage methodologies tend to inherit some of their limitations;
- Many of the studies were developed for a singular launch or entry vehicle and would require considerable modification to make them suitable for other vehicles and their associated missions;
- Explicit guidance is better suited to the terminal area flight phase since it is adaptable and able to cope with off-nominal conditions;
- The current generation of computers makes it possible to perform online trajectory planning for guidance, however online trajectory optimisation is still too computationally intensive;
- The use of a single method or program for trajectory planning and or guidance over the entire mission could provide greater flexibility and reduce system development, complexity and costs;
- Most studies utilise Monte Carlo testing to evaluate guidance performance as it allows the inclusion of a wide variety and combination of off-nominal conditions.

The research presented within this thesis attempts to address the identified current gaps in literature with several aims that are provided in section 2.7. This research also tried to combine the good traits and aims of the research from section 2.3 with the programs developed at the Institut für Raumfahrtsysteme (Institute for Space Systems), Universität Stuttgart.

2.7 Research Aims

The research conducted within this study was focused on extending the trajectory design and guidance methods discussed in section 2.4.3 and detailed in Chapter 3 to the terminal area flight phase. The primary aims of this research to address current gaps in literature were to:

- Develop and evaluate the effectiveness of a trajectory design method for the terminal area flight phase utilising a non-linear optimisation with parameterisation by steering commands;
- Develop and evaluate a real time guidance method for reusable launch vehicle during the terminal area flight phase utilising the restoration steps of an accelerated gradient projection algorithm;
- Demonstrate the adaptability and flexibility of the trajectory design and guidance methods based on steering command parameterisation for general reusable launch vehicles;
- Evaluate the trajectory design and guidance methods against various off-nominal conditions;
- Provide a detailed sensitivity of the terminal area flight phase determining the influence of off-nominal conditions on trajectory design and guidance capabilities;
- Provide detailed research on the terminal area flight phase to assist in the development programs of future reusable launch vehicles, fly back boosters and lifting entry vehicles;
- Provide a comparison of the developed trajectory design and guidance methods against published data and other methods where possible.

Chapter 3

Methodology

The eternal mystery of the world is it's comprehensibility.

Albert Einstein (1879-1955)
Theoretical Physicist

THE following chapter discusses the optimisation and guidance programs including the mathematical formulation, models, off-nominal conditions (applied errors) and assumptions. Additionally the key aspects and developments made to the programs to make them applicable to the terminal area flight phase are presented.

3.1 Problem Formulation

The problem is formulated in the optimisation and guidance programs using non linear programming (NLP) techniques. For the optimisation program the problem is solved using the sequential quadratic programming algorithm NLPQL method contained within the International Mathematics Standard Library (IMSL) (Schittkowski, 1985/1986). For the guidance program an accelerated Gradient Projection Algorithm (GPA) was utilised to provide trajectory updates (Speyer et al., 1971). The flight path optimisation problem was defined to find the control history $\vec{u}(t)$ which would deliver the vehicle from the given initial state $\vec{x}(t_0)$ to the required final state $\vec{x}(t_f)$ such that a cost function F is minimised. The mathematical problem was parameterised to find the set of parameters $\vec{p}$ that minimise the cost function.

$$\min \; F(\vec{p}) \tag{3.1}$$

With final (equality) and in-flight (inequality) constraints given by equations 3.2 and 3.3 respectively.

$$g_i(\vec{p}) = 0, \quad i = 1, \ldots, m_e \tag{3.2}$$

$$g_j(\vec{p}) \leqslant 0, \quad j = m_e + 1, \ldots, m \tag{3.3}$$

Subject to the differential constraints given by equation 3.4.

$$\dot{\vec{x}} = f(\vec{x}(t), \vec{u}(t)) \tag{3.4}$$

Which were the equations of motion in three degrees of freedom given in section 3.1.1, solved by numerical integration of the given initial state by a fourth order Runge-Kutta method. The parameters each have an upper, $p_{i,u}$, and lower, $p_{i,l}$, bound as defined in equation 3.5.

$$p_{i,l} \leqslant p_i \leqslant p_{i,u} \tag{3.5}$$

The state vector $\vec{x}$ of the vehicle is given by equation 3.6.

$$\vec{x} = [r, \lambda, \delta, v, \gamma, \chi, M]^T \tag{3.6}$$

Where r is the distance from the centre of the earth, λ and δ the longitude and latitude respectively, v the vehicle's velocity, γ the flight path angle, χ the azimuth or heading and M the vehicle mass. The mass does not vary during the flight since it is assumed that no propellant is utilised for the terminal area flight phase of the Hopper and X-33 vehicles. The mass is included however because the vehicle mass variations are later investigated during sensitivity and guidance evaluation studies.

3.1.1 Equations of Motion

The equations of motion for a rotating spherical earth are used within this study. The equations of motion are provided in equations 3.7, 3.8, 3.9, 3.10, 3.11 and 3.12.

$$\dot{v} = \frac{F_x}{M} + r \cdot \omega_E^2 \cdot \cos^2\delta\,(\sin\gamma - \cos\chi \cdot \tan\delta \cdot \cos\gamma) \tag{3.7}$$

$$\begin{aligned}\dot{\gamma} &= \frac{F_y}{M \cdot v} + \frac{r}{v} \cdot \omega_E^2 \cdot \cos^2\delta\,(\cos\gamma + \cos\chi \cdot \tan\delta) \\ &\quad +2 \cdot \omega_E \cdot \cos\delta \cdot \sin\chi + \frac{v}{r}\cos\gamma\end{aligned} \tag{3.8}$$

$$\begin{aligned}\dot{\chi} &= \frac{F_z}{M \cdot v \cdot \cos\gamma} + \frac{r \cdot \omega_E^2}{v \cdot \cos\gamma} \cdot \cos\delta \cdot \sin\delta \cdot \sin\chi \\ &\quad -2 \cdot \omega_E \cdot \cos\delta\,(\cos\chi \cdot \tan\gamma - \tan\delta) + \frac{v}{r}\sin\chi \cdot \tan\delta \cdot \cos\gamma\end{aligned} \tag{3.9}$$

$$\dot{r} = v \cdot \sin\gamma \tag{3.10}$$

$$\dot{\lambda} = \frac{v \cdot \cos\gamma \cdot \sin\chi}{r \cdot \cos\delta} \tag{3.11}$$

$$\dot{\delta} = \frac{v}{r} \cdot \cos\gamma \cdot \cos\chi \tag{3.12}$$

The gravitational force vector in the horizontal reference frame is given by equation 3.13. The calculation of the vector elements are given in section 3.2.2.

$$\vec{G} = \begin{bmatrix} G_r \\ G_\lambda \\ G_\delta \end{bmatrix} = M \cdot \vec{g} = M \cdot \begin{bmatrix} g_r \\ g_\lambda \\ g_\delta \end{bmatrix} \tag{3.13}$$

The overall force vector in the velocity system is then given by equation 3.14

$$\begin{aligned}\vec{F} &= \begin{bmatrix} F_x \\ F_y \\ F_z \end{bmatrix} \\ &= \begin{bmatrix} T \cdot \cos(\alpha + \vartheta) - D - G_r \cdot \sin\gamma + G_\lambda \cdot \cos\gamma \cdot \sin\chi \\ \qquad\qquad +G_\delta \cdot \cos\gamma\cos\chi \\ (T \cdot \sin(\alpha + \vartheta) + L) \cdot \cos\mu - G_r \cdot \cos\gamma - G_\lambda \cdot \sin\gamma \cdot \sin\chi \\ \qquad\qquad -G_\delta \cdot \sin\gamma \cdot \cos\chi \\ (T \cdot \sin(\alpha + \vartheta) + L) \cdot \sin\mu + G_{lambda} \cdot \cos\chi - G_\delta \cdot \sin\chi \end{bmatrix}\end{aligned} \tag{3.14}$$

Equation 3.14 can be simplified since from equation 3.47, $g_\lambda = 0$ and since there is no thrust during the terminal flight phase $T = 0$ giving equation 3.15. A more detailed discussion of the equations of motions used within the optimisation and guidance programs is discussed in Burkhardt (2000).

$$\vec{F} = \begin{bmatrix} F_x \\ F_y \\ F_z \end{bmatrix} = \begin{bmatrix} -D - G_r \cdot \sin\gamma + G_\delta \cdot \cos\gamma \cos\chi \\ L \cdot \cos\mu - G_r \cdot \cos\gamma - G_\delta \cdot \sin\gamma \cdot \cos\chi \\ L \cdot \sin\mu - G_\delta \cdot \sin\chi \end{bmatrix} \tag{3.15}$$

3.1.2 NLPQL Subroutine

The optimisation program solves this problem using the FORTRAN NLPQL subroutine contained within the international mathematics standard library (IMSL). Although there is considerable literature for this routine (Schittkowski, 1983, 1985/1986; Schittkowski and Zillober, 2001; Schittkowski, 2003, 2004) it is utilised essentially as a black box for this application, passing the required inputs to the routine. However it is important to present the basic methodology used. The basic concept of the NLPQL outlined here is taken from Schittkowski (1983, 1985/1986); Schittkowski and Zillober (2001); Schittkowski (2003, 2004) where a more detailed description is provided.

The NLPQL routine is a Sequential Quadratic Programming (SQP) method since it generates and successively solves a sequence of quadratic programming sub-problems (Schittkowski, 1985/1986). The non-linear problem presented in section 3.1 is converted to the quadratic sub-problem given by equations 3.16, 3.17 and 3.18.

$$\min \frac{1}{2} d^T \cdot B_k \cdot d + \Delta f(x_k)^T \cdot d \tag{3.16}$$

$$\Delta g_i \cdot (x_k)^T \cdot d + g_i \cdot (x_k) = 0, \quad i = 1, \ldots, m_e \tag{3.17}$$

$$\Delta g_j \cdot (x_k)^T \cdot d + g_j \cdot (x_k) \geqslant 0, \quad j = m_e, \ldots, m \tag{3.18}$$

Where x_k is the k-th estimate for the optimal solution and B_k is a symmetric matrix that approximates the Hessian of the Lagrange function given in equation 3.19. The next iteration is given by equation 3.20 where d_k denotes the k-th solution of equations 3.16, 3.17 and 3.18 and α_k is a step length parameter such that $\alpha_k \in (0, 1]$.

$$L(x,u) = f(x) - \sum_{i=1}^{m} u_i \cdot g_i(x) \tag{3.19}$$

$$x_{k+1} = x_k + \alpha_k \cdot d_k \tag{3.20}$$

The problem can also be redefined as given in equations 3.21, 3.22 and 3.23 which prevents the evaluation of the gradient for the constraints that are inactive. The definition of equations 3.21, 3.22 and 3.23 provides a more efficient program, with J_k^* the set of active constraints including equality constraints and K_k^* is the set of inactive constraints. Where $J_k^* \cup K_k^* = \{1,\dots,m\}$ and a constraint is consider active if the function value is not positive or the corresponding multiplier is greater than zero.

$$\min \ \frac{1}{2} d^T \cdot B_k \cdot d + \Delta f(x_k)^T \cdot d \tag{3.21}$$

$$\Delta g_i \cdot (x_k)^T \cdot d + g_i \cdot (x_k) \left\{ \begin{array}{c} = \\ \geqslant \end{array} \right\} 0, \quad i \in J_k^* \tag{3.22}$$

$$\Delta g_j \cdot (x_k)^T \cdot d + g_j \cdot (x_k) \geqslant 0, \quad j \in K_k^* \tag{3.23}$$

However it is possible that the linear constraints of equation sets 3.16, 3.17, 3.18 and 3.21, 3.22, 3.23 can become inconsistent. Therefore an additional variable ξ, such that $0 \leqslant \xi \leqslant 1$ is introduced to create an $(n+1)$-dimensional sub-problem with consistent constraints resulting in the equations 3.24, 3.25 and 3.26. Equations 3.24, 3.25 and 3.26 have a finite unique solution provided B_k is a positive definite matrix.

$$\min \ \frac{1}{2} d^T \cdot B_k \cdot d + \Delta f(x_k)^T \cdot d + \frac{1}{2} \psi_k \cdot \xi^2 \tag{3.24}$$

$$\Delta g_i \cdot (x_k)^T \cdot d + (1-\xi)\, g_i \cdot (x_k) \left\{ \begin{array}{c} = \\ \geqslant \end{array} \right\} 0, \quad i \in J_k^* \tag{3.25}$$

$$\Delta g_j \cdot (x_k)^T \cdot d + g_j \cdot (x_k) \geqslant 0, \quad j \in K_k^* \tag{3.26}$$

The additional parameter ψ_k can be chosen by equation 3.27 with A_{k-1} given by equation 3.28.

$$\psi_k \doteq \max\left(\psi_0, \frac{\psi^* \cdot \left(d_{k-1}^T \cdot A_{k-1} \cdot u_{k-1}\right)^2}{\left(1-\xi_{k-1}\right)^2 \cdot d_{k-1}^T \cdot B_{k-1} \cdot d_{k-1}}\right) \tag{3.27}$$

$$A_{k-1} \doteq \left(\Delta g_1\left(x_{k-1}\right), \ldots, \Delta g_m\left(x_{k-1}\right)\right) \tag{3.28}$$

3.1.3 Gradient Projection Algorithm

The guidance program uses an accelerated Gradient Projection Algorithm (GPA) with a two step process of restoration and optimisation (Speyer et al., 1971). The parameterisation problem is then solved using non linear programming (NLP) techniques to find the set of parameters $\vec{p}$ using an update scheme given by equation 3.29.

$$\vec{p}^{k+1} = \vec{p}^k + \alpha^k \cdot \vec{s}^k \tag{3.29}$$

$$0 \leqslant \alpha \leqslant 1 \tag{3.30}$$

Where α^k represents the step length taken along the search vector $\vec{s}^k$ and the superscript k indicates the iteration cycle. The GPA used within the guidance program uses only a forward perturbation to find the required gradient, which may be either positive (forward) or negative (backward). The first stage of the accelerated GPA is the restoration step which only fulfils the final constraints. The search direction is calculated using equation 3.31.

$$\vec{s}^k = -\bar{H}^k \cdot \vec{g}_p^k \cdot \left(\vec{g}_p^{k^T} \cdot \bar{H}^k \cdot \vec{g}_p^k\right)^{-1} \cdot \vec{g}^{k^T} \tag{3.31}$$

Where $\vec{g}_p^k = \nabla \vec{g} \cdot \left(\vec{p}^k\right)$ is the Jacobian matrix containing the constraint violation gradients with respect to parameter variation found by a single flight path prediction with the forward perturbation of a single parameter performed separately for each individual parameter. Consequently each additional parameter used within the control vector requires an additional flight path prediction and therefore increased computational effort. $\bar{H}$ is a quasi-Newton matrix which is approximated as the unity matrix for the first assumption and is later updated in the optimisation step. The step length α^k can be assumed to be unity, however the guidance program allows for reductions in the step length.

The second stage is the optimisation step which attempts to minimise the cost function. The search direction for the optimisation step is determined utilising equation 3.32 and with equation 3.33 which is an augmented cost function.

$$\vec{s}^{k} = -\bar{H}^{k} \cdot \tilde{F}_{p}^{k} \tag{3.32}$$

$$\tilde{F}^{k} = F^{k} + \vec{\Lambda} \cdot \vec{g}^{k} \tag{3.33}$$

The augmented cost function combines the original cost function F^{k} and the constraint violations $\vec{g}^{k}$ via the Lagrangian multipliers Λ found using equation 3.34.

$$\vec{\Lambda} = -\left(\vec{g}_{p}^{k^{T}} \cdot \bar{H}^{k} \cdot \vec{g}_{p}^{k}\right)^{-1} \cdot \vec{g}_{p}^{k^{T}} \cdot \bar{H}^{k} \cdot \vec{g}_{p}^{k} \tag{3.34}$$

Where $\vec{g}_{p}^{k}$ is the Jacobian and $\bar{H}$ is the Hessian matrix calculated using the Davidon-Fletcher-Powell (DFP) scheme of equations 3.35, 3.36 and 3.37.

$$\bar{H}^{k+1} = \bar{H}^{k} + \frac{\Delta\vec{p}^{k} \cdot \left(\Delta\vec{p}^{k}\right)^{T}}{\left(\Delta\vec{p}^{k}\right)^{T} \cdot \Delta\vec{\tilde{F}}_{p}^{k}} - \frac{\bar{H}^{k} \cdot \Delta\vec{\tilde{F}}_{p}^{k} \cdot \left(\Delta\vec{\tilde{F}}_{p}^{k}\right)^{T} \cdot \bar{H}^{k}}{\left(\Delta\vec{\tilde{F}}_{p}^{k}\right)^{T} \cdot \bar{H}^{k} \cdot \Delta\vec{\tilde{F}}_{p}^{k}} \tag{3.35}$$

$$\Delta\vec{p}^{k} = \vec{p}^{k+1} - \vec{p}^{k} \tag{3.36}$$

$$\Delta\vec{\tilde{F}}_{p}^{k} = \nabla\tilde{F}^{k+1} - \nabla\tilde{F}^{k} \tag{3.37}$$

The step size α^{k} used for the parameter update in equation 3.29 can be found by the one dimensional search with equation 3.38 using a golden search algorithm.

$$\tilde{F}\left(\vec{p}^{k} + \alpha^{k}\vec{s}^{k}\right) = \min_{\alpha}\left[\tilde{F}\left(\vec{p}^{k} + \alpha\vec{s}^{k}\right)\right] \tag{3.38}$$

3.1.4 Guidance Program Implementation

The guidance program utilises the restoration step of the gradient projection method to conform to the constraints. The optimisation step of the GPA is not utilised as an optimised solution was already found within the optimisation program before being

loaded into the guidance program as the reference trajectory. Utilising only the restoration step reduces the computational effort of the predictor. Although this has previously been used in other studies discussed in section 2.4.3 this method has never been applied to the terminal area flight phase.

Figure 3.1 shows the basic working of the GPA (Telaar, 2005), note this diagram is simplified for ease of understanding in reality the cost function is likely to be non-linear and the whole problem has greater dimensions than the two shown here. The shaded regions represent the viable area that the solution can lie within without exceeding the restriction violations represented by the boundaries. The circular regions represent the various values of the cost function increasing in a concentric manner around the minimum.

Point 1 is the starting location of the initial solution provided. The restoration step occurs moving the solution from point 1 to 2, thus ensuring that the solution is within the restriction violation boundaries. The optimisation step occurs from point 2 toward point 3 where the cost function is being reduced by moving to an inner circle along the restriction boundary provided by the search direction _s. Point 3 represents the optimum solution the minimum achievable cost function still within the restriction violations boundaries.

Within the guidance program only the restoration steps are used. Consequently the

Figure 3.1 – Graphical representation of the GPA (Telaar, 2005)

use of only the restoration steps results in a final solution which is sub-optimal. The optimal solution is not required since the final target values each have an associated tolerance and the restoration steps ensure that these constraints are respected. The minimisation of the cost function is not a primary concern as the final flight is only a slight modification of the reference found with the optimisation program and therefore the change to the cost function should be minimal. The reference trajectory is only *optimal* when the experienced flight conditions were as predicted by the models. However with the inclusion of off-nominal conditions this solution is no longer *optimal*.

3.1.5 Structure of the Optimisation Program

The optimisation program is capable of utilising various models to simulate the vehicle and environment as discussed in section 3.2. The optimisation and sensitivity studies within this study were performed with both the lower and higher order models. However for final results and passing the trajectory solutions to the guidance program the higher order models were used for increased accuracy and to assist in future studies. The optimisation program utilised the NLPQL routine, discussed in section 3.1.2, having both forward and backward parameter perturbations employing a central difference method to determine the gradients (Schittkowski and Zillober, 2001).

3.1.6 Structure of the Guidance Program

There are two major sections to the guidance program the simulator and the predictor. Figure 3.2 shows the structure of the program. The simulator, imitates the real world flight environment experienced by the vehicle. Consequently the simulation environment uses the higher order models to produce an accurate representation of the environment. The simulation environment also includes the disturbances discussed in section 3.2.

The predictor acts as the on-board computer for the launch vehicle taking the sensor data, in this case the vehicle states from the simulator, performing the flight path prediction and determining the required steering commands. The flight path prediction is solved numerically using a fourth order Runge-Kutta integration scheme. Due to the computational requirements of the flight path predictor low order models are

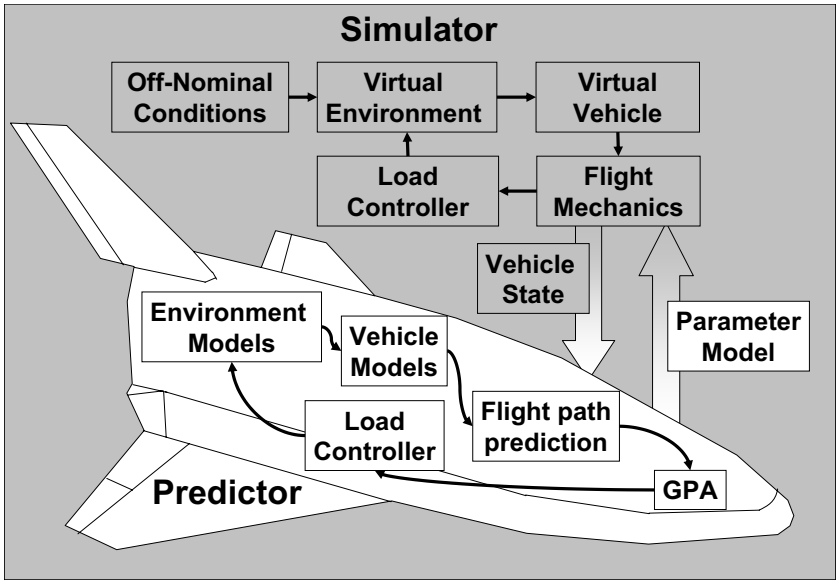

Figure 3.2: Structure of the guidance concept

used for aerodynamics, gravity and the atmospheric environment. During the flight the time for each prediction reduces since less flight path remains and consequently reduced computational effort is required.

3.1.7 Load Controller

To ensure that the vehicle loads were not exceeded during flight within the guidance program a load control was previously introduced (Gräßlin, 2004; Telaar, 2005). The load controller is utilised in the predictor portions of the guidance program to ensure that the vehicles do not exceed their load limits. The vehicle loading is calculated with equation 3.39. The values of the lift and drag forces are determine with equations 3.40 and 3.41, respectively.

$$F_{Aero} = \sqrt{L^2 + D^2} = \frac{1}{2} \cdot \rho \cdot v^2 \cdot S_{ref} \cdot \sqrt{C_L^2 + C_D^2} \tag{3.39}$$

$$L = C_L \cdot q \cdot S_{ref} = C_L \frac{1}{2} \cdot \rho \cdot v^2 \cdot S_{ref} \tag{3.40}$$

$$D = C_D \cdot q \cdot S_{ref} = C_D \frac{1}{2} \cdot \rho \cdot v^2 \cdot S_{ref} \tag{3.41}$$

Where L and D are the lift and drag forces with corresponding lift and drag coefficients C_L and C_D. q is the dynamic pressure given by equation 3.42. ρ is the atmospheric density obtained from the models discussed in section 3.2.1. v is the vehicle velocity as given in the state vector equation 3.6.

$$q = \frac{1}{2} \cdot \rho \cdot v^2 \tag{3.42}$$

After the steering commands are calculated for both the simulator and predictor portions of the guidance program the load controller then checks to ensure that the angle of attack does not result in a load limit violation. If vehicle's load limit is violated the current value for the angle of attack is reduced to a value that will not cause the vehicle to exceed the load limit as given in Telaar (2005).

Although the load limit is included it rarely becomes active for the Hopper vehicle due to the large load limit value given in table 4.2. There are some cases for the X-33 vehicle that the load limiter becomes active however these are only for brief periods of time and under extreme off-nominal conditions.

3.2 Models and Errors

In order for the optimisation and guidance programs to simulate the vehicle and environment several different models were required. These models also differ in their accuracy and computational effort depending on whether they are required for real world simulation (simulator) or for the on-board guidance computer (predictor). The models that simulate the real world environment are only approximations since it is difficult to accurately represent the world. Consequently applied errors, referred to as off-nominal conditions, are utilised to account for possible discrepancies between the actual world and simulated real world models. The following section describes the key models and off-nominal conditions used within the two programs.

There are several different types of off-nominal conditions (applied errors). Environmental errors are those that relate specifically to the vehicle environment. These include variations in density and wind velocities discussed in section 3.2.1. The vehicle characteristic errors are those which related directly to a vehicle property. These include variations in the vehicle's mass and aerodynamic coefficients, discussed in sec-

tions 3.2.3 and 3.2.4. Navigation and Steering errors relate to the accuracy and variation of the on-board vehicle sensors including sensor noise, offset errors and time delays, discussed in sections 3.2.5 and 3.2.6. Initial condition errors modify the vehicle's initial altitude, position, velocity, flight path angle and azimuth from the nominal conditions, discussed more in section 3.2.7.

3.2.1 Atmosphere and Wind

There are several different standard atmospheric models available. The majority of the publicly available ones are discussed in Labitzke et al. (1985); Griffin and French (1991); Hedin (1991); Chabrillat (1995); Justus and Johnson (1999). Although all these models can be implemented within the optimisation and guidance programs the models used for this study were the Mass Spectrometer Incoherent Scatter Extended (MSISE) 1993 (Labitzke et al., 1985; Hedin, 1991; Chabrillat, 1995) and the US Standard 1962 (Griffin and French, 1991).

The MSISE 1993 model is complex and requires considerable computational effort. It was for this reason that only the optimisation program and simulator portion of the guidance program used the MSISE 1993 as they were not time critical. The predictor portion of the guidance program utilised the simpler US Standard 1962 model for reduced computational effort. The MSISE 1993 utilises several complicated subroutines to produce the outputs whilst the US Standard model consists of a single subroutine consequently requiring less computational effort. The MSISE model takes into account; day, time, altitude, latitude, longitude, radiation flux and magnetic index. With these parameters the MSISE 1993 model is able to produce values for density, pressure and temperature. The US Standard atmosphere uses only the altitude as an input to produce density, pressure and temperature. Consequently the US Standard atmosphere has a single density profile that is position and time independent.

For this research the most important value is the density which is used to calculate vehicle aerodynamic forces and dynamic pressure. The density profiles and the associated error difference are shown in Appendix A.2. The profiles shown are for the entire world and the specific areas considered for each vehicle where stated.

To simulate winds the Horizontal Wind Model (HWM) 1993 is used (Hedin et al., 1996). The wind model consists of several subroutines which produce North-South

and East-West wind values based on day, time, altitude, latitude, longitude, radiation flux and magnetic index. The wind model profiles can be seen in Appendix A.3. The wind model similar to the MSISE 1993 model requires more computational effort and was therefore only used within the optimisation program and simulator portion of the guidance program. Some later work on the X-33 vehicle guidance also included a predictor wind model, this is discussed more in section 6.2.6.

Another method used to model the winds is included in the sensitivity studies of sections 6.1.3 and 6.2.4. The sensitivity studies utilise a constant wind velocity or wind velocity that is dependent on the altitude of the vehicle. These type of winds were also used in the study Hoffman et al. (1970) to test the guidance method for the lifting body re-entry vehicle. The constant wind values are randomly varied for each simulation between $\pm 5\,\mathrm{m/s}$ in the North-South and East-West wind directions. The altitude varying winds are randomly varied for each simulation between $\pm 1.5\mathrm{h}\,\mathrm{m/s}\cdot\mathrm{km}$ in the North-South and East-West wind directions. For example a value of $1.5\mathrm{h}\,\mathrm{m/s}\cdot\mathrm{km}$ at an altitude of $10\,\mathrm{km}$ would result in a wind velocity of $1.5\cdot 10 = 15\,\mathrm{m/s}$. Positive values represent a North or East wind and negative values represent a South or West wind. These wind values were only applied to the simulator portion of the guidance program.

Atmospheric perturbations are included in almost all guidance evaluations as these are the most likely off-nominal conditions to be experienced by launch vehicles. Variations in density are of primary concern as they can affect lift, drag and dynamic pressure. The atmospheric perturbations within this study were produced by varying the inputs to the MSISE 1993 and HWM 1993 models. Wind was included such that it could be switched on or off, to allow for either combined effects or only that of the MSISE 1993 model. The atmospheric model parameters varied were; day from 0 to 365, time from 0 to 24 hours, 3 month average radiation flux from 70 to 260, radiation flux of previous day from 70 to 260 and magnetic flux index from 7 to 25. These were the perturbations provided by the source code for the MSISE 1993 (Labitzke et al., 1985; Hedin, 1991; Chabrillat, 1995). The longitude and latitude varied as the position of the vehicle changed during the flight. The influence of the radiation flux and radiation flux from previous days is minimal below altitudes of 80km (Labitzke et al., 1985; Hedin, 1991; Chabrillat, 1995). However they were included in this study for completeness

and because their inclusion did not influence the computational requirement of the predictor portion of the guidance program.

A density noise, although not part of the MSISE 1993 model, was also included to account for discrepancies in atmospheric density due to the monthly averaged data of the MSISE 1993 model. The density error was modelled as a random ±4% discrepancy with a 3 sigma gaussian distribution.

3.2.2 Earth Shape and Gravity

There are several methods of modelling the earth shape; a flat earth, a sphere using the either maximum, minimum, or mean earth radius or an ellipsoid. The ellipsoid model was utilised in this study as it provided increased accuracy and did not require a significant amount of additional computational time over the other models. The ellipsoid earth model is provided in equation 3.43 for the eccentricity and equation 3.44 for the ellipse (Regan and Anandakrishnan, 1993). Where e is the eccentricity, R_E is radius of the Earth, R_e is the Earth equatorial radius, R_p is the Earth polar radius, δ the geocentric latitude.

$$e = \sqrt{1 - \left(\frac{R_p}{R_e}\right)^2} \tag{3.43}$$

$$R_E = \frac{R_p}{\sqrt{1 - e^2 \cdot \cos^2(\delta)}} \tag{3.44}$$

There are two different models for gravity used within this study the Newtonian point mass approximation and a fourth order model which takes into account the oblateness of the Earth's shape. The Newtonian point mass model varies the gravitational acceleration with regards to distance from the Earth's centre. The gravitational acceleration for the Earth at any radius from the centre is given by Newton's gravitational law given by equation 3.45 (Regan and Anandakrishnan, 1993).

$$g = \frac{G \cdot M_E}{r^2} \tag{3.45}$$

Where g is the gravitational acceleration, r the distance from the centre of the Earth, G the universal gravitational constant and M_E the mass of the Earth. This model is relatively computationally efficient and provides a good approximation for the radial

variation in gravitational acceleration. However this model utilises a point mass assumption which does not take into account the effects of inhomogeneous mass distribution of the Earth due to the ellipsoidal shape. For a better approximation of the gravitational acceleration a higher order model is required.

The higher order model for the Earth's gravitational acceleration utilises Newton's gravitational law for point masses but takes into account the oblateness of the Earth by considering the inhomogeneous mass distribution. The model takes into account the additional variation of gravitational acceleration with latitude as well as the altitude of the Newtonian model. Consequently a lateral gravitation acceleration is calculated for the vehicle resulting in a gravitation force vector that is not always orientated towards the Earth's centre which the Newtonian model does. The variation in gravitational potential due to the distance from the Earth's centre g_r, longitude g_λ and latitude g_δ is given by equations 3.46, 3.47 and 3.48 respectively (Regan and Anandakrishnan, 1993).

$$g_r = \frac{G \cdot M_E}{R^2}\left\{1 - \frac{3}{2}\cdot J_2 \cdot \left(\frac{R_e}{R}\right)^2 \cdot \left[3\cdot\sin^2(\delta) - 1\right] - 2\cdot J_3 \cdot \left(\frac{R_e}{R}\right)^3 \cdot \sin(\delta)\cdot\left[5\cdot\sin^2(\delta) - 3\right] - \frac{5}{8}\cdot J_4 \cdot \left(\frac{R_e}{R}\right)^2 \cdot \left[35\cdot\sin^4(\delta) - 30\cdot\sin^2(\delta) + 3\right]\right\} \quad (3.46)$$

$$g_\lambda = 0 \quad (3.47)$$

$$g_\delta = -\frac{3\cdot G\cdot M_E}{R^2}\cdot\left(\frac{R_e}{R}\right)^2 \cdot \cos(\delta)\left\{J_2\cdot\sin(\delta) + \frac{1}{2}\cdot J_3\cdot\left(\frac{R_e}{R}\right)\cdot\left[5\cdot\sin^2(\delta) - 1\right] + \frac{5}{6}\cdot J_4\cdot\sin(\delta)\cdot\left(\frac{R_e}{R}\right)^2\cdot\left[7\cdot\sin^2(\delta) - 3\right]\right\} \quad (3.48)$$

Where G is the universal gravitational constant, M_E is the mass of the Earth, R_e is the radius of the earth at the equator, R is the current distance from the Earth's centre, δ is the geocentric latitude and the constants J_i are the Jeffery Constants which take into account the Earth's oblateness. The constants for the gravity model used within this study are given in table 3.1 (Wertz and Larson, 1999).

The higher order model is more accurate than the Newtonian approximation of equation 3.45 although the method is more computationally intensive. Consequently

NOTE: This table is included on page 70 of the print copy of the thesis held in the University of Adelaide Library.

Table 3.1 – Earth constants for gravity and shape (Wertz and Larson, 1999)

the present study implements the Newtonian model for the predictor and the higher order model for the simulator. The associated errors are small in magnitude so their influence is minimal in comparison to the other model differences such as those of the atmosphere and vehicle aerodynamics.

3.2.3 Aerodynamics

The aerodynamic models for the Hopper and X-33 vehicles used within this study consisted of tabulated values for lift and drag coefficients as a function of Mach number and angle of attack (Spies and Grallert, 2001; Spies, 2002, 2003). Intermediate lift and drag coefficient values were determined using a two dimensional interpolation routines (angle of attack and Mach number). The optimisation program and simulator portion of the guidance program use a higher accuracy fourth order spline interpolation routine and the predictor portion employs a simpler linear interpolation routine to reduce computational requirements. Figures 3.3(a) and 3.3(b) provide the lift-to-drag ratios as a function of Mach number and angle of attack for the Hopper and X-33 vehicles, respectively. The aerodynamic lift and drag forces are then calculated utilising equations 3.40 and 3.41.

The aerodynamics for the Hopper vehicle were only a preliminary model and at the stage of writing only a three degree of freedom model was publicly available taking into account lift, drag and skin friction. The aerodynamic coefficient tables for the Hopper vehicle were only valid for angles of attack less than 20◦ and a Mach number ranges from 0.2 to 20. There was also a correction factor included to account for the variation due to the vehicle's Mach number given by equations 3.49, 3.50 and 3.51

NOTE: This figure is included on page 71 of the print copy of the thesis held in the University of Adelaide Library.

Figure 3.3: The Hopper and X-33 vehicle aerodynamics

(Spies, 2003).

$$Ma_f = 1 + 0.075 \cdot \exp^{-\left(\frac{Ma-1.15}{Ma+1.15}\right)^2} \tag{3.49}$$

$$C_d = \frac{C_{dMach}}{Ma_f} \tag{3.50}$$

$$C_l = C_{lMach} \cdot Ma_f \tag{3.51}$$

The skin friction coefficient, C_f is added to the drag value after the modifications for Mach speed correction to give the update drag value, $C_{dSkin\,Friction}$ as shown in equation 3.52.

$$C_{dSkin\,Friction} = C_d + C_f \tag{3.52}$$

A new development from this research is the utilisation of the vehicle's speed brake as a steering parameter. Traditionally the programs have only been applied to the hypersonic re-entry of the vehicle terminating at the terminal area interface (TAI) point. Consequently the simulated vehicles never reached subsonic speeds, where the speed brake becomes effective. Most traditional terminal area flight phase methods utilise (in some form) a speed brake as a steering variable. The Shuttle TAEM utilises the speed brake as a method for controlling the energy dissipation rate (Ehlers and Kraemer, 1977).

At the time of writing a precise speed brake model for the Hopper vehicle was unavailable. Consequently two separate speed brake models were developed for evaluation. The first model was developed in order to determine the influence that the inclusion of a speed brake would have on the guidance. A simple linear model was selected which added a 10% bias to the drag coefficient as a method for simulating the additional drag of the vehicle as given by equation 3.53. The use of 10% bias was select to simply verify the influence a speed brake has on the vehicles during the terminal area flight. The amount of bias was then controlled via a speed brake setting variable δSB, such that $0 \leqslant \delta SB \leqslant 1$.

$$C_D = C_{d^{\text{Skin Friction}}} + \delta SB \cdot 0.1 \cdot C_{d^{\text{Skin Friction}}} \tag{3.53}$$

The use of speed brake setting instead of an angular deflection allows the speed brake to be applied to multiple vehicles by introducing a different aerodynamic model. The use of the speed brake setting also allows for speed brake modelling in the cases where vehicles do not have a specific speed brake but instead utilise manipulation of several control surfaces to simulate a speed brake.

The simple speed brake model quickly revealed the advantages of including the speed brake setting as a steering variable for the terminal area flight phase. The speed brake was able to provide significant margins (discussed more in section 5.4) for the trajectory without the need of complicated geometric segments or multiple trajectory phases. The additional speed brake setting steering parameters were also useful for the trajectory design and for coping with off-nominal conditions during guidance evaluation.

A more refined speed brake model was then developed as part of this research based on aerodynamic data from two previous NASA research vehicles the HL-20 lifting body (Jackson et al., 1992; Jackson and Cruz, 1992) and the cancelled X-34 suborbital test bed (Pamadi and Brauckmann, 1999; Pamadi et al., 2000). The speed brake model provides an additional drag coefficient, C_S, which is a function of angle of attack, α and Mach number, Ma as given by equation 3.54.

$$C_S(\alpha, Ma) \tag{3.54}$$

The new implementation of the speed brake is given by equation 3.55, again the speed brake setting δSB is used with the same limits.

$$C_D = C_{d^{\text{Skin Friction}}} + \delta SB \cdot C_S \tag{3.55}$$

A detailed model and discussion of the development for the speed brake model generated within this study is contained in Appendix C. Although the developed model was conducted in combination with the rest of the vehicle aerodynamic testing it was generated from well established data for other vehicles and consequently provided the required accuracy to allow proper evaluation of the guidance method. The implementation of the speed brake was also modular, allowing the inclusion of model specifically developed for the Hopper vehicle should one become publicly available in the future.

The X-33 vehicle aerodynamic models from NASA were provided as coefficients for axial and normal forces as a function of angle of attack, side slip angle and Mach number as given by equation 3.56. Within this study the side slip angle was assumed to be zero and therefore not to have an influence on the aerodynamics of the vehicle. Since only a 3 Degrees of Freedom (3DOF) model was available for the Hopper vehicle it was decide to only perform a 3DOF analysis of the X-33 vehicle. Consequently the influence of vehicle roll and inertia was ignored. Although later consideration is given to the vehicle attitude, roll and inertia with the inclusion of time delays for the steering commands discussed in section 3.2.6. For ease of implementation within the existing subroutines of the guidance program the tables of axial C_A and normal coefficient C_N were transformed to tables for lift C_L and drag coefficients C_D using equations 3.57 and 3.58

$$\begin{matrix} C_A\,(Ma, \alpha, \beta) \\ C_N\,(Ma, \alpha, \beta) \end{matrix} \tag{3.56}$$

$$C_l = C_N \cdot \cos\alpha - C_A \cdot \sin\alpha \tag{3.57}$$

$$C_d = C_N \cdot \sin\alpha + C_A \cdot \cos\alpha \tag{3.58}$$

Although the X-33 vehicle does not have specific speed brake surfaces as the Hopper vehicle does a speed break has previously been simulated using split in-board and

out-board elevons within an unpublished NASA study (Dukeman, 2004). The coefficient modification increments were provided in the NASA X-33 vehicle aerodynamic models. The speed brake for the X-33 vehicle was provided as a function of Mach number Ma, angle of attack α and side slip angle β as given by equation 3.59. The speed brake coefficients were also given in terms of axial and normal coefficient which were again transformed to lift and drag coefficients as given by equations 3.60 and 3.61. The speed brake coefficients were then added to the lift, C_l and drag, C_d coefficients with variation via the speed brake setting as given by equations 3.62 and 3.63 to give the total lift, C_L and drag, C_D coefficients. Where C_{S_L} and C_{S_D} are the lift and drag speed brake coefficients respectively and δSB is the speed brake setting.

$$C_S = (Ma, \alpha, \beta) \tag{3.59}$$

$$C_{S_L} = C_N \cdot \cos\alpha - C_A \cdot \sin\alpha \tag{3.60}$$

$$C_{S_D} = C_N \cdot \sin\alpha + C_A \cdot \cos\alpha \tag{3.61}$$

$$C_L = C_l + \delta SB \cdot C_{S_L} \tag{3.62}$$

$$C_D = C_d + \delta SB \cdot C_{S_D} \tag{3.63}$$

The prediction of aerodynamics of new launch vehicles although advanced with the use of Computational Fluid Dynamics (CFD) and wind tunnel testing, it is still insufficient for a completely accurate representation. The first flight of the US Shuttle Orbiter actually showed drastic difference in aerodynamic coefficients than those of pre-flight prediction based on wind tunnel testing (Siemers and Larson, 1979; Harpold and Gavert, 1983; Young and Underwood, 1983). The inclusion of aerodynamic errors in vehicle models is common in mission analysis. Consequently the guidance evaluations within this study have also included modifications to the vehicle aerodynamics to ensure the validity of the result presented here. The variation to the vehicles aerodynamics are modelled using modifying factors for both the lift and drag coefficients during flight, $\pm 5\%$ for the Hopper vehicle (Siemers and Larson, 1979; Telaar, 2005) and

±10% for the X-33 vehicle (Hoffman et al., 1970; Naftel and Powell, 1991, 1993). The random modifying factor was constant for the entire flight of each seperate trajectory.

3.2.4 Vehicle Mass

The terminal area flight phase is unpowered (without thrust) and therefore there is no significant change in the vehicle mass due to propellant usage. In this study it is assumed that the steering commands are achieved utilising the aerodynamic surface deflections. Although it is possible with the Hopper and X-33 vehicles that at higher Mach numbers above 1.0 the reaction control thrusters are required. The centre of gravity is also assumed to have a constant position.

During the development of prototype launch vehicles the exact mass of the final vehicle is never known with complete certainty. Consequently in trajectory propagation and guidance studies a variation of vehicle mass is incorporated such that if the vehicle mass is to increase or decrease during development the guidance program and findings will still remain valid. Mass variation are included in sensitivity studies to determine how the vehicle mass influences the trajectory. The mass is also traditionally varied to account for different mission scenarios in case of failed payload deployment or payload return. For this study the mass was modelled by using a mass factor which varied the Hopper vehicle mass by ±5% (Telaar, 2005) and the X-33 vehicle mass by ±0.5% (Dukeman, 2004).

3.2.5 Navigation Errors

On board a launch vehicle sensors are used to determine the position and attitude of the vehicle. It was assumed for this study that the vehicles use a Space Integrated GPS/INS (SIGI) with additional support from the landing site for altitude prediction, namely a differential Global Positioning System (GPS) (Honeywell International Inc., 2000; Gockel et al., 2004). An Inertial Navigation System (INS) measures the linear and angular acceleration to determine positions and velocities by integrating the signals.

The sensors used within a SIGI have an associated error for position and velocity. To model the position and velocity errors within this a noise error was included at each separate time step to the vehicle state within the simulation environment. The

errors are produced from random number generation using a Gaussian distribution with a 3 sigma range of $\pm$5.0m for position and $\pm$0.5m/s for velocity (Siemers and Larson, 1979; Wolf et al., 1996; Honeywell International Inc., 2000; Gockel et al., 2004; Jategaonkar et al., 2005).

A call was performed to obtain a new position and velocity error value at every time step. If the calls for a new error value were performed every time the error is added to the prediction instead of successive time steps a different error value would be given to the Runge-Kutta integration scheme. This would cause mathematical errors to occur within the program during integration and therefore introduce poorly formed gradients which could possibly cause the program to collapse in rare cases. Although this was never observed during development the possibility still exists. Therefore it was assumed that the position and velocity errors were constant for each time step. This is not entirely correct for real time simulation since position and velocity sensor errors vary greatly with time. However a variation with each time step should be sufficient to approximate the sensor noise while ensuring a level of confidence in the numerical integration scheme.

3.2.6 Steering Command Errors

There were three different errors applied to the steering command in the guidance program. The three different types of errors were all combined during Monte Carlo analysis to account for the sensor resolution, noise and rotational dynamics of the vehicle. The first error was a constant steering command error bias. The trajectories are designed with angles of attack, bank angles and speed brake settings which have numerous decimal points, for example 4.333358958 degrees. However in a real world flight environment the resolution of the sensor is not that accurate. Although the computer is able to command these angles of attacks the actual actuators in a real life flight can only provide the resolution that they have for the commands generally on the order of tenths to hundredths of a degree (Siemers and Larson, 1979). Therefore it is important to test the guidance with the simulation environment including these limitations by providing a bias error to the angle of attacks, bank angles and speed brake settings. The angle of attack and bank angle had a bias error which was randomly varied for every trajectory simulation with limits of $\pm 0.05^{\circ}$ (Siemers and Larson, 1979). Variations in

angle of attack of $\pm 0.5^{\circ}$ were observed to produce large variations in lift-to-drag ratios at subsonic speeds. The speed brake setting bias error was also varied randomly for each trajectory simulation but with limits of $\pm 0.25\%$ (Siemers and Larson, 1979). The values were taken from the data provided for the US Space Shuttle Orbiter in Siemers and Larson (1979). This method did not provide a realistic model as a constant bias error for each would not be the only possible error present, therefore additional errors were included (Wolf et al., 1996; Honeywell International Inc., 2000).

The second steering command error applied sensor noise to account for the imperfections of the on board attitude sensors for angle of attack, bank angle and speed brake. Similar to the navigation errors of section 3.2.5 the steering command sensor noise errors are calculated at each time step to ensure mathematical stability within the program. The noise errors used a Gaussian distribution with 1 sigma limits also taken from the data supplied for the US Shuttle Orbiter provided in Siemers and Larson (1979). The noise error 1 sigma limits were $\pm 0.05^{\circ}$ for the angle of attack, $\pm 0.1^{\circ}$ for the bank angle and ± 0.02 or 2% for the speed brake setting (Siemers and Larson, 1979).

The third error utilised steering command time delays previously introduced in the study Burkhardt (2001); Telaar (2005). The simulations were performed with three degree of freedom (3DOF) but as an effort to take into account the vehicles inertia, rotational and attitude dynamics and improve the error approximation for the angle of attack, bank angle and speed brake setting a time delay was introduced (Telaar, 2005). The time delay is modelled by limiting the rate change of the steering command given by equations 3.64, 3.65 and 3.66 for angle of attack, bank angle and new for this this study the speed brake setting, respectively.

$$\frac{d\alpha}{dt} = \frac{\alpha_c - \alpha}{\tau_\alpha} \tag{3.64}$$

$$\frac{d\mu}{dt} = \frac{\mu_c - \mu}{\tau_\mu} \tag{3.65}$$

$$\frac{d\delta SB}{dt} = \frac{\delta SB_c - \delta SB}{\tau_{SB}} \tag{3.66}$$

Where, α is angle of attack, μ is bank angle, δSB the speed brake setting, with subscript c representing the commanded steering settings, τ represents the time delay with

subscripts α, μ and δSB representing the angle of attack, bank angle and speed brake setting respectively and the dt denominator represents the rate with respect to time.

The time delay was varied for each simulation using a random number generator. The Hopper vehicle utilised a lower limit of 0.1 second and an upper limit of 3.0 seconds for the angle of attack (Telaar, 2005) and speed brake setting. The bank angle time delay had limits of 0.1 and 5.0 seconds (Telaar, 2005). The X-33 vehicle has a reduced upper limit for the bank angle time delay from 5.0 seconds to 3.0 seconds. During Monte Carlo simulations for the X-33 vehicle it was found that the 5.0 second bank angle time delay caused problems for the guidance to adapt the trajectory. A 5.0 second delay was considered excessive as the time required for a vehicle to perform orientation was expected to be less than 3.0 seconds.

3.2.7 Initial Condition Errors

The final conditions for the re-entry flight phase are generally provided with an allowable tolerance to account for deviations from the nominal trajectory caused by off-nominal conditions. For example the initial velocity value for the US Shuttle Orbiter at the commencement of TAEM can be $1000\,\mathrm{ft/s}$ $\mathrm{pm}100\,\mathrm{ft/s}$ (Ehlers and Kraemer, 1977). Consequently the altitude, attitude, heading, initial position and velocity of the vehicles at the commencement of the terminal area flight phase can vary considerably from the reference mission. Thus the simulations within this study included the possible variations of the altitude, attitude, heading, initial position and velocity at the terminal area interface in order to evaluate the guidance program. The initial conditions were varied for each simulation using a random number generator.

For the initial position variations a subroutine was produced which generated the initial position using a random number for the angle and then a distance based on the limits (Spies, 2003). Although this method produces more initial positions closer to the target this is what is commonly observed in re-entry results. To have an equal distribution the square root of the random number should be applied to the distance since the area of a circle is $\pi \cdot \mathrm{Radius}^2$.

The Hopper vehicle modelled the variation in initial position as a circle with a radius of 20 kilometres (Spies, 2003; Telaar, 2005). The initial altitude was varied by $\pm 2.5\,\mathrm{km}$ (da Costa, 2003; Spies, 2003), initial velocity by $\pm 30\,\mathrm{m/s}$ (Hoffman et al., 1970;

Ehlers and Kraemer, 1977), the initial flight path angle from 0 to -30° and the initial heading by $\pm 20^\circ$ (Büchner, 2003; Camara et al., 2002a).

The X-33 vehicle utilised two initial position variations. The first initial position variation used an annulus with an internal radius of 44.448 km (24 nmi) and external radius of 66.672 km (36 nmi) centred at a HAC intersection point (Leavitt et al., 2002). The implementation in this study does not use a HAC and consequently the centre of the annulus was shifted to the ALI target point. The second initial position variation used a circle similar to the Hopper vehicle but with a raidus of 11.112 km (6 nmi) centred at the initial latitude and longitude given in table 4.7. However the results presented here are only for the annulus initial position variation. The initial altitude was varied between ± 1828.8 m (± 6000 ft) (Kluever and Horneman, 2005), the initial velocity by ± 30 m/s (Hoffman et al., 1970; Ehlers and Kraemer, 1977), the initial flight path angle between $\pm 4^\circ$ (Kluever and Horneman, 2005) and the initial heading by $\pm 15^\circ$ (Büchner, 2003; Camara et al., 2002a).

3.2.8 Summary of Off-Nominal Conditions

The off-nominal conditions for the Hopper and X-33 vehicles are summarised in table 3.2. These errors are included in the simulator to account for discrepancies in modelling a real world environment with numerical models. The values of the off-nominal conditions are generated using a psuedo random number generator discussed more in section 6.1.4. The random number utilises the upper and lower bounds of the off-nominal conditions and also takes into consideration the distribution type. There are 3 distribution types Equal, 1 sigma and 3 sigma. An *equal* distribution means that all values between the upper and lower bounds have an equal chance of being generated. A 1 sigma distribution is a Gaussian distribution where the upper and lower bounds are the -1 and +1 sigma values respectively. A 3 sigma distribution is similar to the 1 sigma distribution except the upper and lower bounds represent the -3 and +3 sigma values respectively. It is important to note that the off-nominal conditions are only applied to the simulator and therefore the predictor has no knowledge of the applied errors and can only adapt by observing the errors in the final conditions.

There are several different types of errors such as atmospheric, navigation and aerodynamics which sometimes have a compounding effect as numerous errors can influ-

ence the equations of motion. An example is the aerodynamic forces which have the differences in density due to the different atmospheric models, the density noise and aerodynamic coefficient modifiers resulting in three errors effecting the vehicle loads experienced. The errors applied are also quite large for a greater evaluation of the guidance method ensuring suitability to the terminal area flight phase.

3.3 Assumptions and Limitations

The current problem formulation, models and methods utilised have several assumptions and limitations. As expected whenever a real world system is approximated by a numerical representation errors are expected. The use of a numerical integration is susceptible to errors due to the evaluation of the integration by discrete sampling instead of using the continuous function (Press et al., 1997a). Consequently errors are to be expected if compared to flight test data. However the expected errors due to the numerical integration should be quite small. A small integration step size of 0.1 seconds is utilised for the simulator to reduce the error. The integration scheme utilises a fourth order Runge-Kutta method also to reduce the possible errors of representing continuous functions. Therefore the numerical representation should provide an accurate formulation for this study.

The current formulation of the equations of motion have singularities when the flight path angle is $\pm 90^\circ$ and when the vehicle approaches the poles, $\delta = \pm 90^\circ$. The singularities occur for the flight path angle as the azimuth of the vehicle is undefined and for the poles because all directions will be south at the north pole and vice versa for the south pole. However this never occurs for either the optimisation or guidance programs for the terminal area flight phase of this study.

The GPA utilised within the guidance program requires an initial guess. This initial guess must be reasonable otherwise the program is not guaranteed convergence. The convergence problem is alleviated since an initial optimised reference trajectory (the initial guess) is provided to the guidance program before simulations.

Within the guidance program the high fidelity models utilised to simulate real world atmospheric conditions are based on data taken as monthly averages (Labitzke et al., 1985; Hedin, 1991; Hedin et al., 1996). Consequently the modelling of actual con-

Off-Nominal Conditions	Lower limit	Upper Limit	Distribution
Hopper Vehicle Characteristics			
Mass Factor	−5%	+5%	Equal
Lift coefficient	−5%	+5%	Equal
Drag coefficient	−5%	+5%	Equal
X-33 Vehicle Characteristics			
Mass Factor	−0.5%	+0.5%	Equal
Lift coefficient	−10%	+10%	Equal
Drag coefficient	−10%	+10%	Equal
Atmosphere and Wind			
Day	1	365	Equal
Time	0	24	Equal
3 month average radiation flux	70	260	Equal [a]
Previous day radiation flux	70	260	Equal [a]
Daily magnetic index	4	25	Equal [a]
Navigation			
Density sensor noise	−4%	+4%	3 sigma
X, Y and Z position noise	−5.0 m	+5.0 m	3 sigma
X, Y and Z velocity noise	−0.5 m/s	+0.5 m/s	3 sigma
Steering			
Angle of attack error	−0.05°	+0.05°	Equal
Bank angle error	−0.05°	+0.05°	Equal
Speed brake setting error	−0.25%	+0.25%	Equal
Angle of attack noise	−0.05°	+0.05°	1 sigma
Bank angle noise	−0.1°	+0.1°	1 sigma
Speed brake noise	−0.02	+0.02	1 sigma
Angle of attack time delay	0.1 s	3.0 s	Equal
Bank angle time delay	0.1 s	5.0 s/3.0 s	Equal
Speed brake time delay	0.1 s	3.0 s	Equal
Hopper Initial Conditions			
Altitude error	−2.5 km	+2.5 km	Equal
Velocity error	−30 m/s	+30 m/s	Equal
Flight path angle	−30°	0°	Equal
Azimuth error	−20°	+20°	Equal
Position	10/ 20 km radius circle		Equal
X-33 Initial Conditions			
Altitude error	−1828.8 m	+1828.8 m	Equal
Velocity error	−30 m/s	+30 m/s	Equal
Flight path angle error	−4°	4°	Equal
Azimuth error	−15°	+15°	Equal
Position	11.112 km radius circle		Equal
	66.672 km/ 44.448 km radius annulus		Equal

Table 3.2: The Hopper and X-33 vehicles off-nominal conditions

[a] The influence of the 3 month average radiation flux, previous day radiation flux and daily magnetic index is minimal below altitudes of 80km (Labitzke et al., 1985; Hedin, 1991; Chabrillat, 1995)

ditions experienced in a real mission might be different. These models however are commonly used within numerous trajectory and guidance studies. The possible errors are somewhat alleviated by the extensive random errors of the atmospheric conditions. However it is still possible that all real world situations are not accounted for.

The vehicle dynamics are modelled in 3DOF which does not accurately represent the physical six degrees of freedom (6DOF) system being represented. Some corrections have been made with the introduction of time delays for the steering commands, however this might not be enough to accurately represent the attitude and roll dynamics. Other assumptions made within the vehicle dynamics is that there is no side-slip and that all angle of attack settings are trimable. These assumptions are valid as the commanded steering commands should be able to be achieved and a bias error is applied to account for attitude resolution. The assumption of zero side slip is also common practise within 3DOF studies (Barton et al., 2002).

There was no speed brake data provided for the Hopper vehicle in the existing aerodynamic model or publicly available in the literature. Consequently a model was developed that used existing data from other vehicles to provide the required accuracy to allow proper evaluation of the guidance method (Jackson et al., 1992; Jackson and Cruz, 1992; Pamadi and Brauckmann, 1999; Pamadi et al., 2000). The formulation of the optimisation and guidance programs allows for the introduction of another speed brake model and the required speed brake settings can be modified to achieve the required increase in drag values. The purpose of this study was not to develop a real world aerodynamic model of the vehicle nor was it to determine the accuracy of a speed brake model, which for this study is a 'best guess' model. However some important characteristics of the speed brake model are drawn from basic aerodynamic knowledge (Jackson et al., 1992; Jackson and Cruz, 1992; Pamadi and Brauckmann, 1999; Pamadi et al., 2000).

A limitation of the optimisation program is that the determined solution is often dependent on the initial guess. A *reasonable* initial guess is often required for the optimisation program. This is because the NLPQL is a local optimiser and therefore does not find the global solution. Some general knowledge and experience is required by the user in order to find the more suitable solutions. The flexibility of the program allows for multiple solutions to be valid. Therefore even if the most suitable solution is

not found a 'good' solution is still more than adequate provided it delivers the vehicle within the mission and final condition restrictions.

The guidance program is unable to ensure convergence of the solution during the restoration steps. However the divergence behaviour was not observed during the hundreds of thousands of simulations conducted during this study. If the restoration steps fail the original commands are still stored and can be used which under nominal conditions will deliver the vehicle safely. However in the presence of off-nominal conditions restriction violations can occur.

Due to the high Mach numbers of the X-33 vehicle a reaction control system might be required to control the vehicle attitude. Within this study it is assumed that the steering commands can be reached using aerodynamic surface deflections and therefore there is no propellant usage for reaction control thrusters. The worst case analysis of section 6.2.3 shows that the guidance is effectively able to cope with mass variations and so any possible variation in mass due to propellant usage should not influence the results significantly.

Chapter 4

Vehicles and Missions

Once you get to earth orbit, you're halfway to anywhere in the solar system.

Robert A. Heinlein (1907 - 1988)
Science Fiction Author

THIS study utilises two vehicles and their associated mission for trajectory planning and guidance evaluation: the sub-orbital Hopper vehicle in section 4.1 and the Single Stage To Orbit (SSTO) X-33 concept vehicle is presented in section 4.2. The design mission profiles for the Hopper and X-33 vehicles are considerably different due to the various vehicle characteristics. However both mission profiles include a terminal area flight phase. The terminal area flight phase, discussed in section 4.3, is also different for each vehicle with distinct initial and final conditions.

4.1 The Hopper Vehicle and Mission

The sub-orbital Hopper concept vehicle is an autonomous semi-reusable launch vehicle that carries an expendable upper stage labelled the Payload Assist Module (PAM), which is used to place payloads into orbit. The Hopper vehicle was investigated under the Future European Space Transportation Investigations Programme (FESTIP) study and further researched within the German Advanced Systems and Technologies for RLV Application (ASTRA) program through co-operation of the German aerospace industry and research institutions. The Hopper vehicle concept shown in figure 4.1 was investigated as a possible replacement for the Ariane 5 launch vehicle and was ex-

pected to reduce launch costs over conventional space transportation systems (Spude et al., 2003).

The Hopper vehicle is powered by 3 Vulcain 3R engines and launched horizontally from Kourou, French Guyana ascending with a sub-orbital flight path to 100km where it reaches the Main Engines Cut Off (MECO) point. The Hopper vehicle then glides to an altitude of 130km where the PAM is released and launched into the desired orbit. The Hopper vehicle continues the glide until a maximum altitude of approximately 150km is reached. Following the sub-orbital trajectory the Hopper vehicle performs a re-entry flight (Spies, 2002). The re-entry is a glide trajectory designed to reduce both thermodynamic and structural loading. Depending on the type of mission the Hopper vehicle lands horizontally at either of three landing sites; Ascension Island for Geostationary Transfer Orbit (GTO), Santa Maria for Medium Inclination and Saint Pierre et Miquelon for High Inclination and Sun Synchronous Orbit (SSO) (Berge et al., 2002). These missions can be seen in figure 4.2 (Berge et al., 2002). This study only considers the mission to Ascension Island as a test case, however the program is developed such that it can be applied to other landing sites. Terminal Area Guidance unlike re-entry guidance is similar for the different landing sites. The guidance can be applied to either of the landing sites with minor changes in vehicle position and azimuth. However other initial conditions such as distance to runway, velocity, altitude and flight path an-

NOTE: This figure is included on page 86 of the print copy of the thesis held in the University of Adelaide Library.

Figure 4.1 – The sub-orbital Hopper concept vehicle (Spies, 2002)

gle will be the same. At approximately 15km altitude and a Mach number 1.5 the Hopper vehicle initiates terminal area guidance in order to align with the landing sites (Spies, 2003). An automatic landing system is initiated and after recovery the Hopper vehicle is then shipped back to French Guyana where it is refitted and inspected prior to the next launch.

The Hopper vehicle utilises three Vulcain 3R engines which are evolutions of the current Vulcain 2 engine design used on the Ariane 5 ECA (Berge et al., 2002). The forward section of the Hopper vehicle houses the Liquid Hydrogen (LH2) tanks and rear section houses the Liquid Oxygen (LOX) tanks and the tubular cargo hold for the PAM. The fuselage and wing structure are constructed from Carbon Fibre Reinforced Plastic (CFRP) using sandwich panels with honeycomb cores (Spies, 2002). The overall structure consists of frames and longitudinal stiffeners as can be seen in figure 4.1(b). Important parameters for the Hopper vehicle used within this study are provided in table 4.1, note that the vehicle mass is the value at the commencement of the terminal area flight phase.

Throughout the mission there are several thermodynamic and structural restrictions to ensure that the vehicle returns safely to the landing site. Table 4.2 displays the mission restrictions for the terminal area flight phase of the Hopper vehicle mission. During the terminal area flight phase it was found that only two of the restriction were significant the vehicle loads and dynamic pressure. Due to the low supersonic and subsonic speeds experienced by the Hopper vehicle the aerothermodynamic heat-

NOTE: This figure is included on page 87 of the print copy of the thesis held in the University of Adelaide Library.

Figure 4.2 – The Hopper vehicle mission profiles (Berge et al., 2002)

Characteristic	Value
Vehicle mass, M	60237.0 kg
Aerodynamic reference area, S_{ref}	580.0 m^2

Table 4.1: The Hopper vehicle characteristics

ing was negligible. Additionally the large value for dynamic pressure meant that this restriction had no influence on the results.

4.2 The X-33 Vehicle and Mission

The X-33 vehicle was developed as a sub-orbital test bed for new technologies that are a requirement of future reusable launch vehicles. The program began in July 1996 under a co-operative agreement between NASA and Lockheed Martin Corporation coupled with other industrial technical partners. The aim of the program was to design, build and fly the half scale sub-orbital lifting body shaped test bed a as predecessor to a SSTO reusable launch vehicles named VentureStar™. Figure 4.3 provides a comparison of size between the X-33, VentureStar™and the US Space Shuttle.

The X-33 program was to test several new technologies including, linear aerospike rocket engines, a rugged metallic thermal protection system, light weight composite structures including cryogenic fuel tanks and advanced guidance, navigation and control systems for an autonomous reusable launch vehicle. The expected outcome of the program were the development, testing and proving of key technologies that would allow a cost reduction of sending a pound of payload into orbit by an order of magnitude. Failures in reusable cryogenic composite fuel tanks, program delays and expanding costs resulted in the program being cancelled in March 2001. The important

Mission Restriction	Limit
Re-entry vehicle load	4.5 g
Dynamic pressure	40 kPa

Table 4.2: The Hopper vehicle mission restrictions

NOTE: This figure is included on page 89 of the print copy of the thesis held in the University of Adelaide Library.

Figure 4.3: Vehicle comparison for the X-33, VentureStar™and US Space Shuttle (NASA, 2005)

vehicle parameters used in this study for the X-33 are provided in table 4.3, note that the vehicle mass is that at the commencement of the terminal area flight phase.

The X-33 mission was designed to test the technologies in all the flight phases of operation. The mission was designed such that the flight envelope could be incrementally increased for altitude, range and Mach number. The X-33 vehicle was to launch vertically from Edwards Air Force Base, California and land horizontally at one of three landing sites. The three landing sites were Silurian Dry Lake Bed California, Michael Army Air Field, Utah and Malmstrom Air Force Base, Montana. The landing site and mission considered in this study is the mid range mission to Michael Army Air Field (MAAF), Utah. Figure 4.4 displays the mission profile for the X-33 landing at the Michael Army Air Field. For this landing site the X-33 accelerates up to speeds of Mach 9 to 12 and a maximum altitude of approximately 50.3km (165000ft). The X-33 then continues on the sub-orbital trajectory performing re-entry and the terminal area

Characteristic	Value
Vehicle mass, M	37648.2 kg(83000 lbm)
Aerodynamic reference area, S_{ref}	149.4 m^2(1608 ft^2)

Table 4.3: The X-33 vehicle characteristics

flight phase manoeuvres before landing at MAAF approximately 724.2km (450miles) downrange. The X-33 vehicle restrictions for the terminal area flight phase are given in table 4.4. Similar to the Hopper vehicle the low supersonic and subsonic speeds experienced by the X-33 vehicle meant that the aerothermodynamic heating was negligible.

Although the X-33 program is no longer funded relevant data is still available about the vehicle. This data includes advanced models for vehicle dynamics which were used within this study to produce the aerodynamic and vehicle models. There is also current on going research into new methods for guidance of reusable launch vehicles using the models from the X-33. It is therefore possible to perform significant comparison between this research and the results obtained from other methodologies such as those of Kluever and Horneman (2005). Additionally by proving the guidance concept for multiple vehicle types several of the key attributes of the guidance method adopted for this study are demonstrated. These attributes include the adaptability and flexibility of the method to operate under different mission types including different flight conditions and with vehicles.

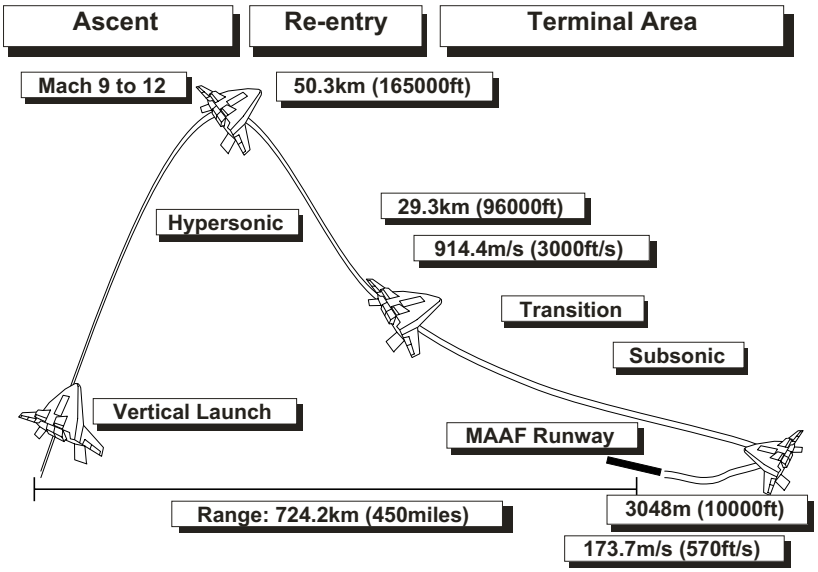

Figure 4.4: The X-33 vehicle MAAF mission profile

Mission Restriction	Limit
Re-entry vehicle load	2.5 g
Dynamic pressure	15.561 kPa(325 psf)

Table 4.4: The X-33 vehicle mission restrictions

4.3 Terminal Area Flight Phase

The terminal area flight phase is the flight region which proceeds the hypersonic re-entry phase. The start point is labelled the Terminal Area Interface (TAI) point. The flight phase ends at the beginning of the landing phase known as the Approach and Landing Interface (ALI) point. An example of the terminal area flight phase of the Hopper vehicle is shown in figure 4.5. The landing point at Ascension Island is shown with the Hopper vehicle (not to scale).

Within the terminal area flight phase there are several important requirements and the environment is quite different to that experienced during hypersonic entry. At the end of the terminal area flight phase the vehicle is required to be aligned with the runway centreline with the appropriate final attitude, altitude, heading and velocity to facilitate a safe landing. A complication of this flight phase is the transition from supersonic to subsonic velocities where the aerodynamics of the vehicle change dramatically. Traditional winged or lifting body re-entry vehicles are unpowered during this phase

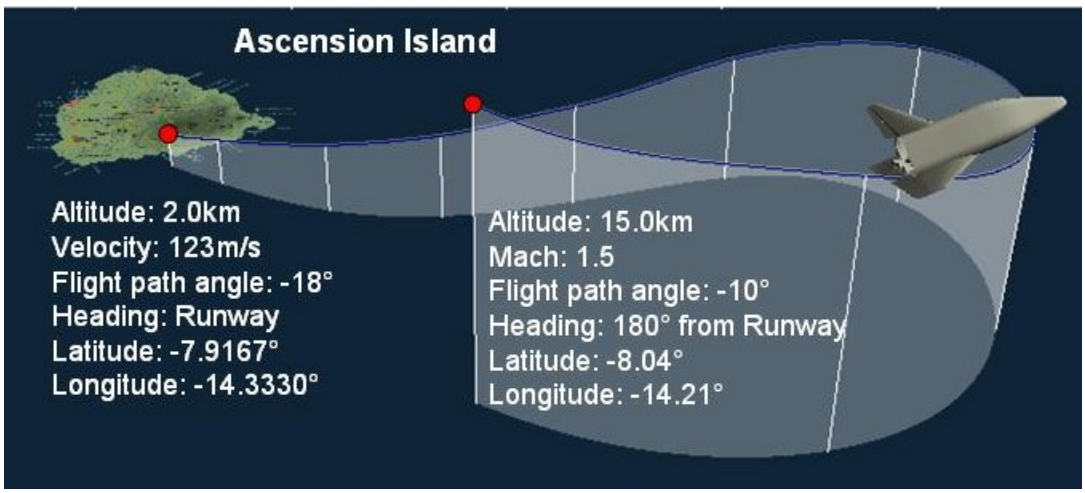

Figure 4.5: The terminal area flight phase of the Hopper vehicle

(without thrust) and more comparable to gliders in this respect. However the vehicles have severely decreased lift-to-drag ratios compared to gliders, making manoeuvres and alignment difficult.

The various initial and final conditions for the terminal area flight phase change depending on the vehicle and mission. The initial conditions for the Hopper and X-33 vehicles are given in tables 4.5 and 4.7 and the final conditions are given in tables 4.6 and 4.8 respectively. Consideration was also given to the variations of the terminal area flight phase initial conditions since they are the final conditions of the hypersonic re-entry phase, this is discussed more in section 3.2.7.

NOTE: This table is included on page 92 of the print copy of the thesis held in the University of Adelaide Library.

Table 4.5 – The Hopper vehicle initial conditions (Spies and Grallert, 2001; Spies, 2002, 2003; Camara et al., 2002a)

NOTE: This table is included on page 93 in the print copy of the thesis held in the University of Adelaide Library.

Table 4.6 – The Hopper vehicle final conditions (Spies and Grallert, 2001; Spies, 2002, 2003; Camara et al., 2002a)

NOTE: This table is included on page 93 in the print copy of the thesis held in the University of Adelaide Library.

Table 4.7 – The X-33 vehicle initial conditions (Kluever and Horneman, 2005)

NOTE: This table is included on page 93 in the print copy of the thesis held in the University of Adelaide Library.

Table 4.8 – The X-33 vehicle final conditions (Kluever and Horneman, 2005)

Chapter 5

Trajectory Design and Optimisation

Insanity is doing the same thing over and over again and expecting different results.

Albert Einstein (1879-1955)
Theoretical Physicist

THE goal of the optimisation program is to find the most suitable solution to solve the problem specified in Chapter 3. The optimisation program was utilised as a design tool for the reference trajectories, see section 5.7. The optimisation program was also utilised as an evaluation tool for the sensitivity studies discussed more in section 5.3. Although it is possible to find the *optimal* solution for the cost functions presented in section 5.6 input from the user was also combined in selection of the reference trajectories. During early investigations into the guidance program it was revealed that the restoration of the various trajectories with off-nominal conditions could be achieved with a variety of *reasonable* solutions. Instead of finding the optimal solution based on specified cost function considerable effort was made to determine the reference trajectories for the guidance program. These reference trajectories included minimisation of the cost functions but were also selected by the user based on the various attributes of the trajectory discussed in section section 5.5. The reference trajectories were selected by the user because it was possible to have a wide variety of trajectory solutions based upon the initial inputs to the optimisation program as discussed in section 5.7.

It is important to note that the optimisation for reference trajectory design is intended to be performed off-line not on-board the vehicle computer. The major reason

for off-line operation is that the optimisation program would not run effectively in real time to design a trajectory as it has a high computational requirement due to the iterative method of finding a solution. However a trajectory could also be further refined, updated or optimised in a coast phase or down time for the on-board computer. The reference trajectory is also designed off-line so that pre-mission analysis can be performed to verify the trajectories suitability. The trajectories designed for the US Space Shuttle are analysed prior to approval (Ehlers and Kraemer, 1977). The difference between the method within this study and that of the US Shuttle is that the optimisation program used for trajectory design is a method which is easily able to be applied to various vehicles and missions without major modifications. Consequently the optimisation program is a much more adaptable and flexible method for trajectory design than some of the previous methods employed for the terminal area flight phase. The optimisation program also allows for the generation of solutions from user specified trajectory constraints and their associated initial and final conditions. These generated solutions can then be analysed later for suitability reducing the required amount of user interaction. Therefore the optimisation program utilised as a trajectory design tool has the possibility of dramatically reducing the required time and personnel for pre-mission planning.

Although within this research only the terminal area flight phase is considered the optimisation program has also been successfully applied to the ascent and re-entry mission phases of various vehicles. The vehicles and missions to date include; the X-38 crew return vehicle (Gräßlin, 2004), the sub-orbital Hopper concept vehicle (Telaar, 2005), the Aeroassisted Orbital Transfer Vehicle (AOTV) (Telaar, 2005) and the Concept of a Lifting Body for Re-entry Investigations (COLIBRI) capsule (Schöttle et al., 1997; Burkhardt, 2001). The optimisation program has also been previously used in comparison to obtained flight data for verification of models with the Micro Re-Entry Capsule (MIRKA) (Tetlow et al., 1999).

The optimisation program is modular allowing for different vehicle, aerodynamic and mission models to be loaded without having to make major modification or reformulate the problem. Consequently the program is highly flexible and adaptable to multiple vehicles and missions. Although the terminal area flight phase for both the Hopper and X-33 vehicles was investigated, they have very different initial and final

conditions, mission constraints and aerodynamic characteristics. To demonstrate the adaptability, flexibility and applicability of this method to various reusable launch vehicles the optimisation program was used as a trajectory design tool for both the Hopper and X-33 vehicles and their associated missions. The optimisation program was also effectively used as a simulation tool investigating the sensitivities of trajectories to the various off-nominal conditions as discussed in section 5.3.

Within this research the trajectory design and guidance programs were quantitatively evaluated and also compared to other available methods on a general basis. To provide a quantitative evaluation of the optimisation and guidance programs a measure of performance was required. It was decided that the results would be evaluated based on the errors in the final conditions, namely target miss, velocity, flight path angle and azimuth. The target miss was defined as the total distance from the target position not including altitude as this was defined as the stopping condition. The final velocity and flight path angle errors were defined as the deviation from the required value with a positive value representing a higher velocity/ flight path angle and a negative value representing a lower velocity/ flight path angle. The final azimuth errors were defined such that a positive error represented an anti-clockwise rotation and a negative error represented a clockwise rotation. The evaluation also included whether vehicle restrictions were violated, namely vehicle loads and dynamic pressure.

5.1 Parameterisation Variable

The problem is formulated to determine a set of parameters $\vec{p}$ solving the problem defined in section 3.1. The optimisation program utilises the steering commands of the vehicle as the parameters $\vec{p}$. Previously the parameters $\vec{p}$ used were angle of attack for the ascent mission phase and pitch rate, angle of attack and/or bank angle for the reentry mission phase (Schöttle et al., 1997; Burkhardt, 2001; Tetlow et al., 2001; Tetlow, 2003; Gräßlin, 2004; Telaar, 2005). This research extends the program to include the terminal area flight phase extending the parameters to include the angle of attack, bank angle and speed brake setting (Chartres et al., 2005b).

The parameters $\vec{p}$ need to be defined over the variable t which in previous implementations had been defined as time or a vehicle state such as velocity or normalised

vehicle energy. It was found that the normalised energy of the vehicle defined in equation 5.1 was the most suited for the terminal area flight phase of the Hopper vehicle (Chartres et al., 2005b).

$$\epsilon_{Norm} = \frac{\epsilon}{\epsilon_{Init}} \tag{5.1}$$

Where ϵ_{Norm} is the normalised energy, ϵ is the instantaneous vehicle energy given by equation 5.2 and ϵ_{Init} is the initial vehicle energy.

$$\epsilon = \epsilon_{Pot} + \epsilon_{Kin} \tag{5.2}$$

ϵ_{Kin} is the kinetic energy and ϵ_{Pot} is the potential energy given by equations 5.3 and 5.4 respectively.

$$\epsilon_{Kin} = \frac{\mu_E}{R_E} - \frac{\mu_E}{R_E + h} \tag{5.3}$$

$$\epsilon_{Pot} = \frac{1}{2}v^2 \tag{5.4}$$

Where μ_E is Earth gravitational potential, R_E is the mean Earth radius, h is the current altitude and v the current vehicle velocity. The normalised energy is most suited because it is steadily decreasing which eliminates any singularities or fluctuations in the parameter definition as can be seen in figure 5.1. The altitude and velocity profiles of figure 5.1 are not steadily decreasing and could cause fluctuations in the steering commands determined from the parameter profiles. The initial and final values for altitude and velocity were also known resulting in a well defined problem for the optimiser to solve.

Other variables considered for t where the flight time, altitude and Mach number (Chartres et al., 2005b). The flight time was found to be unsuitable. Although it was an independent variable and also steadily increasing the final value was unknown. The final flight time for the Hopper vehicle was able to vary from 150 to 600 seconds (Chartres et al., 2005b). Consequently the definition of the parameters was problematic. Defining the steering parameters to the maximum possible value, for example 600 seconds, would cause some parameters to be neglected if the flight time was shorter (Chartres et al., 2005b). Similarly defining the steering parameters to the minimum

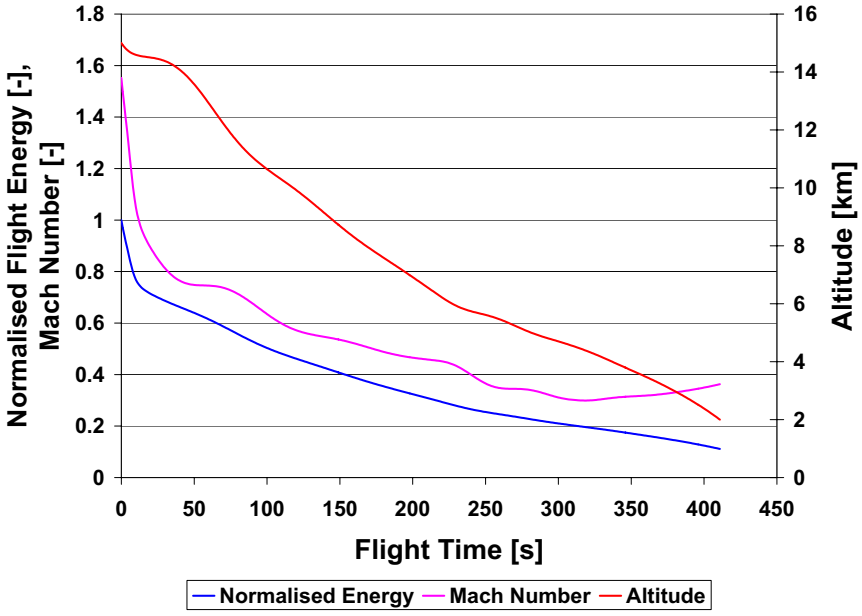

Figure 5.1: Different profiles for vehicle state variables

value, for example 150 seconds, would cause the final parameter to be active for large amount of time if the flight time was longer than the minimum (Chartres et al., 2005b).

The initial and final altitude where known which would mean that the profile could be defined as a function of altitude adequately. However, the altitude was found to be unsuitable because there were cases where it was found not to be steadily decreasing which could cause switching back and forth between parameters (Chartres et al., 2005b). This could be fixed by enforcing an additional restriction on the flight path angle, limiting values to be less than 0.0 degrees as was demonstrated in Büchner (2003) and discussed in section 2.3.6. However, this method was not entirely effective as the altitude profiles were able to have various decreasing slopes or even an almost constant value which resulted in a poorly defined set of parameters (Chartres et al., 2005b).

Similar to altitude the altitude profiles the initial and final values for the Mach number were known. However, it was possible to have points of inflexion in the Mach number profile as can been seen in figure 5.1 where the Mach number begins to increase towards the end of the flight. This would cause switching between parameters and a poorly defined set of parameters for steering commands (Chartres et al., 2005b).

The normalised energy has also been used to define trajectory profiles in other terminal area flight phases including the US Shuttle (Ehlers and Kraemer, 1977) and X-33

vehicles (Burchett, 2004; Kluever and Horneman, 2005). The results from the Hopper vehicle study indicated that the normalised energy would also be the most suitable for other reusable launch vehicles since similar problems would arise in the profile definitions. Therefore the X-33 vehicle also utilises the normalised energy for the variable t during the terminal area flight phase.

5.2 Parameter Profiles

The number of parameters in the parameter vector $\vec{p}$ can be varied by the user within the input files to the optimisation program. The number of parameters and an initial guess of their value is required by the optimisation program. Increasing the number of parameters can increase the accuracy of the guidance program in the presence of off-nominal conditions. Since with more parameters the guidance program has a greater number of parameters that can be updated and therefore more opportunities to adapt the trajectory to off-nominal conditions.

During a guidance call each individual parameter is perturbed separately and a flight path prediction is performed. Therefore for a large number of parameters lots of flight path predictions must be performed. The flight path prediction is the most computationally demanding portion of the program due to the flight path integration. To reduce computational time a minimum number of parameters possible should be used. However, with too few parameters the guidance is not able to effectively compensate for off-nominal conditions since there are only a few parameters to update. Consequently a compromise must be found between the computational requirements and guidance programs ability to compensate for off-nominal conditions.

The problem formulation must also be considered when determining the number of required parameters. In order for the problem to be properly formulated there should be more active parameters at the end of the trajectory than the required number of final condition constraints. The problem was formulated with 4 final condition constraints; position, velocity, flight path angle and azimuth. The position is defined in terms of altitude, latitude and longitude, however altitude was defined as the stopping condition eliminating the need for an additional constraint. The longitude and latitude were also combined into the single position constraint to reduce the number of constraints

simplifying the problem definition. There needs to be at least 4 active parameters at the end of the trajectory to find a solution. This is accomplished by ensuring that the final parameters are never reached leaving the pre-final and final parameters active. This provides 6 active parameters at the end of the trajectory; 2 angles of attack, 2 bank angles and 2 speed brake settings.

Within this research considerable work was performed to determine suitable numbers of parameters for both the Hopper and X-33 vehicles. Although it was found that for both vehicles the number of parameters could be dramatically reduced to only 6 or 7 parameters these were not enough to allow for the guidance program to cope with off-nominal conditions.

Within this study several approaches were developed for selecting the number of parameters. The most effective method was an elimination method. Initially a large number of parameters was utilised within the optimisation program for trajectory design. The number of parameters could then be reduced by the user when a parameter was found to be unnecessary. The parameter vector $\vec{p}$ is a piecewise linear model for values in between individual parameters a linear interpolation routine is utilised. Linear interpolation is utilised as it is computationally efficient and easily defined. The use of splines for interpolation was unsuitable as the definition of splines requires several points. This would cause problems during the flight when parameters became inactive leading to insufficiently defined steering command profiles. A parameter was found to be unnecessary when it lay linearly in between two other parameters as demonstrated by the circled parameters in figure 5.2. The user would continue to remove parameters until no more unnecessary parameters remained. The guidance was then tested to determine if there were enough parameters to cope with off-nominal conditions. It is important to note that the selection of the number of parameters is not an optimisation parameter and is purely performed by the user.

Care must be taken by the user not to reduce the number of parameters to a point where the guidance is unable to cope with off-nominal conditions. With a low level of experience the user would be able to notice profiles that are suitable to be passed to the guidance to determine suitability under off-nominal conditions. When problems occurred the inclusion of an additional parameter generally provided the additionally ability to cope with the off-nominal conditions. However, typically additional param-

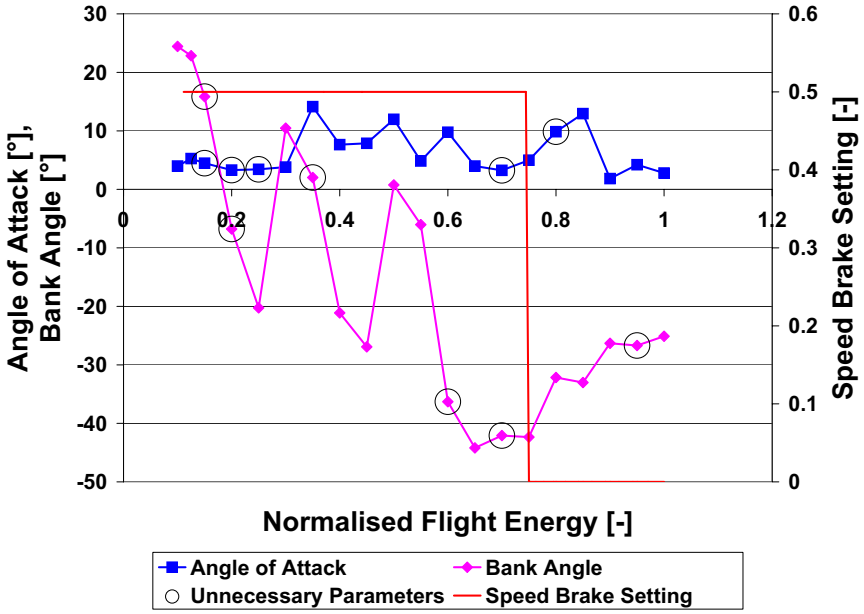

Figure 5.2: A parameter model with too many steering parameters

eters were not required since starting with a large number of parameters initially combined with the use of the cost functions discussed in section 5.6 provided significant trajectory margins to cope with off-nominal conditions.

Another method investigated for the development of reference trajectories involved the use of only a few parameters and the addition of parameters by the user when the optimiser had trouble finding solutions or required a large number of iterations. The solution was also evaluated with the guidance to determine the suitability of the trajectories under off-nominal conditions. The addition method did not work as effectively as the elimination method as it often required more time and effort to develop a suitable parameter model that was able to cope with off-nominal conditions.

For the Hopper vehicle the most suitable number of parameters was found to be 18; 7 for angle of attack, 7 for bank angle and 4 for speed brake setting. For the X-33 vehicle the most suitable number of parameters was found to be 20; 8 for angle of attack, 8 for bank angle and 4 for speed brake setting. The X-33 vehicle required more parameters as the mission profile had a larger velocity and altitude range which resulted in larger vehicle energy variations from the start to finish of the trajectory. The parameter sets provided here are considered the most suitable based on the experience gained through this research. Careful consideration was also given to the computational requirements

and accuracy of the solutions under off-nominal conditions. However, they are not the definitive number of parameters for the vehicles as there were also cases where a reduced or increased number of parameters provided similar guidance results under off-nominal conditions.

The spacing of the parameters with regards to normalised energy could also be varied by the user within the input files of the optimisation program. Within this research it was found that using *unequally* spaced parameters produced better results for the guidance (Chartres et al., 2005b). Although it was also possible for the guidance to cope with off-nominal conditions if the parameters were *equally* spaced the results were improved when utilising *unequally* spaced parameters. During the initial portions of the trajectory the final condition errors caused by off-nominal conditions can be easily adapted too because there are still a sufficient number of active parameters. However, during the closing stages of flight there are less active parameters remaining that can be modified to account for off-nominal conditions. Therefore *unequally* spaced parameters were utilised with more parameters defined towards the end of the trajectory. With more parameters still active towards the end of flight the guidance is better able to update the profile and cope with off-nominal conditions. The unequally spaced parameters were used for both the Hopper and X-33 vehicles.

5.3 Sensitivity Studies

The influence of off-nominal conditions during the terminal area flight phase has to date been unavailable in public literature. Consequently there is insufficient information on the size of errors caused by the various off-nominal conditions. In order to understand which conditions have the greatest effect on a vehicle during terminal area flight phase sensitivity studies were performed. Sensitivity studies also provide knowledge about the kinds of margins that should be designed into trajectories to cope with the dispersions caused by off-nominal conditions.

The sensitivity studies were performed using an initial optimised solution (reference trajectory). The optimisation was switched off, which changes the optimisation program into a simulation tool since it no longer has the ability to perform trajectory modifications to cope with the off-nominal conditions. Thus the trajectories are with-

out any updates and follow the reference commands even with off-nominal conditions present. The off-nominal conditions given in table 5.1 were applied to the Hopper vehicle and mission. The HWM model uses a standard setting with: Date=0, Time=14:00 (50400 seconds), 3 month average radiation flux=150, previous day radiation flux=150 and Daily magnetic index=4.

The results are presented in table 5.2 and figures 5.3 and 5.4 show the ground tracks for the various off-nominal conditions. The results in table 5.2 indicate that the Hopper vehicle mission is sensitive to the model errors for vehicle aerodynamics, atmospheric density and mass. As the mass of the vehicle is well known before flight and after payload jettison the mass variations should not cause a problem. The errors in vehicle aerodynamics and density could be reduced in the guidance by having more accurate vehicle and atmospheric models. For the aerodynamics this would require a larger amount of costly wind tunnel and computational fluid dynamic studies. However, there would still be uncertainties in the models due to the complexity of accurately modelling the real world vehicle aerodynamics, as observed with the US Shuttle (Siemers and Larson, 1979; Cobleigh, 1998). Provided the guidance is able to adapt to the errors contained in table 5.2 this additional testing may not be required.

The initial condition variations also provide some significant errors indicating that the Hopper vehicle mission is sensitive to modelling errors and mission dispersions. Figures 5.3 and 5.4 show the effects on the vehicle ground track due to the model errors and initial condition variations, respectively. The target miss is significantly more pronounced for the vehicle modelling errors, however the initial velocity variations

Conditions	Values
Mass M	$\pm 10\%$
Drag coefficient C_D	$\pm 10\%$
Lift coefficient C_L	$\pm 10\%$
Density ρ	$\pm 10\%$
Winds	HWM 1993
Initial altitude h	$\pm 2500\,m$
Initial velocity v	$-42/58\,m/s$
Initial flight path angle γ	$+10^\circ / -20^\circ$
Initial azimuth χ	$\pm 20^\circ$

Table 5.1: Hopper vehicle sensitivity study for off-nominal conditions

		Errors			
Conditions	Target miss (km)	v (m/s)	T (s)	$\gamma(^\circ)$	$\chi(^\circ)$
Mass +10%	8.089	4.341	-17.925	0.279	12.559
Mass -10%	9.321	-4.596	19.891	-0.320	-14.789
C_D +10%	7.861	-0.596	-33.799	-1.462	14.568
C_D -10%	10.783	0.624	41.736	1.521	-18.214
C_L +10%	18.965	-3.593	57.791	1.069	-31.502
C_L -10%	16.190	4.107	-54.814	-1.497	28.437
ρ +10%	8.445	-4.162	18.055	-0.288	-13.401
ρ -10%	8.910	4.814	-19.791	0.298	13.824
Winds	1.306	1.513	-1.632	0.298	1.628
Initial $v = 400$ m/s	6.164	-3.859	-10.589	0.840	-13.593
Initial $v = 500$ m/s	11.546	5.606	10.494	-1.409	23.098
Initial h +2.5 km	3.908	5.044	29.858	-1.267	7.176
Initial h −2.5 km	0.708	-5.402	-44.034	1.158	3.837
Initial χ +20°	6.626	-0.0170	0.127	0.0199	19.874
Initial χ −20°	6.675	0.0098	-0.0843	-0.0203	-19.999
Initial $\gamma = 0°$	2.752	0.0062	10.737	-0.0058	-5.642
Initial $\gamma = -30°$	5.748	-0.0102	-23.828	0.0162	12.618

Table 5.2: Effect of off-nominal conditions on the Hopper vehicle final conditions without guidance

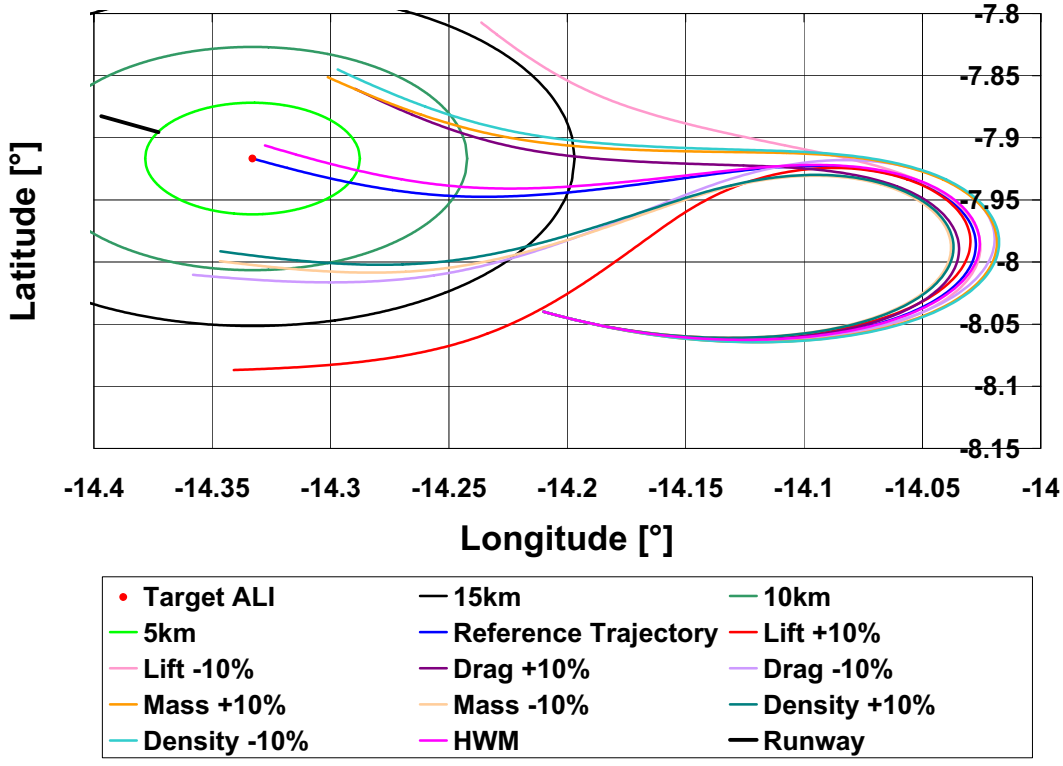

Figure 5.3: Model error effects for a Hopper vehicle trajectory without guidance

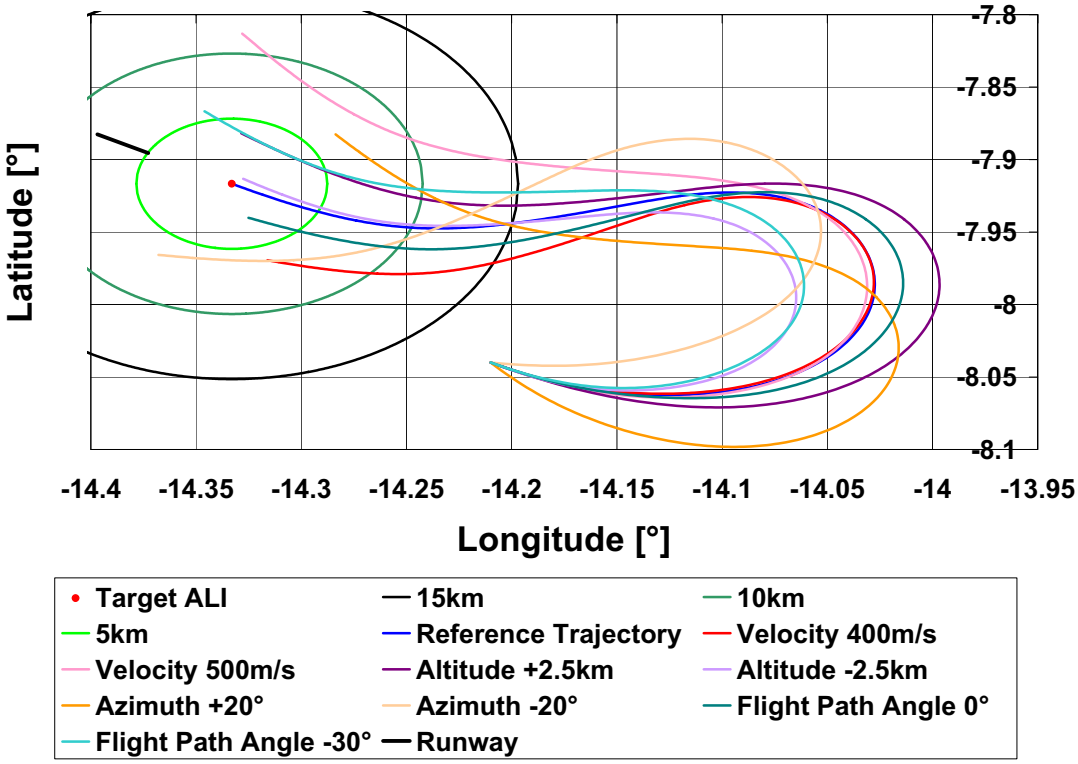

Figure 5.4: Initial condition effects for a Hopper vehicle trajectory without guidance

also produce a large target miss. The target miss for the aerodynamics and density errors were expected as these applied errors significantly change the forces experienced during flight and therefore the range of the vehicle. The variation in the initial velocity results in different aerodynamic characteristics since the vehicle is at a higher or lower Mach number.

The large velocity errors are due to the initial altitude and velocity variations. The variations in initial altitude and velocity modify the vehicle's energy condition and results in decreased or increased vehicle energy at the start of flight. Since the steering parameters are based on normalised energy the steering command profile is modified with respect to the ground track. This results in the profiles seen in figure 5.4.

The flight path angle errors have similar influences to target miss and velocity error, namely vehicle aerodynamics and initial altitude and velocity. There is a coupling between the vehicle velocity and the flight path angle which would explain why applied errors in vehicle velocity also result in final flight path angle errors. The flight path angle errors are however quite small and within tolerance values indicating that

the off-nominal conditions have less effect on the final flight path angle than the target miss or final velocity errors.

The azimuth errors are most likely a side effect of the variations in the vehicle steering profiles for the ground track. The ground tracks of figures 5.3 and 5.4 show how the final azimuth is affected by the overall trajectory. The guidance should be quite capable of adapting the final azimuth errors using modifications to the steering commands, specifically bank angles.

A similar sensitivity study was performed on the X-33 vehicle and mission to investigate the major influences and to determine if they are similar to those observed for the Hopper vehicle. The X-33 vehicle sensitivity study utilised the conditions provided in table 5.3. The results for the X-33 vehicle are given in table 5.4 and figures 5.5 and 5.6. The results indicate that the target miss is sensitive to the aerodynamic, density, mass and initial condition errors. The major influences are similar to the Hopper vehicle and mission indicating that they are common for the terminal area flight phase and/or this problem formulation.

The target miss for the X-33 vehicle is largely influenced by the lift coefficient errors and variation in the initial azimuth. The influence of the initial azimuth as seen in figure 5.6 appears to be more related to the reference trajectory and initial solution than a sensitivity of the terminal area flight phase. The guidance should be able to easily adapt to the error caused by the initial azimuth using modifications to the bank angle steering commands. The X-33 vehicle however appears to be sensitive to the lift coefficient errors which influence the vehicle lift force and therefore range completely

Conditions	Values
Mass M	$\pm 10\%$
Drag coefficient C_D	$\pm 10\%$
Lift coefficient C_L	$\pm 10\%$
Density ρ	$\pm 10\%$
Winds	HWM 1993
Initial altitude h	$\pm 1828.80\,m$
Initial velocity v	$\pm 30\,m/s$
Initial flight path angle γ	$\pm 4^\circ$
Initial azimuth χ	$\pm 15^\circ$

Table 5.3: X-33 vehicle sensitivity study for off-nominal conditions

modifying the ground track for the initial steering parameters as can be seen in the trajectories of figure 5.5.

The final velocity has large errors for the lift coefficient, density and mass errors. The lift coefficient errors result in different aerodynamic characteristic for the same set of steering parameters this influences both the final velocity and flight path angle. The other final flight path angle errors are quite small and below the tolerances given in table 4.8.

Similarly for the Hopper vehicle, the mass of the X-33 vehicle during the terminal area flight phase is known to a much greater accuracy than the errors contained in table 5.3. However the effects of varying the vehicle mass are important in the early design phases where the vehicle mass and fluctuate due to structural or sub-system modifications. The density error seems quite large but looking at the profiles in Appendix A.2 it is possible to have such large errors but perhaps not constant for the entire flight. The final azimuth errors similar to the Hopper vehicle and mission seem to be more a side effect of the trajectory profiles as seen in figures 5.5 and 5.6.

		Errors			
Conditions	Target miss (km)	v (m/s)	T (s)	$\gamma(^\circ)$	$\chi(^\circ)$
Mass +10%	5.8462	9.6593	-20.8464	-2.8710	-8.7046
Mass -10%	7.1756	-11.9421	24.7113	3.5635	10.4595
C_D +10%	2.0116	-4.3097	-27.4631	-2.1252	-3.5877
C_D -10%	3.6735	4.6193	34.8896	2.2644	3.5998
C_L +10%	9.9359	-7.1437	55.7444	5.7466	13.4844
C_L -10%	12.7016	30.1292	-231.3444	-25.6839	-70.0464
ρ +10%	6.4657	-10.7384	22.2724	3.2101	9.4190
ρ -10%	6.4223	10.6245	-22.9700	-3.1519	-9.5789
Winds	2.8669	4.6525	3.9922	0.8882	6.5197
Initial v +30m/s	4.2763	0.9876	-0.3840	2.6249	14.7896
Initial v -30m/s	4.5901	-1.8480	6.8972	-2.3991	-16.4244
Initial h +1828.8m	5.3471	-1.0825	-2.2301	1.6636	11.0836
Initial h -1828.8m	5.9790	0.7412	1.3381	-1.6052	-12.0747
Initial χ $+15^\circ$	14.0874	0.0162	3.3410	0.0346	15.1401
Initial χ -15°	14.0993	-0.0081	3.0299	-0.0437	-15.1094
Initial γ $+4^\circ$	5.7808	-0.0066	11.7488	0.0036	0.6338
Initial γ -4°	5.5701	0.0064	-6.0275	-0.0025	-0.2395

Table 5.4: Effect of off-nominal conditions on the X-33 vehicle final conditions without guidance

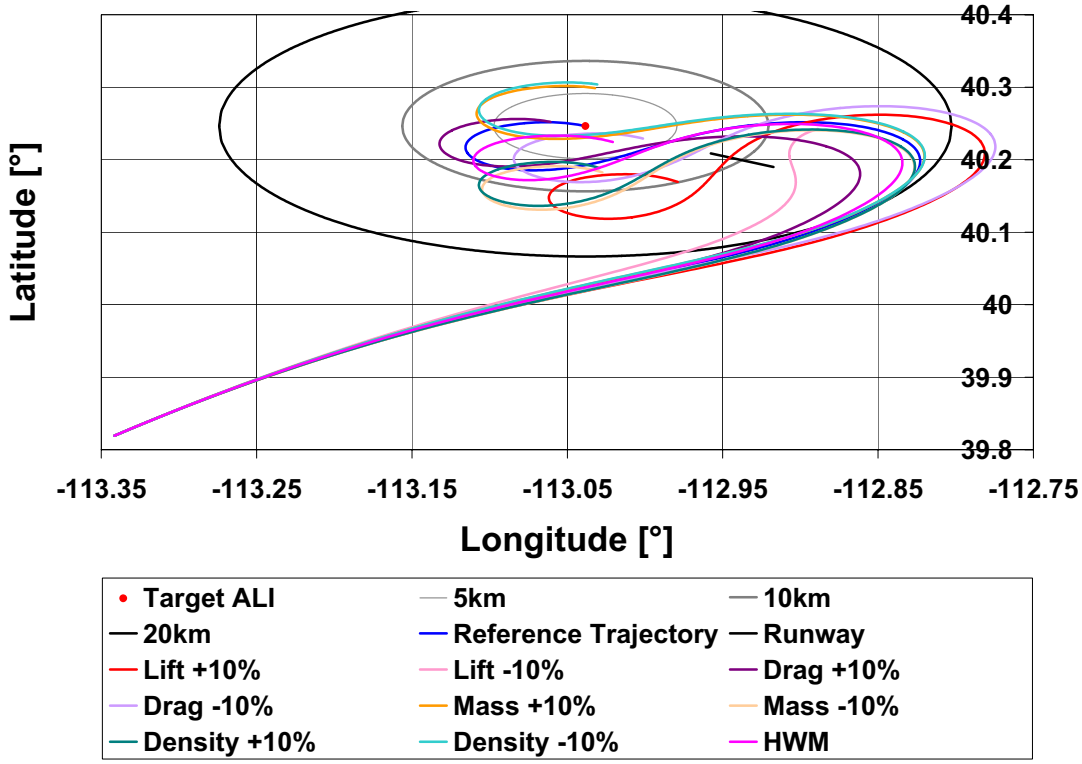

Figure 5.5: Model error effects for a X-33 vehicle trajectory without guidance

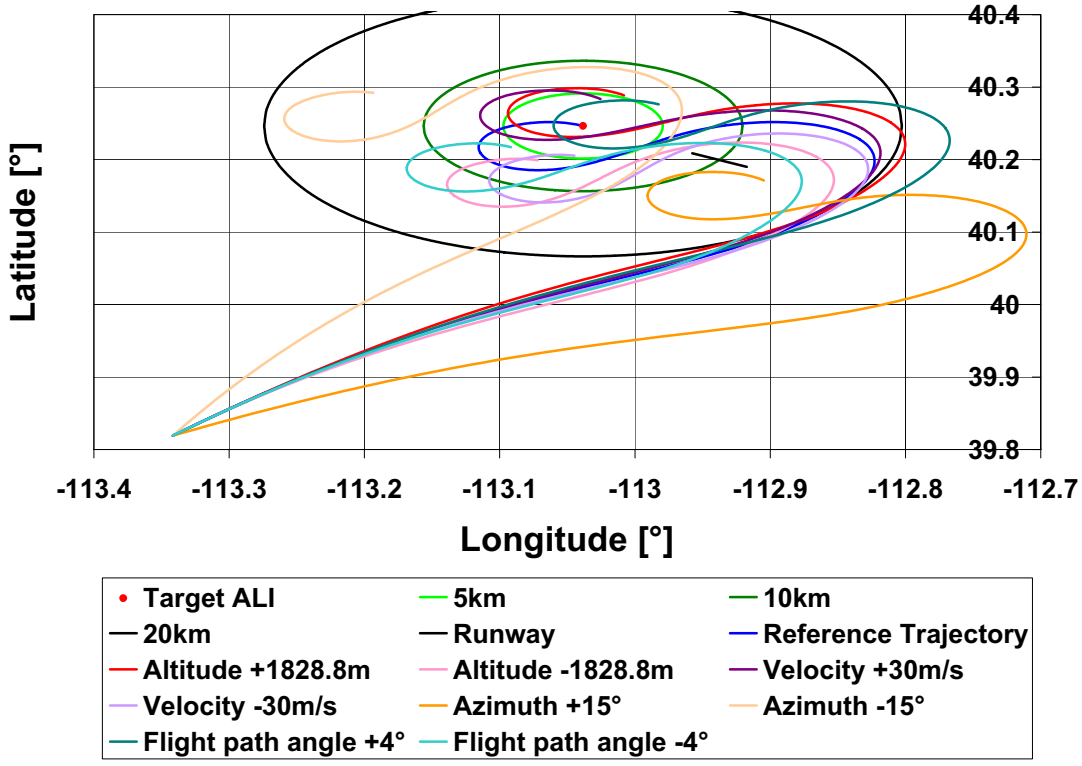

Figure 5.6: Initial condition effects for a X-33 vehicle trajectory without guidance

By utilising two different vehicles and missions for the sensitivity studies the common influences can be identified as generic for the terminal area flight phase instead of vehicle or mission related. However, it is also possible that the sensitivities result from the parameterisation method used within this study. The results for the X-33 vehicle are different to those of the Hopper vehicle, which indicates that some of the sensitivities are vehicle and mission related. There are however some common major influences for the terminal area flight phase. These are the aerodynamic model errors especially related to the lift coefficient errors that produce large target miss and final velocity errors.

Although the modifications to the drag coefficients still produce errors they are not as large as the errors for the lift coefficient. Consequently it seems for both vehicles and therefore generally for the terminal area flight phase that drag errors are less influential than lift errors. That is useful as generally the uncertainties in wind tunnel aerodynamic test are greater for the drag coefficient due to the mounting boom, Reynolds number, real gas and tunnel blockage effects (Cobleigh, 1998). Therefore some modelling errors in drag coefficients can be tolerated but attempts should be made to determine the lift coefficients with an increased accuracy.

The initial velocity errors also seem to have a large influence on the target miss for both vehicles and missions. Since the vehicle velocity heavily influences the vehicle energy state this influence is more likely related to the problem formulation and parameterisation method than a sensitivity of the terminal area flight phase.

5.4 Trajectory Margins

The sensitivity studies of section 5.3 revealed that off-nominal conditions can produce large disturbances in the final conditions without an active guidance system to update the trajectory. A guidance system however can only update the trajectory if there are sufficient margins included within the trajectory or mission. For example if the vehicle is flying at the maximum lift-to-drag ratio it is impossible that the guidance will be able to increase the flight distance since the initial solution was already at the maximum range. Therefore a method was devised in order to ensure that the trajectories had sufficient margins to cope with the expected off-nominal conditions.

The Shuttle TAEM and Buran guidance methods incorporate margins by including the ability to select different locations for the HAC and the use of S-turn manuevers (Ehlers and Kraemer, 1977; Moore, 1991; Kirpischikov, 1997). An S-turn is a series of turns towards and away from the runway performed by re-entry vehicles during the terminal area flight phase which produce an 'S' shaped curve in the ground track. S-turns are often used as a method to dissipate excessive energy at the terminal area interface (Ehlers and Kraemer, 1977). However, they can also be used as a method to later extend the ground track ensuring there is sufficient energy (Kirpischikov, 1997). By eliminating or reducing the size of an S-turn in the trajectory the energy that would have been dissipated during the manoeuvre is now utilised for increasing the range of the vehicle.

The implementation of S-turns was investigated during optimisation however it was found to be problematic for the optimisation method used (Chartres et al., 2005b). The forced inclusion of S-turns within the trajectory via several methods caused the optimiser to include the S-turn as an essential portion of the trajectory thus eliminating S-turn margins within the trajectory. The inclusion of S-turns also eliminated the flexibility in the trajectory design and imposed similar limitations to other methods, namely the inclusion of several flight phases and geometric constraints on the ground track (Chartres et al., 2005b).

The terminal area guidance for the X-33 vehicle discussed in Kluever and Horneman (2005) utilises modifications to the size of the HAC and turns within the trajectory segments to provide margins. The method of providing margins in the trajectory by resizing or reshaping the trajectory has been included in almost all terminal area guidance schemes from those initially developed for the NASA lifting bodies (Hoffman et al., 1970) to the latest schemes utilising fuzzy logic (Burchett, 2004). The method of resizing and reshaping trajectories to provide margins was often implemented through the inclusion of S-turns in the trajectory. However, more recent work utilising online trajectory propagators have extended the resizing and reshaping to include the HAC radius, trajectory segments and curve radii (Barton et al., 2002; Camara et al., 2002b; Büchner, 2003; Burchett, 2004; Kluever and Horneman, 2005). The modification of the trajectory prior to the terminal area interface is often used effectively to eliminate errors that occur at the terminal area interface.

The online update scheme used within this research updates the trajectory in real time to cope with off-nominal conditions via the restoration steps of the GPA contained in the guidance program. The large deviations in final conditions caused by the expected off-nominal conditions indicate that there should be additional attributes or methods included in the initial solution to provide additional margins.

The US Shuttle TAEM guidance method utilises the modulation of the dynamic pressure and speed brake to control the energy state of the Orbiter (Ehlers and Kraemer, 1977). The use of a speed brake for the terminal area flight phase allows rapid modification of the vehicles drag characteristics. By increasing the speed brake setting the drag of the vehicle is increased and therefore the amount of energy dissipation is also increased. The simulations performed in section 5.3 showed that significant changes in range and the final conditions could be achieved via modification of the vehicle's aerodynamic characteristics. Consequently the utilisation of a speed brake was investigated as a method of including margins within the trajectory (Chartres et al., 2005b).

The Hopper vehicle model available in the public domain for simulations did not include a speed brake model therefore an additional model had to be developed. The current study is however only a 3 degrees of freedom study and so an approximate model was valid enough to provide a proof of concept. Before the proposed guidance concept can be flight tested an accurate model of the speed brake and full 6 degrees of freedom studies would need to be performed. The speed brake model and formulation is discussed in section 3.2.3 and the full model used in this study is provided in Appendix C.

Although the speed brake setting, δSB, is included within the aerodynamic and steering models it is not an active optimisation parameter. To ensure the inclusions of margins within the trajectories the speed brake setting, δSB, is set to 0.5 representing 50% of the total additional drag available from the speed brake. This allows the speed brake setting to be modulated by 50% in either direction to decrease or increase the vehicles energy dissipation rate as required. The guidance program discussed in Chapter 6 utilises the speed brake setting as an active steering parameter and as such is able to adjust the value of the setting during flight to adapt to off-nominal conditions.

Section 6.1.6 in the guidance results further discusses the influence of the speed

brake on the guidance and provides some results which do not include the speed brake as a steering parameter. A description of the derivation of the model and the actual model utilised is provided in Appendix C.

5.5 Trajectory Design

Traditional terminal area flight phase trajectories have incorporated a heading alignment cylinder (HAC). These were first implemented in the terminal area energy management of the US Shuttle Orbiter (Ehlers and Kraemer, 1977). The current problem formulation allows for different types of trajectories without the restriction of including a HAC. This makes the trajectory more flexible but it also makes it difficult to determine what are the most suitable trajectories for the terminal area flight phase since there are no baseline trajectories without a HAC for comparison (Chartres et al., 2005b).

There are several criteria which specify a suitable trajectory for the terminal area flight phase. The trajectory must:

- Deliver the vehicle to the final conditions within tolerance;
- Provide the smallest error for the final conditions;
- Provide sufficient margins for off-nominal conditions;
- Minimise the dynamic pressure and vehicle loads experienced during flight;
- Provide a steering profile that can be readily followed by the guidance computer.

The margins were previously discussed in detail in section 5.4. The reduction of the final conditions errors, dynamic pressure and vehicle loads is discussed in more detail in section 5.6.

The method for determining a suitable trajectory generally requires input and evaluation from an experienced user. Although the benefit of having an experienced user cannot be discounted this study has looked at a method for generating trajectories that do not require considerable input and evaluation from a well experienced user. This was achieved by utilising the cost function, discussed in section 5.6, as a design criteria and found to work quite effectively for both vehicles and missions investigated. By looking at the output value of the cost function a user can ascertain with minimal effort

if the trajectory is suitable as a reference trajectory for the guidance. Although a user is still required to evaluate the suitable trajectories this evaluation process is simplified as much of the trajectory design requirements have already been incorporated into the cost functions.

5.6 Cost Functions

The optimisation of a trajectory requires a specified cost function as a performance measure to evaluate the various solutions. The cost function, $F(\vec{p})$ is minimised by the optimiser however the cost function can also be maximised by changing the sign convention such that $F = -F(\vec{p})$.

Careful consideration must be given to the cost function as the solution from the optimiser depends on the chosen performance measure. For example if the performance measure was to maximise the flight time the optimal trajectory which would result in the vehicle flying a large range at the maximum lift-to-drag ratio in order to obtain the largest flight time (Grubler, 2001). Similarly a cost function to minimise the flight time would result in a short range and flying at the maximum dynamic pressure or drag to dissipate the vehicles energy quickly (Grubler, 2001). Both of these cases are undesirable in the presence of off-nominal conditions as the designed trajectory might not be able to adjust in the presence of such disturbances as head or tail winds (Grubler, 2001; Chartres et al., 2005b).

The final constraints, $g_i(\vec{p}) = 0$, are equality restrictions in the problem formulation and the optimiser automatically reduces the errors. However, the in-flight constraints, $g_j(\vec{p}) \leqslant 0$, are inequality restrictions and therefore provided the values are not exceeded the optimiser does not minimise their value.

For the terminal area flight phase of the Hopper and X-33 vehicles the in-flight restrictions were the dynamic pressure and vehicle loads. With the problem formulation given in section 3.1 it is possible to have trajectories where the vehicle is operating at the maximum vehicle loads or dynamic pressure. The operation at maximum levels is undesirable in the presence of off-nominal disturbance which could cause violation of the in-flight restrictions. In the cases of dynamic pressure or vehicle loads this can result in the damage or even loss of the vehicle. Therefore it is often wise to include

the minimisation of the in-flight constraints within the cost function.

The upper limit for vehicle loads and dynamic pressure for the Hopper vehicle given in table 4.2 are quite large for a re-entry vehicle and were seldom reached therefore their inclusion in the cost function was unnecessary.

The X-33 vehicle however had more critical limits as seen in table 4.4. These limits especially the dynamic pressure were often reached during optimisation and trajectory design, so careful consideration was required when designing the cost function to ensure that it included the dynamic pressure and vehicle loads.

To ensure that the maximum dynamic pressure would not be reached during optimisation of the X-33 vehicle trajectory it was determined that including a cost function that provided a dynamic pressure margin was required. To maximise the margin between the dynamic pressure limit and the maximum dynamic pressure experienced, equation 5.5 was utilised as the cost function.

$$F_{\text{Dynamic Pressure}} = -\left[\left(\frac{1}{2}\rho v^2\right)_{Lim} - \left(\frac{1}{2}\rho v^2\right)_{Max}\right] \tag{5.5}$$

Where $\left(\frac{1}{2}\rho v^2\right)_{Lim}$ is the dynamic pressure limit and $\left(\frac{1}{2}\rho v^2\right)_{Max}$ is the maximum dynamic pressure experienced by the vehicle for each time step. The negative modifier results in the optimiser maximising the value instead of the standard minimisation.

Within the optimisation program there is a load controller, discussed in section 3.1.7. The load controller ensures that the commanded angle of attack values do not result in the vehicles violating their load restrictions. However, similar to the dynamic pressure it is undesirable to design a trajectory where the vehicle is operating at the upper load limit or that the load controller must be active for a large portion of the flight. In these cases the guidance does not have the flexibility to increase the angle of attack and so may not be able to effectively adapt to off-nominal conditions experienced. Therefore it is useful to try and reduce the maximum load experienced by the vehicle during trajectory design.

The X-33 vehicle utilises equation 5.6 in the cost function to minimise the maximum loads experienced during trajectory design (Schöttle, 1988; Telaar, 2005).

$$F_{\text{Load}} = \left(\frac{\sqrt{L^2 + D^2}}{M}\right)_{Max} \tag{5.6}$$

Where L and D are the lift and drag forces respectively, M is the vehicle mass and the subscript Max defines the maximum value. Due to the large value for the in-flight loads for the Hopper vehicle it was not necessary to include equation 5.6 within the cost function as the load limits were never reached during trajectory design.

Work such as Kluever and Horneman (2005) revealed that a 'bang bang' (rapid step) steering command profile seemed the most suitable for the terminal area flight phase when using a HAC type trajectory. However, since the optimisation allows for trajectories other than the HAC type it is difficult to determine what a suitable steering profile should be. When considering the use of the trajectory as a reference trajectory for the guidance program the profile should be such that it can be easily followed. Therefore the steering profile should minimise the effort required to switch between two consecutive parameters, control effort. The cost function is referred to as the control effort cost function, $f_{Control}$, defined in equation 5.7 which is a modified version of the cost function used in Telaar (2005).

$$F_{Control} = \sum_{i=1}^{n_\alpha - 1} \left(\frac{p_{\alpha(i+1)} - p_{\alpha(i)}}{t_{\alpha(i+1)} - t_{\alpha(i)}} \right)^2 + \sum_{i=1}^{n_\mu - 1} \left(\frac{p_{\mu(i+1)} - p_{\mu(i)}}{t_{\mu(i+1)} - t_{\mu(i)}} \right)^2 \tag{5.7}$$

Where n is the number of parameters, $p_{(i)}$ is the value of the ith parameter, t_i is the value of the normalised energy for the ith parameter and the subscripts α and μ represent the angle of attack and bank angle respectively. Note here that the speed brake parameters are not included in the cost function since during optimisation they are kept constant at 0.5 to provide margins in the trajectory design. By minimising the control effort a smooth steering parameter model is produced which allows for easy trajectory following by the guidance.

The Hopper vehicle did not have problems with dynamic pressure and vehicle loads therefore another cost function was required in order to have a design parameter for selecting suitable trajectories. A key requirement for the Hopper vehicle was to ensure that there was enough range to allow for the off-nominal conditions. The flight range of the Hopper vehicle is related to the flight time. Experience from numerous simulations was then utilised to determine a suitable flight time that allows sufficient margins.

The Hopper vehicle utilises the cost function give in equation 5.8.

$$F(\vec{p})_{\text{Hopper}} = 1.0 \cdot F_{\text{Control}} + 0.1 \cdot \exp\left(\frac{|400 - t_{end}|^2}{1100}\right) \tag{5.8}$$

Where t_{end} is the final flight time. This provides a suitable trajectory reducing the required control effort and ensuring a flight time that provides sufficient margins for off-nominal conditions. The control effort, F_{Control}, is included to ensure a smooth profile.

Using the flight time is very dependent on the type of vehicle and mission and therefore the cost function and trajectory design parameter would need to be modified for each vehicle and mission. An experienced user would then be required to develop the design parameter which reduces the advantages of other less experienced users being able to utilise the design parameter. The research conducted on the X-33 vehicle provided a more suitable cost function for generic reusable launch vehicles.

The cost function utilised for the X-33 vehicle trajectory design given in equation 5.9 is a combination of several of the cost functions.

$$F(\vec{p})_{\text{X-33}} = 1.0 \cdot F_{\text{Dynamic Pressure}} + 10.0 \cdot F_{\text{Load}} + 1.0 \cdot F_{\text{Control}} \tag{5.9}$$

Where $F_{\text{Dynamic Pressure}}$ is the negative dynamic pressure margin from the in-flight limit, F_{Load} is the maximum loads experienced and F_{Control} is the control effort each defined in equations 5.5, 5.6 and 5.7 respectively. The X-33 vehicle cost function maximises the dynamic pressure margin and minimises the vehicle loads and control effort. Note in equations 5.8 and 5.9 the different modifiers for each element. The modifiers are used as a method to scale the various influences such as dynamic pressure and control.

5.7 Reference Trajectories

The selection of an appropriate reference trajectory is a difficult task as there are many considerations, which are outlined in section 5.5. The utilisation of the cost functions discussed in section 5.6 ensures that a majority of the requirements are considered. However, the problem formulation discussed in Chapter 3 creates a very flexible solution environment. The problem formulation does not require the fixed ground tracks, way points, altitude or drag profiles utilised in other methods discussed in Chapter

2. Instead allowing the trajectory to be designed using the steering commands results in a flexibility to produce various different types of ground tracks and vehicle state profiles.

The sub-orbital Hopper vehicle has a maximum achievable glide range of approximately 115 km for the terminal area flight phase; considerably more range than required. However, the additional range provides a benefit to the guidance updates in the presence of off-nominal conditions. A result of the large range available was that there were several different types of ground track and steering parameter profiles that would provide a solution. This flexibility resulted in some ground tracks such as those shown in figure 5.7 that were unsuitable as a reference trajectory. Some ground tracks included complex turns that would be difficult for the guidance to track under off-nominal conditions. Another type of ground track had the vehicle flying away from the runway and performing a sharp turn around manoeuvre followed by a long flight back towards the runway. This long flight is unsuitable in the presence of off-nominal conditions which can result in a change in the range capabilities of the Hopper vehicle and possibly failure to meet the target conditions. Although the use of the cost functions in section 5.6 eliminated the majority of these types of ground tracks it was still possible to have complex ground tracks that are harder for the guidance to track than a smooth curving ground track.

A common element of the trajectory solutions for the Hopper vehicle was the rapid transition to sub-sonic speeds. Figure 5.8 shows how the velocity and energy is rapidly decreasing during the early portion of the trajectory. The switch to sub-sonic speeds provided more favourable aerodynamic conditions with a larger lift-to-drag ratio. The improved lift-to-drag ratio at sub-sonic speeds provides the Hopper vehicle with increased manoeuvrability and range which is useful at the early stages of the flight where the vehicle is heading away from the target and must turn around.

The flight path angle and velocity also experienced some coupling during flight. A common occurrence towards the end of flight was that the velocity would decrease below the required value then the flight path angle would be reduced to reach the target condition and consequently the velocity would increase to the required value. This coupling behaviour can be seen in figure 5.8.

The selected reference trajectory for the Hopper vehicle mission is shown in figure

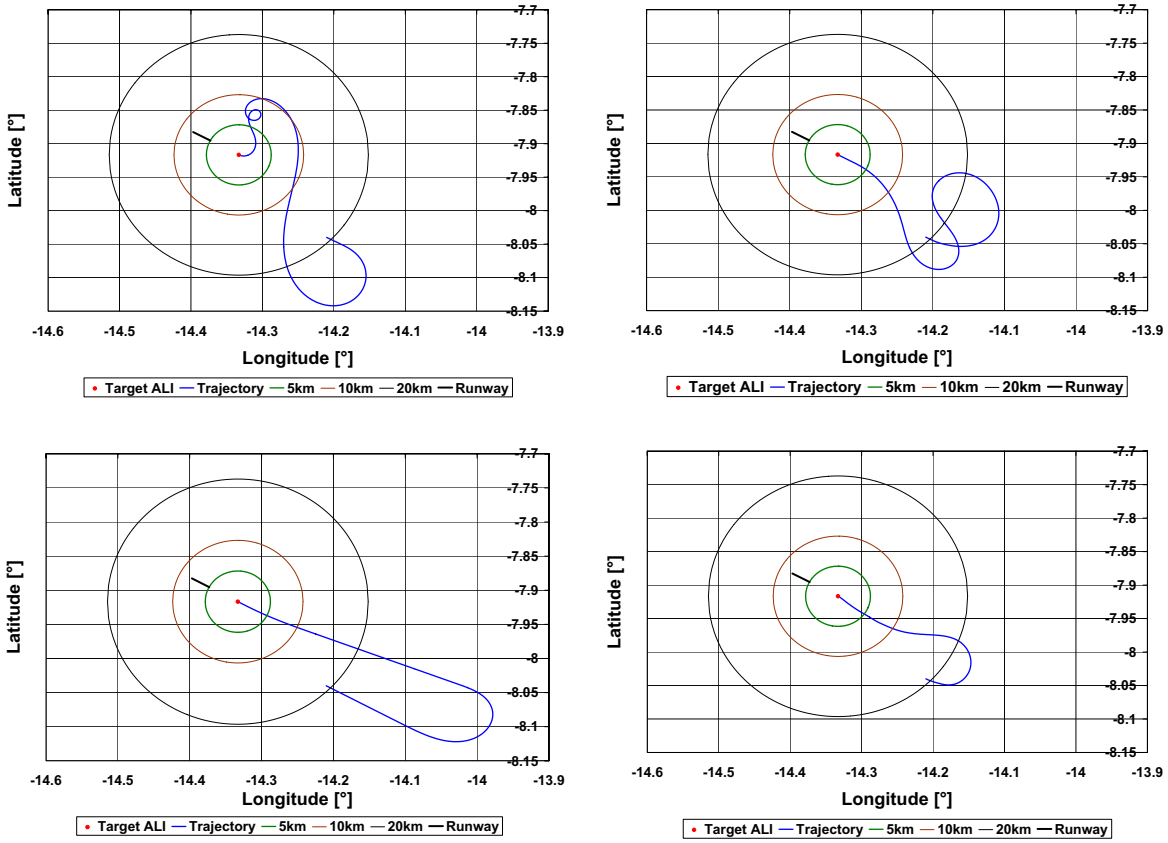

Figure 5.7: Additional Hopper vehicle trajectory solution ground tracks produced during optimisation studies

5.8 including the ground track, steering command and vehicle state profiles. Note that the azimuth is shown using a scale between 0 and 360° so the sharp jump seen in the profile is a result of the definition and not actually present in the trajectory. The steering commands are also shown over normalised energy and therefore progress from right to left. The ground track is a smooth gentle curve which only requires minimal bank angle and angle of attack commands providing margins for increased range or tighter turns in the presence of off-nominal conditions. The low bank angle at the end of the trajectory is also useful as transition to the approach and landing phase of the Hopper vehicle does not require large commands to align with the runway. The speed brake setting is also fixed at 50% to provide margins for energy dissipation rate and only becomes active at sub-sonic speeds.

The research performed on the Hopper vehicle was applied to the generation of the X-33 vehicle reference trajectory. The cost function for the X-33 vehicle discussed

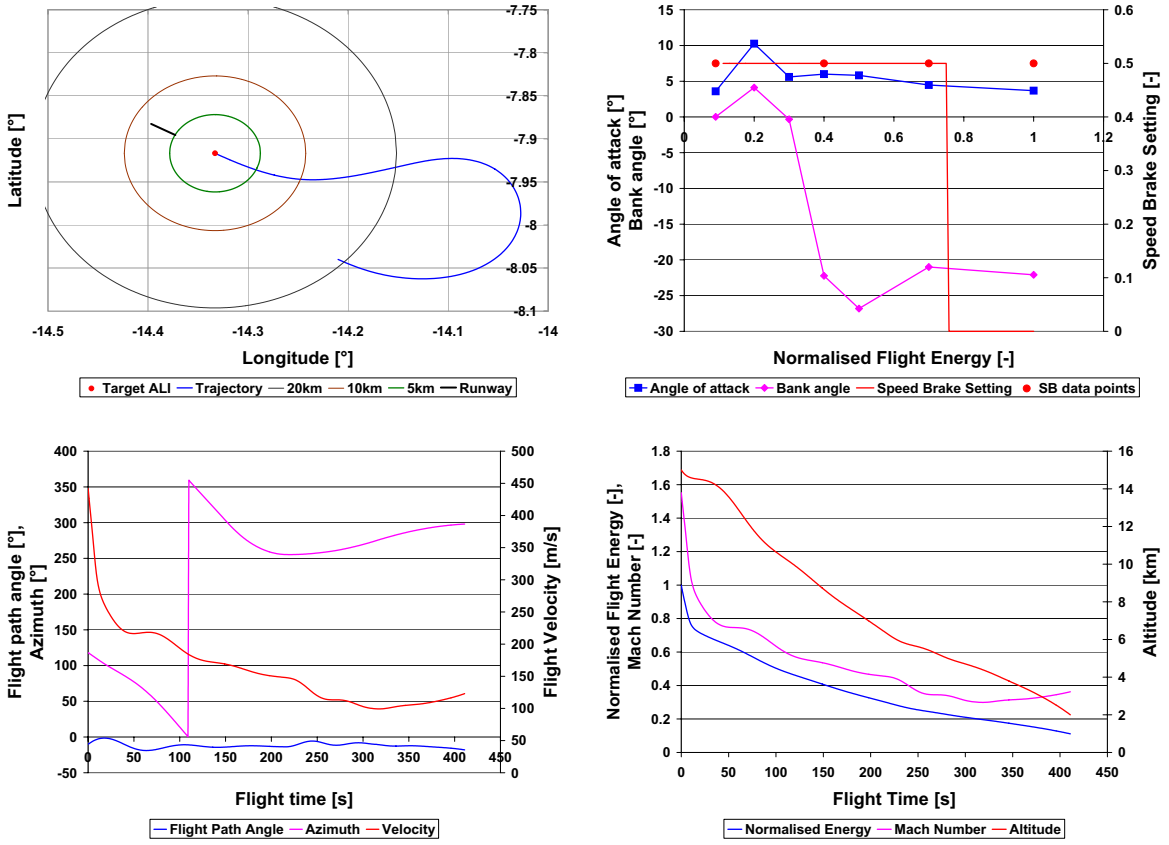

Figure 5.8: The ground track, state and steering command profiles for the Hopper vehicle reference trajectory

in section 5.6 eliminated many of the unsuitable trajectories. However, similar to the Hopper vehicle the X-33 vehicle also had several different types of possible trajectories. These are shown in figure 5.9. The solutions shown here were not selected because they either had too large vehicle loads or dynamic pressure values that did not provide margins for off-nominal conditions. Another problem with the solutions shown in figure 5.9 is that they had large steering commands that did not provide significant margins for tighter turns or increased range. The X-33 vehicle cost function also eliminated the majority of unsuitable trajectory types.

Attempts were made to produce a HAC type ground track for the X-33 vehicle by manipulating the input values to the optimiser. The optimiser however always found solutions of the types shown in figure 5.9. The difficulty of optimising the X-33 vehicle trajectory for a HAC type of solution was also discussed in Kluever and Horneman (2005) where a method of inverse dynamics was utilised with the flight path angle and

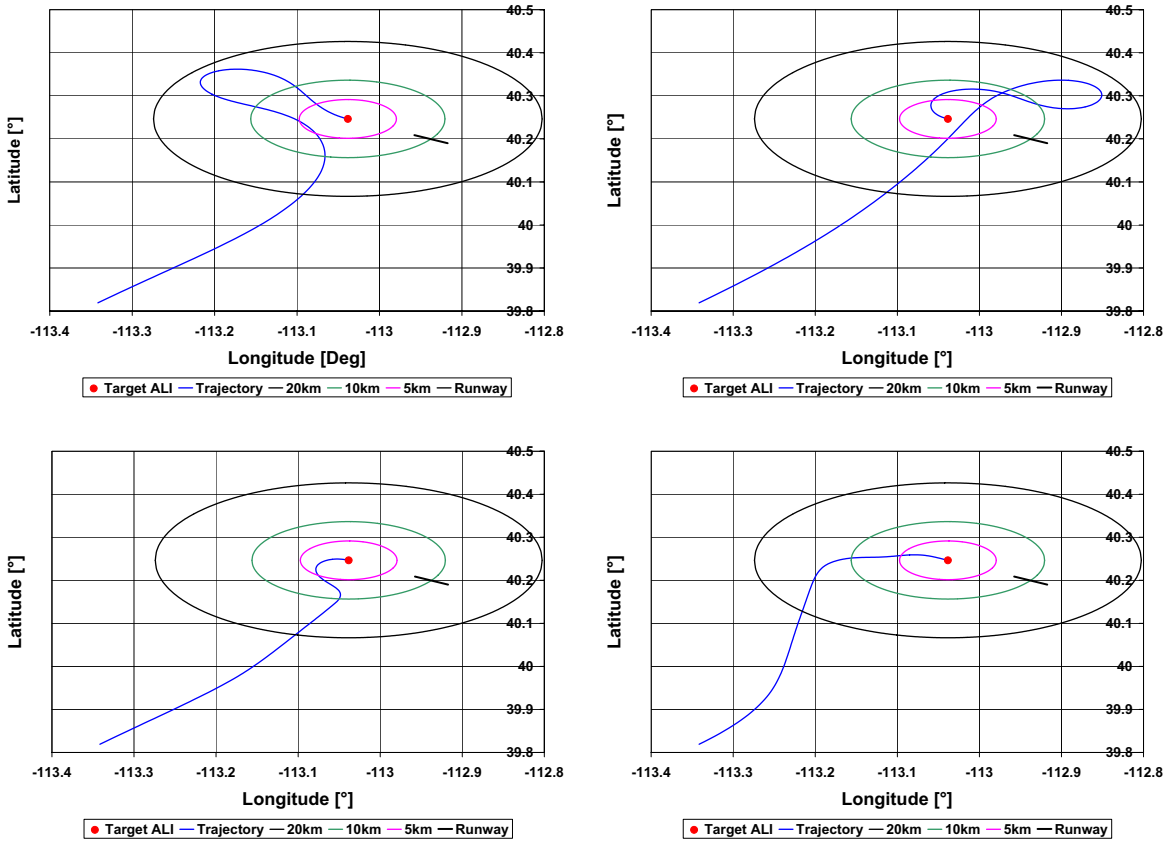

Figure 5.9: Additional X-33 vehicle trajectory solution ground tracks produced during optimisation studies

azimuth used as parameterisation variables. Instead of forcing a HAC type of ground track the formulation discussed in Chapter 3 allows for other solution types.

The selected reference trajectory for the X-33 vehicle is shown in figure 5.10 with the ground track, vehicle state and steering command profiles given. Note that the azimuth is again shown using a scale between 0 and 360° so there is no step in the profile. The steering commands are also shown over normalised energy and therefore progress from right to left.

Although the ground track looks somewhat unusual for a typical terminal area trajectory such as those discussed in Chapter 2 it is an effective ground track. The vehicle loads and dynamic pressure are quite low ensuring sufficient margins are provided for the off-nominal conditions. Looking at the steering commands in figure 5.10 the bank angles are larger than those of the Hopper vehicle. The larger bank angle commands are required for the manoeuvring of the X-33 vehicle due to the lower lift-to-drag ratio

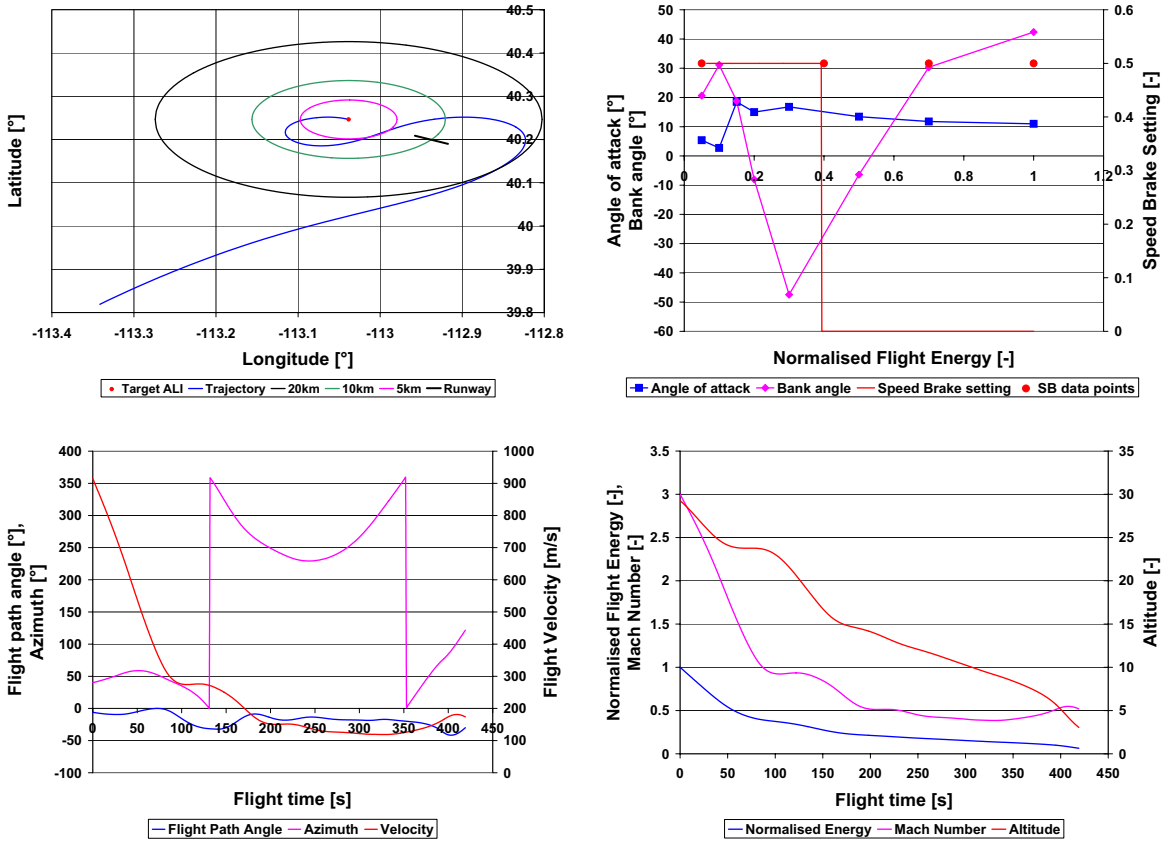

Figure 5.10: The ground track, state and steering command profiles for the X-33 vehicle reference trajectory

when compared to the Hopper vehicle.

The fast transition from supersonic speeds to subsonic speeds is also seen with the X-33 vehicle, indicating that this is common for reusable launch vehicles during the terminal area flight phase. A requirement of Kluever and Horneman (2005) stated that the X-33 vehicle is to be at subsonic speeds during the HAC turn manoeuvre. The larger initial velocity of the X-33 vehicle mission results in a more pronounced occurrence of the transition behaviour as shown in figure 5.10. The large initial velocity of the X-33 vehicle also causes a large initial section of the trajectory which is only slightly curved despite the relatively large values of bank angle. The X-33 vehicle's flight path angle and velocity profiles also exhibit the coupling observed with the Hopper vehicle. The commonalities between the Hopper and the X-33 vehicles could be related to the terminal area flight phase or the method of problem formulation.

The reference trajectories discussed here are later loaded into the guidance program

as an initial solution. The use of the optimisation program to design the reference trajectories has been shown to work remarkably well. The use of the trajectory design criteria and cost functions discussed in sections 5.5 and 5.6 respectively allow a user to easily design and determine suitable trajectories for later use in the guidance program. The guidance program also has significant flexibility such that the *optimal* solution is not required, a reasonable solution is sufficient to ensure success.

5.8 Comparison to Other Methods

A direct comparison to previous trajectory design methods discussed in section 2.3 is difficult. The difficulties arise from the limited amount of published data on some methods, such as the Russian/Soviet Buran-Energia launch system. Other difficulties occur because there has been no effective comparative study of the methods utilising the same simulation environment and models. Many of the methods discussed in section 2.3 include various restrictions on the trajectories relating to the different vehicle types. The greatest problem in a comparison of the various methods is due to their self imposed limitations such as the inclusion of a HAC or redefinition of the flight dynamics in terms of variables, such as dynamic pressure. A direct comparison of the previous methods could be achieved using the same problem formulation such as cost function, in-flight restrictions, initial and final conditions, mission and vehicle models. However, by looking at the other methods and their results it is possible to determine general advantages and disadvantages of using one method over another.

In general there were two types of trajectory planners for the terminal area flight phase. The first trajectory planners designed trajectories off-line through a process of optimisation or a specific method utilising reference profiles and/or trajectory shaping. The second type of methods performed trajectory design entirely on-board utilising geometric segments, way points or calculated reference profiles based on constraints. There were however hybrids of these methods, such as the method discussed in section 2.3.7, where a large variety of trajectories were optimised off-line and then the data was interrogated on-board to construct the reference profile.

The trajectory planning method developed and investigated within this study provides significant advantages over traditional methods such as the US Shuttle TAEM

and Buran Pre-Landing Maneuvering Stage methods, discussed in sections 2.3.2 and 2.3.4 respectively. The trajectory planning method used here allows for trajectories that do not include fixed geometric segments, such as a HAC. The trajectories produced were optimised taking into account the initial and final conditions, in-flight constraints and the selected cost function. The optimisation process combined the longitudinal and lateral dynamics and did not require any sub-phases. Although the method utilises optimisation for trajectory planning the *optimal* solution is not required. Instead it was found that there were numerous suitable solutions. The *optimal* solution would also be dependent on the cost function selected and might not be the *optimal* solution in the presence of off-nominal conditions.

Some of the methods discussed in section 2.3 also provided greater capability to cope with off-nominal conditions over the traditional methods with their ability to provide updates or redesign the reference trajectory on-board. However, some relied upon fixed geometric segments, multiple sub-phases, a HAC or decoupling of the longitudinal or lateral guidance. The optimisation method used within this study eliminates the need for fixed geometric segments, multiple sub-phases and a HAC. The coupling of the longitudinal and lateral dynamics is a benefit of this method as it eliminates inherent errors or the need for correction factors.

Whether the approach utilised within this study is more suitable than the other methods of section 2.3 is hard to determine. These methods are based on instrument flying techniques of military aircraft (Burchett, 2004) and therefore there might be significant merit to their inclusion. Only an investigation utilising a direct comparison of the different types of methods would reveal the one most suited to the terminal area flight phase.

Another benefit of the method investigated within this study was the adaptability for use with multiple vehicles and missions as demonstrated by the results presented for both the Hopper and X-33 vehicles. Some of the other methods, discussed in section 2.3, are also able to be applied to other vehicles. However, some of these methods require considerable modifications including retraining of the fuzzy logic inference systems or detailed optimisation studies. Some methods are vehicle specific and require considerable modification and redefinition of reference profiles in order to be implemented for other vehicles.

There are however disadvantages associated with the method investigated within this study. The computation of a reference trajectory takes into account both the longitudinal and lateral guidance using an iterative optimisation of the vehicle states. Consequently the trajectory planning method requires a large amount of computational effort and is unsuitable for on-board implementation. Other methods, including the methods discussed in sections 2.3.5 and 2.3.9, are able to perform online trajectory design. The online trajectory design was achieved using simplified dynamics or geometric segments which reduced the computational effort of these methods providing the ability for on-board implementation. On-board trajectory generation was useful for these methods as they incorporated it into the guidance calls to adjust the trajectory profiles. However, the guidance method of this study, discussed in sections 3.1.3, 3.1.4 and Chapter 6, was able to re-design the reference trajectory on-board without relying on simplified dynamics or geometric constraints. In theory this would make the method more accurate due to the reduced errors inherent in reduced dynamics such as the decoupling of longitudinal and lateral guidance. The method used within this study would also be theoretically more adaptable and flexible than methods with fixed geometric segments or way points. However, the exact benefits have not been shown as there is no direct comparison to the other methods.

The optimisation of the trajectory was performed utilising a Newtonian gradient based method that does not find a global minimum but rather a local minimum. Consequently the optimised solution was often found to be based on the initial *guess* provided to the optimiser. The method of Schierman et al. (2004b), discussed in section 2.3.7, overcame this by iterating the inputs to the optimisation and then storing the data for on-board interrogation. The method utilised in this study requires the user to have some partial knowledge and experience to develop suitable trajectories. However, it would also be possible to set up a global optimiser by iterating on the initial *guess* provided. Since the trajectory design is performed off-line some pre-mission analysis would still be required however it should be reduced over traditional methods such as the US Shuttle TAEM method.

The optimisation of the ground track for the X-33 vehicle presented in Kluever and Horneman (2005) included a HAC style ground track which makes a direct comparison to the method discussed in Chapter 3 and the results of this method difficult. The

ground track did however allow for variations in HAC size and placement (Kluever and Horneman, 2005). The results showed that bank angle commands were significantly affected by the HAC shape and placement when compared to the un-optimised results using the trajectory planner. Kluever and Horneman (2005) required inverse dynamics to find solutions with a HAC using optimisation, as discussed in section 2.3.9. The results showed a 'bang bang' type profile for bank angle commands. These are different to the bank angle commands observed here since the trajectories generated via the method investigated in this research do not utilise a HAC which must be followed. The bank angle commands do switch directions during the flight, however they are more gradual than the methods of Kluever and Horneman (2005). Thus a direct comparison to the trajectories developed within this study is difficult as the trajectories do not include a HAC and consequently the steering command profiles are dramatically different.

The forcing nature of the Proto-SNAKE trajectory planner, discussed in section 2.3.3, makes a comparison difficult to the results obtained using the optimisation method of this study. The trajectories relied upon forcing bank angle turns and so provided only a single type of solution (Grubler, 2001). The theory behind the Proto-SNAKE method was investigated further by Büchner (2003) which showed that trajectories could be effectively planned. However, comparison to the results of Büchner (2003) is difficult as the initial and final conditions varied between the study and those given in tables 4.5 and 4.6. The method of Büchner (2003) required considerably less distance and heading changes than required for both the Hopper and X-33 vehicles.

The trajectories produced with the fuzzy logic inference system, discussed in section 2.3.8, showed different results to those of the optimisation method of this study and the results from the method of Kluever and Horneman (2005). The difference from the results of the method investigated here were expected as Burchett (2004) included a HAC. However, Kluever and Horneman (2005) also included a HAC and had different steering command and ground track profiles. The difference in the results was most likely due to Kluever and Horneman (2005) using an overhead HAC type trajectory where the vehicle flew past the runway and then around the HAC to land whereas Burchett (2004) had trajectories that flew the vehicle towards a direct HAC turn to the runway.

In general the type of trajectory, problem formulation, initial and final conditions, in-flight constraints and methodology utilised to determine a solution all dramatically affected the trajectories of the terminal area flight phase. Therefore to adequately compare the various methods of trajectory planning, discussed in section 2.3, with the method investigated here would require a study conducted with the same mission profile, vehicle and environmental models. Generally however the results of the study seem plausible as the trajectories flown are similar to those of the other methods. The method used within this study increases the computational accuracies of the trajectory at the expense of computational effort requiring pre-mission planning and analysis. The method does however allow for a considerable amount of flexibility in the trajectory design eliminating the need for multiple sub-phase, fixed geometric segments or decoupling of the longitudinal and lateral dynamics. The method investigated here is also suitable for multiple vehicles as demonstrated by the investigations with both the Hopper and X-33 vehicles.

5.9 Discussions From Trajectory Design

As mentioned in the introduction to this chapter the optimisation program is utilised as a design tool for the reference trajectories. The reason for user selection of the reference trajectories and not just the *optimal* solution with the lowest cost function is that there are many possible solutions all with closely related cost function values. Perhaps this is a problem in the definition of the cost functions discussed in section 5.6 but the cost functions are designed to produce the required *types* of trajectory that would be suitable for the terminal area flight phase.

The reference trajectories are selected by the user evaluating the cost function values, the trajectory solutions produced by the optimisation program, the considerations outlined in section 5.5 and user experience. The evaluation of the trajectories by the cost function values could have been performed to determine the *optimal* solution based upon the selected cost function. However, it was difficult to include all of the considerations given in section 5.5 within a single cost function. Additionally with numerous terms in the cost function two trajectories could have very similar value but different characteristics as seen in figures 5.7 and 5.9. For example two X-33 vehicle

trajectories could have similar values but one might have reduced dynamic pressure values but greater vehicle loads. Therefore user experience and evaluation is required in selecting the required reference trajectories.

An important adjustment not previously mentioned is the modification of the Hopper vehicle's final flight path angle value from two values quoted in literature. The final flight path angle value provided in a presentation from Astrium now known as EADS Space Transportation (at the time of writing) was $-28{+}10^\circ$ (Camara et al., 2002a). The Phoenix demonstrator a test bed for landing guidance of reusable launch vehicles based on a $\frac{1}{7}$th scale of the Hopper vehicle utilised a value of -23° for the final flight path angle (Gockel et al., 2004). It was found in this study that both the optimisation and guidance program worked more effectively if a final flight path angle value of $-18 \pm 5^\circ$ was used. This new flight path angle value was still within the quoted tolerance for the Hopper (Astrium) and Phoenix values.

The optimisation program often had difficulty to find an acceptable solution with the lower flight path angle values. The determined reason for this difficulty is the conflicting nature of the final velocity and flight path angle values where a large velocity is required. This can be seen in the flight path angle and velocity curves shown in figure 5.8. The curves are closely related towards the end of the terminal area flight phase to achieve the required flight path angle. The velocity drops below the target value and then increases due to the decrease in the flight path angle. Investigations showed that if the velocity constraint was removed the optimisation program was easily able to achieve a trajectory solution meeting various different flight path angle values. However the final velocity values were well outside the values required. Similarly if the final flight path angle constraint was removed the optimiser had no trouble in determining suitable trajectories.

During the approach and landing phase of reusable launch vehicles a constant glide slope is utilised with constant flight path angle and velocity. A constant glide scope can be modelled using equations 5.10 and 5.11 provided there are no other external accelerations such that the velocity is constant.

$$L = -M \cdot g \cdot \sin\gamma \tag{5.10}$$

$$D = -M \cdot g \cdot \cos\gamma \tag{5.11}$$

Therefore the flight path angle can be related to the lift-to-drag ratio by equation 5.12.

$$\tan\gamma = \left(\frac{L}{D}\right)^{-1} \tag{5.12}$$

The lift-to-drag ratio for the aerodynamic models used in this study are a function of angle of attack and Mach number. The lift-to-drag ratios for various flight path angle, γ values calculated from equation 5.12 are shown in table 5.5

Using the equations B.1 and B.2 contained in Appendix B.2 the Mach number for the final velocity range of the Hopper vehicle was determined. For an altitude of 2km the US Standard 1962 Atmosphere gives a temperature of 281.43°K, resulting in Mach numbers of 0.336, 0.365 and 0.395 for velocities 113 m/s, 123 m/s and 133 m/s respectively.

A portion of the Hopper vehicle aerodynamic model with the required flight path angles for the various lift-to-drag ratios are shown in figure 5.11. Here it can be seen that for each of the various glide slopes, corresponding flight path angles and lift-to-drag ratios can be readily achieved through variations in angle of attack. Although the new flight path angle value of $-18°$ requires a larger lift-to-drag ratio the value is still readily achievable with the lift-to-drag values of the Hopper vehicle. Therefore, there is still significant margin with the new glide slope should the required lift-to-drag ratio need to be increased.

It was decided that since the velocity of the Hopper vehicle was important to the energy condition at the commencement of the approach and landing phase it made more sense to slightly modify the final flight path angle value instead of the vehicle velocity. The information presented in the presentation to Astrium did not match the

Flight path angle, γ	L/D
$-13°$	4.33
$-18°$	3.08
$-23°$	2.36
$-28°$	1.88

Table 5.5: Flight path angles and corresponding L/D ratios for constant glide slope

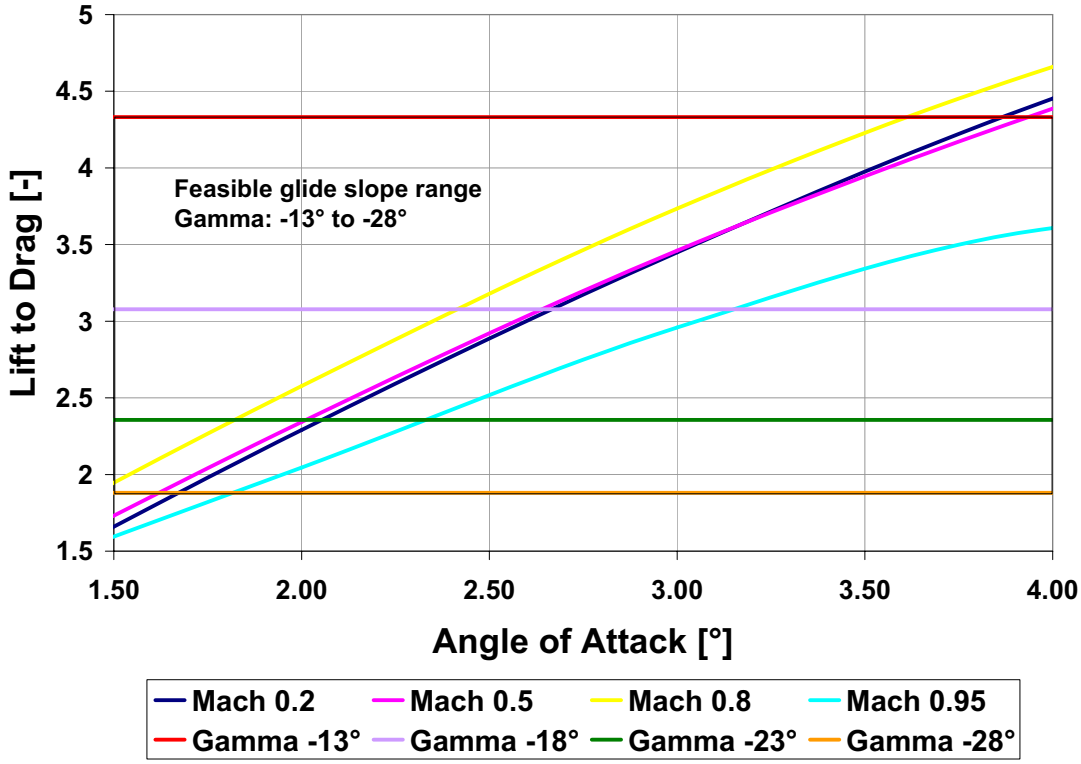

Figure 5.11: The Hopper vehicle aerodynamic model for the feasible glide slopes

results achieved within this study possibly due to the fact that it was determined while performing preliminary studies. It was thought that the influence of the change to the final flight path angle made within this research could be incorporated in future studies of the approach and landing phase.

5.10 Conclusions from Trajectory Design

The major improvements from this research to the optimisation program, continually developed through the studies of Schöttle et al. (1997); Burkhardt (2001); Tetlow (2003); Gräßlin (2004); Telaar (2005), is the adaption and extension to the terminal area flight phase. The adaption was achieved through the addition of a speed brake setting steering parameter and development of a speed brake model. The research also shows that the improved optimisation program is an effective method of performing off-line trajectory design and analysis for the terminal area flight phase. This study presents a sensitivity analysis for the terminal area flight phase using the discussed methodology of chapter 3 and with application to the Hopper and X-33 vehicles. By performing

the sensitivity study on both of the vehicles common influences for the terminal area flight phase are revealed. Additionally attributes that are vehicle specific were identified through the sensitivity studies. This study also highlights the adaptability and applicability of the optimisation program to multiple vehicles by the application to two vehicles with different characteristics and mission profiles.

The use of the optimisation program has been shown to be an effective method for performing trajectory design and sensitivity analysis for the terminal area flight phase. Using non-linear programming methods combined with the NLPQL sub-routine a new method for trajectory design is achieved through the definition of steering commands. Using the steering commands to design the trajectories helps to solve some of the limitations discussed in Chapter 2 and highlighted in section 2.6. By removing the need for fixed ground track segments such as the HAC and way points the trajectories can be designed to suit the vehicle type and mission.

The majority of methods for terminal area guidance described in section 2.3 utilised a HAC. The method used within this study does not utilise a HAC in order to provide a greater amount of flexibility in the design and restoration of trajectories. The definition of a HAC within trajectories for the terminal area flight phase might provide additional benefits that are unknown to the author. Although not investigated in this study the use of a HAC could be incorporated with the method of this study. If the inclusion of a HAC was a requirement it could be included by changing the termination point of this method from the ALI point to a HAC intersection point. This would still allow flexible trajectories to be designed using this method. A HAC tracking phase could then be included to track the HAC and terminate at the ALI point.

The results of section 5.7 show that trajectories can vary significantly for different vehicles and missions. The optimisation program has been shown to be an effective trajectory design tool for both the Hopper and X-33 vehicles. The optimisation program can also be easily extended to other lifting re-entry bodies by loading in new vehicle models and mission initial and final conditions. The tool can also be used for other planets or moons by loading in the appropriate atmospheric model.

The comparison to the other methods discussed in section 5.8 reveal the versatility of this method as an off-line design tool allowing improved mission analysis for multiple vehicles and missions. The comparison also revealed that the optimisation

program is computationally intensive for trajectory design and is unable to be performed in the on-board guidance computer like some other methods. Although it is a benefit to have a flexible trajectory defined by the steering parameters this definition does not allow for specific sizes and shapes to be designed into the trajectory such as a HAC. This was revealed in section 5.4 where S-turns could not be effectively included in the trajectory as margins. The inclusion of margins was however achieved through the cost functions discussed in section 5.6 and the nominal speed brake setting of 50% allowing for variations in the vehicle's drag and thus energy dissipation rate.

The sensitivity studies of section 5.3 show that there are commonalities for two different vehicles during the terminal area flight phase. The results show that the aerodynamic, density and mass errors caused the largest errors in the final conditions. These commonalities can be a trait of the problem formulation based on the parameterisation of the trajectory via the steering parameters, discussed in section 5.2, or they could be common to the terminal area flight phase. The other methods of trajectory design discussed in section 5.8 utilised similar errors especially aerodynamic errors which would seem to indicate that the influence of aerodynamic errors is related to the terminal area flight phase and not the steering parameter parameterisation method. The sensitivity studies also showed what level of margins should be designed into the reference trajectories and assisted in the development of the guidance program discussed in Chapter 6.

Chapter 6

Guidance

One test result is worth one thousand expert opinions.

Wernher von Braun (1912-1977)

Rocket Scientist

THE goal of the guidance program is to adapt the trajectory during flight to cope with off-nominal conditions such that the vehicle arrives safely within the specified tolerances for the final conditions and vehicle restrictions. This is accomplished by solving the problem specified in Chapter 3 by utilising the restoration steps of the gradient projection algorithm (GPA).

A considerable amount of the developmental work of the guidance program for the terminal area flight phase was performed using the sub-orbital Hopper concept vehicle and associated mission. It was decided that the testing of a single vehicle and associated mission especially the vehicle that was used to further develop the method was insufficient to verify the guidance program. Consequently the guidance program required additional verification. The guidance program was developed such that it could be easily adapted to other vehicles and missions. Therefore proper evaluation would require actual testing of the guidance program for different vehicles and their associated missions. Another reason for further analysis was that although the basic guidance program had been applied to other vehicles and missions, see section 2.4.3, a considerable amount of modifications were made to adapt the guidance program to the terminal area flight phase. These modifications include the addition and development of steering and aerodynamic models combined with modifications to existing models

and the inclusion of the speed brake setting as an additional steering parameter. Errors in any of these modifications could considerably alter the effective operation of the guidance program or even the validity of the results. Therefore the guidance program was also applied to the terminal area flight phase of the NASA/Lockheed Martin single stage to orbit concept vehicle, X-33.

There were several reasons for the selection of the two different vehicles and missions. The major reason was that both vehicles had a significant amount of data available to the author or in the public domain to allow for modelling and comparison to other methods to verify the results. Another significant reason was that although both vehicles and missions operate in the terminal area flight phase allowing for an effective verification of the program there are still considerable differences. The Hopper vehicle has considerably different aerodynamics since it is a winged re-entry vehicle compared to the lifting body aerodynamics of the X-33 vehicles. The X-33 vehicle terminal area flight phase has different initial and final conditions to that of the Hopper vehicle resulting in completely different trajectories. These differences in the vehicles and missions allow the evaluations to demonstrate the versatility and adaptability of the guidance program. Additionally the sensitivity studies conducted with the guidance program for both vehicles revealed common influences from off-nominal conditions.

6.1 The Hopper Vehicle Results

To evaluate the guidance program several tests were required to prove the applicability, flexibility and adaptability of this method to the terminal area flight phase. The following sections present and discuss the results for the guidance program applied to the Hopper vehicle and mission. Previous results have been presented in Chartres et al. (2005a), however significant improvements and additional detailed sensitivity studies have since been performed.

An initial guidance trial was performed to ensure that the guidance was able to deliver the Hopper vehicle to the required final conditions and to ensure that the guidance was operating appropriately. A single guidance trial was performed without any applied errors. The results are displayed in figure 6.1 and table 6.1.

The results show that the guidance is effectively able to deliver the Hopper vehicle

Conditions	Target miss (m)	v (m/s)	$\gamma(^\circ)$	$\chi(^\circ)$
Target conditions	0 ± 100	123.0 ± 10	-18 ± 5	-62 ± 5
Guidance results	9.6727	124.9097	-18.0928	-61.9928
Errors	9.6727	1.9097	-0.0928	0.0072

Table 6.1: The Hopper vehicle guidance results without off-nominal conditions

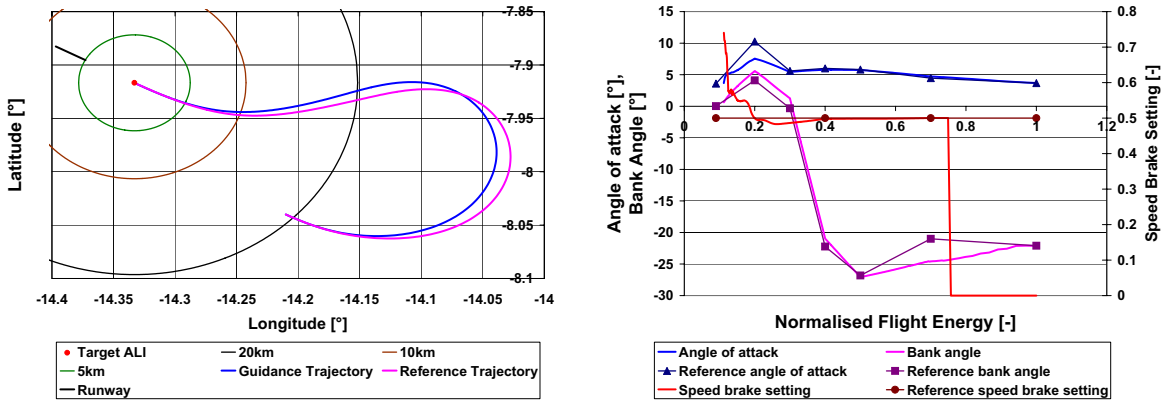

Figure 6.1: The Hopper vehicle ground track and steering profile of the initial solution and solution after restoration steps for nominal conditions

to the final conditions. There are some slight errors which result from the variations in the models of predictor and simulator. The target miss of 9.67m was quite large, however still within the acceptable tolerance limits of the final conditions. The target miss was most likely caused by the variation in the density profiles for the different atmospheric models of the simulator and predictor.

Looking at the ground track for the guided trajectory and the reference trajectory in figure 6.1 it is possible to see the difference between the two trajectories. During the restoration cycles of the guidance program the steering profiles are modified. The major difference between an optimised reference trajectory and a guidance solution is the speed brake setting. The speed brake setting is not an optimisable steering parameter during trajectory design instead it is set to a constant value to provide margins, see section 5.4. However, within the guidance program the speed brake setting parameters are active and therefore modified during the restoration cycles. The speed brake setting is also a very influential parameter towards the end of the trajectory. This often results in the speed brake setting being largely modified towards the end of flight, as

shown in figure 6.1.

Note with figure 6.1 the steering profiles are displayed with respect to normalised vehicle energy and therefore the start of the trajectory occurs on the right hand side and progresses to the left. Here the speed brake setting is increased towards the end of the flight. The angle of attack profile is also modified decreasing the profile towards the end of the flight. The bank angle is also modified with a slight increase in the settings. Interesting is the second parameter for bank angle which has been placed such that it intersects a line between the first and third parameters. This might indicate that this bank angle parameter is unnecessary. However, in the presence of off-nominal conditions especially initial condition variations the guidance requires this parameter in order to meet the final conditions. The influence of off-nominal conditions on the steering parameters is discussed more in section 6.1.2.

6.1.1 Real Time Operation

In order for the guidance to be effective on-board the unmanned Hopper vehicle it must be able to operate in real time. Therefore a guidance evaluation was performed to determine the suitability of the guidance method for on-board operation. The guidance normally utilises a call interval (time between successive calls) of 1.0 seconds. The guidance call interval needs to be larger than the required calculation time of the predictor in order to be effective for real time on-board operation. An analysis utilising 1000 first calls of the predictor revealed an average calculation time of 249.1 ms. The evaluation was performed on an Intel™ Pentium™ 4, 2.4 Ghz desktop computer running Windows XP™ and Compaq™ Visual Fortran Professional Edition 6.6.C. The first call to the predictor is the longest as a complete flight path integration must be performed for each of the steering parameters plus an additional integration with the modified parameters. Consequently as parameters become inactive the number of flight path predictions reduces. Additionally as the trajectory progresses the time to the final conditions is reduced and therefore less of the trajectory must be integrated. The result reveals that the guidance is able to operate on-board in real time provided that all other on-board computational operations can be performed within 750 ms.

The guidance was also evaluated to determine the influence that guidance call intervals and integration step size has on the final conditions. The guidance call interval

and integration step size were varied between 0.1 and 10.0 seconds with intervals of 0.1 seconds and a guidance simulation performed for each time. The results for the guidance call variations are shown in figure 6.2 and the results for the guidance integration step size are shown in 6.3.

The results for the guidance call interval variations reveal that as the guidance call interval increases the target miss and final velocity errors become greater. This was expected as the updates become less frequent the guidance is unable to adjust for the errors as often. The final flight path angle error also becomes worse and seems to settle at around 0.6 seconds. The final azimuth is not significantly effected by the variations in guidance call interval.

A large guidance call interval does not allow the guidance to adjust for the off-nominal conditions very often, however minimal computational effort is required. Alternatively a small guidance call interval provides a greater ability to adapt to off-nominal conditions but also increased computational requirements. Looking at figure 6.2 it can be seen that significant performance improvement is not achieved below 1.0 seconds. Consequently a guidance interval of 1.0 seconds is the most suitable since it provides accurate results and reduces the required computational effort.

Interesting to note in the results for the guidance call interval is that there are several places in which although the guidance interval has varied but the results are still the same. This seems to indicate that variations of the guidance call interval around some values provides no difference in performance. Such that there are sets of results for different guidance intervals. However, it is obvious to see the detrimental effects

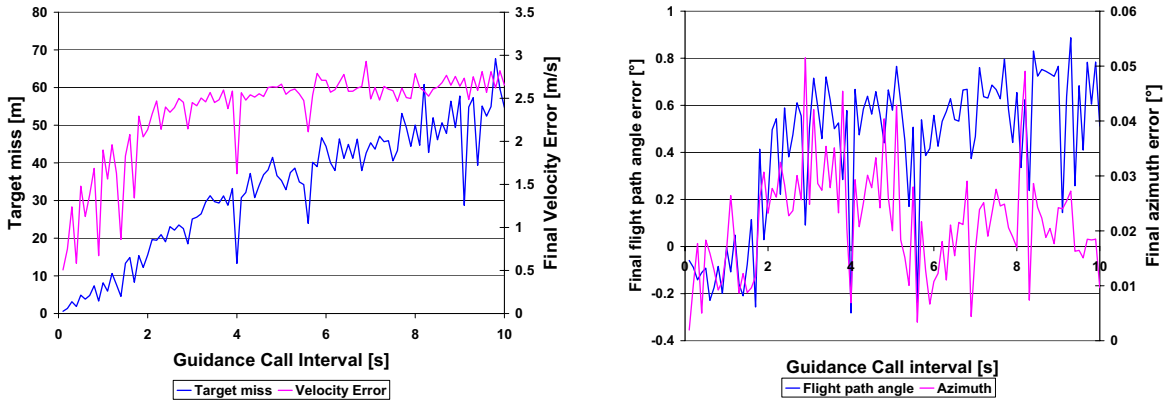

Figure 6.2: Guidance call interval influence on Hopper vehicle final conditions

produced by larger guidance call intervals.

The results for the integration step size, shown in figure 6.3, are also as expected with a larger step size producing larger errors. The integration step size influences the accuracy of the predictor's ability to simulate the actual trajectory flown. Similar to the results seen for the guidance call interval the influence on the final azimuth is quite small. The target miss restriction is actually violated for integration step sizes greater than 8 seconds.

The results of figure 6.3 show that no significant performance gain is achieved by using an integration step size less than 1.0 seconds. Thus the standard predictor integration step size of 1.0 seconds is suitable for the Hopper vehicle guidance program.

A possible compromise between computational effort and final condition accuracy could be achieved by implementing adaptive guidance call intervals and integration step sizes. The guidance call intervals and integration step sizes could be larger at the beginning of the trajectory where reduced accuracy is acceptable and become smaller towards the end of the trajectory where increased accuracy is required. This adaptive method could reduce the overall computational effort required by the on-board computer due to the reduced number of guidance calls and integration steps. However, these adaptive guidance call intervals and integration step sizes were not investigated in this study.

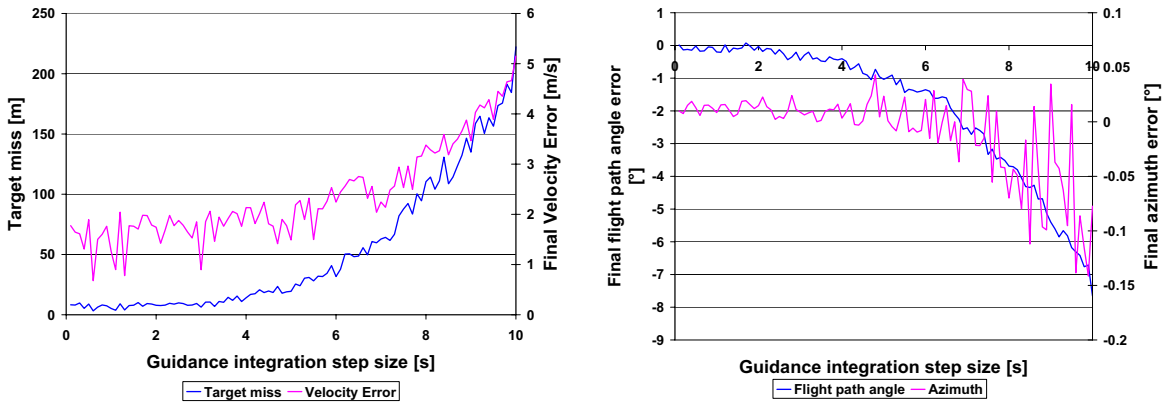

Figure 6.3: Guidance integration step size influence on Hopper vehicle final conditions

6.1.2 Guidance Worst Cases

The sensitivity studies conducted during trajectory design and optimisation, discussed in section 5.3, indicated that the guidance needed to be able to cope with large errors in the final conditions. To ensure that the guidance was successfully able to cope with the errors given in table 5.1 representing worst case situations an evaluation of the guidance was performed. The results are presented in figures 6.4 and 6.5 and table 6.2.

The results in figure 6.4 show the effects to the ground track caused by the various off-nominal conditions which are utilised to account for model uncertainty of the vehicle and environment models. The variation of the ground tracks is quite significant looking at the reference trajectory, which is the optimised solution, each of the solutions are modified in a similar manner to that of the initial guided solution, shown in figure 6.1. Having the ability to modify the steering commands the guidance program modifies the solution to the form seen when there were no errors present. The inclusion of the model errors cause only minor modification in the ground track compared to the guidance solution without errors.

Figure 6.5 shows the effects to the ground track caused by variations in initial conditions. The ground tracks are different to those seen in figure 6.4 with the model errors. The variations in altitude produce ground tracks that are further away or closer to the target during the turn around manoeuvre, this behaviour can be related to the aerodynamic properties of the vehicle. In section 5.7 it was discussed how the Hopper vehicle is better able to manoeuvre at sub-sonic speeds due the aerodynamic characteristics. The increased altitude results in a lower density. The lower density reduces the drag forces and it takes the Hopper vehicle a longer time period to dissipate the required energy to reduce the velocity to the more manoeuvrable sub-sonic speeds. Consequently the vehicle requires a greater ground track to turnaround. Similarly the reduced altitude results in a reduced ground track to reach the more manoeuvrable sub-sonic speeds.

The modifications applied to the initial velocity produce similar results to those observed for the altitude variations but are less pronounced. The reduced initial velocity results in a shorter ground track to reach the more manoeuvrable sub-sonic speeds and the increased initial velocity results in a slightly larger ground track. Here the increased initial velocity of $500\,\mathrm{m/s}$ results in a ground track more similar to that ob-

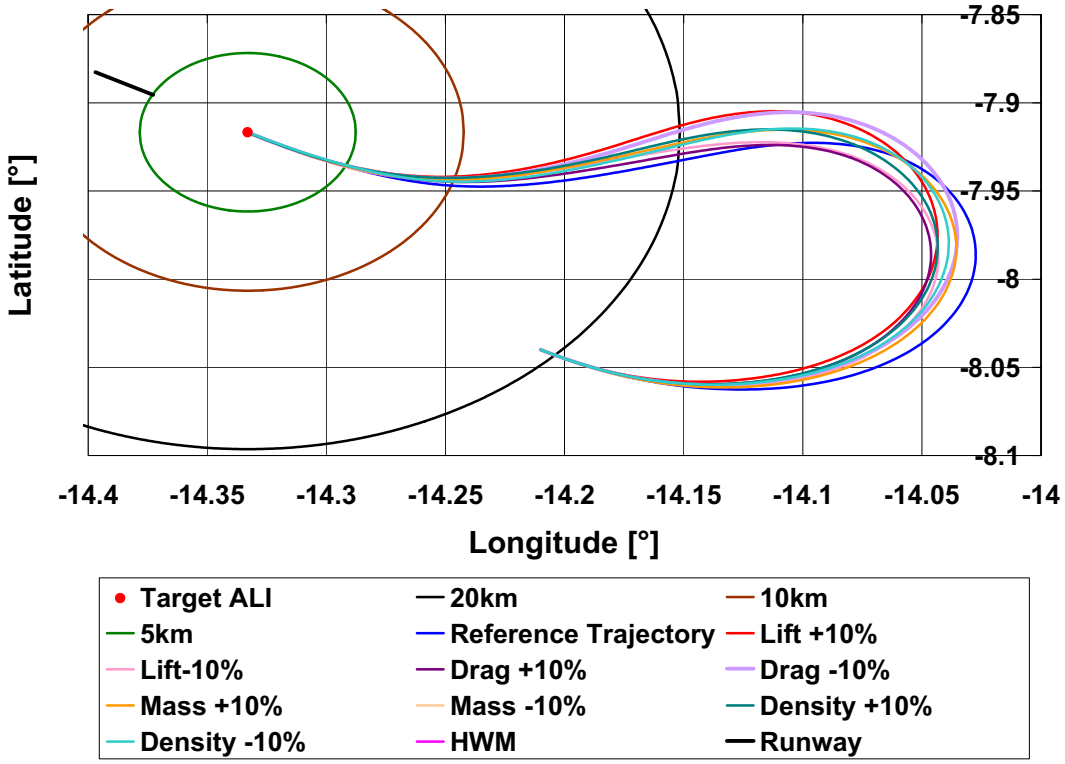

Figure 6.4: The Hopper vehicle guidance results with worst case off-nominal conditions for vehicle and environment models

served in the optimised solution of figure 6.1 instead of the guidance solution without errors. The guidance solution ground track appears to lay in between the two velocity trajectories.

The results for the initial azimuth variation are as expected, the ground track becomes slightly skewed but the guidance is able to correct for the initial variation. The results for the initial azimuth variations are similar to those presented in the results of Hoffman et al. (1970) and Kluever and Horneman (2005). The modification to the initial flight path angle are interesting, a small value for the flight path angle, such as zero, results in a reduced vertical component of the velocity and hence the vehicle is able to fly further down range which results in the increased ground track before turn around. Similarly with the initial flight path angle at -30 degrees the vertical velocity is increased and results in the vehicle descending more rapidly to the higher density region of the atmosphere resulting in a quicker transition to sub-sonic speeds and hence increased manoeuvrability.

The results of table 6.2 show that the guidance is effectively able to cope with all

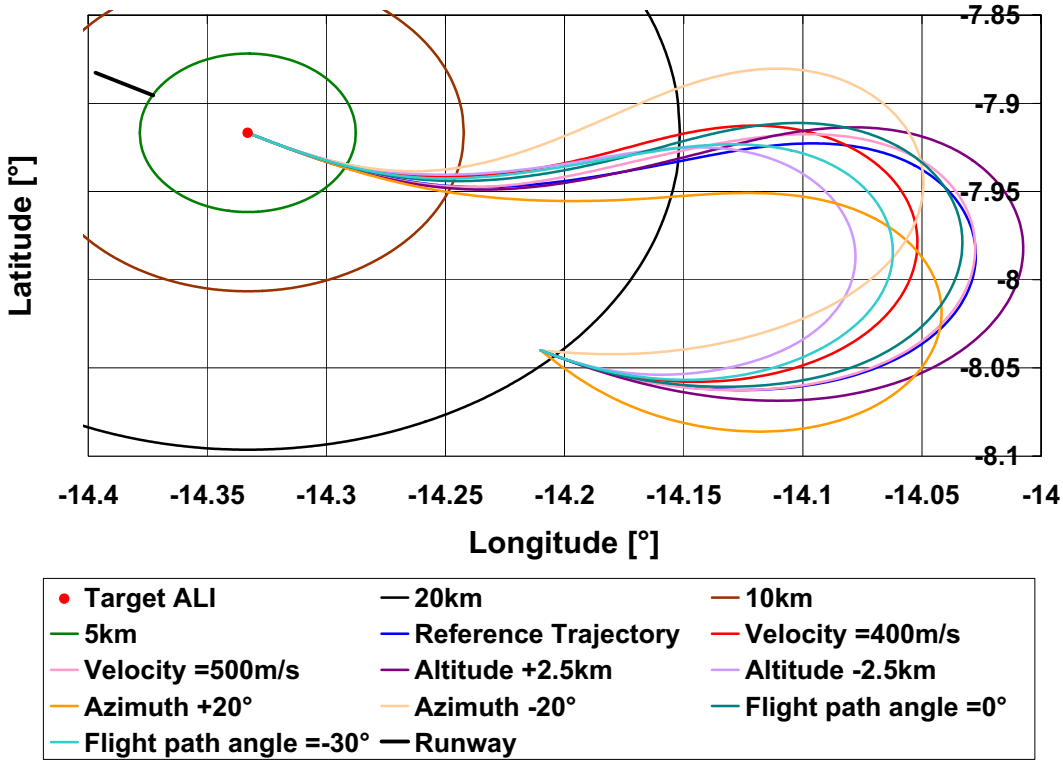

Figure 6.5: The Hopper vehicle guidance results with worst case initial conditions

		Errors			
Conditions	Target miss (m)	v (m/s)	T (s)	$\gamma(^\circ)$	$\chi(^\circ)$
Mass +10%	29.4314	3.3397	-4.4988	0.1501	0.0489
Mass -10%	18.6075	-0.7373	3.0203	1.4792	0.0696
C_D +10%	5.7069	-0.0661	9.3665	-0.3095	-0.0018
C_D -10%	15.7660	6.7080	-7.9798	1.3858	0.1647
C_L +10%	10.6298	7.6890	-12.4847	0.8206	0.1353
C_L -10%	78.7699	3.0557	-5.5717	0.2462	0.0263
ρ +10%	28.2513	3.9720	-13.5739	0.2367	0.0270
ρ -10%	20.0852	-0.7149	17.8027	1.4623	0.0678
Winds	16.5076	3.0502	1.5422	0.0603	-0.0138
Initial $v = 400$ m/s	9.5351	1.7785	-15.8988	0.0561	-0.0008
Initial $v = 500$ m/s	5.1072	1.3772	21.7007	-0.1641	0.0204
Initial h +2.5 km	4.6923	1.1046	39.0742	-0.1997	0.0140
Initial h −2.5 km	9.0349	2.1986	-42.8190	0.2061	-0.0092
Initial χ +20°	4.6354	1.2310	2.7739	-0.1621	0.0116
Initial χ −20°	12.3071	1.6380	-6.3787	-0.1184	0.0157
Initial $\gamma = 0^\circ$	5.6355	1.3717	9.1349	-0.1325	0.0113
Initial $\gamma = -30^\circ$	3.2088	0.7199	-26.0054	-0.2189	0.0085

Table 6.2: The Hopper vehicle guidance results with worst case off-nominal conditions

of the extreme cases provided in table 5.1. The guidance is better able to cope with some of the off-nominal conditions than others. The target miss of the Hopper vehicle is largely influenced by the reduced lift coefficient and increased mass and density. The final velocity errors are influenced by the disturbances of lift and drag coefficients, mass, density and winds. The target miss and final velocity errors for the guidance are both strongly influenced by the aerodynamic errors of the vehicle. This was expected as the aerodynamics of vehicle modify the ability to dissipate energy which is directly related to the range and velocity of the vehicle (Chartres et al., 2005b). To ensure accurate results from the guidance the vehicle aerodynamics need to be known with a level of certainty, this is discussed more in section 6.1.3.

The final flight path angle errors are small in comparison to the target miss and final velocity errors. The final flight path angle errors are sensitive to similar disturbances as the velocity, due to the relationship between the flight path angle and the vertical velocity given by equation 3.10. The coupling between the velocity and flight path angle is discussed in more detail in section 5.7. The final azimuth errors are also small for all of the extreme cases indicating that the guidance is more able to correct errors for final azimuth than those for final velocity or target miss. This was expected as errors in azimuth can be easily accounted for by bank angle steering commands.

The modifications of the lift coefficient in the trajectory design sensitivity studies of section 5.3 produced large errors in the majority of final conditions, especially target miss. Most of the errors for the guidance are also sensitive to applied errors for aerodynamic coefficients. Figure 6.6 displays the modifications made to the steering profile for the lift coefficient, C_L disturbances of $\pm 10\%$.

Of significance here is the steering profile for the speed brake setting with $C_L + 10\%$ the guidance increases the speed brake setting to provide extra drag. Normally the guidance will increase the speed brake setting to a larger value towards the end of the flight as see in figure 6.1. However, here the speed brake setting is increased to the maximum value instead of the 0.75 value seen in figure 6.1. The speed brake setting is also decreased for $C_L - 10\%$ to compensate for the reduced lift. The guidance utilises the speed brake setting as a method to compensate for errors in the aerodynamic model as discussed more in section 6.1.3

Although the guidance is effectively able to cope with the various worst case set-

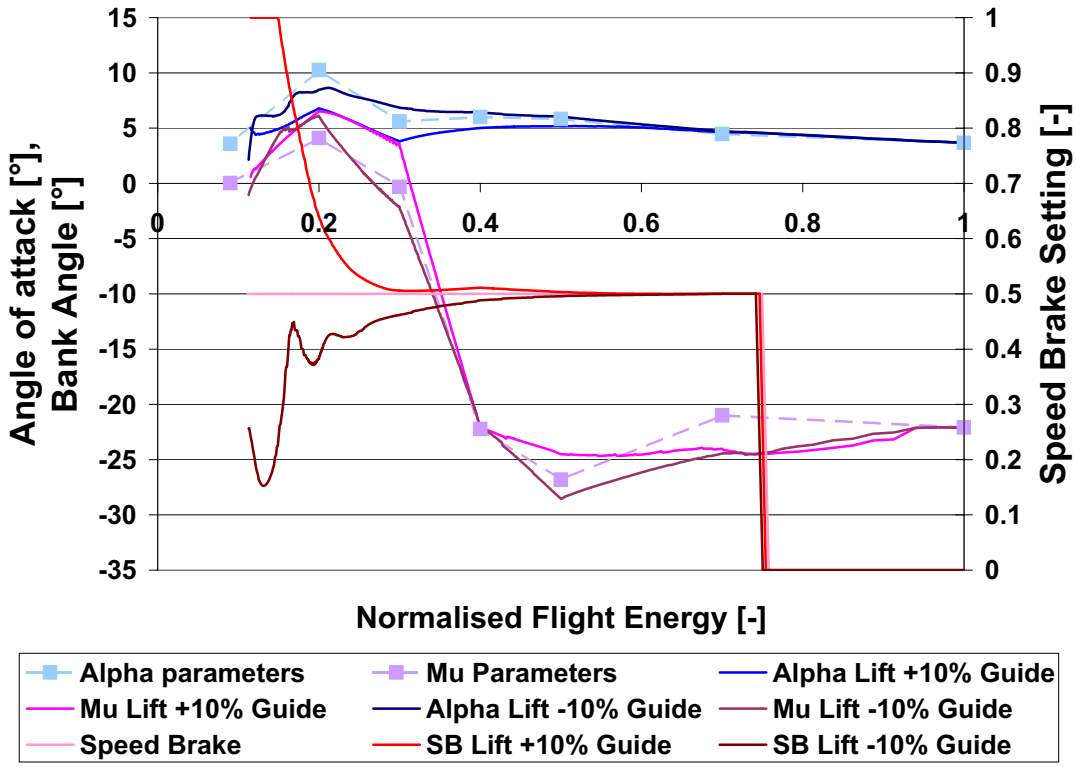

Figure 6.6: The Hopper vehicle steering profile for initial solution and $C_L \pm 10\%$

tings for each individual applied error this does not completely verify the overall effectiveness of the guidance methodology. Other errors given in table 3.2, which include sensor noise and time delays in the vehicle steering commands have yet to be evaluated. Further investigations were required to evaluate the most influential errors to the guidance and what the effects of combined applied errors would have on the final conditions. The influence of the various errors is discussed in the sensitivity studies of section 6.1.3 and the effects of combined applied errors is discussed in the Monte Carlo evaluation of section 6.1.4.

6.1.3 Sensitivity Studies

The terminal area flight phase requires the guidance to direct the Hopper vehicle to the correct final conditions, namely altitude, azimuth, flight path angle, position and velocity. The problem was formulated such that the stopping condition would be the altitude of the vehicle as this has traditionally been used to switch to the approach and landing guidance phase for other vehicles (Hoffman et al., 1970; Ehlers and Kraemer,

1977; Barton and Tragesser, 1999; Kirpischikov, 1997; Kluever and Horneman, 2005). However, the other four final conditions each had varying values of tolerance and the final velocity and flight path angle displayed coupling during trajectory optimisation and initial simulations.

To evaluate the guidance it is useful to determine the feasible operating range and whether it is able to cope with a large variety of off-nominal conditions. The investigations utilised random errors for off-nominal conditions provided in table 3.2 with 100 simulation for each error type. The error types were mass, aerodynamics, atmosphere, atmosphere and wind, density noise, constant winds, altitude varying winds, position noise, velocity noise, steering bias, steering noise, steering time delay and initial conditions. The maximum, minimum, average and standard deviation results for target miss, final velocity, azimuth and flight path angle errors are shown in figures 6.7, 6.9, 6.11 and 6.13, respectively.

The results shown in figure 6.7 reveal that the guidance for the Hopper vehicle is sensitive to winds, steering time delays, aerodynamic errors and position noise. Figure

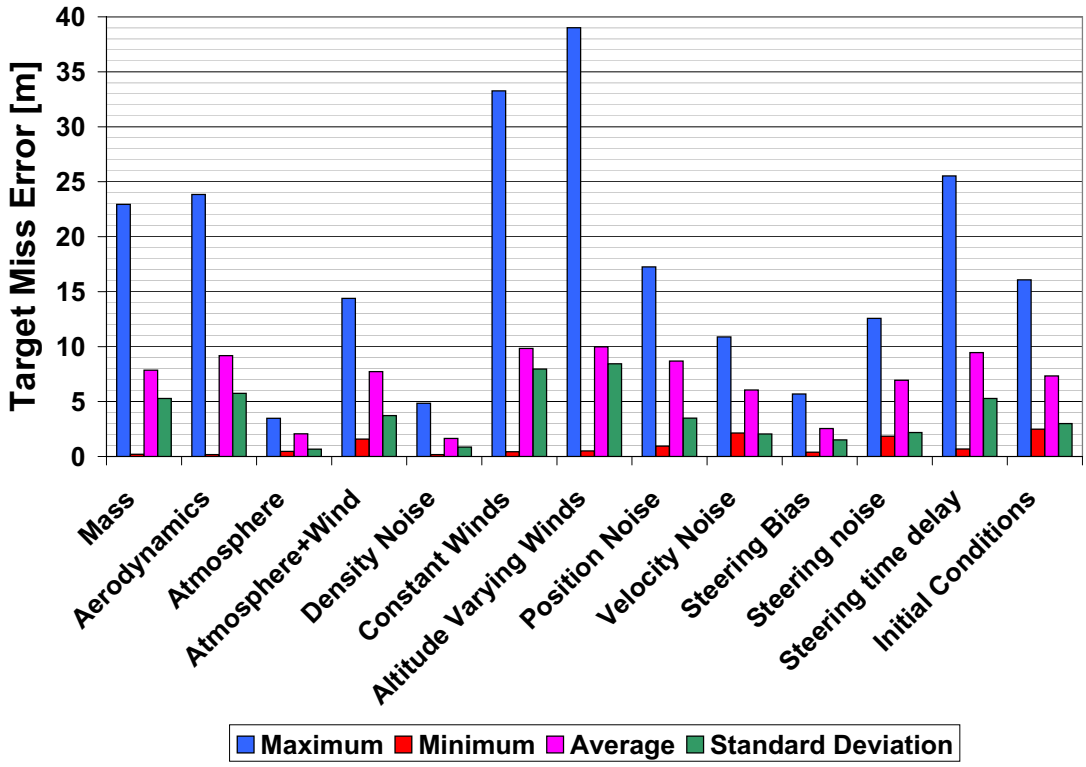

Figure 6.7: The Hopper vehicle target miss errors due to off-nominal conditions

6.8 shows the effects of the individual errors in the most influential error sets.

Figure 6.8(a) only shows the influence of the time of year on the target miss as the influence from the time of day is only slight with some scattering around the values produced due to the day of the year. The target miss errors shown in figure 6.8(a) show that at different times of the year the influence of the wind changes with the middle period of the year producing the smallest errors. There is also scattering of the results with certain days of the year producing reduced target miss errors. The influence of the wind on the vehicle velocity is not known to the predictor and therefore a slight position error would be expected as the vehicle's actual velocity is different from the predicted value.

The bank angle time delay produces the largest errors of the steering time delays for the target miss. The steering time delay effects shown in figure 6.8(b) reveal that below a time delay of 1.0 seconds the target miss error increases with increasing time delay for all cases. After 1.0 second a linear increase with some random scattering is seen for each of the time delays with only slight error increases for the angle of attack and speed brake setting time delay. The bank angle time delay reduces the ability for the vehicle to turn and align with runway centreline resulting in lateral target miss errors.

The applied aerodynamic errors modify the lift-to-drag ratio of the vehicle resulting in reduced range and manoeuvrability that leads to target miss errors. The effect of the applied aerodynamic coefficient errors is shown in figure 6.8(c) where the reduced lift coefficients produce the greatest error. Reduced drag coefficients also produce errors that slightly decrease with increasing drag coefficient modifiers.

The target miss errors due to position noise were expected since towards the end of the flight the predictor needs to accurately know where the vehicle is in order to perform the restoration steps. If the position is not correctly known then the modified steering commands can lead to larger errors. The altitude error produced the largest target miss errors of the position errors as shown in figure 6.8(d). The altitude is used as a stopping condition and so any error in the altitude will have the predictor stopping the integration too late or too soon resulting in an undershooting or overshooting of the target due to the large horizontal velocity in comparison to the vertical velocity.

The effects of the different applied error sets on the Hopper vehicle final velocity are

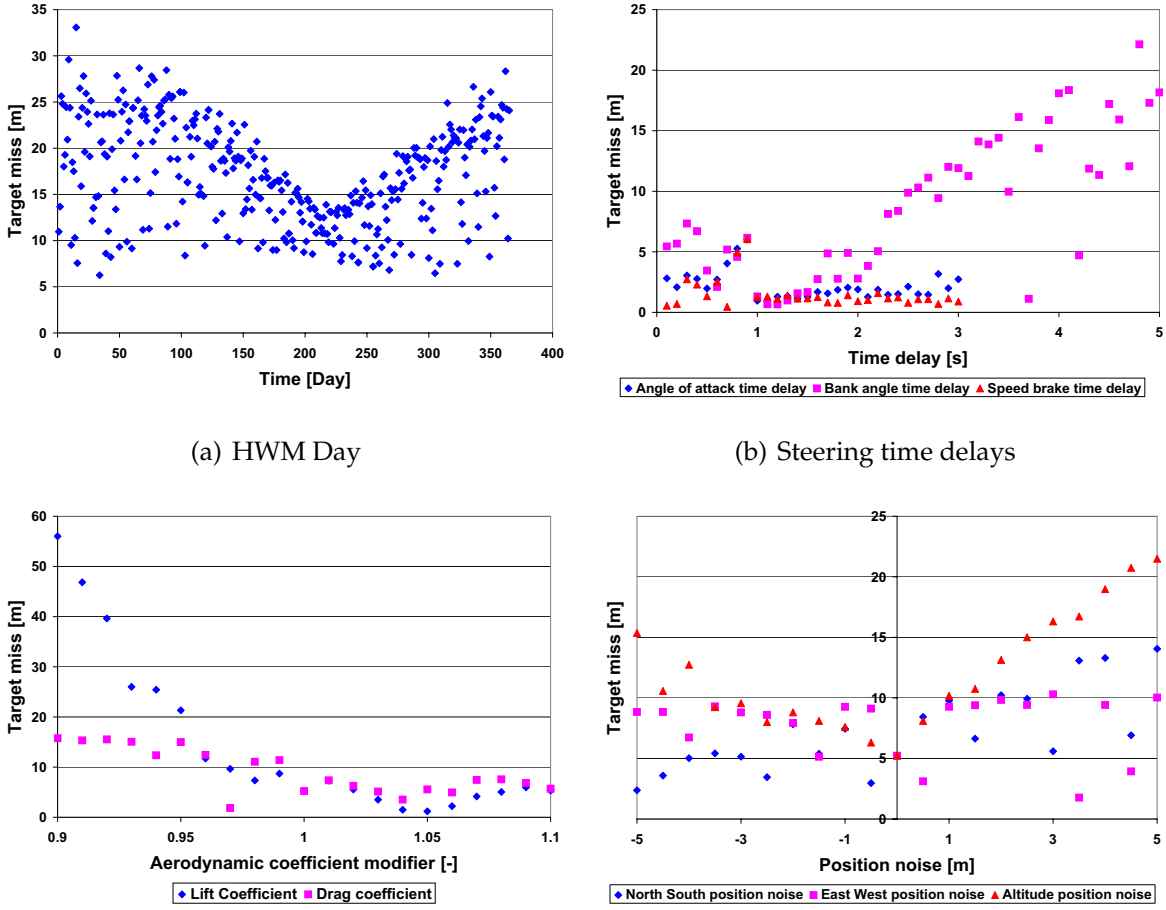

(a) HWM Day

(b) Steering time delays

(c) Aerodynamic coefficients

(d) Position noise

Figure 6.8: The influence of off-nominal conditions on the Hopper vehicle target miss error

shown in figure 6.9. The most influential applied errors were found to be winds, steering time delay, initial conditions and aerodynamic errors. The effects of the individual applied errors for these different error sets is shown in figure 6.10.

The influence of the Horizontal Wind Model (HWM) on the final velocity is similar to the target miss error results as it is also more related to the time of year than the time of day as shown in figures 6.10(a) and 6.10(b). The time of day has a slight influence there is scattering around a central value. The time of the year still has the scatter but a general trend can be seen. The time of the year has a similar influence on the final velocity error as the target miss error with the middle period of the year from the HWM producing reduced errors.

The steering time delays cause final velocity errors because towards the end of flight

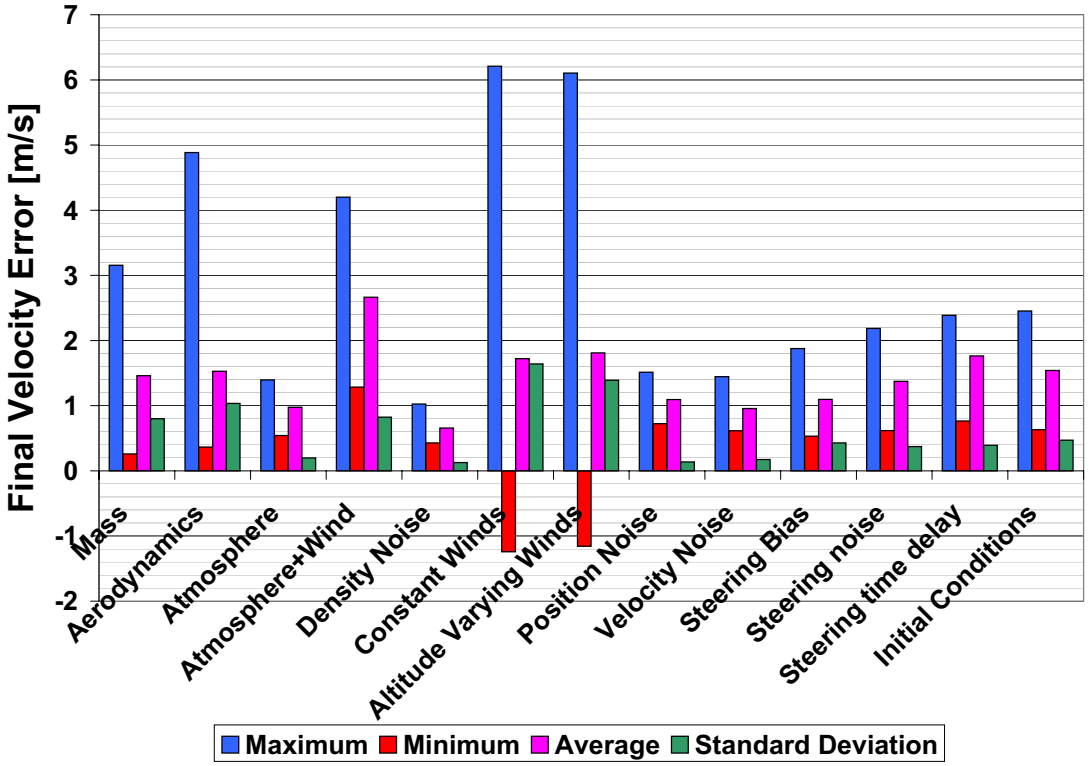

Figure 6.9: The Hopper vehicle final velocity errors due to off-nominal conditions

the vehicle is not able to adjust the attitude fast enough to dissipate the required energy. This can be seen in figure 6.10(c) where increased time delays result in increased final velocity errors. Here the energy dissipation problem can be seen with larger final velocity errors caused by the speed brake setting rather than the angle of attack because the speed brake setting is utilised at the end of flight to control the drag and thus energy dissipation rate.

The initial conditions were already shown to have an influence on the final velocity in sections 5.3 and 6.1.2. Figures 6.10(d) and 6.10(e) show how the individual errors have slightly decreasing final velocity errors with increasing initial condition error. There is also significant random scattering of the results. Each of the separate individual initial condition errors seems to produce a similar final velocity error value.

The aerodynamic coefficient modifiers have previously caused velocity errors for the Hopper vehicle as discussed in section 5.3, especially for the lift coefficient modifier with the guidance inactive. In section 6.1.2 it was also seen that the drag coefficient modifiers produced significant final velocity errors with the guidance active. Figure

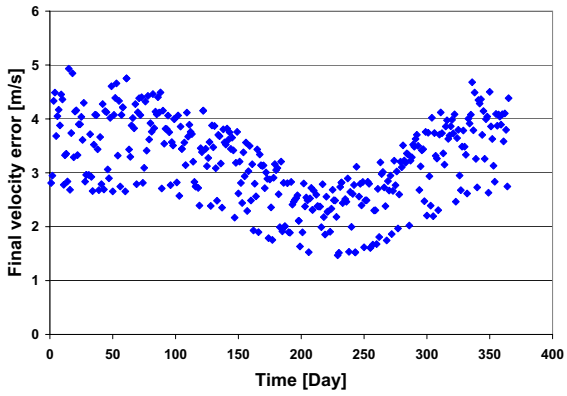

(a) HWM Day

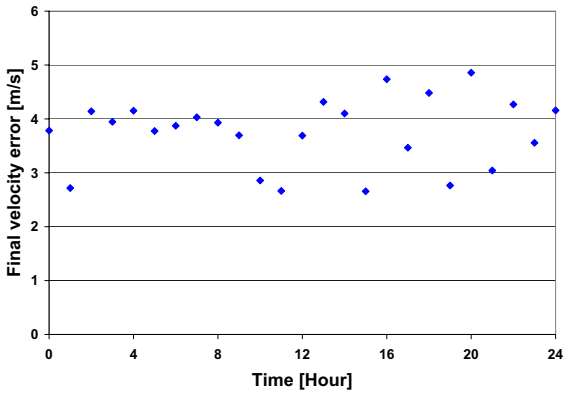

(b) HWM Time

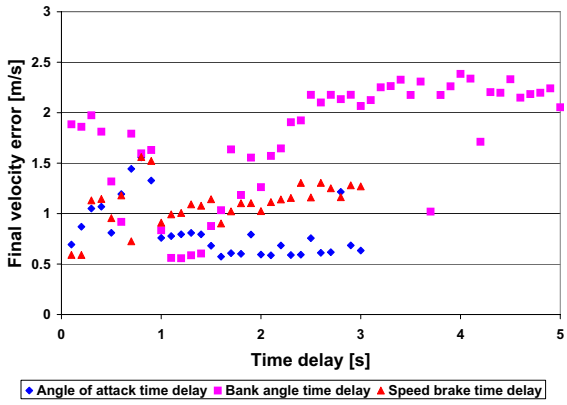

(c) Steering time delays

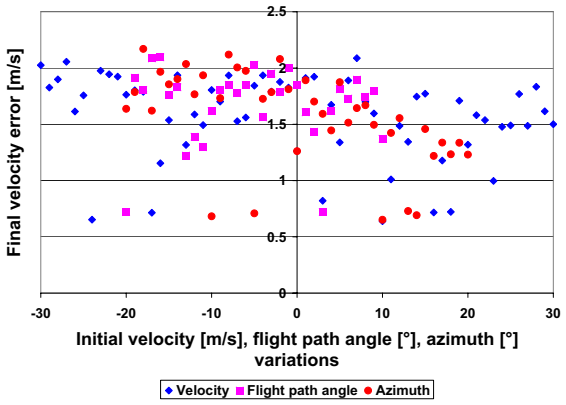

(d) Initial conditions

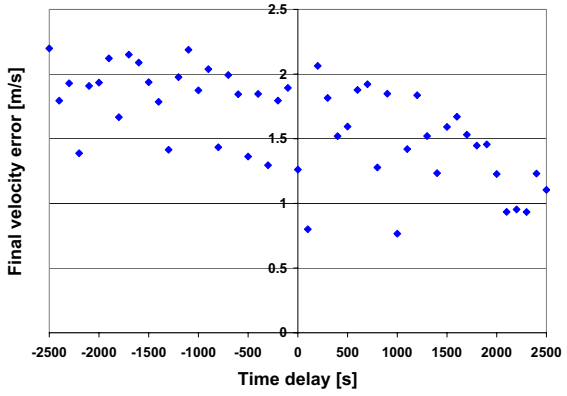

(e) Initial altitude

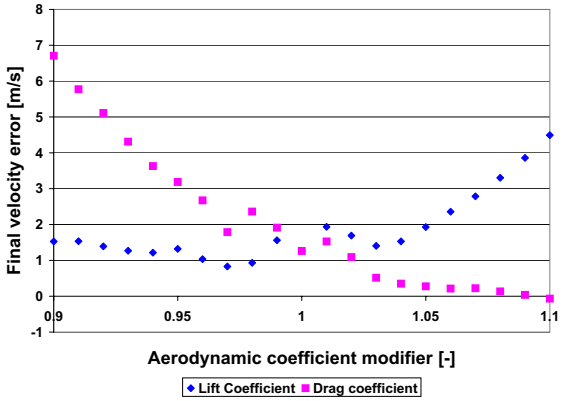

(f) Aerodynamic coefficients

Figure 6.10: The influence of off-nominal conditions on the Hopper vehicle final velocity error

6.10(f) shows how the individual aerodynamic coefficient modifiers influences the final velocity. The final velocity error increases for increasing lift coefficient after a mostly stable error below neutral. The final velocity error decreases for the drag coefficient modifier. The modification of the Hopper vehicle aerodynamic characteristics has a similar effect to the steering time delay modifying the accuracies of the predicted energy dissipation rate and producing a higher velocity for reduced drag and increased lift.

The final azimuth errors due to the different off-nominal condition sets is shown in figure 6.11, here the errors are much smaller than those for target miss or final velocity. The errors observed are not critical and well within the limits provided. The steering time delay, atmosphere and wind and velocity noise were found to be the most influential on the final azimuth errors with the individual errors of these sets shown in figure 6.12

The effect of the steering time delay especially that of the bank angle time delay is shown in figure 6.12(a). The bank angle time delays were expected to cause the

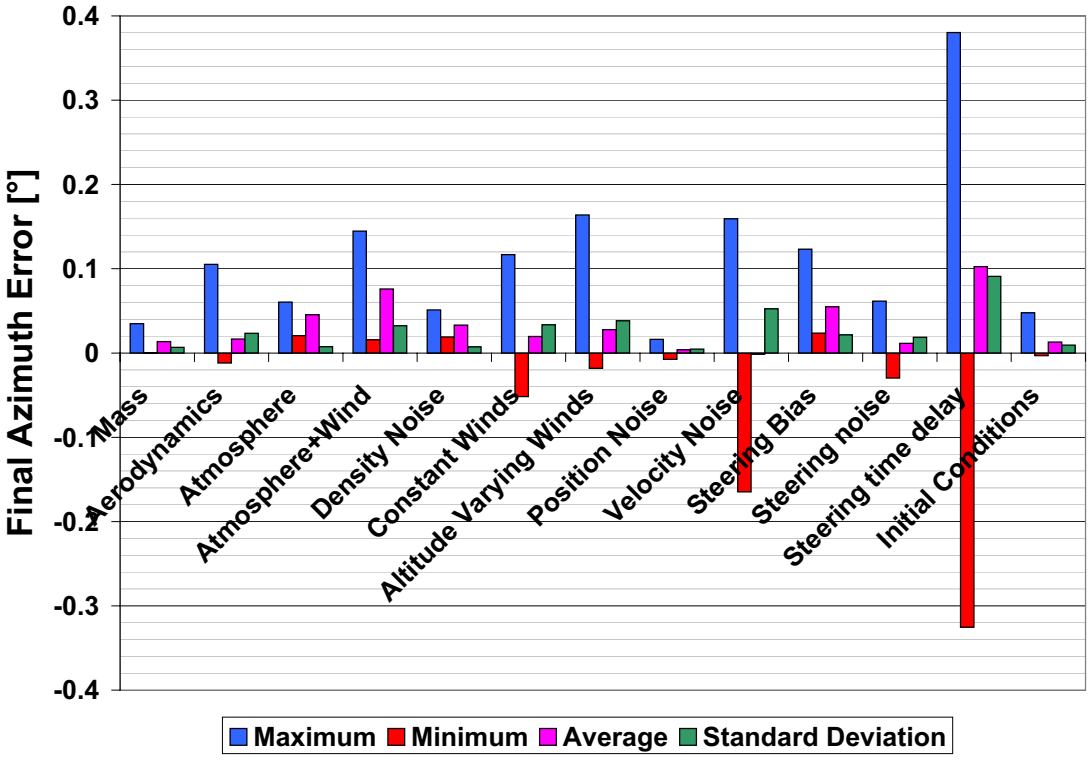

Figure 6.11: The Hopper vehicle final azimuth errors due to off-nominal conditions

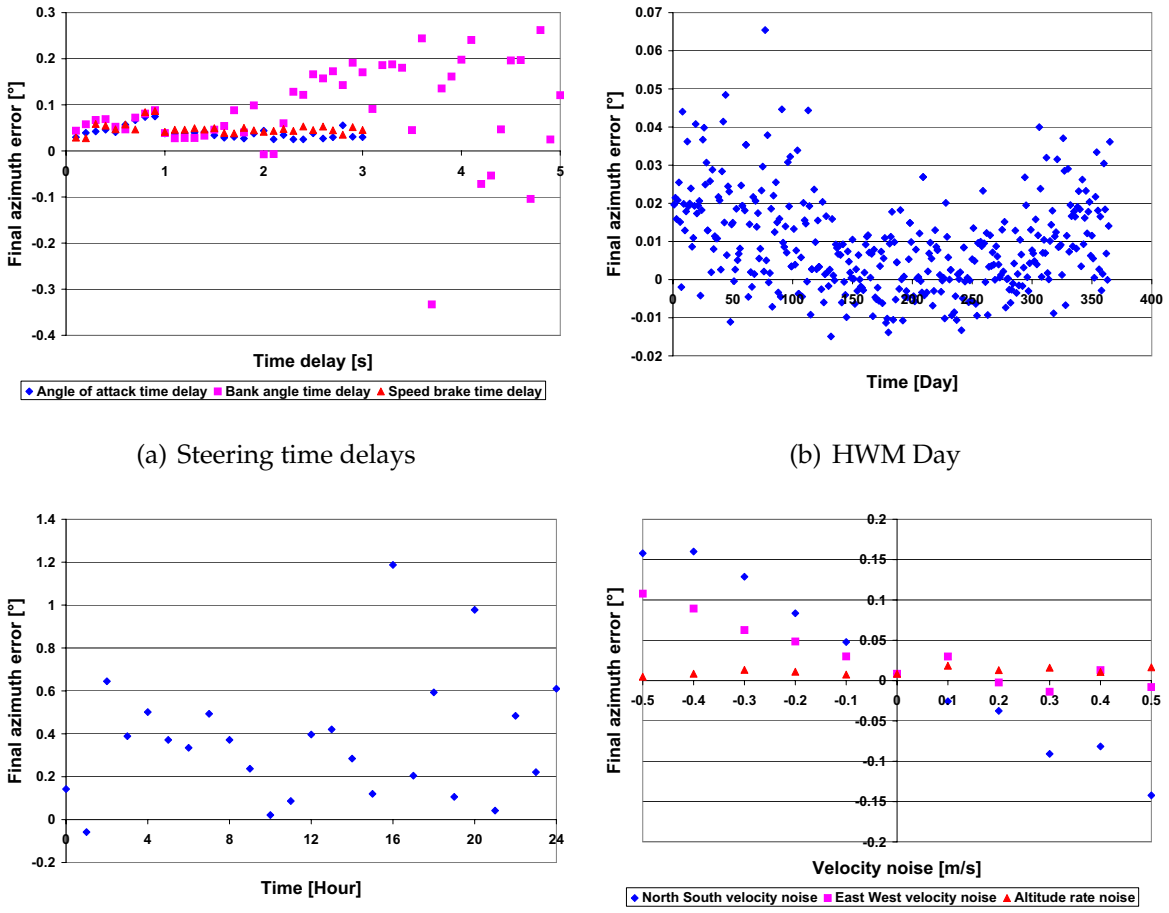

(a) Steering time delays

(b) HWM Day

(c) HWM Time

(d) Velocity noise

Figure 6.12: The influence of off-nominal conditions on the Hopper vehicle final azimuth error

largest azimuth errors because delays in achieving the correct bank angle result in delays in turning and lateral manoeuvring. This also results in a poor alignment with the runway centreline. The final azimuth errors are small showing that the guidance is effectively able to cope with the off-nominal conditions. The angle of attack and speed brake setting time delays produce similar results with small errors in the final azimuth.

For the HWM the time of day has a greater influence on the final azimuth than the time of year as shown in figures 6.12(b) and 6.12(b). The time of day produces larger errors but with a somewhat random pattern. The time of year exhibits similar behaviour to that of the target miss and final velocity error with the middle period of the year having reduced errors and scattering of the results. The HWM would change the actual velocity of the vehicle and produce a small error in the predictor which

explains the very slight final azimuth errors.

The velocity noise also produced only small errors in the final azimuth of the Hopper vehicle. Figure 6.12(d) shows the individual velocity noise errors with the altitude rate producing the smallest final azimuth errors of the three. The influences show a somewhat linear relationship with the final azimuth error decreasing for increased velocity noise or velocity noise in the North and East directions.

The errors for the final flight path angle are larger than those observed for the final azimuth as shown in figure 6.13. The most influential error sets are the atmosphere and HWM, steering time delay and aerodynamics with their individual errors shown in figure 6.14.

The influence of the winds on the final flight path angle can be seen in figures 6.14(a) and 6.14(b). The general trends show that the time of year has a greater influence than the time of day. Figure 6.14(a) also shows that the reduced errors for the middle period of the year. The HWM effects the velocity of the vehicle. In section 5.7 it was discussed how the flight path angle and velocity exhibited coupling. Therefore any influence on the Hopper vehicle velocity also influences the flight path angle. This can also be seen in figures 6.9 and 6.13 where similar error sets influence the final velocity and flight path angle.

The steering time delays cause delays in the Hopper vehicle's attitude which leads to the errors seen for the other final conditions. The steering time delays also influence the final flight path angle. Figure 6.14(c) shows the final flight path angle errors for each of the steering time delays. It was expected that the angle of attack time delay would have the greatest influence on the final flight path angle but instead it seems that the bank angle time delay does. The final flight path angle errors seem to increase with time delay in a similar fashion to the final velocity errors.

The aerodynamic coefficient modifiers are shown in figure 6.14(d) where reduced drag coefficients produced the largest final flight path angle errors. Increases in the drag coefficient modifier results in negative errors that have a magnitude smaller than the positive errors. Complementary to this the reduced lift coefficient modifiers also result in the negative final flight path angle errors. Increased lift coefficient modifiers produce the positive final flight path angle errors but at a reduced level to that of the reduced drag coefficient modifiers.

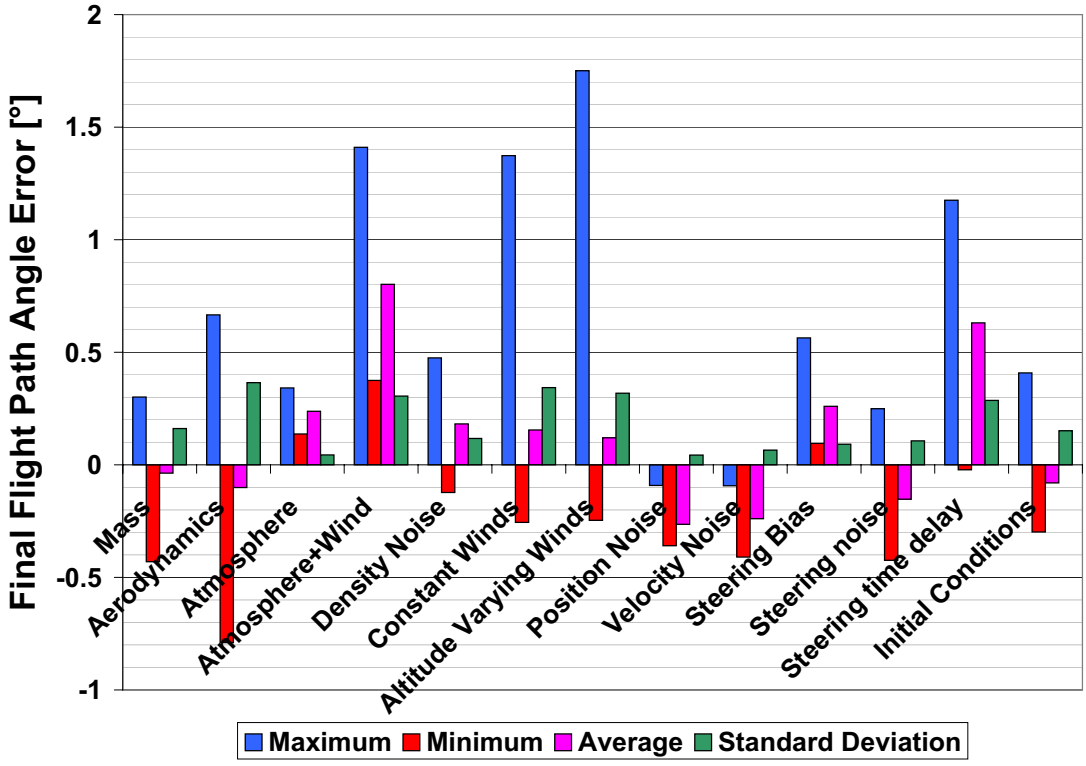

Figure 6.13: The Hopper vehicle final flight path angle errors due to off-nominal conditions

The results presented show that the guidance is effectively able to cope with the individual error sets. The winds and aerodynamic errors were revealed to have been the greatest influence on the final conditions. The evaluation of the guidance program also requires a study of the final conditions errors when all of the off-nominal conditions from table 3.2 are combined. The combined results are discussed in section 6.1.4. An additional evaluation is discussed in section 6.1.5 utilising the initial conditions from the re-entry studies instead of those specified in table 3.2.

6.1.4 Guidance Evaluation

A standard method for evaluating the performance of a guidance method is the utilisation of Monte Carlo simulations. The Monte Carlo method utilises random number or pseudo random number generation of the off-nominal conditions. For the current research a pseudo random number generator was utilised in order to provide the same set of random numbers so continual improvements in the guidance program could be

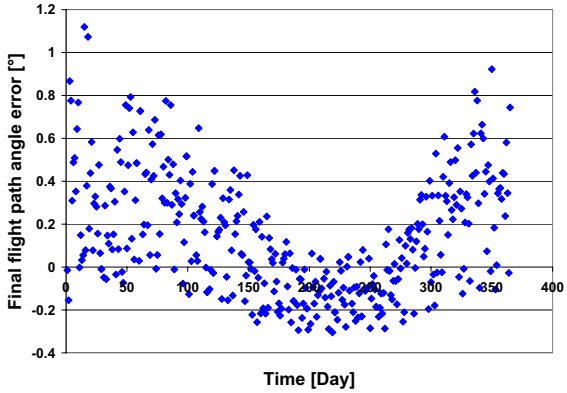

(a) HWM Day

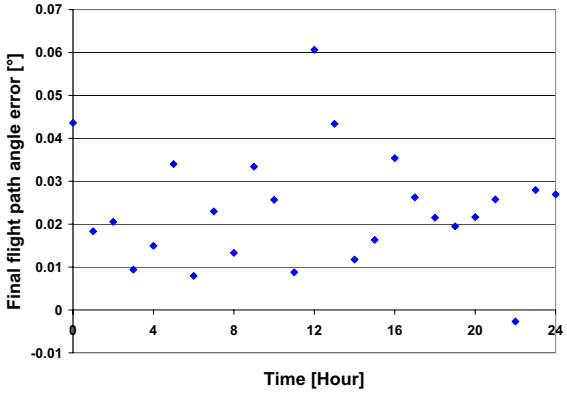

(b) HWM Time

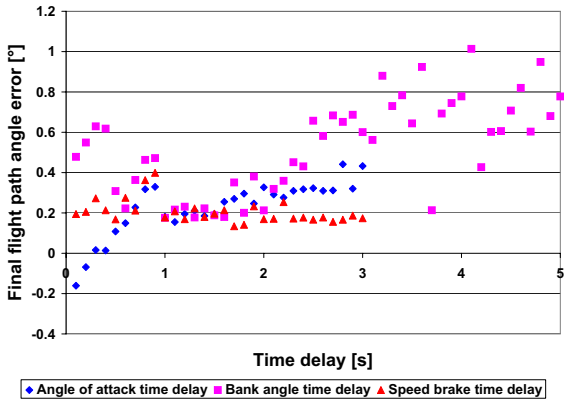

(c) Steering time delays

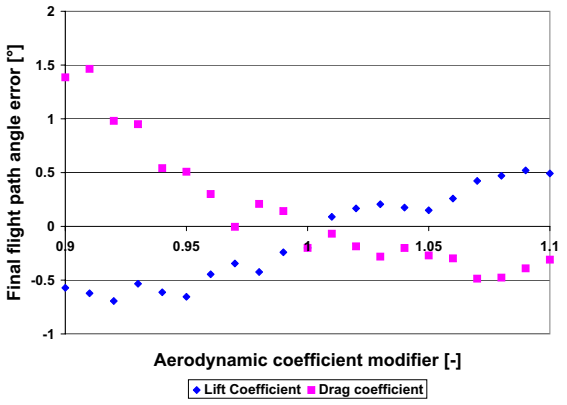

(d) Aerodynamic coefficients

Figure 6.14: The influence of off-nominal conditions on the Hopper vehicle final flight path angle error

properly evaluated. The random number generators were obtained from Press et al. (1997a,b) using routine *rand3*. The Gaussian distribution used for noise errors was also obtained from Press et al. (1997a,b) using routine *gasdev* and a separate *rand3* for the required random number inputs.

A 1000 simulation Monte Carlo analysis was performed using the off-nominal conditions and distributions specified in table 3.2. For the initial position variation there were two different values quoted in the literature. Camara et al. (2002a), Büchner (2003) and da Costa (2003, 2005) state that a circle with a 10 km radius should be used whereas Spies (2003) and Telaar (2005) state a 20 km radius. To provide a comparison to other methods and their results it was important to consider the 10 km radius. However, the re-entry study for the Hopper vehicle in Telaar (2005) utilised a target position

tolerance of 20 km radius and therefore it was also important to consider this in the terminal area flight phase study. If the guidance is able to cope with a 20km radius initial position then it will also be able to cope with a 10km radius consequently the larger variation was utilised. The results for an initial position variation with a 20 km radius circle are presented in figures 6.15 and 6.16 and table 6.3.

The results show that the guidance is effectively able to cope with the off-nominal conditions given in table 3.2. Out of the 1000 simulations performed none failed to reach the final condition tolerances. The largest target miss was 61.0 m which is well within the specified tolerance for the Hopper vehicle mission. Although a specification was given that the lateral error was to be ±100 m (Spies, 2003), the down range tolerance was not specified and therefore the error tolerance was assumed to be a 100 m radius circle for ease of implementation. Figure 6.15 shows that the larger target miss errors are down range and not lateral indicating that if failures occurred they would be minor.

The target miss results in figures 6.15, 6.16 and table 6.3 show that the majority of target miss errors are within 0 to 25 m radius of the target, above 25 m the results are more scattered. The standard deviation of 8.8 m indicates that there is further scattering around the average value of 13.2 m. The further scattering of the results have some lateral and undershooting errors seen in figure 6.15 but are well within tolerance. The target miss errors observed are quite small considering the influences that the various errors can have on the final position as discussed in sections 5.3 and 6.1.3.

The final velocity errors are interesting as all of the errors are positive. The average velocity error is approximately 3.0 m/s with a standard deviation of 1.7 m/s indicating that the majority of values occur with an error of 1 to 5 m/s. There are a few cases where the error is below 1m/s but there are also some cases with larger error values approaching 7 to 9 m/s. However these errors are still within the specified tolerances.

The final flight path angle errors and azimuth errors are quite small as expected as it was revealed in sections 5.3, 6.1.2 and 6.1.3 that they are not as influenced by the off-nominal conditions as the target miss or final velocity errors. Figure 6.16 shows that the values for both the flight path angle and azimuth vary around a slight positive error.

The errors seen for the final conditions were expected as the results in section 6.1.3

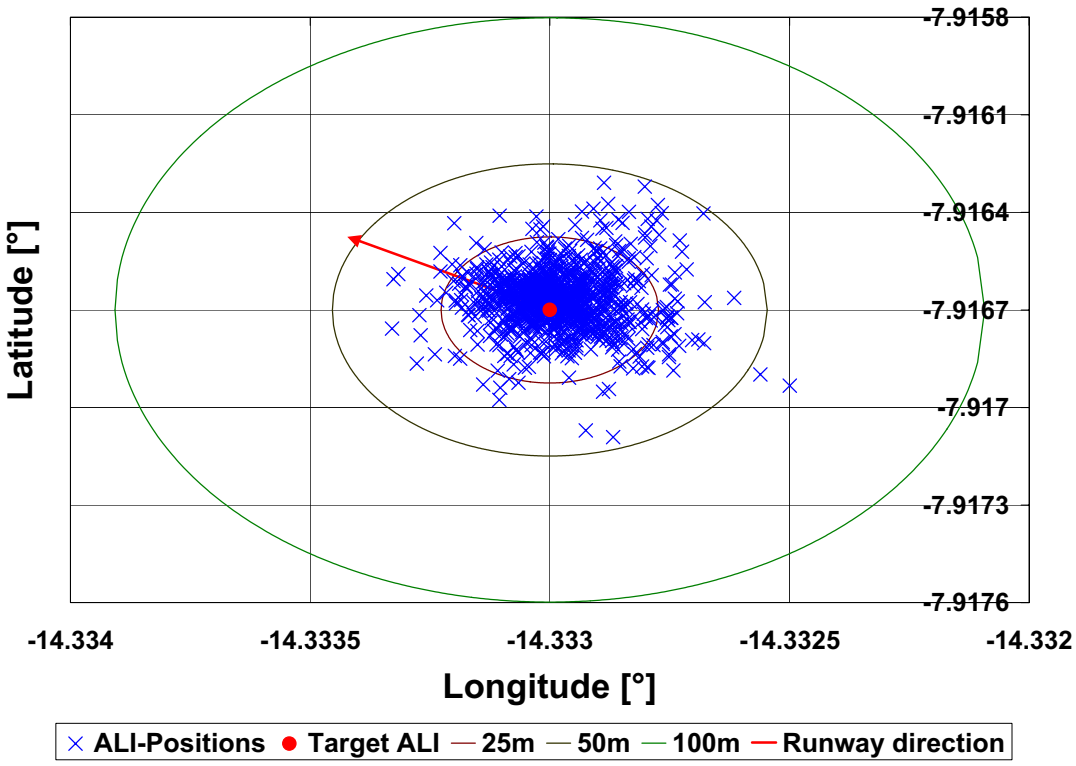

Figure 6.15: Final position results for the Hopper vehicle 1000 simulation run Monte Carlo analysis with off-nominal conditions

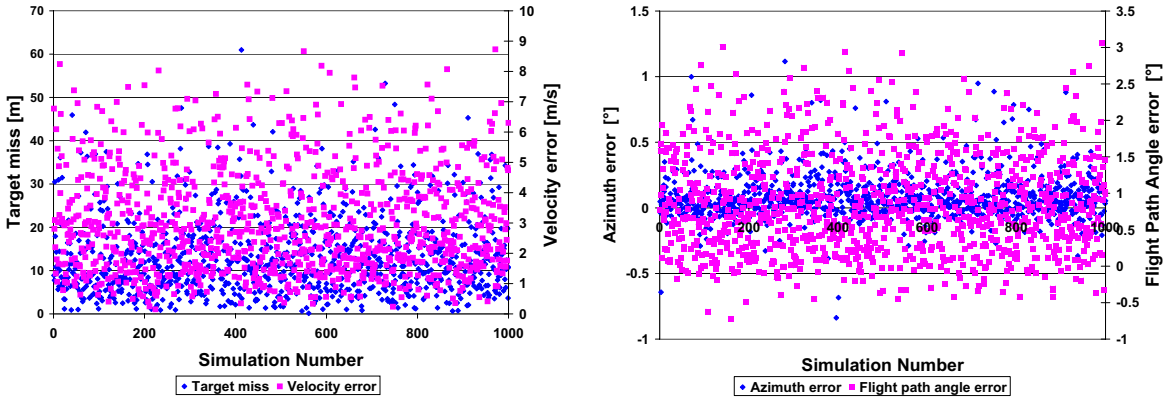

Figure 6.16: The final condition errors for the Hopper vehicle 1000 simulation run Monte Carlo analysis with off-nominal conditions

Restrictions	Target miss (m)	v (m/s)	γ (°)	χ (°)
Number of violations	0	0	0	0
Maximum	60.9695	8.7303	3.0618	1.1160
Minimum	0.1317	0.1502	-0.7267	-0.8376
Average	13.2011	3.0267	0.8474	0.0812
Standard Deviation	8.7659	1.7001	0.6771	0.1708

Table 6.3: Results for the Hopper vehicle 1000 simulation run Monte Carlo analysis with a 20km radius circle initial position variation

already revealed that several of the off-nominal conditions cause significant errors. Therefore when off-nominal conditions are combined together this causes larger errors than those seen in the results of section 6.1.3. However, the results show that the guidance is effectively able to cope with the combined off-nominal conditions specified in table 3.2.

6.1.5 Re-Entry Study Results

The problem formulation described in section 3.1 has been previously applied to the ascent and re-entry phase of the Hopper vehicle mission (Telaar, 2005). Several studies were performed including a 1000 simulation Monte Carlo evaluation with off-nominal conditions (Telaar, 2005). The final results from this evaluation are shown in figure 6.17 and table 6.4.

These results represent the final states of the Hopper vehicle from re-entry and therefore simulated initial conditions for the terminal area flight phase. Looking at the results in figure 6.17 and table 6.4 it is easy to see that several of the trajectories failed to meet the final conditions of the re-entry phase. Although the trajectories failed the final re-entry conditions it might be possible that the terminal area guidance could still recover the vehicle and successfully complete the mission.

The re-entry studies produced results for the final altitude and velocity which are quite different to those specified by Spies (2003). The velocity is lower, approximately 300 m/s for the average value and the altitude is greater, approximately 20 km for the average value. It would seem that the values given by Spies (2003) are not optimal and that the new results from Telaar (2005) should be considered. The velocity and altitude from Telaar (2005) were determined by considering the vehicle's final energy condition

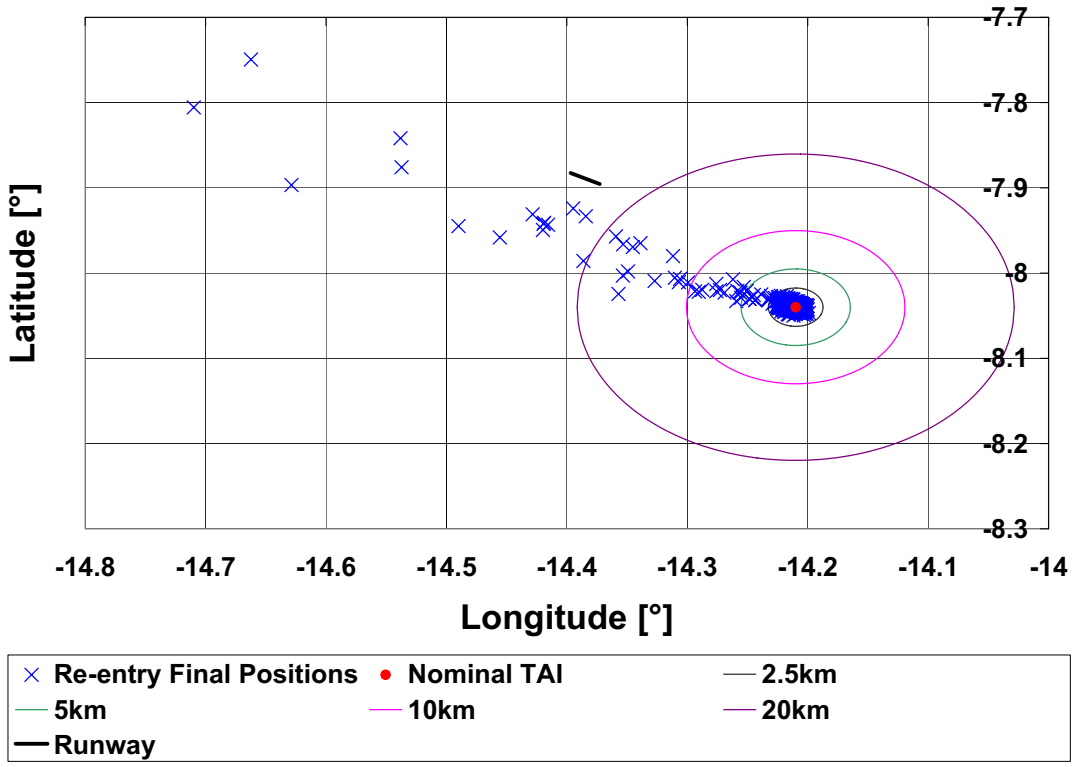

Figure 6.17: Final positions from the Hopper vehicle re-entry studies

Restrictions	Target miss (m)	h (km)	v (m/s)	γ (°)	χ (°)
Maximum	60954.8102	22.1018	389.4199	1.7908	264.6830
Minimum	10.6205	17.2794	239.8281	-51.0334	57.1229
Average	1491.0453	20.3598	299.1692	-26.3745	115.9987
Standard Deviation	4674.7903	1.3858	44.8141	8.1681	18.3983

Table 6.4: Final results from Hopper vehicle re-entry studies

and not specific altitude or velocity values. There are also considerable variations in the azimuth and flight path angles. The flight path angles have some extreme values which are quite steep for the start of the terminal area flight phase as seen in table 6.4. The azimuth in some cases has the vehicle initially heading in the other direction from the standard mission.

To further test the guidance each of the final states from the re-entry phase were loaded into the guidance as the initial conditions including the failed trajectories. Initially no additional errors were applied to the guidance and the results are shown in figure 6.18 and table 6.5.

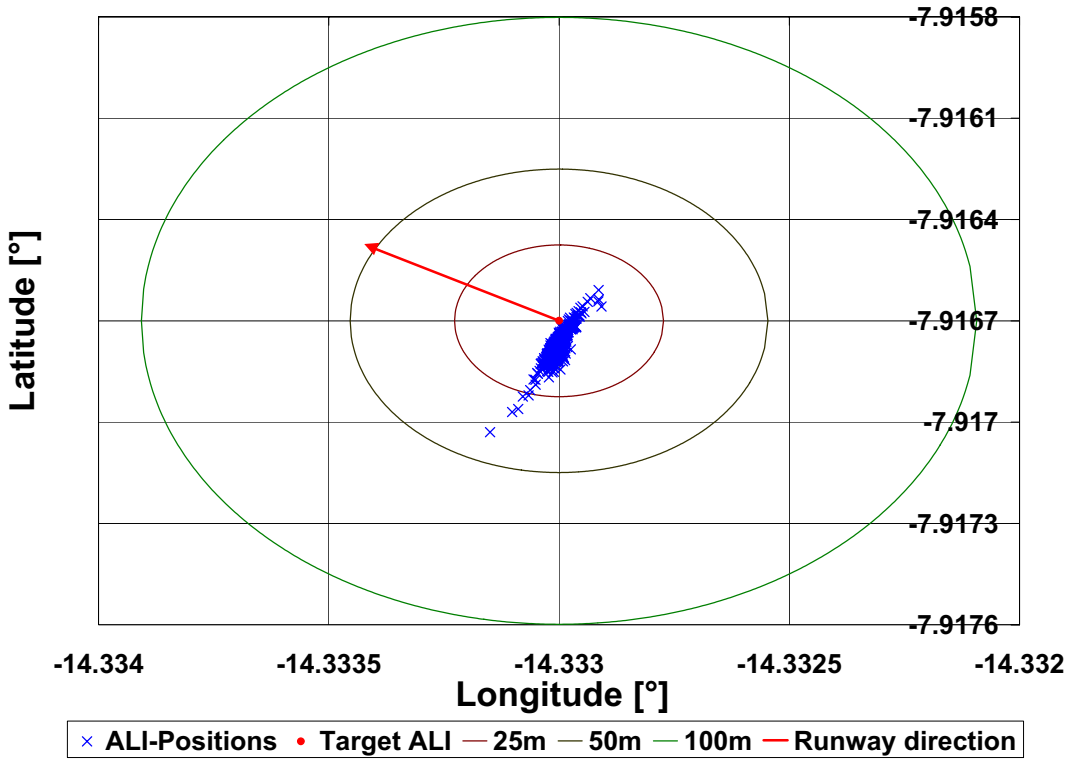

Figure 6.18: Final positions with re-entry study inputs

Restrictions	Target miss (m)	Velocity (m/s)	γ (°)	χ (°)
Maximum	40.2454	2.5810	0.8381	0.7020
Minimum	2.1357	0.6331	-0.2912	-0.0137
Average	8.2577	1.6400	-0.0427	0.0170
Standard Deviation	3.6454	0.1705	0.3554	0.0279

Table 6.5: Final results with re-entry study inputs

The results show that the guidance is effective at coping with the initial conditions provided by the re-entry studies. The guidance is even able to cope with the failed re-entry cases which have a large range-to-go safely delivering the vehicle to the required final terminal area flight phase conditions. The guidance is also able to reach the required final conditions even with extreme cases of initial flight path angle and azimuth well outside of the expected initial conditions for the terminal area interface. The results demonstrate the flexibility and adaptability of the guidance method to cope with large initial condition disturbances. Trajectories which were thought to have failed during the re-entry studies were able to be recovered using the terminal area guidance

suggesting that the guidance method is able to cope with disturbances outside of the specified tolerances for the terminal area interface.

Although the guidance was shown to be adaptable to the initial condition variations obtained from the re-entry studies to prove the applicability of the guidance method the other off-nominal conditions must also be included. Therefore initial conditions obtained from the re-entry studies were also combined with the off-nominal conditions (excluding the initial condition variations) specified in table 3.2 and another 1000 simulation Monte Carlo evaluation was performed. The results are shown in figures 6.19, 6.20 and table 6.6.

The spread of final positions shown in figure 6.19 reveal the effectiveness of the guidance with a large majority of the results within a 25 m radius. The target miss errors are caused by the combination of the errors which have been previously observed and discussed in section 6.1.3. The most influential off-nominal condition sets for the target miss was found to be the HWM, steering command time delays, aerodynamic errors and position noise.

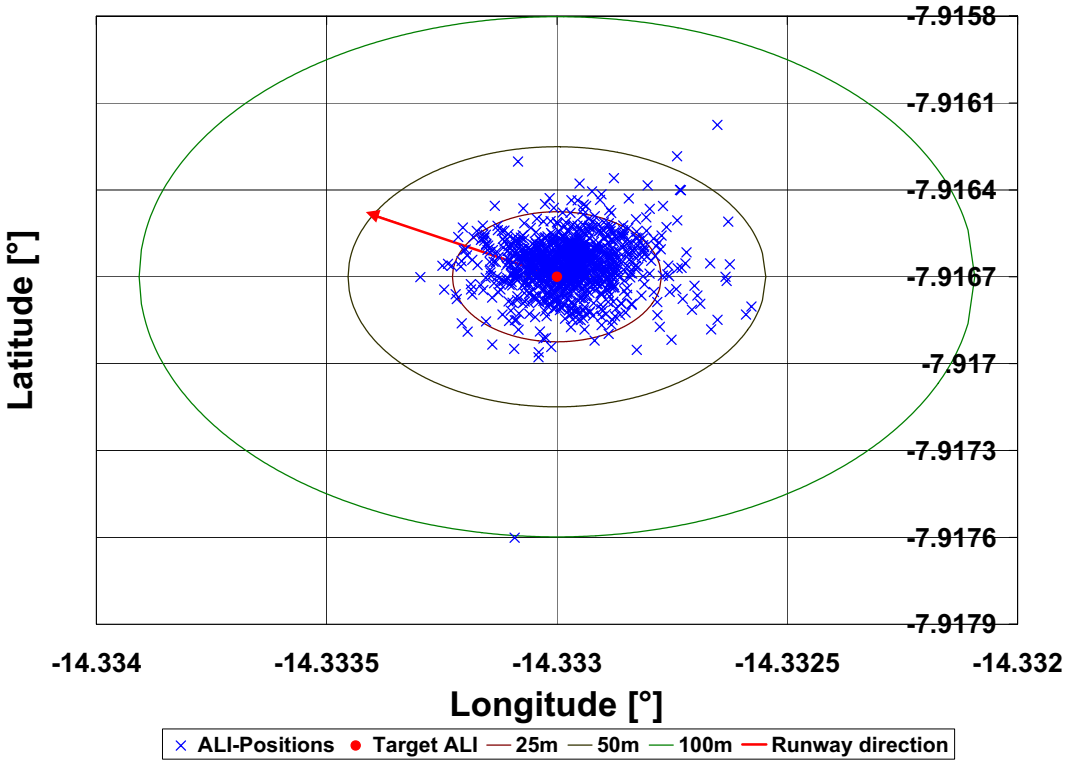

Figure 6.19: Final points with re-entry study inputs and off-nominal condition errors

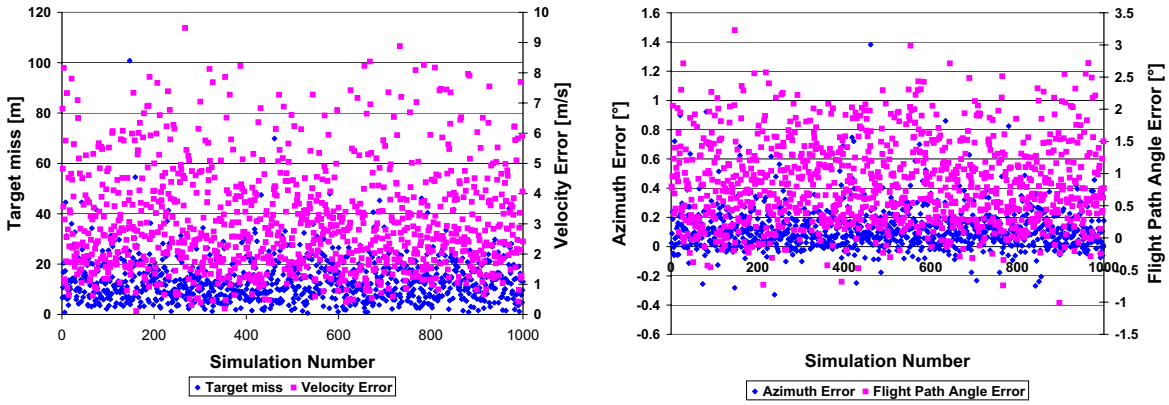

Figure 6.20: Hopper vehicle final condition errors with re-entry study inputs

Restrictions	Target miss (m)	Velocity (m/s)	γ (°)	χ (°)
Violations	1	0	0	0
Maximum	100.8146	9.4825	3.2300	1.3820
Minimum	0.5547	0.1138	-1.0084	-0.3287
Average	13.5650	3.0881	0.8528	0.1148
Standard Deviation	8.8486	1.7073	0.6568	0.1439

Table 6.6: Final results with re-entry study inputs and off-nominal condition errors

There was a single violation of the final condition tolerances with a single trajectory number 147 having a target miss of 100.8 m. The trajectory included the initial conditions from the re-entry results with the largest target miss. Looking at the trajectory the Hopper vehicle reached the bank angle limits for a brief moment in the flight. This could be a possible explanation why the vehicle was unable to reach the target as no other trajectory reached the bank angle steering command limits.

The Phoenix vehicle is a Hopper vehicle demonstrator that was used to test the approach and landing guidance with drop tests discussed in Jategaonkar et al. (2005). The drop tests had a larger initial position error than expected, with the third drop test starting with a 126 m lateral offset and during the trajectory the lateral offset reached a maximum of 245m (Jategaonkar et al., 2005). Camara et al. (2002b) utilised a larger down range tolerance of 500 m. Consequently it should be possible for the approach and landing guidance to recover the trajectory and safely land the Hopper vehicle for the case where the target miss tolerance is marginally exceeded. A more useful tolerance for the target miss based on this information would be a circle with a 250 m

radius.

In figure 6.17 there are several trajectories where the initial positions lay to the North-West (behind) the target ALI point. These results were expected to cause a problem for the guidance program as the reference trajectory is quite different to the trajectory required for these positions. However, as can be seen from the results, the guidance program is able to adapt the trajectory to deliver the vehicle to the required final conditions. The guidance significantly modified the steering command profiles increasing the angle of attack and bank angle values. Figure 6.21 shows the ground track and steering command profile for trajectory #393 and the initial reference trajectory. The trajectory #393 initially had a distance from the TAI of 59433.5 m the second largest distance from the TAI after the failed trajectory #147 with 60954.8 m. The angle of attack was increased to increase the lift-to-drag ratio and therefore range of the Hopper vehicle. The bank angle values were increased to provide sharper turns to enable the vehicle to align with the runway. The speed brake setting was increased towards a setting of 1.0 as shown in figure 6.21.

There were some extreme cases where the initial vehicle velocity was well below the initial values specified by Spies (2003). The initial velocity and altitude provided a Mach number that was less than 1.0 resulting in the instant activation of the speed brake. However, the rest of the steering commands are very similar to those observed in the Hopper vehicle guidance solution without errors shown in figure 6.1. The low velocity initial conditions have associated high altitude due to the energy stopping criteria used in the re-entry study (Telaar, 2005).

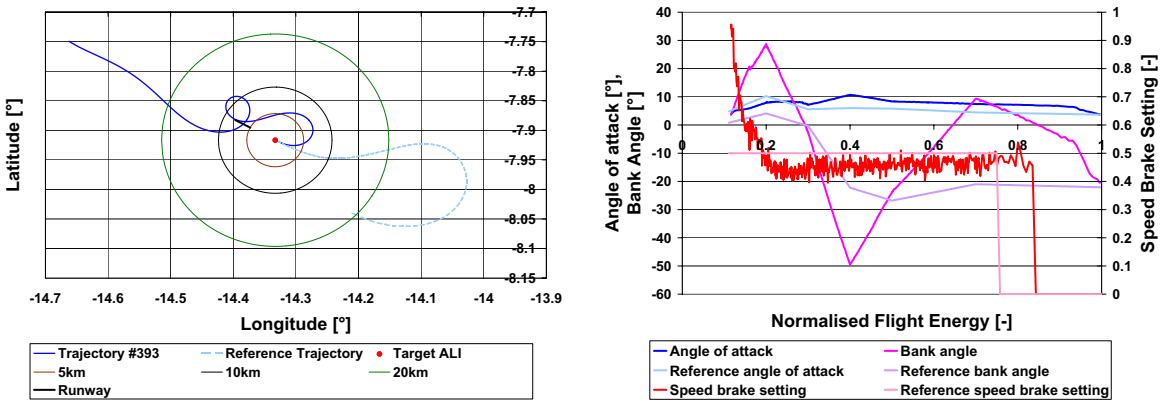

Figure 6.21: Hopper vehicle re-entry trajectory #393 and reference trajectory

The extreme cases for flight path and azimuth angles were also expected to cause problems for the guidance due to the large difference in comparison to the reference trajectory. However, as with the altitude and velocity variations the guidance is effectively able to cope with the flight path angle and azimuth dispersions. For the cases with extreme values for flight path angle the trajectories were modified to include decreased bank angle commands for the initial half of the profile and increased bank angle commands for the final half of the profile. The angle of attack is reduced in a similar manner to the Hopper vehicle guidance solution without any errors shown in figure 6.1. The speed brake setting in a few trajectories increases which is similar to the Hopper vehicle guidance solution without any errors shown in figure 6.1. For the large azimuth errors the trajectories were modified via the bank angle commands with the modifications depending on the direction of the initial heading. The angle of attack and speed brake setting have similar modifications to those made to the Hopper vehicle guidance solution without any errors shown in figure 6.1.

The guidance is able to cope with the wide dispersion of initial conditions from the re-entry studies and in-flight off-nominal conditions to deliver the Hopper vehicle to the required final conditions. These results were accomplished with only a single stored reference trajectory that in almost all of the cases was quite different to conditions experienced during flight. The results show the adaptability and flexibility of the guidance method as it is able to adapt to the conditions experienced even when these conditions are completely different to the stored reference trajectory.

6.1.6 Results Without Speed Brake

To analyse the guidance method further and determine the influence of using the speed brake setting as a steering parameter an evaluation of the guidance program was performed without the speed brake setting. A new initial solution was therefore required without a speed brake utilising the optimisation program and methodology of Chapter 5. Figure 6.22 shows the initial solutions without the speed brake.

The ground track, vehicle state and steering command profiles are considerably different without a speed brake. Larger commands are utilised for the bank angle during the middle stages of the trajectory in order to perform the turn around manoeuvre. At the later stages of the trajectory the angle of attack is increased to compensate for the

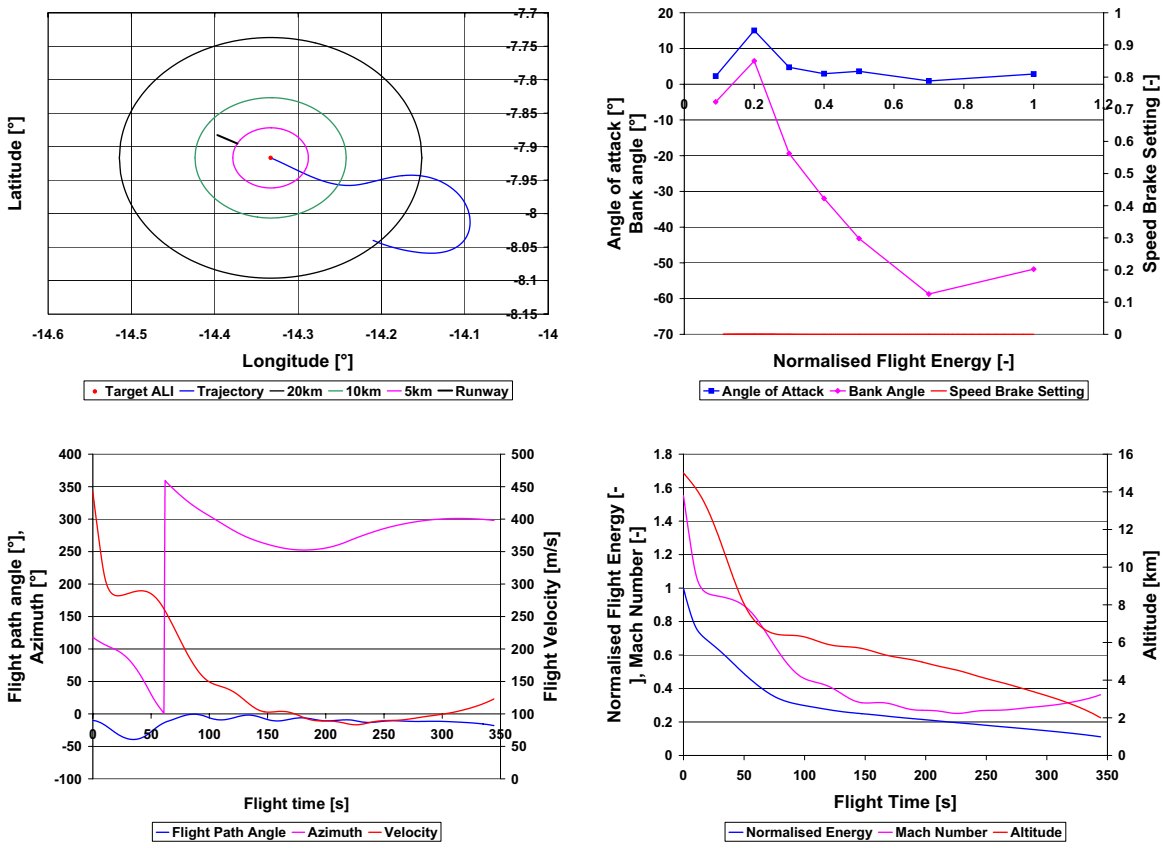

Figure 6.22: Reference trajectory without speed brake

lost drag without the speed brake. There are some commonalities to the trajectory with a speed brake including the rapid transition from supersonic to subsonic speeds. The coupling between the flight path angle and velocity can still be seen at the later stages of the trajectory in figure 6.22.

The initial and off-nominal condition variations given in table 3.2 were utilised to determine how the guidance copes with the dispersions without the speed brake setting as a steering variable. A 1000 simulation Monte Carlo run was performed utilising the new initial solution without speed brake. Figures 6.23 and 6.24 and table 6.7 display the results.

A total of 949 trajectories had one or more restriction violations. The majority of violations were related to the target miss, this can be seen in figures 6.23 and 6.24. The final position results shown in figure 6.23 reveal that without a speed brake the vehicle either overshoots or undershoots the target. The guidance for the Hopper vehicle utilises the speed brake as a method to control the range of the vehicle by varying

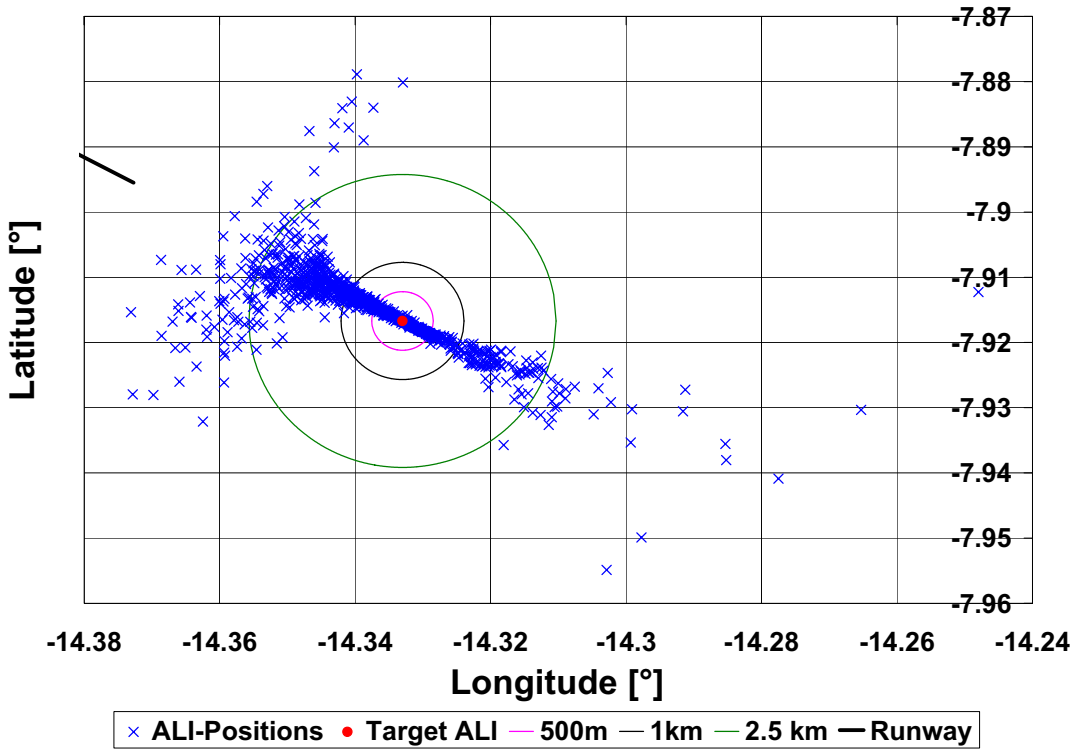

Figure 6.23: Final positions for the Hopper vehicle without a speed brake

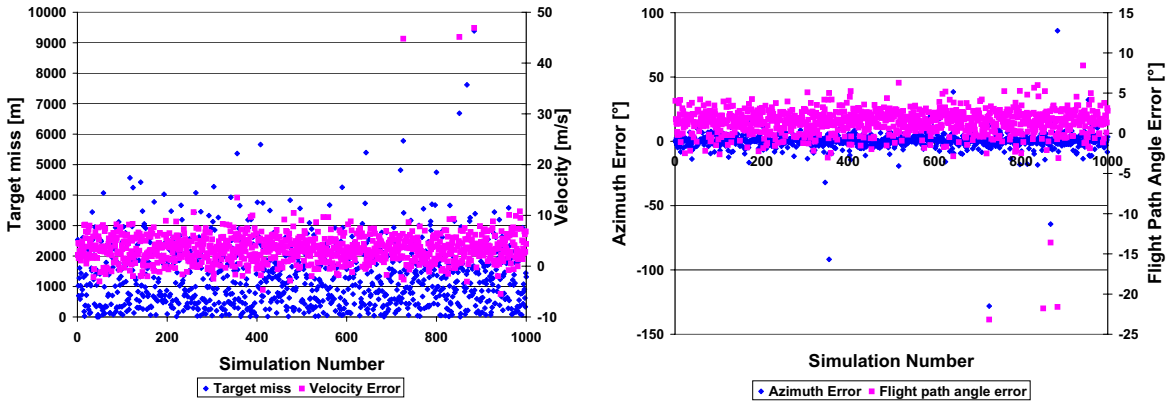

Figure 6.24: Hopper vehicle final condition errors without a speed brake

Restrictions	Target miss (km)	ν (m/s)	γ (°)	χ (°)
Number of violations	949	8	15	54
Maximum	9.3876	46.9230	8.4375	86.0018
Minimum	0.0036	-5.4596	-23.1657	-128.1162
Average	1.3116	3.5104	1.3671	0.0523
Standard Deviation	1.0423	3.3872	1.9581	7.7339

Table 6.7: Results for the Hopper vehicle without a speed brake

the drag and therefore energy dissipation rate. Consequently it is easy to see that the speed brake setting is an important inclusion in terminal area guidance as it provides a method for better control of the energy dissipation rate.

Looking at the results of section 6.1.4 and how the parameters are modified throughout the trajectory the speed brake setting steering parameters are more active at the end of flight than the angle of attack parameters. The speed brake setting command parameter used in the Hopper vehicle guidance program allows the predictor to modify the Hopper vehicle's drag without affecting the lift. Therefore an increased energy dissipation rate can be achieved with only a change in drag. Whereas a modification to the angle of attack would modify the vehicle's drag and lift coefficients. The speed brake setting then becomes important towards the end of flight where energy needs to be dissipated without significantly changing the vehicle's runway alignment or position.

The other restriction violations seem to be extreme cases where the overshooting or undershooting caused by the speed brake also results in failures for the final velocity, flight path angle and azimuth. As mentioned in section 6.1.5 it is possible to increase the target miss tolerances. When a target miss tolerance of 250 m is considered then there are 885 trajectories that fail to reach the target miss limit.

6.1.7 Comparison to Other Methods

There has been previous research into the development of terminal area guidance for the Hopper vehicle using the methodologies that were discussed in section 2.3.6. The Hopper vehicle concept has undergone various stages of development especially with regards to refining the vehicle models most importantly the aerodynamic model. Consequently the various studies Camara et al. (2002b), Büchner (2003), da Costa (2003) and da Costa (2005) might have different models than those used within this study for the Hopper vehicle. The studies performed also use different assumption for the flight environment. For example Büchner (2003) utilised a flat Earth where this study utilises a 4th order Earth shape model. The studies Büchner (2003), Camara et al. (2002b), da Costa (2003) and da Costa (2005) are papers presented at conferences and consequently do not provide a detailed evaluation of the guidance for all the off-nominal conditions considered here. Another major difference between this research and other methods is that within this research the final altitude is utilised as the stopping con-

dition allowing no variation of the final altitude whereas the other results generally have some allowed variation in the final altitude. These attributes make it difficult to perform a direct comparison between this research and the studies of Camara et al. (2002b), Büchner (2003), da Costa (2003) and da Costa (2005). However, a generalised comparison can be made with regards to the results and the strengths and weaknesses of the methodology used.

Camara et al. (2002b) utilises a modified Shuttle based methodology discussed in section 2.3.6. Camara et al. (2002b) performed a Monte Carlo variation with simultaneous variation of the initial conditions namely azimuth, Mach number and position. A mean wind velocity was also included. The values of variation for the errors are not specified and the initial and final conditions are different to those used within this study. The final position results show similar results to those discussed in section 6.1.4 with the guidance working effectively for the unspecified error values.

Büchner (2003) utilises a method more closely related to that of Grubler (2001) separating the lateral and longitudinal guidance, this is discussed more in sections 2.3.3 and 2.3.6. Büchner (2003) presented results for the initial position variation within a 10 km radius circle and initial heading variation of $\pm 20^{\circ}$. The results were exceptional with the final position errors less than 1m and stated that the 'final conditions are met with high accuracy (position and heading)' (Büchner, 2003). Additionally all the constraints were respected indicating no restriction violations.

The final position error for initial azimuth variations of this study had an average value of 7.5 m with a maximum value of 12.7 m. The position variations using a 20 km circle produce an average target miss of 8.0 m with a maximum of 19.6 m. The results presented in Büchner (2003) are exceptional. However it should be noted that the initial position and heading utilised are different to those used in this study with the heading being towards the target and the initial position is 12 km downrange. Consequently the vehicle does not require the difficult turnaround manoeuvre common to the results of this study. Additionally the results for the final velocity and flight path angle are not presented. The velocity errors were shown to be quite large for the guidance method of this study and it would be interesting to perform a comparison.

da Costa (2003) and da Costa (2005) summarises and provide additional results using the methods of Camara et al. (2002b) and Büchner (2003). da Costa (2003) reveals

that using the method of Büchner (2003) with a 10 km radius circle initial position variation, 99.2% of trajectories meet the requirements of the ALI and there were 'no catastrophic failures'. The results from this study show that using a 20km radius circle position variation all trajectories are able to reach the required ALI conditions within the specified tolerances.

da Costa (2005) also presents results for the advanced path control activities discussed in section 2.3.6. The results presented utilised a Monte Carlo evaluation with dispersions for wind and vehicle aerodynamics, 15% lift and drag errors with a 3σ distribution. da Costa (2005) states that 99.1% of the results met the required ALI conditions. Using the same errors, 92.7% of the results using this guidance method meet the required ALI conditions. If a target miss of 250 m is considered then 95.5% of the trajectories reach the required conditions. The errors are caused by the large aerodynamic errors with large increases in lift-to-drag ratios resulting in final velocity violations and large reductions of the lift-to-drag ratio resulting in target miss violations. The guidance method utilised in this study appears to be more sensitive to the aerodynamic errors than the method presented in da Costa (2005).

A direct comparison to the results of Camara et al. (2002b), Büchner (2003), da Costa (2003) and da Costa (2005) does not provide a quantitative evaluation due to differences in vehicle and simulation environments, applied errors and mission conditions. However, the general comparison of the results reveals that the guidance method investigated in this study provides similar results to those published in literature.

6.2 The X-33 Vehicle Results

To verify the flexibility and adaptability of the guidance method it was decided to utilise the guidance program for a different vehicle type and mission. It was also important to be able to provide a comparison to other methods both utilised and under development. The X-33 vehicle was selected as much of the recent work on terminal area guidance such as Burchett (2004) and Kluever and Horneman (2005) has been applied using the X-33 vehicle. The X-33 vehicle and mission data were also available to the author. Another reason for the selection of the X-33 vehicle was that significant work had been performed on the vehicle models especially with regards to aerodynam-

ics.

The mission for the X-33 vehicle discussed in section 4.2 is significantly different from that of the Hopper vehicle and therefore would provide a useful evaluation of the guidance program under different conditions. The higher initial velocity and altitude would allow for a useful extension of the guidance envelope. The lifting body type aerodynamics of the X-33 vehicle results in different manoeuvrability characteristics and sensitivities useful for identifying the applicability and adaptability of this guidance methodology to other types of reusable launch vehicles.

Similar to the Hopper vehicle an initial guidance simulation was performed to ensure that the models and the guidance were operating correctly. Another reason was highlighted by the results for the Hopper vehicle, figure 6.1 showing how the steering profile especially the speed brake setting changed for the guided trajectory. It is useful to see how the guidance modifies the trajectory for the X-33 vehicle especially with regard to the different speed brake model. The results for an X-33 vehicle trajectory without off-nominal conditions are shown in figure 6.25 and table 6.8.

Here the X-33 vehicle guidance works exceptionally well even better than the results provided for the Hopper vehicle guidance in table 6.1. Similar to the Hopper vehicle guidance the errors in table 6.8 are due to the difference in predictor and simulator models. The target miss and velocity errors are reduced when compared to those previously observed with the Hopper vehicle guidance. An implication of this is that the X-33 vehicle guidance might be better able to adapt to model discrepancies and errors than the Hopper vehicle guidance. However, further evaluations revealed problems with the X-33 vehicle guidance coping with winds, discussed more in section 6.2.6.

The flight path angle and azimuth errors are larger than those observed for the

Conditions	Target miss (m)	v (m/s)	$\gamma(^\circ)$	$\chi(^\circ)$
Target conditions	0 ± 100	173.7 ± 10.67 (570 ± 35ft/s)	-30 ± 5	121.5 ± 5
Guidance results	3.4790	173.5560	-29.3986	121.7742
Errors	3.4790	-0.1440	0.6014	0.2742

Table 6.8: X-33 vehicle guidance results without off-nominal conditions

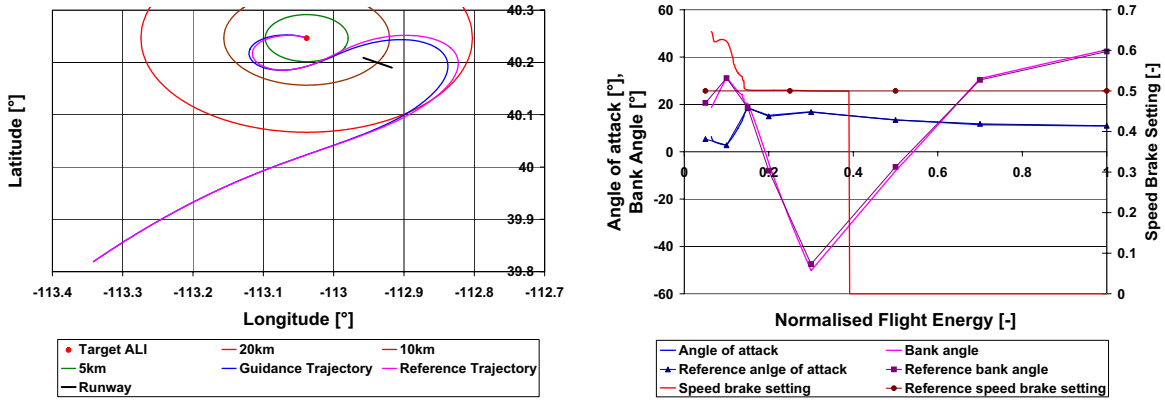

Figure 6.25: X-33 vehicle ground track and steering profile of the initial solution and solution after restoration steps for nominal conditions

Hopper vehicle guidance. This is most likely a cause of the scaling modifications made for the X-33 vehicle guidance discussed in section 6.2.1.

The restoration steps of the X-33 vehicle guidance also modified the steering commands. This was again caused by the speed brake setting parameter being active within the guidance program but fixed during trajectory design and optimisation. Figure 6.25 shows the ground track and steering profile for the X-33 vehicle guidance without off-nominal conditions and the reference trajectory.

6.2.1 X-33 Vehicle Guidance Modifications

The guidance program is designed to be modular allowing for quick and easy modifications to perform analysis on different vehicles and missions. To perform studies on the X-33 vehicle the mission and vehicle data was required. The mission data included: reference trajectory, initial and final conditions, in-flight restrictions and some modifications to the values of off-nominal conditions. The vehicle data included the aerodynamic model subroutine and vehicle properties such as mass and reference area. The modular nature meant that no significant modifications were required to other subroutines within the guidance program showing the flexibility and adaptability of the program to be quickly applied to another mission and vehicle.

Performance analysis of the guidance revealed that the X-33 vehicle was having some problems initially coping with meeting all of the target requirements, especially the target miss and final velocity errors. Slight modifications to the target miss and

final velocity error scaling were made to increase their importance with regards to the other final conditions, which resulted in improved performance for the X-33 vehicle. It is important when scaling the restrictions to ensure that they are of similar magnitude because otherwise the guidance will be biased to achieve one restriction. These modifications were not required for the Hopper vehicle mission because the scaling of the restrictions had already been investigated during the early guidance studies (Chartres et al., 2005a).

The X-33 vehicle guidance also appeared to be having problems coping with the wind profiles produced from the HWM 1993, this is discussed more in section 6.2.5. An improvement was made to the X-33 vehicle guidance by utilising an on-board wind profile predictor which used simple models that could be uploaded from the landing site, this is discussed more in section 6.2.6.

6.2.2 Real Time Operation

A real time evaluation of the X-33 vehicle guidance was also performed using the same methods as that for the Hopper vehicle guidance discussed in section 6.1.1. The average X-33 vehicle guidance computation time for the first call was 260.8 ms. This is slightly greater than that of the Hopper vehicle and can probably be related to the increased number of parameters requiring two additional flight path predictions. Note that although this was the computation time required the code is experimental and research based, building upon previous work which consequently contains redundant lines of code. The guidance program has also never been optimised for speed. Instead it was written by several different authors including students and is designed for ease of use over computational speed.

The results for the guidance call interval and integration step size variations are shown in figures 6.27 and 6.26 respectively. The results for the guidance call variation exhibit similar results to that of the Hopper vehicle guidance except that the final condition errors are larger. It would seem that the X-33 vehicle is more sensitive to variations in guidance call interval than the Hopper vehicle. Again it can be seen that guidance call intervals below 1.0 seconds provide no significant improvements in final condition errors except for small improvements in the final velocity error. Considering the average computation time of the first call, a guidance call interval of 1.0 second is

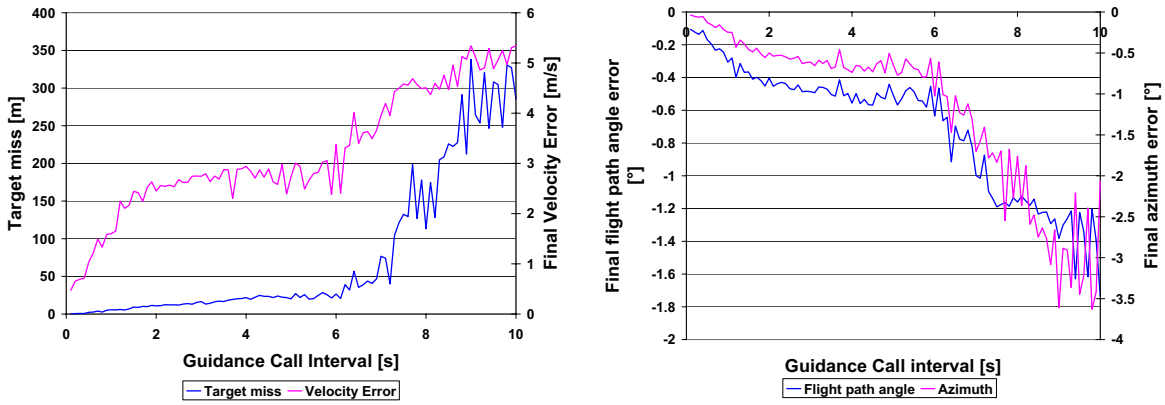

Figure 6.26: Guidance call interval influence on X-33 vehicle final conditions

suitable for both the Hopper and X-33 vehicles guidance.

The results for the integration step size are similar to the results for the Hopper vehicle guidance discussed in section 6.1.1. The target miss and final velocity conditions are violated at large integration step sizes. The results show that below 1.0 seconds no significant improvement in final condition errors is achieved. Therefore to minimise the computational effort an integration step size of 1.0 seconds is used for the predictor.

6.2.3 Guidance Worst Cases

The sensitivity studies conducted for the X-33 vehicle in section 5.3 revealed that the guidance would need to be able to cope with large final condition errors caused by poor vehicle aerodynamic modelling especially with regards to the lift coefficient. The

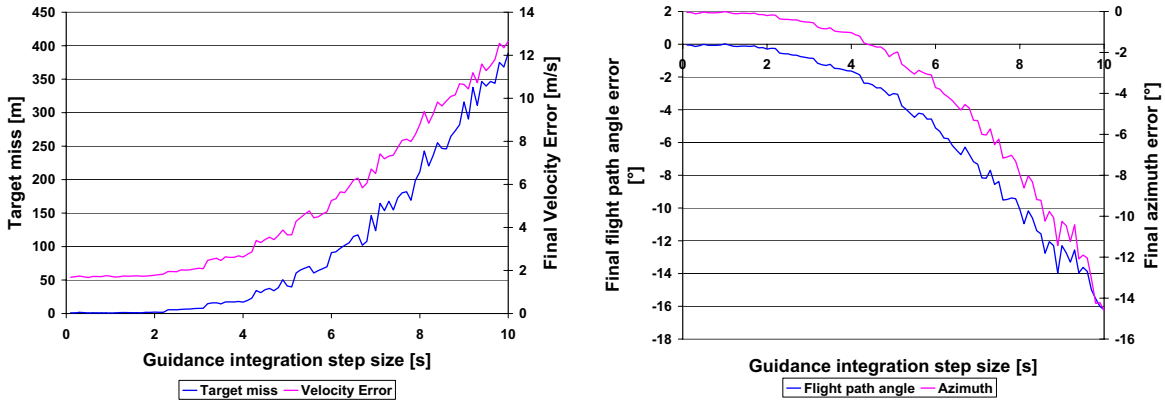

Figure 6.27: Guidance integration step size influence on X-33 vehicle final conditions

X-33 vehicle and mission were also influenced by density, mass and initial condition errors. The guidance was evaluated using the off-nominal conditions from table 5.3. The results are shown in figures 6.28, 6.29 and table 6.9.

The results show that the guidance for the X-33 vehicle is capable of handling the off-nominal conditions and delivering the vehicle to the required final conditions. All of the final condition errors shown in table 6.9 are well within the required tolerances indicating that the guidance program also works for the X-33 vehicle without any major changes.

The ground tracks shown in figure 6.28 reveal how the guidance adapts the ground track for the various off-nominal conditions relating to the simulated model errors. Different to the Hopper vehicle results presented in section 6.1.2 the X-33 vehicle ground tracks appear to be more closely related to the initial reference solution during the majority of the ground track. There are some variations occurring during the first and second turn around manoeuvres where the modifications to the steering profiles result in variations of turn radius at the location of the manoeuvres. The start of the trajectories are almost identical. This is expected since the X-33 vehicle is not very manoeuvrable at the early stages of flight due to the high initial Mach number and aerodynamic characteristics of the vehicle.

Similar to the Hopper vehicle results discussed in 6.1.2, the trajectory variations for the X-33 vehicle are more pronounced for the aerodynamic errors. The applied drag errors result in ground tracks that either have tighter turns or more delayed turns for the positive and negative errors respectively. Interesting is that a positive lift error has a similar effect to the negative drag error but not of the same magnitude. The trajectories that most relate to the guided solution shown in figure 6.25 are those that include the errors for mass -10% and density +10%.

A comparison to the optimisation sensitivity study results presented in figure 5.5 show that the guidance primarily modifies the steering commands so that the turn around manoeuvres occur more like the reference trajectory. The plots for the various steering command modifications due to the off-nominal conditions are included in Appendix D.

The ground tracks shown in figure 6.29 present how the guidance modifies the ground tracks for the variations in initial conditions given in table 5.3. The results for

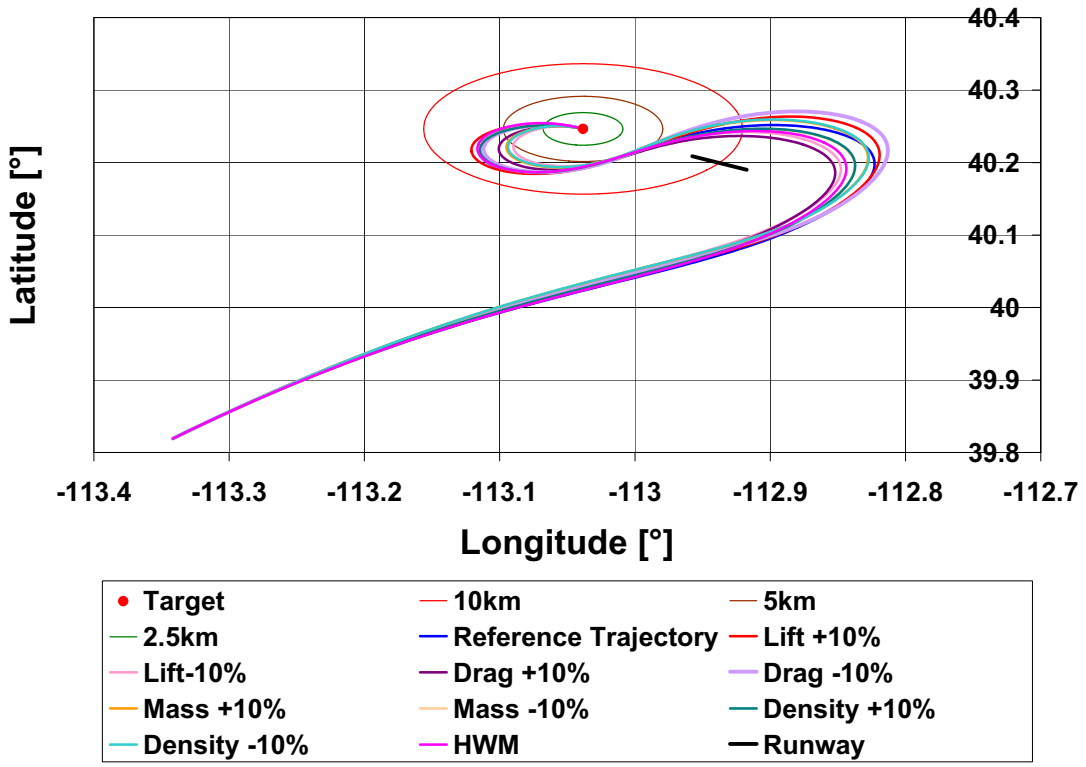

Figure 6.28: X-33 vehicle guidance results with worst case off-nominal conditions for vehicle and environment models

the X-33 vehicle studies are again different to those of the Hopper vehicle. The ground tracks for the X-33 vehicle are much closer to the reference trajectory and initial guided solution shown in figure 6.25. A comparison to the optimisation results presented in figure 5.6 and the results of figure 6.29 show that the guidance modifies the steering commands such that the ground track becomes more similar to the reference trajectory solution except for the $\pm 15^{\circ}$ initial azimuth modifications.

In figure 6.25 it was shown that the speed brake setting increased towards the end of flight. Looking at figures D.15, D.16, D.17 and D.18 it can be seen that the speed brake setting is increased to the maximum value in order to adapt to the off-nominal conditions.

The azimuth errors as expected resulted in a skewed ground track. However, the results were also unexpected as the guidance modified the turn around manoeuvres within the ground track. The modifications to the ground track were achieved via significant modifications to the bank angle profile, as shown in figure D.16. The variation of the bank angle commands for some of the data points are evenly distributed with

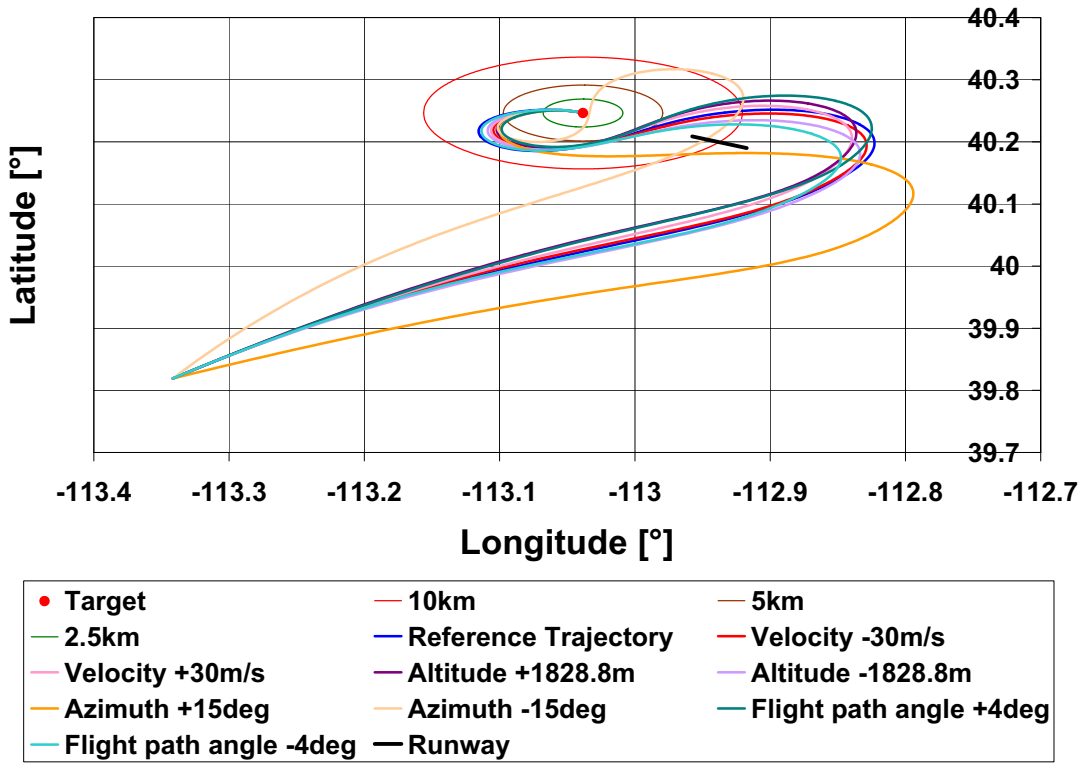

Figure 6.29: X-33 vehicle guidance results with worst case initial conditions

the reference trajectory in the middle.

The final azimuth and flight path angle errors shown in table 6.9 are exceptionally small for almost all cases. The applied model errors seem to have a bigger influence on the guidance results than the initial condition variations. Similar to the Hopper vehicle the mass of the X-33 vehicle is well known before the terminal area flight phase and so the ±10% mass error is much greater than would occur in a real flight. However, the adaptability of the guidance program with increased mass allows for possible payload return or abort capabilities. The density and lift coefficient errors had the greatest influence on the guidance indicating that improvements in the guidance could be achieved by more accurate atmospheric and aerodynamic models for the vehicle. However, the guidance works effectively with the current errors with all results well within the final condition tolerances.

Kluever and Horneman (2005) also performed experiments on their guidance system with variations of the initial altitude and azimuth. The results for the initial conditions are provided in table 6.10 (Kluever and Horneman, 2005).

Conditions	Target miss (m)	Errors v (m/s)	γ(°)	χ(°)
Mass +10%	20.3901	5.8254	-0.9065	-1.4400
Mass -10%	8.9546	-0.8848	1.2188	0.7030
C_D +10%	3.1044	-0.0068	-0.4129	-0.3411
C_D -10%	5.2795	8.9507	0.6158	0.3629
C_L +10%	5.7535	3.2863	0.7829	0.3524
C_L -10%	16.4204	2.2899	-0.9270	-1.4574
ρ +10%	8.3511	-0.6371	1.0177	0.6004
ρ -10%	22.0380	6.2095	-0.7728	-1.3157
Winds	3.6578	3.3948	0.4935	0.1882
Initial v +30 m/s	1.1077	1.6759	-0.0669	-0.0613
Initial v −30 m/s	2.0355	1.7632	-0.1901	-0.1371
Initial h +1828.8 m	0.9577	1.6906	-0.0489	-0.0504
Initial h −1828.8 m	0.9584	1.7201	-0.0629	-0.0489
Initial χ +15°	0.9075	1.6994	-0.0468	-0.0474
Initial χ −15°	0.6809	1.6486	-0.0072	-0.0138
Initial γ +4°	2.6148	1.8854	-0.2880	-0.2459
Initial γ −4°	0.9224	1.6898	-0.0734	-0.0611

Table 6.9: X-33 vehicle guidance results with worst case off-nominal conditions

Dispersions	Target miss (m)/(ft)	v (m/s)/(ft/s)	γ (°)
None	3.35 (11)	6.46 (-21.2)	0.1
Initial h + 1828.6 m(6000 ft)	51.82 (170)	2.77 (-9.1)	0.1
Initial h − 1828.6 m(6000 ft)	1.52 (5)	5.73 (-18.8)	0.0
Initial χ + 15°	0.30 (1)	6.61 (-21.7)	0.1
Initial χ − 15°	9.14 (30)	6.43 (-21.1)	0.1

Table 6.10: Results from Kluever and Horneman (2005) for initial altitude and azimuth variations

Although the same errors were applied the same environment models were not utilised and this makes a direct comparison difficult since there is no commonality in the methods of testing. A partial comparison can be made by looking at the results of the tables 6.9 and 6.10. From these tables it can be seen that the method used within this research seems to provide better results. This would seem to indicate that the restoration steps are more effective at coping with these errors than the trajectory planning guidance method discussed in section 2.3.9. However, as shown in sections 6.1.3 and 6.2.4 even the modelling of the atmosphere can have an influence on the results. To perform a proper evaluation the same simulation environment should be utilised.

Although the X-33 vehicle guidance was successfully able to cope with the off-nominal conditions specified in table 5.3, these simulations only included a single error of fixed value for certain types of errors. Further evaluation of the guidance which looks at the influence of initial position, sensor, navigation and time delay errors is discussed in section 6.2.4. A Monte Carlo evaluation of the guidance is discussed in section 6.2.5 looking at the combined influences of all the off-nominal conditions.

6.2.4 Sensitivity Studies

A sensitivity study was also used to evaluate the influence of the off-nominal conditions on the X-33 vehicle guidance. Similar to the Hopper vehicle sensitivity study 100 simulations were performed with a random spread for each of the different type of off-nominal conditions; mass, aerodynamics, atmosphere, atmosphere and wind, density noise, constant winds, altitude varying winds, position noise, velocity noise, steering bias, steering noise, steering time delay and initial conditions. The results for these studies are presented in figures 6.30, 6.32, 6.36, 6.34 and 6.38. These studies allowed the most influential error sets to be determined and then the individual errors of the influential sets were further analysed.

Figure 6.30 shows the maximum, minimum, average and standard deviation of the X-33 vehicle target miss for the various sets of off-nominal condition. The results show that winds, steering time delays and aerodynamic errors have the greatest influence on the X-33 vehicle target miss. Figure 6.31 shows how each of the individual errors from the influential error sets affect the final conditions.

The influence of the Horizontal Wind Model (HWM) on the target miss is shown in figures 6.31(a) and 6.31(b). Here it can be seen that the results for target miss vary for the time of year and day due to the strong wind values contained in the HWM. The influence of the time of day is partially random with no discernible pattern, however it can be seen that there are certain times of the day which have reduced winds. The time of the year shown in figure 6.31(a) is much more interesting as there is an obvious pattern to the results, although there is still some scattering. It seems that during the middle of the year the target miss results are lower due to the reduce wind velocities from the HWM. Figures A.9 and A.10 show the North-South and East-West wind profiles generated from the HWM. It can be seen that the East and West winds are

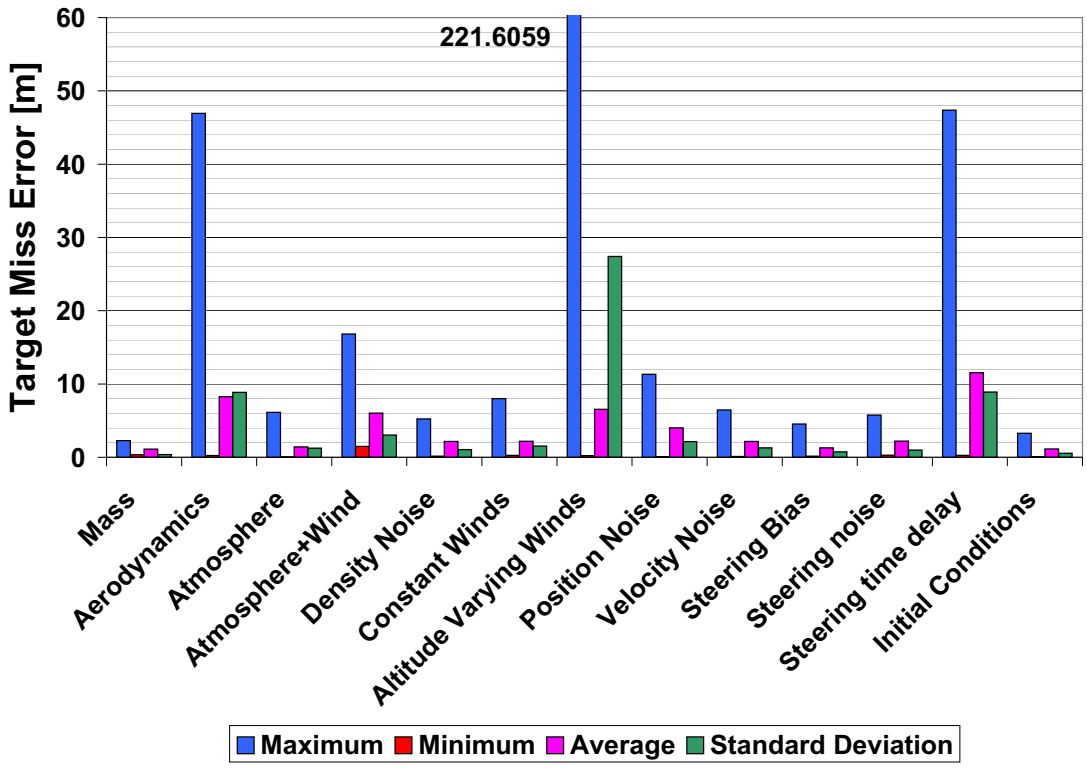

Figure 6.30: X-33 vehicle target miss errors due to off-nominal conditions

much stronger than the North and South winds. Figures A.11, A.12 and A.13 show the change in West and East wind strengths throughout the year. It seems that the guidance is better able to cope with the low strength winds which are present in the HWM during the middle portion of the year.

A time delay is used to mimic the time required for the vehicle to change from one attitude to another. This was used as a simple way of including transition errors so that the commands are not assumed to be instantaneous. The X-33 vehicle guidance had a greater problem than the Hopper vehicle guidance coping with the time delays. This can be related to the aerodynamics of the vehicle since figure 6.31(c) shows that both the angle of attack and bank angle have a larger error with increasing time delay. The speed brake setting exhibits a somewhat random behaviour with errors oscillating around the 5m mark.

The influence of the aerodynamics on the target miss shown in figure 6.31(d) reveal that the lift coefficient modifier is more influential than the drag coefficient modifier. Values of the lift coefficient modifier below 0.95 increase the target miss error in a poly-

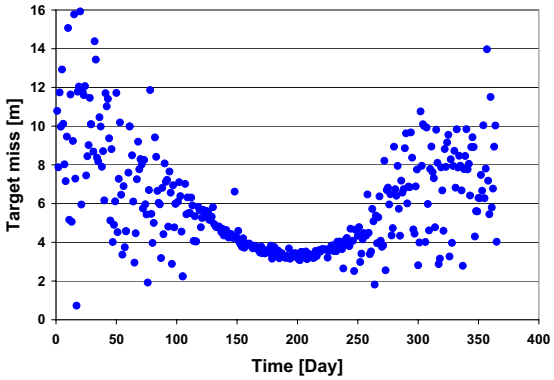

(a) HWM Day

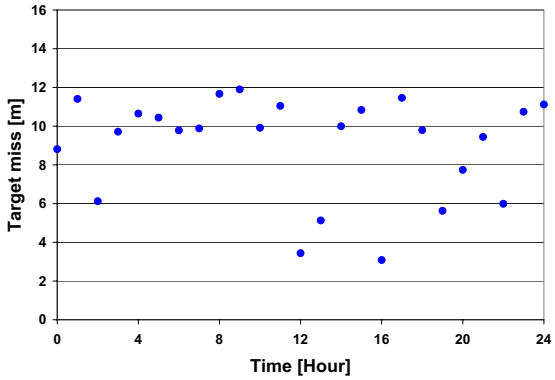

(b) HWM Hour

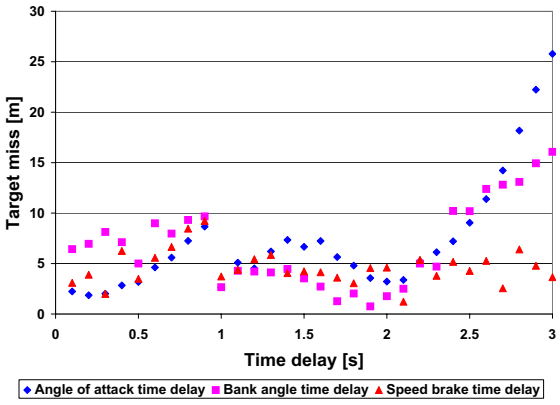

(c) Steering time delays

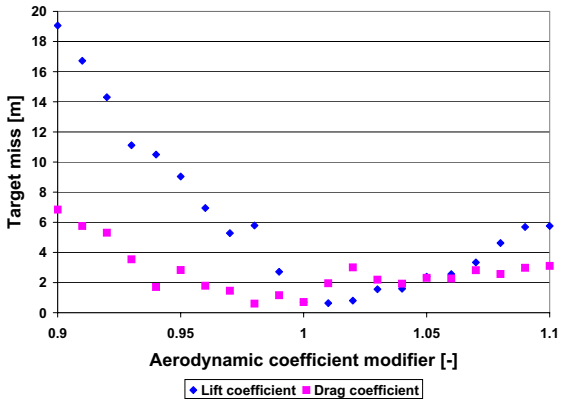

(d) Aerodynamic coefficients

Figure 6.31: The influence of off-nominal conditions on X-33 vehicle target miss error

nomial fashion. This is important for the guidance because the lift coefficient modifier utilised in guidance evaluation in section 6.2.5 has a lower limit of 0.90 which could explain some of the large target miss errors observed. The decreased lift coefficient results in a lower lift-to-drag ratio and changes the ranging capabilities of the X-33 vehicle severely affecting the manoeuvring (turn rates) and trajectory.

Figure 6.32 shows the maximum, minimum, average and standard deviation of the final velocity errors for the various sets of off-nominal conditions. The results show that similar to the target miss, winds, aerodynamics and steering time delays have the greatest influence on the final velocity error. The influence of each of the individual off-nominal conditions from these sets are shown in figure 6.33.

The HWM similar to the target miss error also affects the final velocity error based on the time of year with the strong winds present in the middle portion of the year

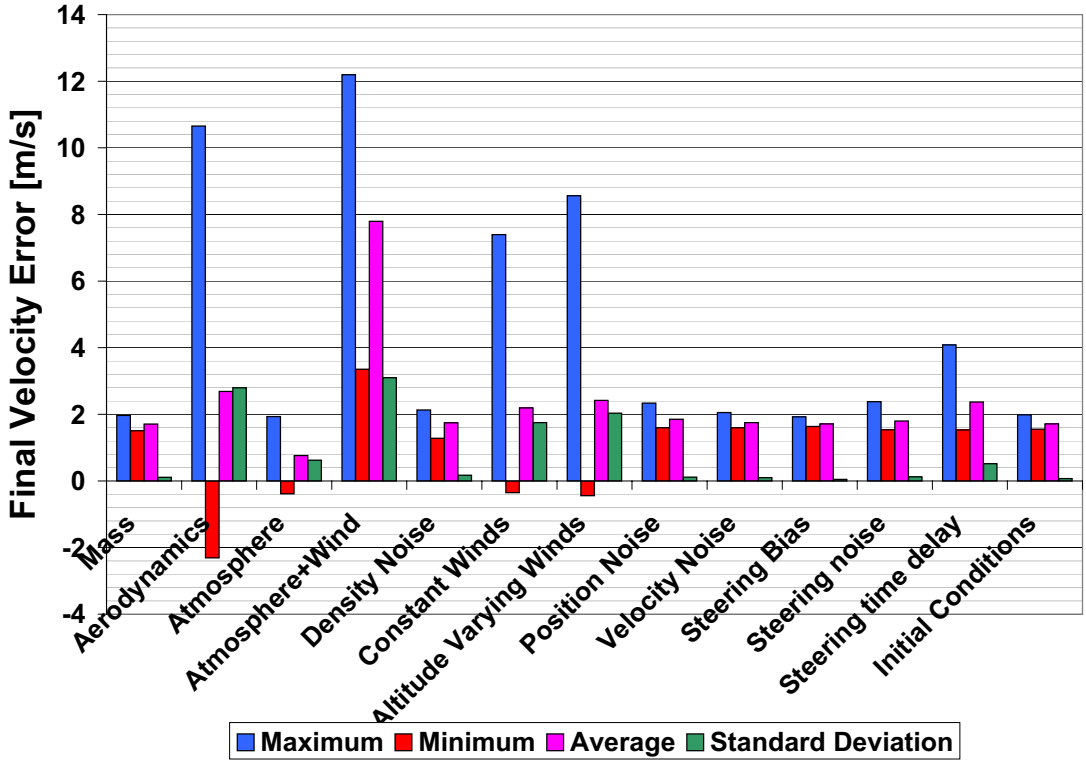

Figure 6.32: X-33 vehicle final velocity errors due to off-nominal conditions

producing reduced errors, shown in figure 6.33(a). The problem seen here is that the upper limit on the velocity error is 10.67 m/s (35 f/s) which is exceeded in numerous cases due to strong winds as shown in figure 6.33(a). Consequently the final velocity restriction is already violated with just the HWM errors, this is discussed more in section 6.2.5. A method for coping with these errors is discussed in section 6.2.6. The errors seen in figure 6.33(b) are due to the fact that the standard day used for single trajectory evaluations is 0 which already has a large error. However, figure 6.33(b) also shows that the final velocity error does not vary much due to the time of day.

The individual aerodynamic coefficient errors shown in figure 6.33(c) reveal that the drag coefficient has a greater influence on the final velocity error than the lift coefficient. For increasing drag coefficient modifiers the final velocity error decreases reaching zero and then becomes negative. For decreasing drag coefficient modifiers the final error increases with a value of 0.9 resulting in an error of 8.78 m/s, which is close to the final velocity limits. The increased velocity results from a higher vehicle energy since with less drag the energy dissipation rate is reduced. The trajectory updates attempt to

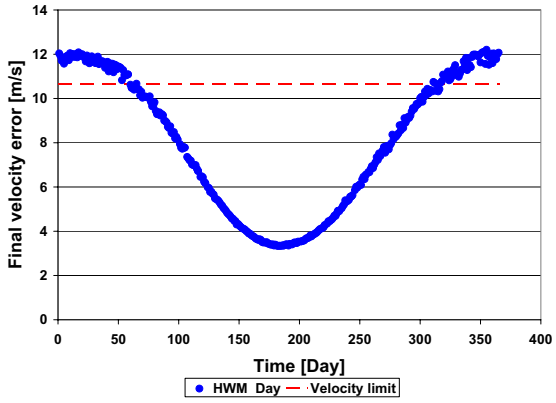

(a) HWM Day

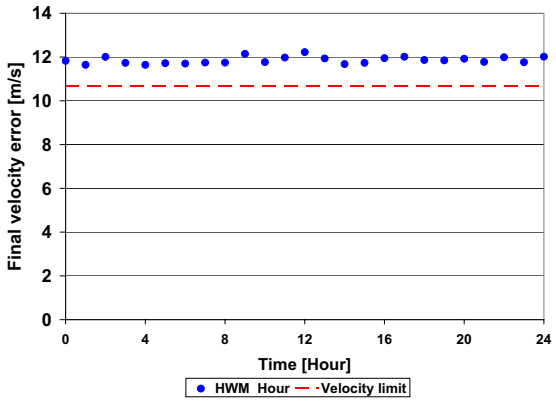

(b) HWM Time

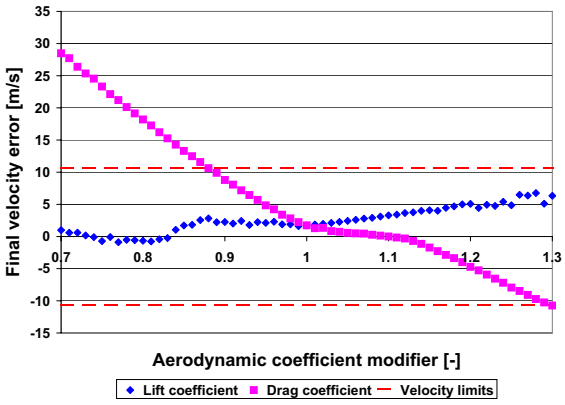

(c) Aerodynamic coefficients

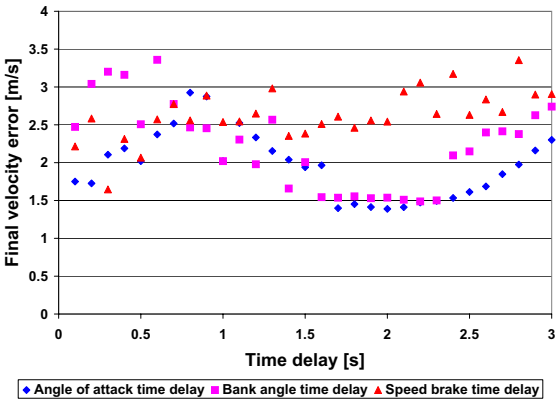

(d) Steering time delays

Figure 6.33: The influence of off-nominal conditions on X-33 vehicle final velocity error

compensate for this by increasing the speed brake setting and angle of attack however they appear to be unable to compensate for the decrease drag. The drag error when combined with other errors such as winds could result in a trajectory which violates the final velocity constraint. This was observed in the results of section 6.2.5. The lift coefficient modifier results in smaller final velocity errors than the drag coefficient modifier with the error slightly increasing for increased lift coefficient modifier.

The speed brake setting time delay seems to have the biggest effect of the three steering command time delays on the final velocity error, as seen in figure 6.33(d). The error due to the speed brake setting seems to randomly oscillate about a velocity error which is linearly increasing with increased time delay. The angle of attack and bank angle time delays produce large final velocity errors below 1.0 seconds then decreasing

error towards 2.0 seconds and then increasing errors again towards 3.0 seconds in a somewhat sinusoidal fashion. Further investigation into what happens with increased time delay for the angle of attack and bank angle showed that the final velocity error is linearly increasing after 2.0 seconds.

Figure 6.34 shows the maximum, minimum, average and standard deviation of the final azimuth errors due to the various off-nominal condition sets. It seems that for the X-33 vehicle only 3 error types are of significant importance with the final azimuth being influenced by the aerodynamic errors, winds and steering time delays.

The aerodynamic coefficient modifiers shown in figure 6.35(a) reveal that the final azimuth is influenced by large variations of the lift coefficient modifier. However, the errors with modifier values between 0.9 and 1.1 are quite small compared to the errors for target miss and final velocity. The final azimuth error increases for increasing lift modifiers and decreases for increasing drag modifiers. The lift and drag both modify the shape of the ground track as was seen in section 5.3 but the guidance is able to adjust the final azimuth via the restoration steps.

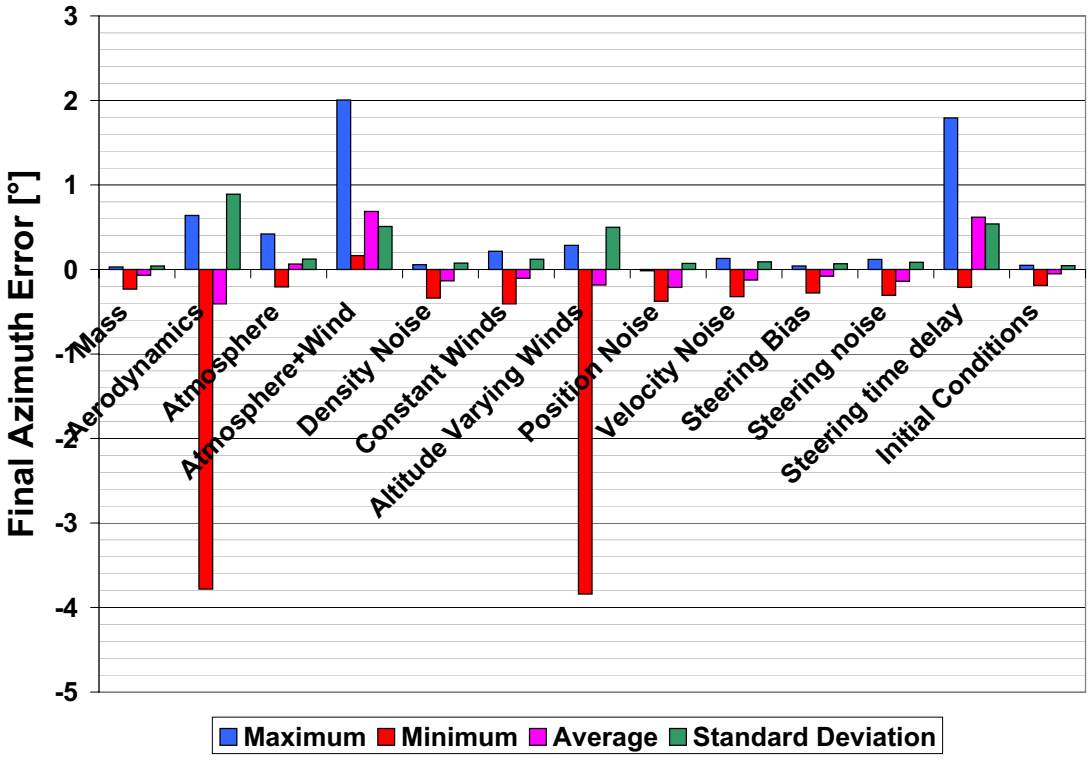

Figure 6.34: X-33 vehicle final azimuth errors due to off-nominal conditions

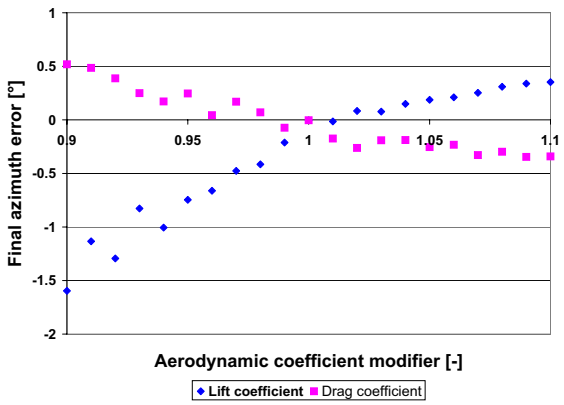

(a) Aerodynamic coefficients

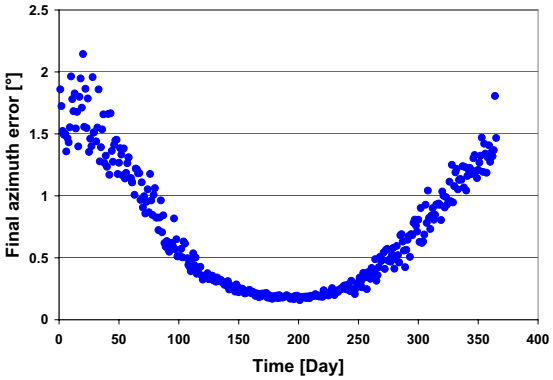

(b) HWM Day

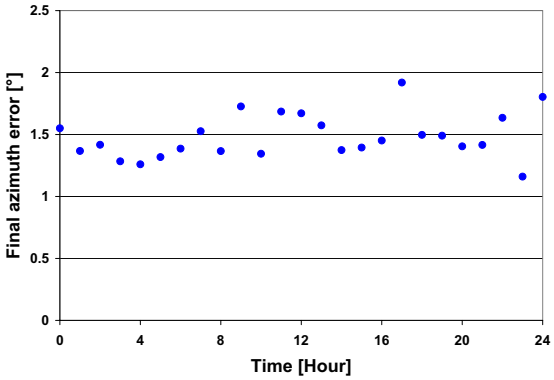

(c) HWM Time

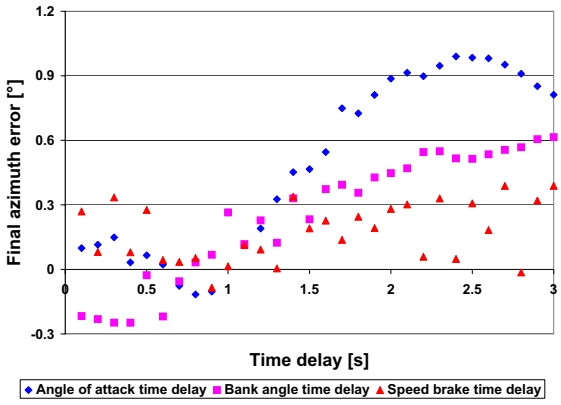

(d) Steering time delays

Figure 6.35: The influence of off-nominal conditions on X-33 vehicle final flight path angle error

The effect of the HWM has a similar influence on the final azimuth the X-33 vehicle, as shown in figures 6.35(b) and 6.35(c). The time of day has a small random influence on the final azimuth errors. The strong winds dependent on the time of year within the HWM have a greater influence on the final azimuth errors. Again the middle portion of the year has reduced error due to the reduced strength winds when compared to the start and end of the year.

The steering time delay effects on the final azimuth shown in figure 6.35(d) have a similar result to the target miss seen in figure 6.31(c). The angle of attack is the most influential. The final azimuth error is linearly increasing for increasing bank angle time delay. The angle of attack increases until around 3.0 seconds where it begins to decrease. Further investigations revealed that the angle of attack produces negative

errors at around 3.0 seconds and decreases linearly with increased time delay. The final azimuth error due to the speed brake setting time delay is also randomly scattered around a slight linear increase with increasing time delay similar to the target miss results.

Figure 6.36 shows the maximum, minimum, average and standard deviation of final flight path angle due to the various off-nominal condition sets. It is also true for the final flight path angle that the same 3 error sets steering time delays, winds and aerodynamic errors are the most influential. Figure 6.37 shows the influence of the individual errors within the 3 error sets.

The steering time delays were the most influential on the final flight path angle error. The angle of attack time delay was the most influential as seen in figure 6.37(a), exhibiting the same behaviour as observed with the final azimuth error. As the pitch of the vehicle is controlled by angle of attack it was expected that the delay would cause final flight path angle errors. The bank angle error instead of linearly increasing with time delay also reaches a zenith like the angle of attack and then produces linearly

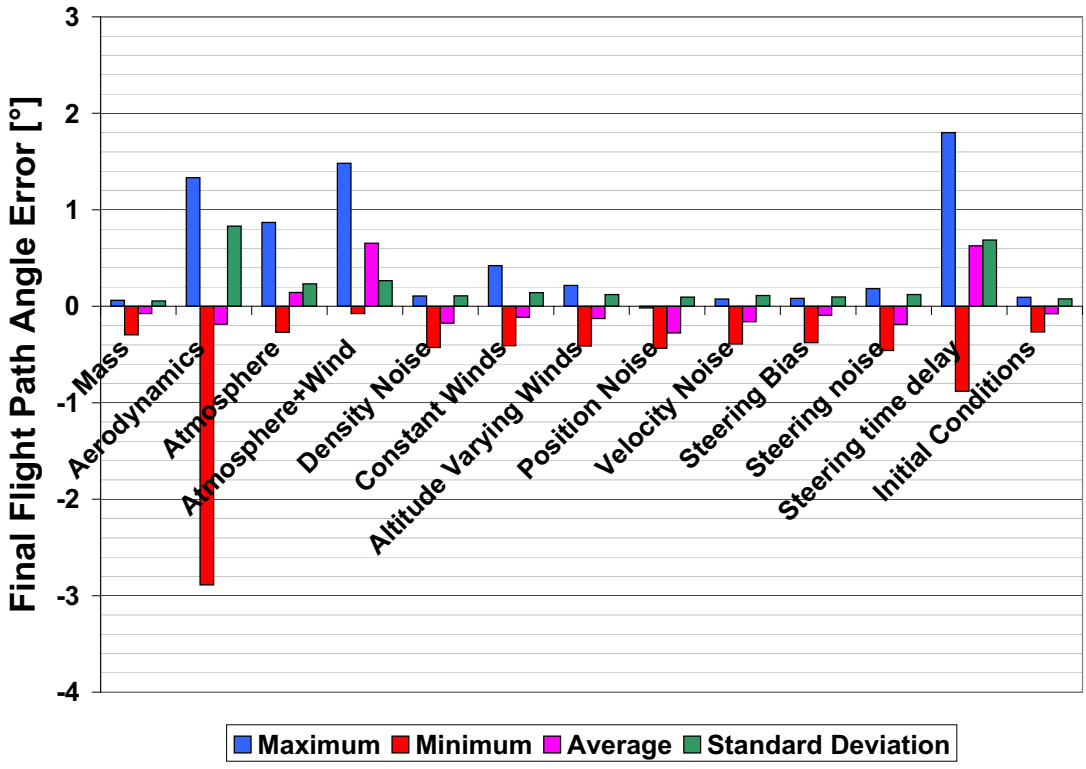

Figure 6.36: X-33 vehicle final flight path angle errors due to off-nominal conditions

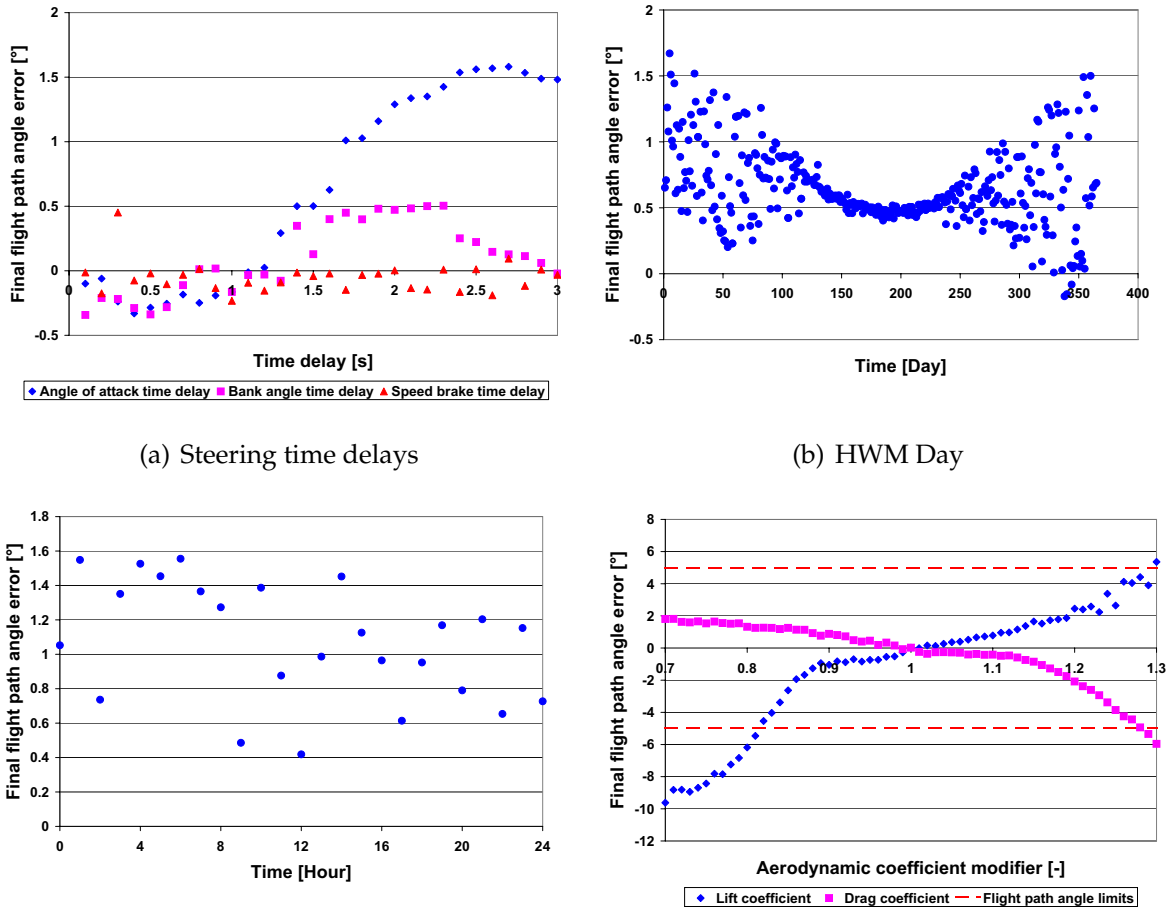

(a) Steering time delays

(b) HWM Day

(c) HWM Time

(d) Aerodynamic coefficients

Figure 6.37: The influence of off-nominal conditions on X-33 vehicle final flight path angle error

decreasing negative error with increasing time delay. The speed brake setting time delay again oscillates except for the final flight path angle error the values are negative with a linearly decreasing error with increased time delay.

The effect of the HWM on the final flight path angle also has similar influences as the target miss, final velocity and azimuth shown in figures 6.37(b) and 6.37(c). The time of day has a greater influence than seen in the other final conditions, however the pattern is still somewhat random. This indicates that small difference in the wind profile can have a large affect on the flight path angle but not the other final conditions. The time of year similar to the other final conditions has a dramatic effects on the error with the middle period of the year producing the lowest errors because of the reduced wind velocities.

Figure 6.37(d) shows the influence of the aerodynamic coefficient modifiers with the final flight path angle error increasing for increased lift coefficients and decreasing for increased drag coefficients. The influence of both the drag and lift coefficient modifiers is similar.

Figure 6.38 shows the influence of the different error sets on the dynamic pressure margin. The dynamic pressure margins are defined as the difference between the dynamic pressure restriction limit and the maximum dynamic pressure experienced by the vehicle. There are again a few types of errors that influence the dynamic pressure margin aerodynamic error, atmosphere and wind variations, density errors and steering time delays. The variations in margins observed in figure 6.38 are quite small indicating that the off-nominal conditions only have a small influence on the dynamic pressure margins. This is also observed in the results of sections 6.2.5 and 6.2.6 where dynamic pressure violations are only small and as a side effect to other larger final condition violations.

Interesting for the X-33 vehicle results is that the same set of errors, namely aero-

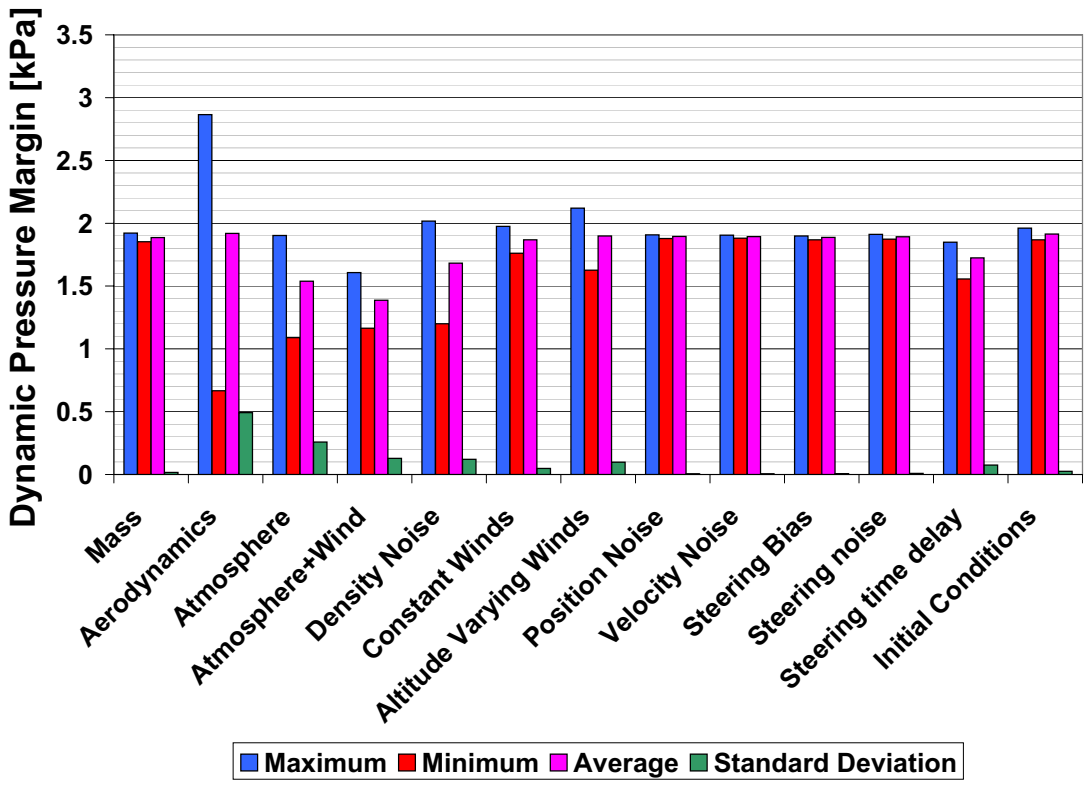

Figure 6.38: X-33 vehicle dynamic pressure margins due to off-nominal conditions

dynamics, winds and steering command time delays, are the greatest influence on the final condition errors. The Hopper vehicle results discussed in section 6.1.3 had various error sets affecting the different final conditions. It would seem that with the X-33 vehicle and mission the guidance program is able to cope with the other types of errors quite well. Consequently in the evaluation of future guidance methods for the terminal area flight phase a focus should be placed on the vehicle aerodynamics, winds and steering command time delays.

6.2.5 Guidance Evaluation

The initial position variations of the X-33 vehicle within this study originally used a circular variation similar to that of the Hopper vehicle. However, the standard mission design defined for the Advanced Guidance and Control Study led by NASA Marshall Space Flight Center (Leavitt et al., 2002) details an annulus centred at the HAC intersection point, discussed more in section 3.2.7.

Both methods are valid for representing the initial position variations of the X-33 vehicle and within this study both methods were investigated. Although the circular initial position was also considered the results presented here are for the annulus type of initial position variations. The annulus was selected since it provides for a much larger spread of initial positions and was defined in the NASA analysis work. The annulus is generated in a similar manner to that of the circular variation used for the Hopper vehicle. A random number is generated for the angle and then for a distance which is inside the inner and outer diameters. Once the position is known the initial heading is modified such that it is heading to the ALI point.

The results for the guidance program using a 1000 simulation Monte Carlo evaluation with the off-nominal conditions given in table 3.2 are provided in figures 6.39, 6.40 and table 6.11.

A total of 468 trajectories had one or more restriction violations indicating that the guidance is not adequate in coping with the combination of off-nominal conditions in table 3.2. The results of sections 6.2.3 and 6.2.4 revealed that the winds, steering command time delays and aerodynamic errors had the greatest influence on the X-33 vehicle guidance.

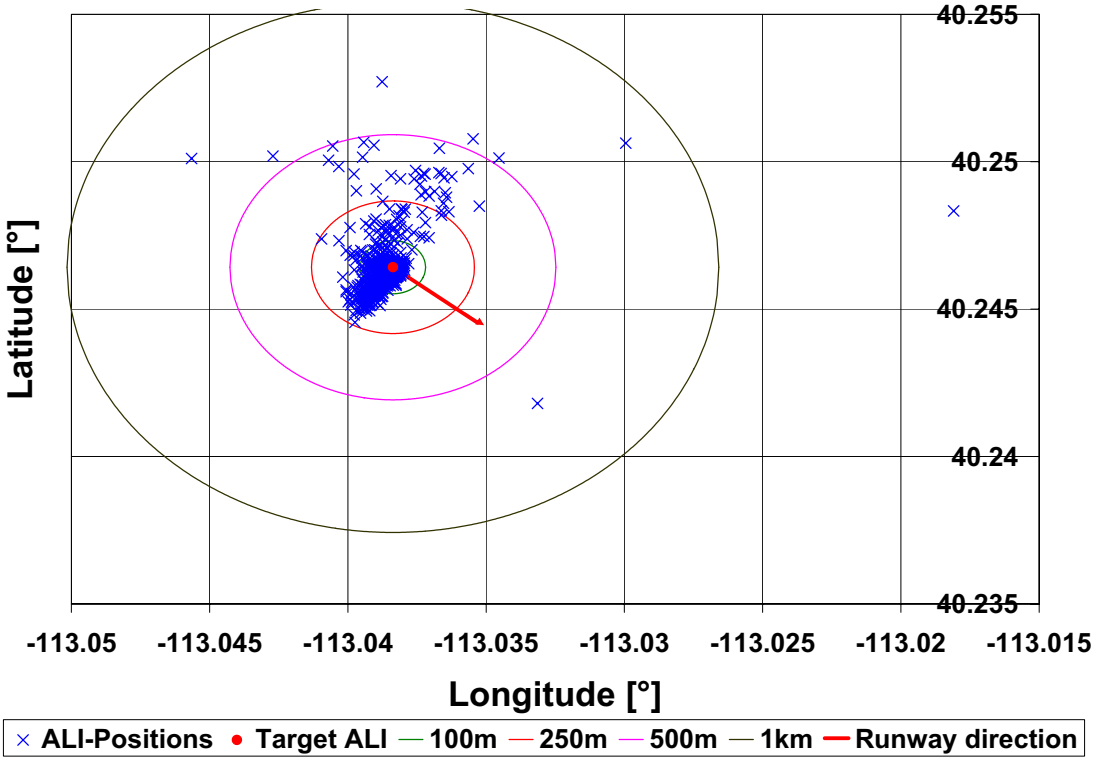

Figure 6.39: Final position results for X-33 vehicle 1000 run Monte Carlo analysis with off-nominal conditions

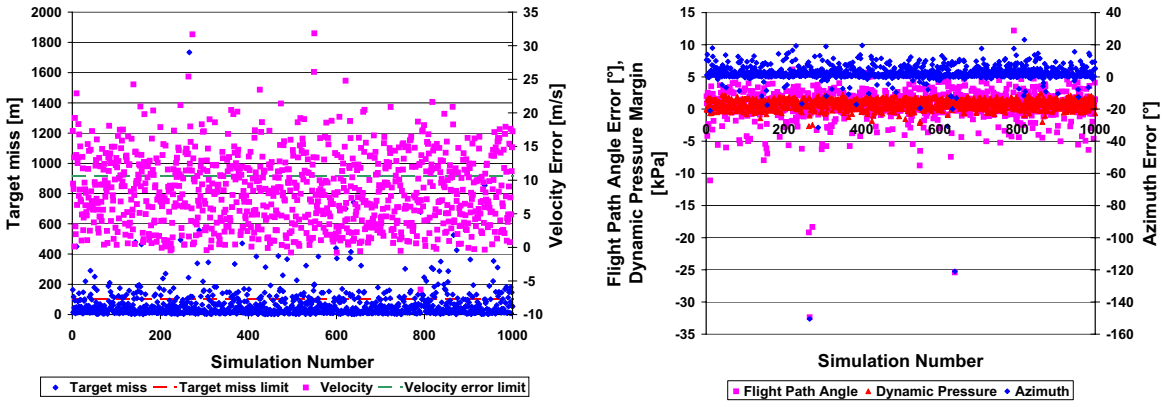

Figure 6.40: X-33 vehicle final condition errors with off-nominal conditions

Restrictions	Target miss (m)	v (m/s)	γ (°)	χ (°)	q (kPa)
Number of violations	210	344	37	76	165
Maximum	1733.5345	31.8299	12.2037	23.1648	2.4077
Minimum	0.8952	-6.2965	-32.3611	-150.4613	-2.6610
Average	68.1854	8.4606	0.5035	2.2261	0.7535
Standard Deviation	104.4097	5.3193	2.5663	7.7360	0.7392

Table 6.11: Results for X-33 vehicle 1000 run Monte Carlo analysis

The large number of trajectories with final condition restriction violations was expected as the results in section 6.2.4 already revealed that the guidance had problems coping with the target miss and final velocity in the individual studies of the wind and aerodynamic errors. When the off-nominal conditions are combined there are a larger number of violations for both the target miss and final velocity.

The results of section 6.2.4 revealed that for certain times of the year the strong winds from the HWM would cause velocity restriction violations. This influence when combined with the large velocity errors caused by reduced drag coefficients was expected to cause a large number of trajectories with final velocity violations. There were 344 trajectories with final velocity violations where the failures can be related to low drag coefficient modifiers and the strong wind conditions. Looking at the failed trajectories the majority occur when there are large velocity errors due to winds from the HWM which occur within the model at certain times of year. For the trajectories with final velocity violations that occur when the wind strength is reduced (typically during the middle portion of the year within the HWM) they have associated large reduced drag coefficient modifiers. Therefore to improve the guidance either the aerodynamic model accuracy must be improved or a wind model provided to the predictor.

The final positions shown in figure 6.39 reveal that a large number of the trajectories fail to reach the required 100 m tolerance. The results shown in figure 6.40 and table 6.11 identify a total of 210 trajectories that fail to meet the target miss tolerance with the largest target miss of approximately 1.73 km. The large average and standard deviation values for target miss show that the X-33 vehicle guidance is not as effective as the guidance for the Hopper vehicle with the combined off-nominal conditions.

The X-33 vehicle terminal area flight phase mission studies performed by NASA utilised a modified US Shuttle TAEM method but the results from this work were

never published in the public domain (Dukeman, 2004). The work of Kluever and Horneman (2005) had a maximum target miss error of 105.46 m, however only the results for individual studies of drag, initial altitude and heading errors were presented. Consequently there is limited information on acceptable target miss limits for the X-33 vehicle mission. Therefore the specified limits for the Hopper vehicle mission were assumed. Section 6.1.5 discussed how the final position error could be greater than that specified by the Hopper vehicle mission. If a target miss limit of 250 m is considered only 42 trajectories exceed the tolerance. Burchett (2004) presented results that allow a target miss with a total range of approximately 870 m. For the Russian Buran Orbiter a lateral target miss of $\pm$500 m was acceptable (Kirpischikov, 1997). If a 500 m target miss tolerance is considered then only 8 trajectories fail to reach the target miss restriction.

The target miss errors are caused by a combination of the winds, steering command time delays and aerodynamic errors. The effects of these errors was discussed in section 6.2.4. The majority of the target miss errors are due to the strong winds from the HWM with the time of year outside of the middle region. The middle period of the year normally does not produce such large target miss errors due to the winds but combined with large steering command delays and low aerodynamic coefficient modifiers there are target mission violations that occurred.

The majority of azimuth errors are within the specified tolerances. Only 76 of the 1000 simulations exceed the final azimuth limits. In section 6.2.4 the azimuth errors were related to the aerodynamic errors, winds and steering command time delays. None of the trajectories with final azimuth violations occur in the middle period of the year indicating a significant influence from the strong winds of HWM. The final azimuth violations are also related to one or more large steering command time delay.

There were some extreme cases for the azimuth where the vehicle is heading almost completely away from the runway. The largest azimuth error of 150 degrees occurs in trajectory #266. The error is caused because the vehicle reaches the bank angle and speed brake setting limits for a large portion of the flight. A possible solution to this problem would be to increase the bank angle limits so that the vehicle is better able to manoeuvre and align with the runway.

The majority of the final flight path angle errors are also within the specified limits with 37 trajectories exceeding the restriction tolerances. The results shown in figure

6.40 and table 6.11 reveal excellent results for the final flight path angle errors with small average and standard deviation values.

Note results presented in figure 6.40 and table 6.11 are for the dynamic pressure margins and the dynamic pressure is only violated for negative values. There were 165 trajectories which have dynamic pressure restriction violations, with a largest violation of 2.66 kPa (55.57 psf). The few trajectories with large dynamic pressure errors occur where there are 3 or more final condition restriction violations, indicating that the large dynamic pressure violations are due in part to the other violations especially large final velocity violations exceeding 20 m/s.

The likely cause of the smaller violations are due to the difference in atmospheric models, density noise and velocity errors. If the on-board guidance predicts a smaller density value than the actual value in the simulation environment the predictor might think it is at the limit when in fact it is slightly exceeding the limit. A method to cope with this would be to have the predictor use a slightly higher value for dynamic pressure calculations. A simpler method would be to set the limit on dynamic pressure to a lower value to ensure that the predictor is always below the initial limit even with errors between the density profiles.

The results using the circular initial position variation instead of an annulus provide similar results with almost the same number of restriction violations 466 compared to 468. The errors also exhibit the common cause of violations namely large steering command time delays, poor aerodynamic coefficient modifiers and winds. Consequently using either method should be adequate to demonstrate and evaluate the effectiveness of the guidance program and applied methodology.

The results indicated that the X-33 vehicle guidance had trouble coping with the winds from the HWM, aerodynamic errors and steering command time delays. Consequently the X-33 vehicle guidance could be improved by improving the aerodynamic accuracy and reducing the steering command time delays.

A study was performed utilising reduced aerodynamic coefficient modifiers of $\pm 5\%$ to simulate improved aerodynamic model accuracy. The results were an improvement of those presented in table 6.11 with only a total of 366 trajectories failing to meet one or more of the restrictions instead of the 468. The results show that the majority of restriction violations occur outside of the middle period of the year which indicates

that the strong winds from the HWM are the primary cause of the final condition violations. There are however some target miss and dynamic pressure violations that occur during the middle period of the year. These target miss errors are caused by large steering command time delays, especially bank angle. Large time delays were previously shown in section 6.2.4 to cause large target miss errors. The combination of the steering command time delays and the other off-nominal conditions resulted in the final condition violations. Although the results were improved with reduced aerodynamic model errors, achieving increased aerodynamic accuracy would require additional wind tunnel, computational fluid dynamic (CFD) or flight testing adding significant cost to a project.

The time delays were assumptions taken from Telaar (2005). Changes in the vehicle attitude would require a certain amount of time however the amount of time would depend upon vehicle rotational dynamics and should be investigated further in detailed 6 degrees of freedom evaluations. The results also indicated that if the predictor had some knowledge of the wind profiles a significant reduction could be achieved in the final restriction violations. Section 6.2.6 discusses the use of simple wind models for the predictor in an attempt to reduce the errors related to the strong winds contained in the HWM.

6.2.6 Predictor Wind Models

A strong correlation was observed between the wind errors and the time of year. Therefore further investigations were performed on the wind profiles for the X-33 vehicle including the variation of various days. The profiles for the terminal area flight phase of the X-33 vehicle were considerably greater than those observed for the Hopper vehicle, as shown in figures A.7, A.8, A.9 and A.10. The East-West winds for the X-33 vehicle terminal area flight phase were larger by an order of magnitude than the North-South winds. The East-West winds were determined to be responsible for the large amount of the final condition violations especially related to final velocity and target miss.

A possible method to alleviate the large number of trajectories with restriction violations seen in section 6.2.5 was to incorporate an approximate wind profile in the predictor. Generally the weather is monitored around the landing site of a vehicle to determine if the environmental conditions are within design tolerances. Using this

data it would be possible to upload an approximate wind model to the X-33 vehicle after the black out phase of re-entry where loss of communication occurs due to atmospheric ionisation.

A test was performed using a single wind profile model which was generated based on the wind profile data contained in Appendix A.3. This simple model was then incorporated into the predictor and a 1000 simulation Monte Carlo evaluation performed. A notable improvement in the guidance results was observed. However the results still had a large number of trajectories where restrictions and final conditions were violated.

To further improve the guidance additional investigations were performed into the wind profiles and how they varied due to the time of the year. It was determined that although the wind profiles had considerable variation during the year it would be possible to group the wind profiles into 3 distinct groups representing different periods of the year. The groups represented low, medium and high winds. A profile was generated for each group and any further variation from this profile could be adapted for within the restoration steps of the guidance. The three profiles generated are provided in table 6.12 and a plot of the profiles with wind profiles from the HWM for various days is provided in figures A.11, A.12 and A.13.

The profiles are very simplistic to minimise storage space and the computational requirements for the predictor. The predictor utilises a linear interpolation routine similar to that used for the steering parameters to determine the intermediate values.

The guidance was then evaluated with the new predictor wind profiles and the off-nominal conditions given in table 3.2. The results are displayed in figures 6.41, 6.42 and table 6.13.

High winds		Medium winds		Low winds	
Days: 0-75, 330-365		Days: 76-134, 271-329		Days: 135-270	
h (m)	v (m/s)	h (m)	v (m/s)	h (m)	v (m/s)
0	3	0	3	0	2.5
10000	22	9000	17	7500	12
12500	22	12000	17	10000	12
25000	7	25000	-1	23000	-6
31500	13	31500	4	31500	-8

Table 6.12: The X-33 vehicle predictor wind profiles

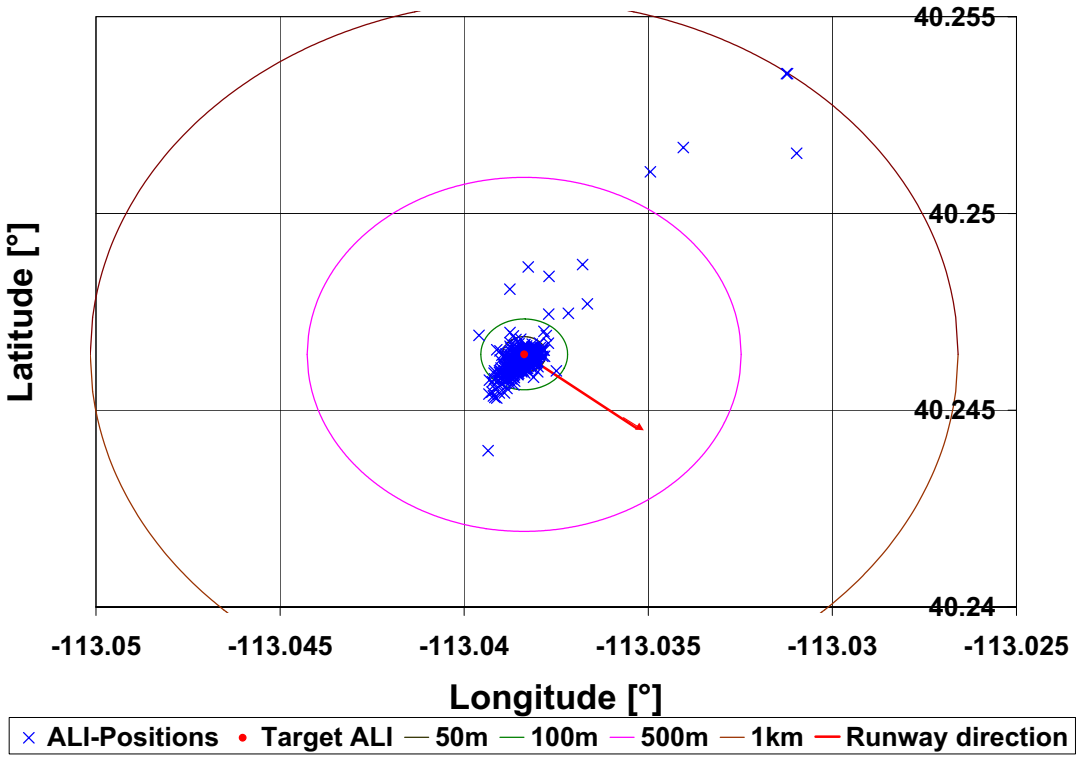

Figure 6.41: Final position results for X-33 vehicle 1000 simulation Monte Carlo analysis with predictor winds

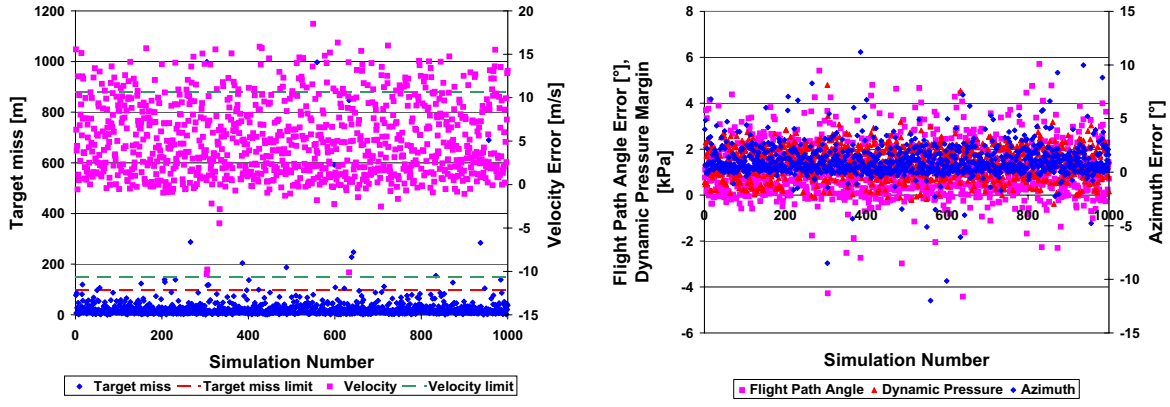

Figure 6.42: The final condition errors for X-33 vehicle 1000 simulation Monte Carlo analysis with predictor winds

Restrictions	Target miss (m)	ν (m/s)	γ (°)	χ (°)	q (kPa)
Number of violations	27	127	2	3	10
Maximum	998.5710	18.5125	5.7088	11.2108	4.7927
Minimum	0.1869	-10.3118	-4.4193	-11.9813	-0.3834
Average	28.3424	5.1961	1.0511	1.0610	1.4560
Standard Deviation	64.0034	4.2818	1.1748	1.5899	0.6724

Table 6.13: Results for X-33 vehicle 1000 run Monte Carlo analysis with predictor winds

The total number of trajectories with one or more restriction violations was 155 an improvement over the 468 in section 6.2.5. The majority of these violations are related to the final velocity error. Although the average value is relatively small at 5.2 m/s approximately half the allowable tolerance the standard deviation shows that there are a significant number of values which violate the tolerance. The figure 6.42 also shows the size and distribution of the velocity violations. The guidance for the X-33 vehicle has problems reaching the required velocity. This again can be related to the combined final velocity errors of the winds, vehicle aerodynamic errors and steering command time delays.

A new sensitivity study was performed on the X-33 vehicle guidance with predictor winds. The final velocity errors due to the HWM and time of year for the X-33 vehicle guidance with and without predictor winds is shown in figure 6.43. The results show that the predictor winds are able to reduce the final velocity errors below the specified tolerance. However, the start and end periods of the year still have large errors that when combined with aerodynamic errors and steering time delays cause final velocity restriction violations.

The target miss violations are also considerable with 27 trajectories failing to reach the target miss requirements. Looking at figures 6.41 and 6.42 it can be seen that the maximum target miss is 999 m and the majority of the failures occur within a 100 to 150 m radius of the target. There is some scattering of solutions around the target mostly with lateral variation.

In section 6.2.5 it was mentioned that larger errors for target miss could be tolerated. When a target miss tolerance of 250 m is considered only 7 trajectories exceed the limit. If the Russian Buran Orbiter target miss tolerance of $\pm$500 m (Kirpischikov, 1997) is

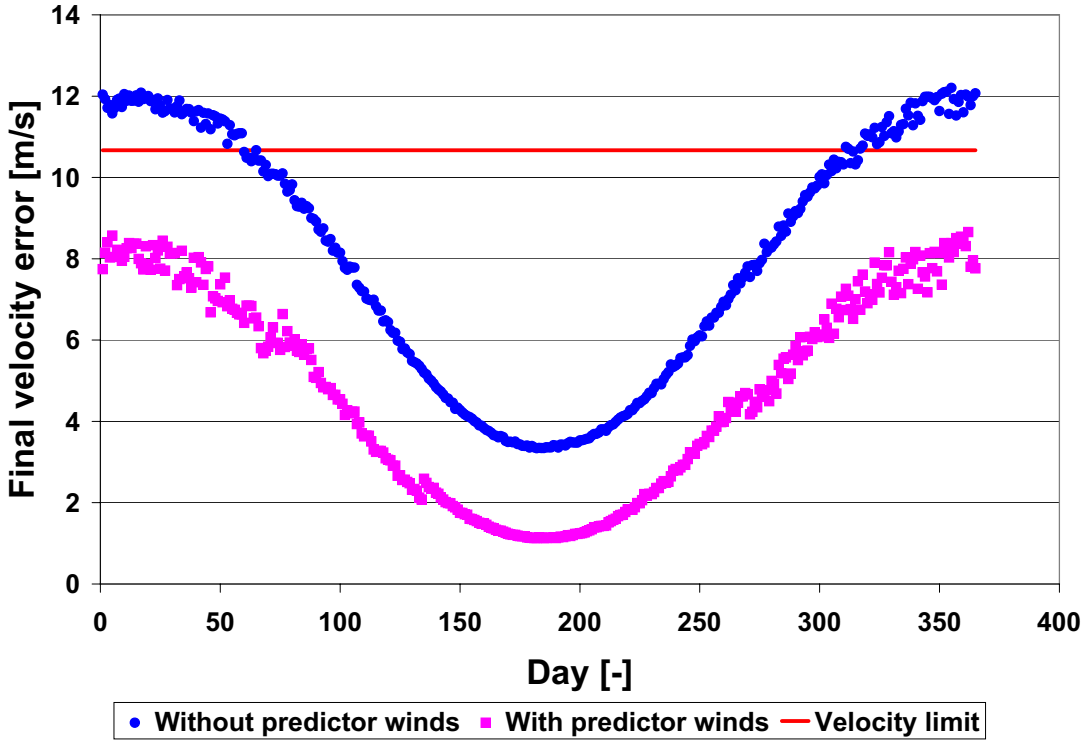

Figure 6.43: X-33 vehicle final velocity errors with HWM and predictor winds

considered then only 5 trajectories fail to reach the required limit.

The largest target miss from trajectory #559 is smaller than that seen in section 6.2.5. Investigations revealed that the trajectory failed because the steering commands were saturated for the majority of the flight. The bank angle commands reached both the upper and lower limits for approximately 70% of the flight time. The speed brake setting is also at the maximum limit for approximately 55% of the flight time. The large aerodynamic errors and angle of attack time delay combined with the other off-nominal conditions resulted in the large target miss. Consequently it seems that this combination of off-nominal conditions resulted in a trajectory where the restoration steps were ineffective.

There are 5 trajectories that fall in the range of 500 to 1000 m. These trajectories also have steering command saturation problems although not as extreme as those seen in trajectory #559. The saturation occurs for the bank angle commands and the speed brake setting towards the end of flight. Therefore a possible improvement could be made to the guidance if the bank angle commands could be increased during the

later stages of flight. If the speed brake setting is set to maximum to try and achieve the maximum amount of drag, consequently resizing the speed brake control surfaces could the provide additional drag required for energy dissipation control. The X-33 vehicle does not have specific speed brake control surfaces instead the inboard and outboard elevons were split to approximate a speed brake. Specific speed brake control surfaces could be included in the vehicle design to provide additional drag control.

There are 4 trajectories with target miss violations that fall within the middle period of the year which would indicate that the HWM was not the primary cause. These trajectories however have large errors for vehicle aerodynamics and steering command time delays. These off-nominal conditions were previously shown in section 6.2.4 to also have a large effect on the target miss. The results also indicate that the target miss errors from each of the error sets in section 6.2.4 do not just add together but instead the combined error sets produce errors that are greater indicating a coupling effect of the errors.

The final flight path angle restriction was only violated in 2 trajectories; an improvement over the results without predictor winds discussed in section 6.2.5. The final flight path angle violations occur for trajectories with strong winds at the initial and final periods of the year. The final flight path angle violations seem to have a combination of steering time delays or aerodynamic errors where the majority of failures have large angle of attack time delays. The results in section 6.2.4 revealed that the angle of attack time delays produce large final flight path angle errors. This combined with the off-nominal conditions for vehicle aerodynamics and winds produce the final flight path angle restriction violations.

Only 3 trajectories failed to meet the final azimuth tolerance with the maximum final azimuth error exceeding the limits by 2.0 degrees. The largest error occurred with trajectory #559 which also violated all the other final conditions. The azimuth error of trajectory #559 is thought to be a side effect of the other errors which caused the vehicle to fail all final conditions. The cause of the failure in the final azimuth was because the bank angle limits were reached and so the X-33 vehicle turn rates were at maximum such that it could not align with the runway centreline.

The trajectories with final azimuth violations all occur near the start and end of the year and all have large drag coefficient modifiers and angle of attack time delays. These

errors when combined with the other off-nominal conditions resulted in the trajectories exceeding one or more of the final condition limits. The results in section 6.2.4 revealed the influence of the time of year, drag coefficient modifier and angle of attack time delay on the final azimuth error.

Note that in figure 6.13 and table 6.13 the dynamic pressure is only violated when the value is negative. Positive values represent the margin for the dynamic pressure. There were 10 violations of the dynamic pressure however the violations are small with a maximum violation of 0.3834 kPa (8.0075 psf). Similar to the dynamic pressure restriction violations observed in section 6.2.5 the likely cause of the violations is the difference in atmospheric models, density noise and velocity errors. The velocity errors are the most likely causes because the value is squared and consequently any error becomes more pronounced. Velocity errors are due to wind errors between the predictor and simulator and the applied velocity noise errors. A method to correct the dynamic pressure violations and the other final restriction violations would be to improve the on-board wind models of the predictor to reduce the wind errors which are the primary cause of the restriction violations. This would require ground support updating the wind profile with readings from the landing site weather tracking station.

Of the 127 velocity restriction violations none occurred in the middle period of the year indicating that the winds still cause the majority of violations. An evaluation of the guidance was performed without the winds, the results showed that only 38 trajectories failed to meet the final condition requirements as opposed to the 155 with predictor winds and the 468 without predictor winds. This indicates that the strong winds from the HWM are the primary cause of the restriction violations. The majority of the violations without winds were dynamic pressure violations which were thought to have the same cause as those mentioned above and in section 6.2.5.

The other violations without HWM are 6 target miss, 7 final velocity, 2 final flight path angle and 4 final azimuth errors. Two of the target miss violations only just exceed the tolerance by 0.7 and 9.6 m. The other target miss errors are caused by the steering commands saturating and reaching the limits for angle of attack, bank angle or speed brake setting. The velocity violations without winds are only just outside of the tolerance values except for the two extreme trajectories #266 and #599 which violate multiple restrictions. The velocity violations are caused by the increased lift-to-drag ra-

tio and steering command time delays in combination with the other off-nominal conditions. The influence of the aerodynamic errors especially reduced drag coefficients and steering command time delays on the final velocity were discussed in section 6.2.4. The influence of the time delay errors could be reduced using well designed controllers for the control surface movements based on the steering commands. A reduction in steering command time delays would provide improved results. The flight path angle violations appear to be a side effect of the two extreme trajectory violations. The final azimuth violations with winds only occur in the trajectories with large target miss errors which indicate that they are a side effect of the bank angle limits being reached.

The results again revealed that even with the predictor having a simplistic approximation of the winds the combination of errors still cause restriction violations. The major occurrence for error is as a result of poor vehicle aerodynamic modifiers and strong winds which result in large final velocity errors. An additional investigation was performed with reduced aerodynamic coefficient modifiers of $\pm 5\%$ and the results were improved with only 45 restriction violations shared between target miss and final velocity violations. The violations again exhibit the main three off-nominal conditions large steering command time delays, poor aerodynamic coefficient modifiers and strong wind profiles.

6.2.7 Comparison to Other Methods

Some other studies have utilised the X-33 vehicle and mission for analysis of different methods for terminal area guidance. These include Burchett (2004) and Kluever and Horneman (2005). As mentioned in section 6.1.7 and 6.2.3 the comparison to other methods is difficult since different simulation environments and vehicle models are used to evaluate the guidance. To effectively evaluate the performance between the different terminal area guidance methods a set of common models for the vehicle and simulation environment is required, similar to the study presented in Hanson and Jones (2004).

Kluever and Horneman (2005) presented results from the evaluation of the trajectory planning guidance method, discussed in section 2.3.9. Kluever and Horneman (2005) utilised disturbances of the initial altitude and azimuth the comparison of these results has already been discussed in section 6.2.3. Additional experiments looked

at the influence of drag errors using modifications of 10, 20 and 30% of the nominal drag value. However different to the study of the thesis, the on-board guidance was assumed to have *perfect knowledge* of these aerodynamic errors (Kluever and Horneman, 2005). When the guidance knows the applied errors only the trajectory planning method is tested. It does not test the guidance program as there are no errors between the simulation and predictor models. The study of this thesis only applies the off-nominal conditon errors to the simulator and therefore the predictor has no knowledge of the applied errors and must adapt by observing the errors in the final conditons. The results presented in table 6.14 detail the errors observed using the method of Kluever and Horneman (2005). The errors detailed here are those for an overhead HAC and with updated ALI targets.

The method utilised in this research was also tested using drag errors of 10, 20 and 30% and assuming that the on-board guidance had *perfect knowldege* of these errors. The results are shown in table 6.15. The trajectory planning guidance method of Kluever and Horneman (2005) has smaller flight path angle errors than the restoration step method used within this research. However, the trajectory planning guidance method has larger errors for target miss and final velocity.

Burchett (2004) utilises fuzzy logic for trajectory design and guidance during the terminal area flight phase, which is discussed more in section 2.3.8. Burchett (2004)

Drag errors (%)	Target miss (m)/(ft)	v (m/s)/(ft/s)	γ (°)
0	3.35 (11)	-6.55 (-21.5)	0.14
10	39.93 (131)	-6.43 (-21.1)	0.2
20	105.46 (346)	-7.92 (-26.0)	0.6
30	82.60 (271)	-10.21 (-33.5)	0.6

Table 6.14: Results from Kluever and Horneman (2005) for drag variations

Drag errors (%)	Target miss (m)	v (m/s)	γ (°)	χ (°)
0	0.7070	1.7327	0.0231	-0.0036
10	3.1030	1.6119	-0.3758	-0.2387
20	5.2792	2.2478	-0.9540	-0.4918
30	8.3302	5.9077	-2.7413	0.4748

Table 6.15: X-33 vehicle results for drag variations with on-board guidance knowledge

also utilised the X-33 vehicle concept providing results for a bounding box of initial conditions and the results observed at ALI. The results for the final ALI seem to have similar tolerances to those used in this study, however the different final conditions make it difficult for a comparison.

The other methods for terminal area guidance applied to the X-33 vehicle have limited evaluations for a large variety of off-nominal conditions in comparison to this study. It is hoped that this study with a large amount of off-nominal conditions can be used to perform comparative studies in the future.

6.3 Discussions From Guidance

The results of this chapter have revealed the significant benefits that the guidance method based on the GPA restoration steps can provide. The guidance method allows for real time autonomous trajectory updates to cope with a variety of off-nominal conditions including mass variations, poor aerodynamic modelling, atmospheric disturbances, steering command time delays, initial condition variations and position, velocity and steering noises. The guidance method used within this study also combines the longitudinal and lateral dynamics to eliminate the possibility of errors within the flight path prediction which are possible within some other methods, such as the US Shuttle TAEM methodology. The guidance method used here does not utilise defined geometric segments, way points or multiple sub-phase for the guidance instead the guidance updates the entire trajectory via steering commands to cope with the off-nominal conditions and eliminate final condition errors.

There are however some disadvantages of the guidance method used within this study. The flight path prediction utilises a large amount of integration and therefore computational effort in comparison to some other methods. The restoration step within the GPA does not provide for a guarantee of solution convergence. Although it has never been observed during this or other studies conducted using this methodology it is possible that the solution can diverge with increasing final conditions errors. This however is very unlikely and if such a case was to occur the initial steering commands from the reference trajectory are still stored on-board. The better solution will be to load the previous steering commands prior to the failure of the updates provided

that each successive update is stored and not over written each time. The results of section 5.3 presents what happens to a reference trajectory under worst case off-nominal conditions. Although not sufficient to reach the required target miss it might be enough to facilitate vehicle recovery in the event of catastrophic guidance failure.

The trajectories developed within this study are not of the HAC type seen in a majority of the literature for the terminal area flight phase. The reason for this is that constraining the vehicle to a HAC type trajectory can cause a variety of problems in the presence of off-nominal conditions including not being able to achieve required range or turn rates. Another problem with traditional methods that use HACs is that they only accommodate a small range of energy conditions based on limited HAC placement. However, the inclusion of S-turns eliminates this problem and current studies have looked at resizing the HAV and a large range of different HAC positions to further address the problem. Within this study the trajectory can be designed to suit the energy conditions since a HAC or way points do not need to be reached. There may however be additional reasons for the inclusion of a HAC based on previous pilot trajectories for runway approach.

The restoration steps of the GPA are an effective method for adapting the reference trajectories under off-nominal conditions. The reference trajectory is an optimised solution determine using the optimisation program discussed in sections 3.1.2, 3.1.5 and Chapter 5. The results of Chapter 6 have shown that under off-nominal conditions the trajectories are updated to meet the required final conditions. It might be argued that since the reference trajectories for both the Hopper and X-33 vehicles are modified on-board there is no reason to perform optimisation in determining the reference trajectory. It is true a different method could be utilised to determine the reference trajectory. However the optimisation method provides significant benefits over other methods. The optimisation method allows for reference trajectory design taking into account the vehicle and environmental models, specified initial and final conditions and in-flight restrictions. The optimisation method of this study also provides a useful method for including margins within the trajectory to allow for possible off-nominal conditions. Another benefit of the optimisation method is that it does not rely upon fixed segments, geometric segments or multiple sub-phases. Consequently the trajectories can be designed to be more flexible than traditional trajectories which rely on these

additional constraints for definition. The optimisation method used within this study is also applicable to multiple vehicle types as demonstrated by the studies for both the Hopper and X-33 vehicles. Consequently the optimisation method used within this study provides a perfect tool for trajectory design taking into account all consideration and providing effective solutions.

The results of section 6.1.6 revealed that the speed brake setting provides a benefit to the guidance method used within this study. The results showed that without the speed brake the vehicle could not effectively control the energy dissipation rate as the Hopper vehicle either under or over shot the target position. The results indicated that a speed brake variable provided a greater ability to adapt to off-nominal conditions during flight. However, it is also possible that based on the method used for trajectory design and guidance a speed brake is not required. The method and results presented in Kluever and Horneman (2005) do not utilise a speed brake. The method of this study requires a speed break setting since the problem formulation requires that an equal number or that there are more active parameters than restrictions. The trajectories designed within this study utilised the speed brake as a method for providing margins. It would also be possible to reformulate the trajectory design process to include margins by another method. However it was found that using the speed brake setting was the most suitable method which allowed flexible and adaptable trajectories (Chartres et al., 2005b). Consequently a possible reason for the inclusion of S-turns and HAC type trajectories within literature is to provide margins without reliance upon the speed brake.

Another interesting consequence of the results of section 6.1.6 is that for the Hopper vehicle it would appear that if a speed brake failure occurred during flight the vehicle would be unable to reach the required target conditions. Therefore it would seem that some sort of redundancy would be required to overcome this problem. Further investigations for the Hopper vehicle should identify if trajectory recovery is available when vehicle actuators or control surfaces fail. This has previously been modelled by the inclusion of additional drag by Schierman et al. (2004b). The guidance method of this study has already demonstrated the ability to cope with additional vehicle drag errors. Therefore presumably the guidance should be able to adapt for control surface failures.

The sensitivity studies of sections 6.1.3 and 6.2.4 revealed that the steering command time delays had an influence on the final condition errors. As discussed in section 3.2.6 the steering command time delays are used as a method to simulate some of 6DOF attitude dynamics. The steering command time delays could be reduced by using well developed control algorithms for the actuators provided large steps in in the commands are not present. A reduction in the time delays would result in reduced final condition errors.

The guidance results from a general comparison reveal that this method provides similar results to the other methods presented in literature. A direct comparison was not possible based on the lack of publicly available detailed studies in the literature as well as the use of different vehicle and environmental models. However, the comparisons of sections 6.1.7 and 6.2.7 reveal that the guidance method is well suited to the terminal area flight phase providing significant results under a larger variety of off-nominal conditions than traditionally published in literature.

When comparing the results to the other methods there are two distinct explicit guidance methods utilised for the terminal area flight phase. Both types of methods perform trajectory updates to cope with errors and off-nominal conditions, however the methodology behind the updates is different. The first type of method, which is utilised in this study, is to perform updates to a reference trajectory that was determined off-line. The second type of method completely redesign the reference trajectory on-board. The second type of method tend to use simplified trajectories based on geometric segments or way points to reduce the computational requirements. They have the added advantage of being able to design the trajectories for a wide case of dispersions and some methods could possibly be utilised for other flight phases or aborts.

The first type of methods rely upon update schemes with a pre-loaded trajectory and have generally been thought to be less capable of coping within errors and off-nominal conditions. However, the results presented in sections 6.1 and 6.2 show that the update scheme utilised within this study is capable of coping with a wide variety of errors and off-nominal conditions with a single reference trajectory. The first type of methods traditionally requires larger amounts of computational effort that have not be available in the past due to computer processor speed limitations. However, the current generation of computer processors provide significant increases in performance

which would allow for the real time use of such methods within on-board guidance computers. The use of technologies such as Field Programmable Gate Arrays (FPGAs) could provide significant increases in computation capacity allowing for the use of methods similar to those used in this study. The use of a single reference trajectory can also possibly reduce the required pre-mission planning and analysis over other methods that require a significant number of trajectories to be calculated prior to flight and then interrogate the data online. However, the single trajectory requires a larger number of evaluations to verify applicability under all possible conditions. It would be interesting to perform a direct comparison to the different methods to determine which is the most suitable for the terminal area flight phase.

The final condition errors for the guidance evaluations of sections 6.1.4, 6.1.5, 6.2.5 and 6.2.6 are greater than the sum of errors from the individual off-nominal condition sets discussed in section 6.2.4 and 6.1.3. The larger final condition error values indicate that the combinations of off-nominal conditions have a detrimental effect producing greater errors than the summation of the individual errors. This was expected as the off-nominal conditions do not just affect one characteristic of the vehicle but modify the applicability of the vehicle and environment models which impacts on all of the state variables. An example is the aerodynamic coefficient, density noise, atmospheric model difference, and velocity noise errors which all affect the calculated lift and drag forces changing the trajectory of the vehicle for the given steering commands. Consequently there is considerable coupling of the various off-nominal conditions to account for model uncertainties resulting in multiple errors within calculations. This results in the calculations having greater errors than would actually be experienced but also provides a greater evaluation of the guidance program.

6.4 Conclusions From Guidance

The results for the guidance program have revealed the effectiveness of the steering command parameterisation method investigated within this study. The restoration steps of the GPA were effectively able to deal with the variety of off-nominal conditions including mass variations, aerodynamic errors, atmospheric disturbances, steering command time delays, initial condition variations and position, velocity and steer-

ing noises.

The sensitivity studies of section 5.3 conducted within the optimisation program revealed large errors under off-nominal conditions without guidance. The worst case studies of sections 6.1.2 and 6.2.3 showed the effectiveness of the guidance method at adapting the steering parameter profiles to cope with a wide variety of off-nominal conditions.

The results of sections 6.1.1 and 6.2.2 for the Hopper and X-33 vehicles show that the guidance is effectively able to operate in real time with the current generation of computer processors. The computational effort although high when compared to traditional guidance methods provides for the capability of real time on-board implementation. The real time operation provides significant benefit to the guidance as it is able to deal with the large variety of off-nominal conditions in real time.

The sensitivity studies for the Hopper vehicle revealed that major sensitivities are winds, steering time delays, aerodynamic errors and position noise. The sensitivities for the X-33 vehicle are winds, steering command time delays and aerodynamic errors. Consequently when considering both vehicles the generic sensitivities for the terminal area flight phase were found to be winds, aerodynamic errors and steering command time delays. Although with the use of the two different vehicles and missions it is plausible to assume that common sensitivities are generic to the terminal area flight phase. However it is also possible that these sensitivities are generic to the methods used within this study. To reveal the generic sensitivities for the terminal area flight phase several different methods for the terminal area flight phase should be investigated simultaneously.

The winds caused larger final condition errors for the X-33 vehicle than the Hopper vehicle. Winds can be analysed at the landing site and as seen with the predictor wind results of the X-33 vehicle this data could possibly be uploaded to the vehicle prior to landing to provide a better model of the vehicle environment and to assist in guidance updates. The inclusion of the predictor wind models for the X-33 vehicle resolved a majority of the trajectory violations witnessed providing improved results. The sensitivities to the aerodynamic errors can be overcome with accurate aerodynamic models for both vehicles through a combination of CFD, wind tunnel and flight testing programs that traditionally occur for the development of launch and re-entry vehicles.

The steering command time delays were included as a method to model delays in achieving the correct vehicle attitude due to vehicle inertial dynamics, command signal processing and actuator rates. Consequently further research into the terminal area flight phase should include evaluation of the vehicle dynamics in 6 degrees of freedom to properly account for these effects and quantitatively identify their influence on the results.

The study conducted on the Hopper vehicle and mission without a speed brake setting as a steering parameter revealed that it is necessary to include a speed brake during the terminal area flight phase for the method used within this study. The speed brake is utilised as a method to control the energy dissipation rate of the vehicle and to include margins within the trajectory.

The evaluation of the guidance method under a variety of off-nominal conditions has revealed the flexibility and applicability of this guidance method to the terminal area flight phase. Using the restoration steps of the GPA the guidance method is effectively able to cope with the off-nominal conditions with only a single stored reference trajectory. The results for the X-33 vehicle provide a demonstration of the flexibility as the guidance program is able to redesign the trajectory for different initial positions and headings based on a large annulus for initial conditions.

An evaluation for the Hopper vehicle utilising the final conditions of re-entry from the study of Telaar (2005) revealed that the guidance was able to recover trajectories from a wider dispersions than required. A consequence of this was that trajectories which failed to meet the required re-entry final conditions were able to be recovered during the terminal area flight phase. This increases the flexibility and adaptability of the guidance algorithm as it is able recover trajectories well outside of the designed constraints.

The results of this chapter have revealed that the guidance method based on restoration steps for the steering commands works effectively for the terminal area flight phase. The studies conducted on both the Hopper and X-33 vehicles reveal the applicability of this guidance method to different vehicles and missions with a minimum amount of modification required. In combination with the ascent and re-entry studies of Telaar (2005) these methods of trajectory parameterisation via steering commands have been shown to be effective for almost the entire flight envelope with only the

approach and landing phase not investigated at this time.

Chapter 7

Conclusion

Make your work to be in keeping with your purpose.

Leonardo da Vinci (1452-1519)

Italian Scientist, Mathematician, Engineer, Inventor and Artist

The conclusion chapter provides a summary of the major findings of this research, the additions to the optimisation and guidance programs and the pertinent additions to current literature. Finally possible avenues for future work are discussed.

7.1 Summary of Major Findings

The research presented in this thesis has provided numerous findings for literature and future researchers. These findings are summarised below (with links to the appropriate section and/ or sections).

- Trajectory design and guidance by parameterising the trajectory based on steering commands was found to work effectively for the terminal area flight phase. Consequently this guidance method has now been shown to work effectively for ascent, re-entry and terminal area flight phases of reusable launch vehicles. See Chapters 5 and 6;
- The guidance system was found to be fast enough such that it could be effectively implemented in a real time on-board system utilising current level computer processors. However, the trajectory design utilising the optimisation techniques would need to be performed off-line. See sections 5.8, 6.1.1 and 6.2.2;

- The normalised vehicle energy was found to be the best method for defining the trajectory command points as it was well defined and steadily decreasing resulting in a well defined trajectory. See section 5.1;

- The cost functions developed in the study were designed to maximise the possible margins provided by a trajectory. However it was often found that several different trajectories could be determined that had similar cost function values. Consequently a user with some experience is required in order to determine the most suitable trajectories during the design process. see section 5.6;

- The trajectories for the terminal area flight phase include a rapid energy loss during the initial portions of the flight until sub-sonic flight is achieved. The trajectories transition to denser atmosphere and subsonic velocities because this region provides for greater lift to drag ratios, increased cross range capability and the ability to dissipate larger amounts of energy. See section 5.7;

- The recommended final flight path angle for the Hopper vehicle of $-28+10^{\circ}$ was found to be not viable resulting in a change to $-18 \pm 5^{\circ}$. The problem occurred due to coupling between final velocity and flight path angle. The change resulted in better results and was proven to be feasible based on the Hopper vehicle characteristics. See section 5.9;

- As expected increasing the amount of time between consecutive guidance calls and integration step size results in increases in final condition errors but provides reduced computational requirements. Reducing the time between consecutive guidance calls and integration step size below one second provides no significant benefit in final condition results. Consequently the guidance call interval and integration step size is selected as one second. See sections 6.1.1 and 6.2.2;

- The terminal area flight phase of the Hopper and X-33 vehicles was found to be sensitive to winds, vehicle aerodynamics and time delays in the steering commands which modelled vehicle inertial dynamics. The commonalities observed for the two different types of vehicle suggest a common attribute for the terminal area flight phase. However these sensitivities could also be related to the param-

eterisation method of this study. See sections 5.3, 6.1.2, 6.1.3, 6.2.3, 6.2.4, 6.3 and 6.4;

- The use of a speed brake for the Hopper vehicle as an additional steering parameter provides significant benefit to the guidance system providing an increased ability to modulate energy dissipation. See sections 5.4, 6.3, 6.4 and Appendix C;
- The strong winds experienced by the X-33 vehicle caused the guidance system to fail to achieve the required final conditions. Inclusion of a model to predict the winds allowed the guidance to achieve improved results. The predicted wind models are analogous to wind models that could be uploaded to the vehicle after the blackout stage of re-entry flight or included on-board based on estimated wind conditions. See section 6.2.5 and 6.2.6;
- The results for the Hopper and X-33 vehicle under a variety of off-nominal conditions showed the effectiveness of this guidance methodology of adapting the trajectory in real time. See sections 6.1.4, 6.2.5 and 6.2.6;
- The use of the guidance program for the ascent, hypersonic re-entry and terminal area flight phases has demonstrated the possibility of the program to work effectively for an entire vehicle mission. See section 6.1.5.

7.2 Conclusions of the Research

The results provided the required information to complete the original aims of the study. The use of the parameterisation method based on the vehicle steering commands for trajectory design was shown to be feasible and worked effectively. Several modifications were required for utilisation within the terminal area flight phase including speed brake models, modifications of environmental models and inclusion of the speed brake steering parameter and predictor wind models. However the results proved that the method is valid and well suited for designing trajectories combining longitudinal and lateral dynamic, eliminating the need for sub-phases, providing significant margins for off-nominal conditions and flexibility to multiple vehicles.

The guidance method utilising the restoration cycles of an accelerated gradient projection algorithm (GPA) was proven to operate effectively in the terminal area flight

phase. The results of the studies for the Hopper and X-33 vehicles showed the flexibility of the method to different vehicle types and also demonstrated the ability to cope with a wider variety of off-nominal conditions than published in other publicly available literature.

The development of the optimisation and guidance programs provided two power tools for performing sensitivity analyses of the terminal area flight phase. The investigations conducted for both the Hopper and X-33 vehicles showed that the method used within this study was sensitive to winds, vehicle aerodynamics and steering command time delays. Although the analyses with two vehicles showed commonalities for the terminal area flight phase it is quite possible that the sensitivities are also an attribute of the problem formulation used within this study. Comparison to other results using different methods for the terminal area flight phase could have revealed whether these sensitivities were or were not induced based on the steering command parameterisation method. However, there is a lack of detailed sensitivity studies in publicly available literature to provide a thorough comparison.

A comparison to other methods was performed. However since the other methods utilised different simulation environments and vehicles a direct comparison was difficult to achieve. A comparison based on general results and those relating to the Hopper and X-33 vehicles revealed that the method used within this study provided comparable results to the other methods. However, since only a general comparison could be performed it was not possible to perform comparative evaluation to determine if the method presented in this research provided significant improvements over the other methods. Future research should involve a direct comparison of the various methods to provide more quantitative results on areas for improvement similar to those studies presented in Hanson et al. (1995) and Hanson and Jones (2004).

The research and results determined in this study provide a significant basis for further research into the terminal area flight phase. The results show the influence of off-nominal conditions on the final conditions both with and without active guidance. The results have also provided detailed and quantitative information on the sensitivities of trajectories which can be utilised in further research to identify the areas of greatest concern and those that require the most development. The results have also identified areas where significant improvements are required such as the predictor wind models

for the X-33 vehicle. The method used within this study has also proven to work effectively and in conjunction with the ascent and re-entry study results has been shown to be an overall effective methodology for trajectory planning and guidance of reusable launch vehicles.

Several of the models used within this study were more accurate than required such as the fourth order Earth shape and non point mass gravity models. This was done to provide as detailed as possible background information for the terminal area flight phase and the vehicles studied. By utilising more detailed models the results presented here can be used as a basis for future studies, such as those proposed in section 7.5. Another reason for the utilisation of higher order models was so that the ascent, re-entry and terminal area flight phases could be coupled into a single program as proposed in section 7.5.

7.3 Additions and Improvements to Programs

During the research conducted in this study the optimisation and guidance programs went through continuous improvements and refinements to make them more suited to the terminal area flight phase. The additions and improvements to the optimisation and guidance programs include:

- Refinement of the environmental models for the terminal area flight phase;
- Inclusion of a speed brake setting as an additional steering parameter;
- Development of a speed brake model for the Hopper vehicle;
- Development of X-33 vehicle and aerodynamic models;
- Demonstration of flexibility and adaptability in trajectory design for the terminal area flight phase;
- Design of trajectories with margins for the terminal area flight phase based on the speed brake setting and cost functions.

7.4 Additions to Terminal Area Flight Phase Research

The results and findings from this research have also provided some significant additions to the literature and research on the terminal area flight phase. The additions and improvements to the terminal area flight phase literature include:

- Development and verification of a new trajectory design method based on nonlinear programming and the parameterisation of the trajectory by steering parameters through the use of a gradient based optimiser;
- Development and verification of a new guidance method utilising restoration steps of an accelerated gradient projection algorithm to update the steering parameters in real time;
- Detailed studies of trajectory design including cost functions, margins and the number and spacing of the steering parameters;
- Detailed sensitivity studies for two vehicles and missions;
- A general comparison to other published methods to identify the strengths and weaknesses of the developed methods;
- Detailed identification of pertinent off-nominal conditions for a 3DOF study for reusable launch vehicles;
- Detailed data on trajectory modification due to off-nominal conditions.

7.5 Future Work

Don't worry about the world coming to an end today. It's already tomorrow in Australia

Charles M. Schulz (1922 - 2000)
American Cartoonist

The trajectory design and guidance programs further developed within this research were only evaluated within a computer simulation environment. The various

models were based on observed data, such as wind tunnel and atmospheric measurement and off-nominal conditions were included to simulate real world conditions and account for modelling inaccuracies. However, further development and evaluation of the trajectory design and guidance programs can be achieved. There are several different steps of development:

1. Improvements can be made to the results for the X-33 vehicle via further development including the possible inclusion of a more detailed but computationally efficient wind models and by utilising multiple initial solutions based on the location and direction of the vehicle within the annulus;

2. Other improvements could be made to reduce the computation time of the programs. Currently the programs are in an unoptimised state as portions of the code have become disused and redundant. Optimisation of the code would allow for faster operating speeds than previously discussed in sections 6.1.1 and 6.2.2 further enhancing the guidance program's suitability for real time operation;

3. Further evaluations of the Hopper and X-33 vehicle studies including the expansion of off-nominal conditions to define large operating ranges. Although this was partially performed in the sensitivity studies of sections 5.3, 6.1.3 and 6.2.4 more detailed studies could be achieved that would provide greater information on the programs and the terminal area flight phase;

4. The evaluations could be extended to include other vehicles including previous vehicles such as US Space Shuttle, sub-orbital X-34 or even future vehicles such as the proposed Russian Clipper. These evaluations will further extend to the flexibility and versatility of the programs as was observed when the X-33 vehicle was included to provide an additional evaluation;

5. Further detailed analysis could be conducted in a 6 degrees of freedom simulation environment which would include side slip forces, vehicle inertial and rolling dynamics. The analysis could also be extended to include models of control surface movements and their influence on the aerodynamics of the vehicle. Such analysis would require detailed aerodynamic models of the vehicles

of which only the NASA lifting bodies and X-33 vehicle are currently available in public literature;

6. Further evaluation of the guidance under additional off-nominal conditions such as actuator or control surface failures to see if the vehicles can still reach the required target final conditions;

7. Comparison to the other methods discussed in section 2.3 could be achieved by performing simulations in a common analysis tool consisting of the same vehicle and environmental models, mission profile and off-nominal conditions. Such studies have previously been conducted for ascent (Hanson et al., 1995) and re-entry (Hanson and Jones, 2004) and could potentially provide valuable information on the terminal area flight phase as well as further developing advance methods for trajectory planning and guidance of reusable launch vehicles;

8. The ultimate evaluation of the trajectory planner and guidance would be to perform real world flight test. However, such flight test programs are prohibitively expensive for university based research without the support of major aerospace companies or government assistance. Flight test could be achieved through several methods including drop test from either a large aircraft or atmospheric balloon or via a test bed vehicle such as the proposed Phoenix 2 studies of Gockel et al. (2004).

An extension of the program to include the ascent and re-entry flight phases from the study of Telaar (2005) combined with the terminal area flight phase of this research into a single program could provide for a complete mission analysis until the ALI point. Further research could also be undertaken to extend the trajectory planner and guidance methods utilised within this study for the approach and landing flight phase of reusable launch vehicles. This would allow the use of only a single tool for trajectory planning of an entire mission. The development of a single guidance method for all flight phases of reusable launch vehicles could significantly reduce the amount of pre-mission planning and analysis, consequently reducing the overall cost of a mission. Such tools were also identified as key tools for the development of advanced guidance and control techniques (Hanson, 2002). However the approach and landing

phase allows for reduced model requirements and simple vehicle dynamics that could be achieved without the sophisticated predictor of this method. Methods similar to those of Barton and Tragesser (1999) and Schierman et al. (2004a) have already been shown to be effective for this flight phase.

Major influences of the terminal area flight phase were revealed within this study with the sensitivity studies. The commonalities and disparities of the observed results utilising the two different vehicles revealed what effects were inherent to the terminal area flight phase and what effects were properties of the vehicle. However, it was also possible that the commonalities could also be attributed to the methods used within this study. Therefore additional investigations of the terminal area flight phase should be undertaken using different methods to validate the findings from this research. Additional studies could provide a greater more in depth understanding of the terminal area flight phase and further assist in the development of improved methods for trajectory planning and guidance.